Etude des conformations et des transitions de forme de l'ADN et des polynucléotides par la diffraction RX de fibres et la modélisation moléculaire

Guy Albiser

Université de Nancy I
Faculté des Sciences

U.F.R. S.T.M.P.
G.D.R. Sciences et
Génie des Matériaux

THESE

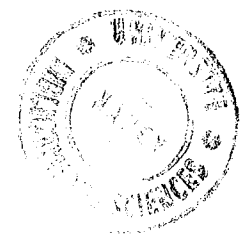

présentée à l'Université de Nancy I
pour obtenir le grade de

DOCTEUR ES SCIENCES PHYSIQUES

par

Guy ALBISER
Maître de Conférences

ETUDE DES CONFORMATIONS ET DES TRANSITIONS DE FORME DE L'ADN ET DES POLYNUCLEOTIDES PAR LA DIFFRACTION R.X. DE FIBRES ET LA MODELISATION MOLECULAIRE

Soutenue le 12 Mars 1992 devant la Commission d'Examen

Membres du Jury

Président :	**M.**	**HORN P.**	**Professeur**
Examinateurs :	**MM.**	**LECOMTE C.**	**Professeur**
		MARRAUD M.	**Directeur de Recherche**
		PREMILAT S.	**Professeur**
	MME	**TAILLANDIER E.**	**Professeur**
	M.	**WITZ J.**	**Directeur de Recherche**

AVANT PROPOS

Ce travail a été effectué au ***Laboratoire de Biophysique Moléculaire*** *de l'Université de Nancy I (équipe de recherche associée au C.N.R.S., groupe Biostructures, U.R.A. N° 494), sous la direction de Monsieur le* ***Professeur S. PREMILAT.***

Je suis profondément reconnaissant à Monsieur le ***Professeur P. HORN*** *de m'avoir accueilli dans ce laboratoire et je tiens à lui formuler mes plus vifs remerciements pour le souci permanent qu'il a eu de faciliter mon travail de recherche sur les plans à la fois humains et matériels. Je le remercie aussi de l'honneur qu'il me fait de présider ce jury de thèse.*

C'est à plus d'un titre que je suis heureux de remercier chaleureusement Monsieur le ***Professeur S.PREMILAT.*** *En effet, il a guidé en permanence ce travail avec une grande rigueur scientifique associée à une patiente amitié. Je lui suis également redevable de toute la partie modélisation moléculaire de ce travail. C'est grâce à sa direction et à une collaboration active et constante que l'essentiel des recherches entreprises ont pu faire l'objet des publications rassemblées dans cette thèse.*

Je tiens à remercier tout particulièrement Madame le ***Professeur E. TAILLANDIER*** *d'avoir accepté de juger ce travail mais aussi de l'attention qu'elle a toujours portée à l'activité et à la vie du laboratoire.*

Que Monsieur ***J. WITZ, Directeur de Recherche au CNRS,*** *trouve ici l'expression de ma gratitude pour avoir bien voulu examiner cette thèse et pour l'aide amicale qu'il m'a apportée*

lors d'un stage au Laboratoire de Biologie Moléculaire de Cambridge (G.B.).

J'exprime mes sincères remerciements à Monsieur ***M. MARRAUD, Directeur de Recherche au C.N.R.S.*** *et Directeur de l'URA 494 pour l'intérêt qu'il porte à notre domaine de recherche et pour avoir accepté de faire partie du Jury.*

Je tiens également à exprimer mes vifs remerciements à Monsieur le ***Professeur C. LECOMTE*** *qui a bien voulu consacrer du temps pour prendre connaissance de ce travail et participer au Jury.*

L'esprit de camaraderie qui lie les chercheurs du laboratoire a crée une ambiance de travail et de collaboration efficace. C'est un plaisir pour moi de citer en particulier, Messieurs ***M. HARMOUCHI et A. ABOUELKASSIMI.***

Il m'est très agréable de remercier ici Monsieur ***M. GRECO*** *pour sa coopération à l'élaboration et à la réalisation des chambres R.X. spéciales et en général pour toute son assistance technique.*

Je suis très reconnaissant à Madame ***D. HENRYON*** *pour sa grande compétence et sa maîtrise dans la réalisation de ce mémoire.*

Je remercie également Monsieur ***Y. SERE*** *pour m'avoir toujours aimablement aidé avec sûreté et rapidité pour l'entretien des générateurs R.X.*

Enfin, je remercie les responsables de Services Communs de l'Université de Nancy I pour leur concours dans l'utilisation d'appareils de mesure.

SOMMAIRE

CHAPITRE V : ETUDES DES DIFFERENTES TRANSITIONS CONFORMATIONNELLES DE L'ADN ET DES POLYNUCLEOTIDES EN FIBRE

INTRODUCTION GENERALE

"We wish to suggest a structure for the salt of deoxyribose nucleic acid (DNA). This structure has novel features which are of considerable biological interest".

J.D. WATSON, F.H.C. CRICK, Nature 1953, 737

La proposition d'une conformation en double hélice droite pour l'acide désoxyribonucléique (ADN) par Watson-Crick est, sans contestation possible, à l'origine de découvertes capitales en biologie moléculaire. En effet, cette structure a permis de comprendre comment l'ADN stockait et transmettait l'information génétique,et de découvrir les mécanismes de duplication de l'ADN, permettant à l'information génétique d'être recopiée et transmise au cours des générations successives .

Avec la découverte de l'universalité du code génétique, la biologie moléculaire a pu décrire les mécanismes de transcription de l'ADN qui dirigent la synthèse des protéines (1). De nombreux événements se sont ensuite succédés en biologie moléculaire : découverte du clonage, des enzymes de scission, possibilité de déterminer des séquences d'un ADN quelconque, mise au point de sonde spécifique, synthèse d'ADN qui code une protéine donc synthèse de protéine, insertion d'une séquence dans un gène et ouverture d'un nouveau domaine de recherche avec le génie génétique (2).

Les propriétés chimiques et physiques de toutes ces macromolécules biologiques sont étroitement liées à leur structure tridimensionnelle. Des questions essentielles se

posent donc pour comprendre comment une structure comme celle de l'ADN conditionne sa fonction au niveau moléculaire . Ces problèmes sont ceux de la biophysique moléculaire qui dispose de plusieurs types de méthodes pour les appréhender : méthodes d'analyses physico-chimiques en solution (absorption U.V. et infrarouge, dichroïsme circulaire, RMN, diffusion R.X...), la diffraction des rayons X, l'analyse conformationnelle et la dynamique moléculaire.(3,4) Parmi ces méthodes, la diffraction des rayons X constitue une méthode d'analyse structurale incontestée mais elle présente aussi les inconvénients majeurs liés à la nécessité d'obtenir des cristaux de bonne qualité et d'étudier la matière biologique dans des conditions non physiologiques. De plus, dans le cas de l'ADN, l'obtention de cristaux n'est possible que pour des oligonucléotides. Néanmoins, on peut approcher les conditions d'existence de l'ADN en solution en utilisant les avantages que donne la diffraction des rayons X en organisant les molécules d'ADN en fibres étirées et orientées. C'est du reste ce moyen qui a permis de proposer la structure en double hélice de l'ADN (5). Cette structure de l'ADN semble très rigide mais de nombreux faits expérimentaux laissent, au contraire, supposer une grande souplesse de conformation. Par exemple, dans l'organisation des chromosomes, la molécule d'ADN subit des enroulements successifs pour obtenir un volume compact. De même, les récentes études d'association ADN-protéine révèlent une flexibilité de la double hélice (6,7). Pour les ADN circulaires des surenroulements de la double hélice existent localement lors de la transcription et peuvent induire des changements de sens de la double hélice (8). Il est également

connu que la structure de l'ADN peut facilement être perturbée par des insertions de colorant ou de drogues (9). Dans le cas d'une séquence complémentaire sur un même brin, la séparation locale des deux chaînes peut créer des conformations cruciformes (10). Lors d'interaction de recombinaison on obtient même des échanges de brin entre deux molécules d'ADN avec le type de jonction Holliday (11). Tous ces faits dénotent donc une très grande plasticité de la conformation de cette molécule d'ADN et montrent que les structures secondaire et tertiaire sont facilement perturbées par les conditions dues à l'environnement(12).

Dans ce vaste champ de recherches, l'objectif du travail présenté ici est restreint à l'étude de la structure secondaire de l'ADN et de polynucléotides placés dans un environnement très simple mais modifiable. Cette étude est faite en utilisant la diffraction des rayons X par l'ADN étirée en fibres orientées.

Les résultats obtenus, rassemblés dans des publications s'inscrivent sur une certaine période, ce qui explique des études répondant à un problème très précis comme, par exemple, l'étude sur la validité d'un modèle conformationnel de l'ADN constitué de la succession d'hélices droites et gauches. Cette période a également été marquée par la découverte d'une structure en double hélice gauche dans un cristal d'un duplex d'hexanucléotide (13). Cet événement s'est traduit par une remise en cause de beaucoup de modèles conformationnels de l'ADN ou de polynucléotides résultant de l'analyse par la diffraction RX de fibres (14).

C'est ainsi que les premiers travaux présentés portent sur des modèles conformationnels de la forme B de l'ADN placé dans un environnement de cation alcalin et d'hydratation très élevée.

Après l'étude sur l'incidence de la composition en bases de l'ADN sur les résultats expérimentaux obtenus par la diffraction des rayons X, il apparait, que pour opérer une discrimination entre les modèles, il est nécessaire d'utiliser les résultats provenant de techniques complémentaires comme le dichroïsme linéaire infrarouge sur film ou la RMN (15,16). Cette démarche s'étant révélée pertinente, elle a pu être poursuivie pour analyser les conformations de l'ADN placé dans d'autres conditions d'environnement. Ainsi, les conformations appelées A et C ont pu être précisées. Ces formes correspondent à un état d'hydratation moyen des fibres et dans le cas de sel de sodium associé, à une très faible concentration pour la forme C. De la même façon, la conformation de la forme D du poly (dA-dT). poly (dA-dT) a été établie en tenant compte des contraintes résultant des données des techniques envisagées .

Disposant alors de modèles conformationnels de l'ADN pour un environnement proche des conditions physiologiques, l'action d'autres types de cation métallique a été étudiée expérimentalement afin d'en déduire l'incidence sur la conformation. La motivation essentielle est d'expliquer certains comportements de l'ADN en solution comme dans le cas de l'étude de la fixation d'argent (17). D'autre part, l'intérêt biologique n'est pas négligeable puisque la teneur en métaux dans la cellule et celle de l'ADN en particulier,

varient considérablement pendant les phases critiques de l'embryogenèse. De même, il a été remarqué que les cellules cancéreuses avaient beaucoup plus besoin de métaux pour fonctionner ou se reproduire(18). Nous avons poursuivi notre travail de recherche en introduisant une contrainte nouvelle, souvent implicitement appliquée aux fibres d'ADN, la tension mécanique. Ce facteur peut intervenir du fait de la structure tertiaire de la molécule d'ADN. L'influence de la tension mécanique est analysée en particulier lors des transitions conformationnelles pour des ADN naturels, les passages de A à B et de B à C étant induits par des changements d'hydratation des fibres.

Les derniers travaux expérimentaux présentés sont consacrés uniquement aux transitions entre les différentes formes des ADN et polynucléotides. Ces analyses étant réalisées dans des conditions précises de cation alcalin associé aux fibres en fonction de l'hydratation. Pour préciser les types de transition et l'état des conformations en présence ansi que les variations d'hydratation de la molécule d'ADN, une méthode complémentaire à la diffraction RX de fibre a été utilisée. Cette méthode fait appel à la mesure des dimensions des fibres ; elle est fondée sur l'établissement de rapports entre les paramètres géométriques des fibres et les paramètres cristallographiques.

CHAPITRE I : METHODES THEORIQUES ET EXPERIMENTALES

A) INTRODUCTION

La diffraction des rayons X par un cristal parfaitement ordonné est un moyen adéquat pour déterminer la structure d'une molécule. L'utilisation de la diffraction des rayons X, dans le cas de molécules constituées de longues chaînes d'unités identiques, comme l'ADN, qui ne permettent pas l'obtention de cristaux, est également possible si on associe ces chaînes en fibres orientées.

Une fibre peut être considérée comme un groupement ordonné de micro-cristallites résultant de l'assemblage ordonné de ces chaînes. Mais ces cristallites sont disposés de façon aléatoire autour de la direction de l'axe la fibre *(figure n°1)*.

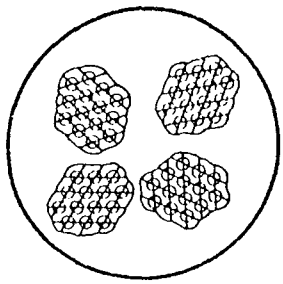

Figure n°1

Section d'une fibre polycristalline.
Les petits cercles représentent les molécules et les régions irrégulières, les cristallites.

Dans le cas de l'ADN, ces molécules en chaîne ont souvent la particularité de former des hélices. En fait des doubles hélices de deux chaînes antiparallèles, chaque chaîne étant constituée par la succession de nucléotides. Un nucléotide comprend un enchaînement phosphate-désoxyribose et sur le désoxyribose se greffe une chaîne latérale, la base, qui est soit purique, soit pyrimidique. Les deux chaînes sont liées par des liaisons hydrogène entre bases complémentaires

(Adénine avec Thymine et Guanine avec Cytosine) selon le schéma de Watson-Crick (19).

La théorie de la diffraction des rayons X par des structures en hélice a été faite par Cochran, Crick et Vand en 1952 (20). Cette théorie a été complétée par Vainshtein (21). Elle est également présentée dans des ouvrages plus récents (22,23).

L'hélice est définie par son pas P mais aussi par la distance C de répétition du motif élémentaire dans la direction de l'axe de l'hélice et par le paramètre p distance entre les projections axiales de deux unités consécutives *(figure n°2)*.

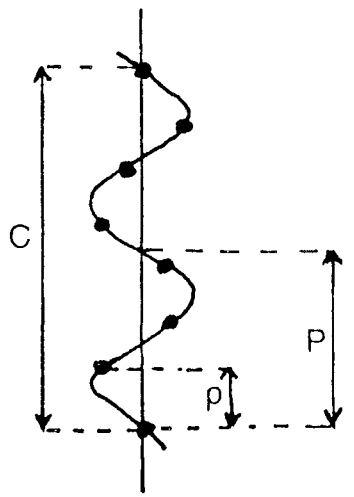

Figure n°2

Hélice discontinue, de pas P comportant 7 unités en 2 tours.

Ces paramètres d'hélice sont facilement déterminés à l'aide des clichés RX de fibre.

Pour avoir des renseignements précis sur la conformation atomique du motif élémentaire (le nucléotide pour l'ADN), il est nécessaire d'établir un modèle moléculaire et de confronter les intensités théoriquement diffractées par celui-ci aux intensités expérimentales. Un bon accord entre ces grandeurs constitue un critère de validité du modèle.

Dans ce chapitre, quelques résultats théoriques sur la diffraction par les structures en hélice sont rappelés. L'exploitation pratique des clichés de fibre de l'ADN, la construction de modèles moléculaires sont également précisées. Enfin, des détails pratiques sont présentés sur la technique d'orientation des fibres d'ADN et sur les moyens expérimentaux pour obtenir de bons clichés RX.

B) THEORIE DE LA DIFFRACTION DES RAYONS X PAR DES FIBRES DE MOLECULES HELICOIDALES

I. Hélice continue

On considère une hélice uniforme, d'épaisseur infiniment petite, de longueur infinie, de rayon r et de pas P ; cette hélice sera représentée ***(figure n°3)*** dans l'espace réel par :

$$x = r \cos \frac{2\pi z}{P}$$

$$y = r \sin \frac{2\pi z}{P}$$

$$z = z$$

et dans l'espace réciproque par :

$$x^* = R \cos \psi$$

$$z^* = R \sin \psi$$

$$z^* = z$$

Hélice droite continue et sa représentation en coordonnées cylindriques.

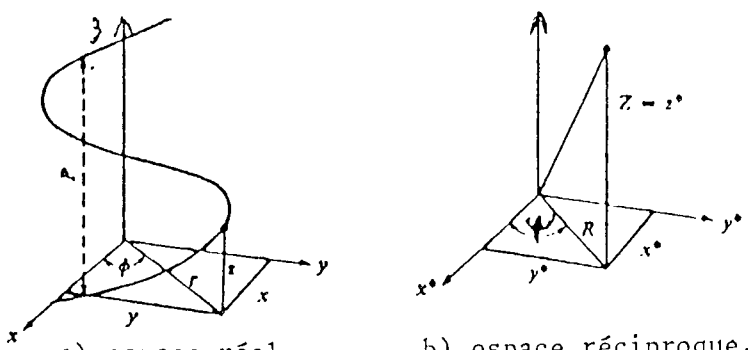

a) espace réel b) espace réciproque.

Figure n°3

Si la densité électronique le long de l'hélice continue est prise uniformément égale à l'unité, le facteur de structure, $F(x^*, y^*, z^*)$, est donné par la transformée de Fourier de la fonction "forme" $H(x, y, z)$.

$$F(x^*, y^*, z^*) = \int_{-\infty}^{+\infty} H(x, y, z) \exp 2\pi i (x x^* + y y^* + z z^*) \, dv$$

La fonction $H(x, y, z)$ étant égale à zéro partout sauf sur l'hélice ou on suppose qu'elle a une valeur égale à l'unité et en remarquant que dv est proportionnel à dz , on peut écrire, en fonction des coordonnées cylindriques :

$$F(x^*, y^*, z^*) = \int_{-\infty}^{+\infty} \exp 2\pi i \left[r R \cos \left(\frac{2\pi z}{P} - \psi \right) + z z^* \right] dz$$

La fonction H a pour période P selon la variable z. La transformée de Fourier de cette fonction périodique est différente de 0 seulement pour les valeurs $z^* P = n$, avec n entier. Le diagramme de diffraction sera donc réduit à des courbes d'intensité situées sur les strates d'ordre n, à distances de 0, $1/P$, $2/P$ de l'équateur du cliché ***(figure N°4)***. On a donc :

$$F(R, \psi, \frac{\ell}{P}) = \int_{0}^{P} \exp 2\pi i \left[r R \cos \left(\frac{2\pi z}{P} - \psi \right) + \frac{nz}{P} \right] dz$$

En utilisant une relation relative aux fonctions de Bessel, on obtient : ***(figure N°5)***

$$F(R, \psi, \frac{\ell}{c}) = J_n (2\pi r R) \exp i n \left(\psi + \frac{\pi}{2} \right)$$

Le calcul de F^2 donne une quantité proportionnelle à l'intensité diffractée par cette hélice continue.

Figure n°4

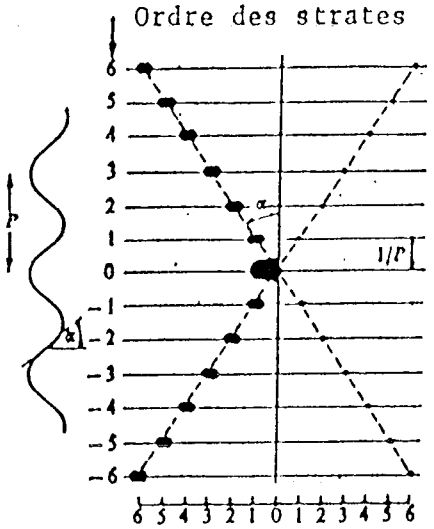

Caractéristique du diagramme de diffraction d'une structure en hélice continue.

Figure n°5

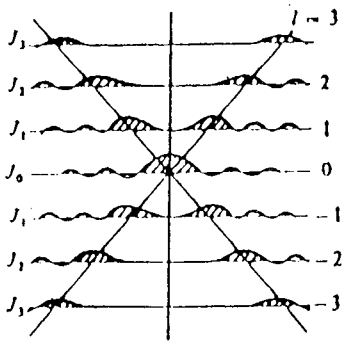

Disbribution des fonctions de Bessel sur les strates

II. Hélice discontinue

Pour figurer la distribution d'atomes identiques sur une hélice de pas P, (ces atomes ayant des projections axiales distantes de p) on considère une distribution de points représentés par l'intersection de l'hélice continue de rayon r et de pas P avec une série de plans parallèles et distants de p *entre eux* ***(figure N°6).***

Figure n°6

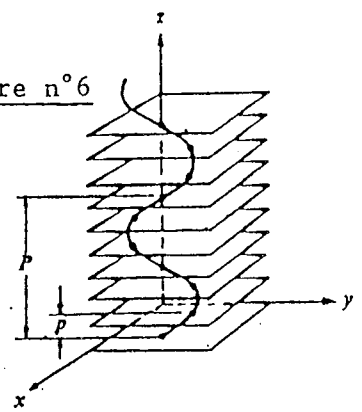

hélice discontinue formée par l'intersection entre une hélice continue et série de plans parallèles.

Figure n°7

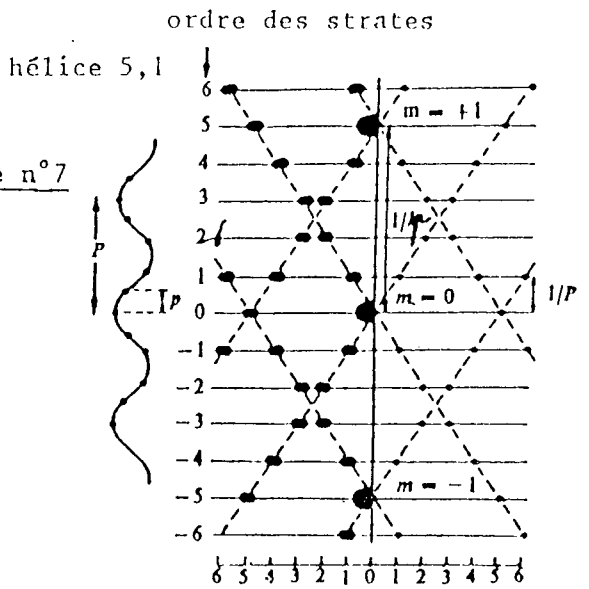

Caractéristique du diagramme de diffraction d'une structure en hélice discontinue.

Connaissant la transformée de Fourier de l'hélice continue qui n'a de valeurs différentes de zéro que sur les strates $z^* = n/p$ et sachant que la transformée de Fourier de plans équidistants de p donne une distribution de points alignés distants de $z^* = m/p$ (m entier) sur une droite perpendiculaire à ces plans, la transformée de Fourier de l'hélice discontinue est le produit de ces deux transformées. Ainsi, le facteur de structure aura des valeurs finies seulement pour :

$$z^* = n/P + m/p$$

De plus, s'il y a t tours d'hélice pour la périodicité cristallographique C avec un nombre u de points, on a : $t\,P = up = C$. En considérant une strate l définie par :

$z^* = l/C$, on obtient la règle de sélection qui fixe l'ordre n des fonctions de Bessel sur cette strate avec m entier :

$$l = n\,t + m\,u$$

Le facteur de structure pour la strate l s'écrit dans ces conditions :

$$F_l(R, \psi, \frac{\ell}{c}) = \sum_n J_n\,(2\pi r R)\exp i n (\psi + \frac{\pi}{2})$$

L'allure du diagramme de diffraction est du type de celle donnée par la *figure n°7* :

III. Molécule en hélice

Une molécule en hélice est constituée d'un nombre j d'atomes de différents types dans chaque motif élémentaire. Chaque atome j de coordonnées (r_j, Φ_j, z_j) est situé sur une hélice. Chaque type d'atome a son facteur atomique f_j. Pour

la strate l, le facteur de structure d'une telle molécule est alors donné par :

$$F_l(R, \psi, \frac{\ell}{c}) = \sum_n \sum_j f_j J_n(2\pi r_j R) \exp i \left[n \left(\psi - \Phi_j + \frac{\pi}{2}\right) + \frac{2\pi \ell z_j}{c}\right]$$

avec la même règle de sélection pour les ordres n des fonctions de Bessel de chaque strate, à savoir :

$$l = n\ t + mu.$$

Dans le cas de l'ADN, le nucléotide contient en moyenne 21 atomes en ne tenant pas compte des atomes d'hydrogène qui diffractent très peu les rayons X.

IV. Intensités théoriques

Le fait qu'une fibre de double hélices d'ADN soit constituée d'un grand nombre de molécules parallèles organisées dans des cristallites d'orientation quelconque autour de la direction de l'axe de la fibre revient à dire que chaque molécule individuelle est orientée au hasard autour de cette direction. Par conséquent, l'intensité diffractée par ces molécules en fibre doit être une valeur moyenne sur les orientations, c'est-à-dire la moyenne pour toutes les valeurs de Ψ , puisque Ψ est l'angle qui définit la position de la molécule dans le réseau réciproque.

En écrivant le facteur de structure d'une molécule sous une autre forme :

$$F(R, \psi, \frac{\ell}{c}) = \sum_n (A_n + i B_n)\ e^{i n \psi}$$

avec :

$$A_n = \sum_j f_j J_n (2\pi r_j R) \cos \left[n\left(\frac{\pi}{2} - \Phi_j\right) + 2\pi \frac{\ell}{c} z_j\right]$$

$$B_n = \sum_j f_j J_n (2\pi r_j R) \sin \left[n\left(\frac{\pi}{2} - \Phi_j\right) + 2\pi \frac{\ell}{c} z_j\right]$$

L'intensité I s'écrit alors :

$$I = F F^*$$

$$I = \sum_n \sum_m \left[(A_n A_m + B_n B_m) + i (A_m B_n - A_n B_m)\right] \exp^{i(n-m)\psi}$$

Cette valeur moyenne vaut 0 sauf pour n = m, on a alors :

$$I = F^2 \overline{\psi} (R, \frac{\ell}{c}) = \sum_n (A_n^2 + B_n^2)$$

n étant les ordres des fonctions de Bessel de la strate l.

Ajoutons que dans le cas de l'ADN, du fait de la présence de deux chaînes antiparallèles, il y a un axe de symétrie (axe dyade) situé dans le plan des bases et perpendiculaire à l'axe de l'hélice. Cette symétrie annule les termes B_n.

V. Réseau

Dans le cas où l'on considère que les cristallites constituant la fibre d'ADN sont parfaitement ordonnées, les molécules en double hélice vont être distribuées aux noeuds d'un réseau cristallin. De cet ordre, dans l'agencement des molécules, il va résulter, sur le cliché de rayons X, des taches de diffraction (ou taches de Bragg) correspondant aux

plans réflecteurs d'indices h, k, l propres à chaque type de réseau cristallin.

Le cliché de diffraction de la fibre résulte donc d'une part de la diffraction de la molécule en double hélice et d'autre part, de l'assemblage des molécules en réseau cristallin. En fait, les taches de Bragg du cliché résultent d'un échantillonnage, aux positions des noeuds du réseau cristallin, des courbes continues des intensités diffractées sur chaque strate. La *figure (8 a et b)* donne un exemple des taches de Bragg ainsi obtenues.

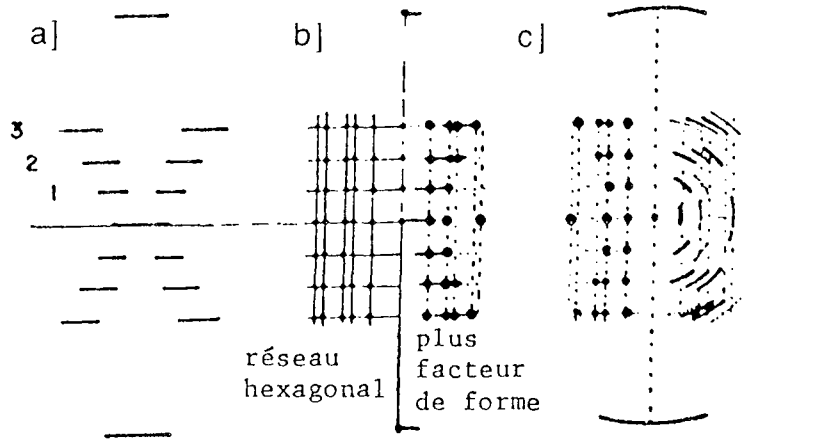

Figure n°8

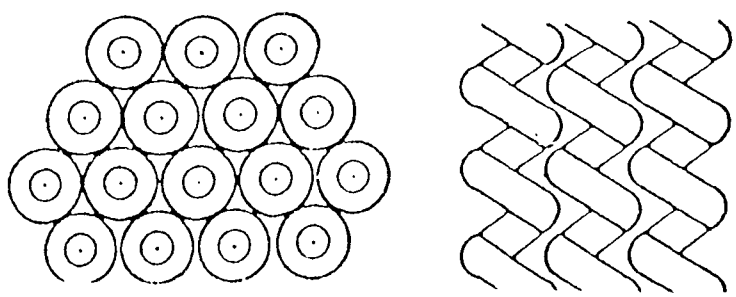

Cliché de diffraction dû à l'assemblage en réseau de molécules en structure hélicoïdale.

L'analyse de la distribution des taches de Bragg permet de déterminer le type de réseau et les absences éventuelles de taches sur certaines strates donne le groupe d'espace avec l'agencement des molécules dans la maille.

En pratique, les clichés de diffraction ne présentent pas de taches ponctuelles de Bragg mais des arcs de la largeur angulaire approximativement constante ***(figure N°8 c)*** . Ceci est dû à une distribution D (α) des axes des cristallites autour de la direction de l'axe de la fibre ***(figure n°9)***.

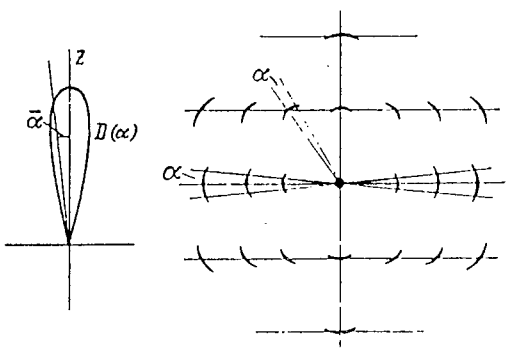

Figure n°9

La fonction D(α) et élargissement angulaire des reflexions sur le cliché RX.

De plus, la régularité de la distribution des molécules dans les cristallites est souvent perturbée. L'analyse des différents types de désordre et de leurs effets sur les diagrammes de diffraction sont détaillés par plusieurs auteurs (21-24-25). Un type de désordre fréquent donne des clichés de diffraction appelés semi-cristallin (avec désordre de type "vis") (26). Ce type de cliché se distingue par des taches de diffraction bien définies au centre et par des distributions continues d'intensité sur les strates supérieures et à des distances éloignées de l'axe du réseau réciproque.

On remarque également que les fibres d'ADN qui sont sensibles à l'humidité relative environnante ont des réseaux cristallins dont les paramètres et quelques fois le type varient en fonction de l'humidité. Ces évolutions entraînent souvent l'accroissement du désordre dans la fibre.

C) EXPLOITATION DES CLICHES RX (CAS DE LA CHAMBRE PLANE)

I. Tâche méridienne

La recherche de la première tache méridienne sur un cliché de diffraction de fibre d'ADN est importante car elle apporte deux types de renseignements : le nombre de nucléotides par tour et l'espacement entre nucléotides successifs p projeté sur l'axe de la fibre.

L'évaluation du nombre de nucléotides par tour résulte du fait que seules les fonctions de Bessel d'ordre zéro ont des valeurs différentes de zéro pour un argument nul et dans ce cas la règle de sélection des fonctions de Bessel s'écrit :

$l = 0\ t + 1\ u$, soit $l = u$.

L'ordre de la strate donne donc en principe le nombre de nucléotides. Néanmoins, il faut remarquer que dans le cas où les strates ne sont pas régulièrement espacées sur le cliché, l'ordre de la strate est délicat à évaluer.

Pour obtenir la valeur de p, il est nécessaire d'obtenir correctement cette tache méridienne. En effet, le noeud qui correspond à cette tache est sur l'axe du réseau réciproque, or, en principe, cet axe est perpendiculaire , comme la fibre, au faisceau de rayons X, donc dans la zone aveugle de la sphère de réflexion (sphère d'Ewald). Pour obtenir la tache méridienne, il est donc nécessaire d'incliner la fibre d'un angle α par rapport à la perpendiculaire au faisceau RX *(figure n°10)*.

Figure n° 10

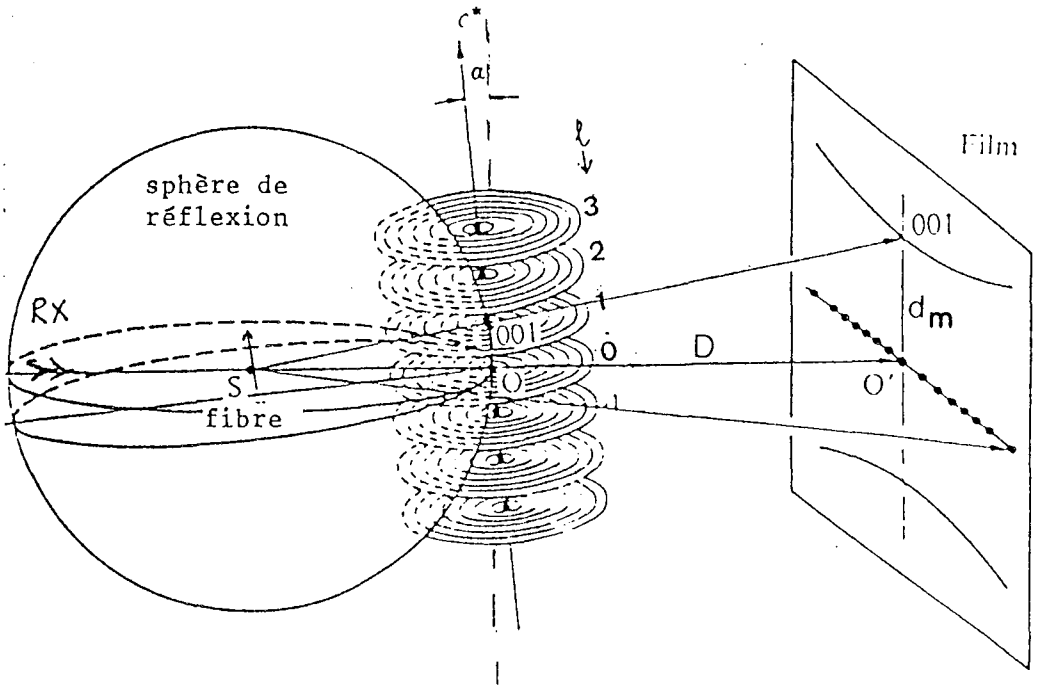

Effet de l'inclinaison de la fibre sur le diagramme de diffraction.

La loi de Bragg donne immédiatement pour p : $p = \lambda/2.\sin\alpha$ avec λ, longueur d'onde du rayonnement X utilisé. On évalue l'angle α en remarquant que $tg\ \alpha = dm/D$, avec dm distance de cette tache méridienne au centre du film et D distance film fibre.

Cette tache méridienne peut apparaître pour une fibre faiblement inclinée du fait de la désorientation des cristallites à l'intérieur de la fibre.

II. Détermination du pas de l'hélice

Le pas de l'hélice est évalué à partir de la distance entre l'équateur du cliché et la première strate, la fibre étant perpendiculaire au faisceau de rayons X. Du fait de

l'utilisation d'un film plan, il résulte que les strates ne sont pas parallèles à la strate équatoriale l = 0. En prenant, sur le cliché, la direction équatoriale et la direction méridienne comme axes de coordonnées (x, z), chaque tache de la strate aura une position bien définie. D étant la distance de la fibre au film *(figure n°11)*,

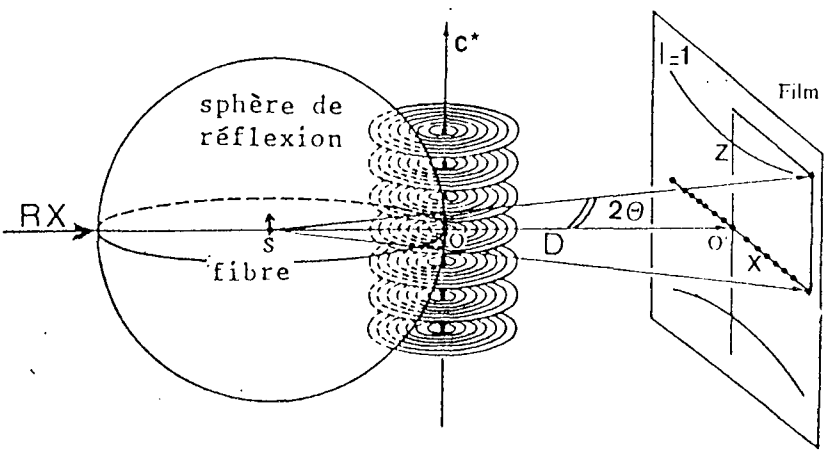

Figure n°11

Coordonnées définissant la position d'une tache de diffraction sur le film-plan.

on définit le pas P pour la strate l par :

$P = P_l = \lambda \ (D^2 + x^2 + z^2)^{1/2}/z$ avec λ la longueur d'onde du faisceau RX. De plus, pour toute strate d'ordre l, on a également : $P = l\ P_l$, ce qui définit parfaitement le pas de l'hélice.

Dans le cas où l'on constate une dissymétrie du cliché par rapport à l'équateur, cela est dû à une inclinaison de la fibre par rapport à la perpendiculaire au faisceau RX. Il est alors possible d'obtenir le pas de l'hélice en tenant compte de l'angle d'inclinaison γ (27). Cet angle est évalué en mesurant les pas P_{L1} et P_{L2} de part et d'autre de l'équateur pour une tache donnée de la strate d' ordre L. Pour une tache de Bragg sur cette strate à la distance d, on a:

$$\operatorname{tg}\gamma = d^2/\lambda \left| 1/P_{L2} - 1/P_{L1} \right|$$

et la correction sur le pas devient :

$$P_{L_{corr}} = \frac{2}{\cos\gamma} \left(\frac{P_{L_1} P_{L_2}}{P_{L_2} + P_{L_1}} \right)$$

III. Détermination du pas cristallographique

Le pas cristallographique c est défini à partir de la relation : t P = u p = c

P le pas étant déterminé ainsi que p et u, on peut vérifier la cohérence de ces valeurs par le calcul de t. En effet, la règle de sélection montre que l = t pour n = l et m = 0. Or, n = l implique des réflexions très intenses proches du méridien . Le paramètre t est donc défini par l'ordre de la strate comportant des réflexions intenses quasi méridiennes.

En pratique, on détermine les paramètres P et p, puis on calcule le rapport P/p : s'il est entier t = l alors C = P. Par contre, si P/p est non entier, il faut que le produit P/p x t soit un entier avec t le plus petit nombre possible.

Pour l'ADN en forme A, on évalue ainsi P = 28,15 A, p = 2.56 A, soit P/p = 11 = u/t. On trouve la strate de la tache méridienne à l'ordre 11. Donc : u = 11 et t = 1 dans ce cas. De plus c = P et la règle de sélection s'écrit : l = n + 11 m.

Par contre pour l'ADN de Lithium en forme C on remarque des strates qui ne sont pas parfaitement équidistantes. Avec la première strate, on obtient P = 30,8 A. La tache méridienne donne p = 3.3 A, P/p = 9,33= u/t. u et t étant des entiers, cela signifie que u = 28 et t = 3, alors C = 3 P = 92.4 A et

la règle de sélection s'écrit : $l = 3n + 28m$. On remarque que la réflexion méridienne se trouve sur la 28e strate.

IV. Détermination du réseau

L'identification du réseau cristallin fait appel à l'évaluation de toutes les distances inter-réticulaires : d_{hkl} (hkl étant les indices de Miller (24), avec l étant l'ordre de la strate). Ces distances sont évaluées pour chaque tache de diffraction du cliché par la loi de Bragg :

$$d_{hkl} = \lambda / 2 \sin \Theta_{hkl}$$

Dans le cas du cliché plan, la valeur de l'angle Θ_{hkl} de chaque tache est obtenu par la relation :

$$\text{tg } 2\,\Theta_{hkl} = \Phi_{hkl} / 2D$$

D étant la distance de la fibre au cliché et Φ_{hkl} la distance radiale entre deux taches hkl symétriques.

Pour les formes classiques A, B C de l'ADN et D,Z des polynucléotides les types et les paramètres de réseau ont été bien établis après un processus de raffinement (28,29,30,31). L'analyse de la distribution des taches de diffraction sur les clichés a également conduit à préciser l'arrangement des molécules d'ADN dans chaque type de cellule unité (30,31).

En pratique, on retrouve pour les fibres d'ADN dans des conditions expérimentales différentes, le type de réseau parmi ceux proposés mais avec des paramètres qui peuvent être variables.

V. Mesure des intensités expérimentales

Etant donné que l'on utilise les films photographiques pour collecter les informations diffractées par les fibres, il est nécessaire d'employer au moins trois films superposés pour couvrir toute la gamme des intensités diffractées. Le développement de ces films devant être réalisé avec soin (température de 20°C, bains neufs, agitation pour éviter les inhomogénéités de développement).

Les intensités sont mesurées à l'aide d'un densitomètre. Pour chaque arc de diffraction on obtient une trace radiale. L'estimation du fond continu sous cette trace est faite empiriquement en mesurant l'intensité entre les strates voisines de la tache puis on mesure au planimètre la surface S comprise entre la trace du densitomètre et l'estimation du fond continu. Comme il y a quatre taches de diffraction par cliché correspondant à la même valeur théorique de l'intensité observée, cette dernière est en fait la moyenne des valeurs trouvées pour les quatre taches. Pour utiliser ces valeurs, il faut leur appliquer des facteurs correctifs dont le détail, pour la diffraction de fibre, est donné par différents auteurs: Franklin (27), Arnott (32), Fuller (33). Certains facteurs correctifs sont négligés comme la polarisation (du fait des angles de diffraction impliqués) mais également le facteur d'absorption.

Par contre, l'utilisation de film plan implique l'introduction d'une correction pour tenir compte de la variation de la distance fibre-tache de diffraction et de l'incidence oblique du faisceau sur le film. De même, du fait de la désorientation autour de l'axe de la fibre, l'intensité

observée est proportionnelle à la longueur L de l'arc observé (28).

Outre le facteur correctif dû à la multiplicité des noeuds n_o du réseau réciproque contribuant à la même tache, il faut prendre en compte le facteur de Lorentz; étant donné les faibles angles de diffraction rencontrés sur les clichés de fibre d'ADN ce facteur est proportionnel à R, distance de la tache de diffraction à l'axe du réseau réciproque (28).

Avec $R = \sqrt{\left(\frac{2 \sin \theta}{\lambda}\right)^2 - \left(\frac{l}{c}\right)^2}$

θ : angle de Bragg ; l : ordre de la strate ;

C : pas cristallographique ; λ : longueur d'onde

Après la correction de la distance, l'intensité expérimentale désignée par F_{obs}^2 s'écrira :

$$|F_{(obs)}|^2 = \frac{S L R}{n_0}$$

Les valeurs ainsi obtenues sont directement comparables à celles résultant du calcul théorique.

D) MODELES CONFORMATIONNELS DES ADN

I. Méthode

Pour calculer les intensités théoriques diffractées par l'ADN en fibre orientée, il est nécessaire de connaître les coordonnées de tous les atomes constitutifs du motif répétitif, à savoir, le nucléotide. Pour ce faire, un

programme de calcul a été réalisé. Il est basé sur la méthode matricielle d'Eyring (34) et dérive de la méthode de construction mise au point par J. Hermans et D. Ferro (35) pour la construction de chaînes protéiques.

Cette méthode de calcul utilise un modèle "d'arbre" qui assimile une chaîne de polymères à un arbre (le squelette de la chaîne principale constituant le tronc et les chaînes latérales les branches). Par cette méthode, on peut donc construire une chaîne macromoléculaire quelconque à partir des données géométriques caractérisant les unités qui composent cette chaîne. Ces données géométriques sont les longueurs de liaisons, les angles de valence et les angles dièdres autour des liaisons entre atomes.

II. Les nucléotides

Dans le cas de l'ADN, l'unité constitutive du "tronc", est formée, dans le sens 5' 3', par trois carbones du désoxyribose C5'- C4'- C3' suivis par O3'- P- O5' du groupe phosphate. Sur C1' se greffe également C2' et sur le phosphore les deux oxygènes O1 et O2. La branche greffée sur C4' est constituée de O4'C1' suivi d'une base. Les quatre bases différentes impliquent que l'on distingue quatre nucléotides différents.

Les longueurs des liaisons entre atomes de même que les angles de valence sont pris comme des constantes. Les valeurs de ces grandeurs sont fixées en prenant les données moyennes obtenues avec différents cristaux de nucléotides et d'oligonucléotides (36-39). Ces grandeurs sont donc astreintes à rester dans des intervalles de valeurs trouvées par des études sur des cristaux de petites molécules.

Pour le désoxyribose, ces grandeurs ont été plus particulièrement fixées à partir des histogrammes publiés par S. Arnott (40). De même, la géométrie des quatre bases proposée par S. Arnott (41) a été utilisée sans modification *(figure n° 12)*

Figure n°12

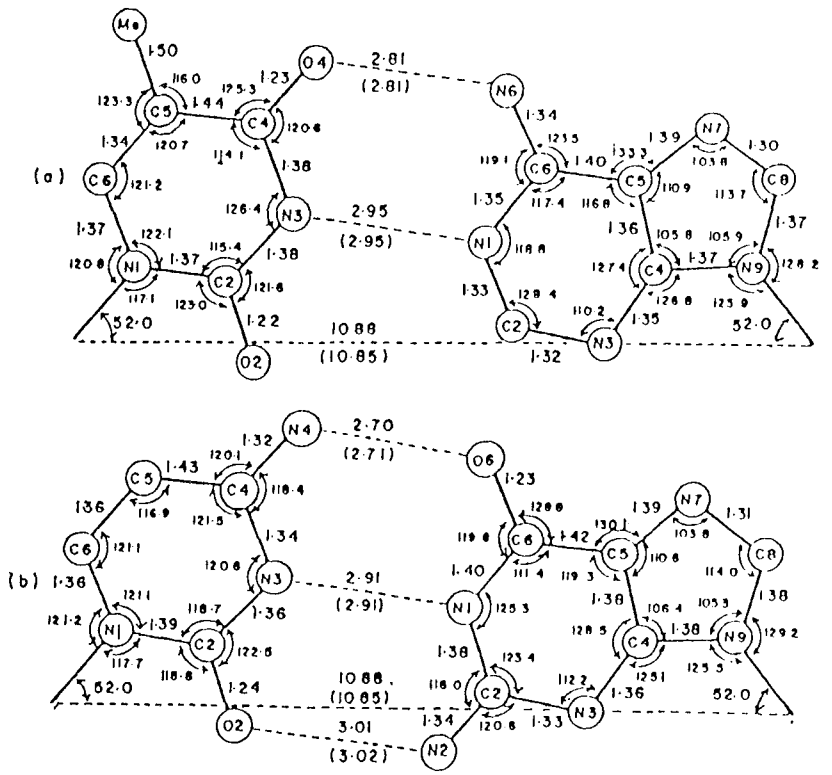

Longueurs de liaisons (Å) et angles de torsion (°) dans l'association Watson Crick des bases.
a) Thymine avec Adénine ; b) Cytosine avec Guanine

Pour réaliser une conformation du nucléotide il reste en fait à fixer les valeurs des six angles dièdres de la chaîne principale ; ces angles sont donc des variables définies selon la nomenclature :

$$\overset{\alpha}{-}\ P\ -\ O1\ \overset{\beta}{-}\ C5\ \overset{\gamma}{-}\ C4\ \overset{\delta}{-}\ C3\ \overset{\varepsilon}{-}\ O3\ \overset{\zeta}{-}\ P\ -$$

un septième angle dièdre variable χ permet de définir la position du plan de la base par rapport au désoxyribose.

III. Les structures hélicoïdales

La conformation hélicoïdale est construite par la succession de nucléotides. Chaque forme particulière d'hélice dépend essentiellement du choix des six angles dièdres qui doivent être les mêmes pour tous les nucléotides.

Le programme de calcul donne les coordonnées cartésiennes de chaque atome de l'hélice dans un repère arbitraire et les transforme en coordonnées cylindriques avec l'axe z selon l'axe de l'hélice et l'axe radial qui passe par le premier atome de la chaîne.

De plus, en utilisant les relations de Sujeta et Miyazawa (42) on peut exprimer, à partir des six angles dièdres variables, les paramètres d'hélice p et θ du nucléotide (p étant la projection axiale du déplacement entre atomes homologues et θ l'angle de rotation entre ces atomes). Cet angle s'évalue par le rapport :

$\theta° = 360° \; p/P$ (P : pas de l'hélice))

IV. Ajustement des paramètres d'hélice du modèle aux données expérimentales.

Etant donné le nombre important de variables qui définissent la conformation du nucléotide, il est nécessaire, au départ du processus de modélisation, d'avoir un ordre de grandeur pour celles-ci. Pour cela, on construit un modèle physique de type Kendrew et on évalue les 6 angles dièdres qui imposent les paramètres d'hélice p et θ ainsi que le sens

de rotation sur l'hélice. En fait, on réduit à 5 le nombre de variables en définissant le type de conformation du désoxyribose (type C2' endo, C3' endo...(43)) et en fixant la valeur de l'angle correspondant. Un programme de calcul permet de modifier progressivement les 5 angles variables afin d'obtenir les paramètres d'hélice expérimentaux θ et p. En pratique, le fait d'ajouter d'autres contraintes (distance à l'axe du C1' pour permettre l'appariement des bases complémentaires, fixation de l'orientation du groupe phosphate...) rend le processus assez long et nécessite même des modifications des angles de valence et des distances inter-atomiques.

V. Appariement des bases des chaînes antiparallèles : axe - dyade

Le calcul des coordonnées cylindriques d'un nucléotide permet de réaliser une projection du modèle sur un plan perpendiculaire à l'axe de l'hélice afin de vérifier l'appariement des bases complémentaires. En effet, c'est surtout la projection de la liaison C1'N9 pour une purine (ou C1'N1 pour une pyrimidine) qui conditionne la position de la base. Un schéma de l'appariement correct des bases complémentaires est alors positionné sur la liaison C1'N9 obtenue. On vérifie que la médiatrice de N9 N1 située dans le plan des deux bases passe par la projection de l'axe de l'hélice. Si ce n'est pas le cas, des ajustements sur les angles dièdres sont réalisés pour vérifier cette contrainte tout en maintenant les valeurs de p et θ.

Par cette méthode d'approximations progressives, les bases sont correctement appariées avec des longueurs de liaisons hydrogéne conformes à celles mesurées sur des oligonucléotides (44). De plus, l'ajustement de l'angle dièdre initialement déterminé en imposant au plan des bases de rester au voisinage de la perpendiculaire à l'axe de l'hélice, permet d'établir le **"tilt"** ou le **"propeller twist"** entre bases appariées *(figure n°13)*.

Figure n°13

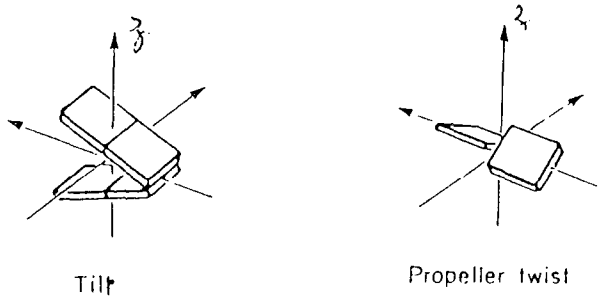

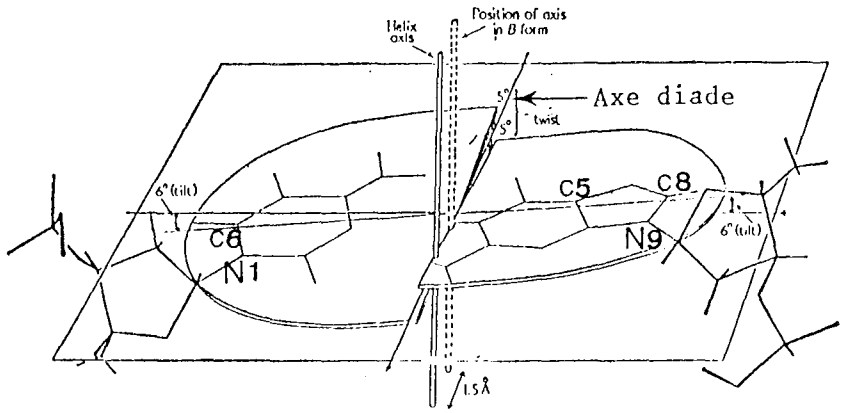

Conventions pour les angles de "tilt" et de "twist".

Dans ces conditions, on remarque que, c'est en fait la médiatrice de la droite passant par C6 (pyrimidine) et C5 - C8 (purine) et qui est perpendiculaire à l'axe de l'hélice qui devient axe de symétrie des deux chaînes antiparallèles. Cet axe appelé axe "dyade" va être pris comme origine des angles et des côtes z des atomes des nucléotides. Ainsi, chaque atome

de coordonnée (R , Φ , z) dans une chaîne aura son homologue de coordonnées (R , - Φ , - z) sur la chaîne complémentaire antiparallèle.

VI. Vérification de la stéréochimie du modèle moléculaire

La construction de plusieurs nucléotides avec des bases différentes est nécessaire pour contrôler la stéréochimie du modèle en double hélice. En effet, il faut vérifier que les distances entre atomes à l'intérieur d'un nucléotide et entre nucléotides, particulièrement au niveau de l'empilement des bases, sont acceptables. Une première approche est obtenue en étudiant le modèle de type Kendrew construit avec les angles dièdres résultant du calcul. Une autre méthode, plus sûre, consiste à utiliser un programme de calcul de l'énergie de van der Waals pour la conformation envisagée avec une mise en évidence des distances inter-atomiques défectueuses. Dans ce cas, tous les atomes d'hydrogène sont placés dans la structure étudiée et les encombrements des atomes sont définis par leur rayon de van der Waals. Si certaines distances inter-atomiques entraînent des empêchements stériques, un nouvel ajustement des paramètres variables est entrepris.

E) INTENSITES DIFFRACTEES CALCULEES A PARTIR DU MODELE

I. Evaluation des facteurs atomiques

Le calcul du facteur de structure d'une molécule en hélice nécessite de connaître les facteurs atomiques des atomes présents dans la structure et au voisinage de cette dernière. Or, dans le cas de fibre d'ADN, chaque double hélice d'ADN est

entourée d'un certain nombre de molécules d'eau mobiles qui ne forment pas une structure périodique et dont les coordonnées cylindriques ne peuvent être déterminées. Par conséquent, l'effet dû à ce "solvant" (en fait eau et cation alcalin présents) ne peut pas être directement calculé. L'approximation introduite (Wrinch 1950 (45)) consiste à considérer le solvant comme un gaz électronique uniforme qui remplit l'espace entre les molécules d'ADN. Le facteur de structure peut être calculé en utilisant le principe de Babinet's (Langridge et al, 1960) (28). Le facteur de structure de l'ADN immergé dans l'eau est égal au facteur de structure de celui-ci diminué d'une grandeur caractéristique de la densité électronique moyenne du solvant. Mais plus simplement, le terme de correction peut être incorporé au facteur atomique f_j (R) de chaque atome (28). Finalement, l'expression du facteur atomique corrigé f_j (R) utilisé dans ce travail est celle proposée par Fraser 1978 (46) et qui résulte d'une amélioration de l'expression donnée par Arnott 1973 (41) :

$$f'_j(R) = f_j(R) - V_j \rho_{sol} \exp\left(-\pi V_j^{\frac{2}{3}} R^2\right)$$

avec R coordonnée radiale dans l'espace réciproque, V_j volume de déplacement de l'atome (Langride) ; ρ_{sol} densité électronique de l'eau prise à 0,334 électron par A^3.

Les facteurs atomiques des atomes de l'ADN immergés dans le solvant, multipliés par le facteur de température

$$\exp(- B^2_{,} R^2 / 4)$$

avec B étant égal à 4 A^2 (28) sont donnés dans le tableau I .

On remarque que l'on doit distinguer, pour les oxygènes, les carbones et les azotes, différents facteurs atomiques qui tiennent compte de l'environnement local et par conséquent, du caractère plus ou moins hydrophobe des atomes.

Atome \ RA^{-1}	0.	0.05	0.10	0.15	0.20	0.25	0.30	0.35	0.40
P	7.20	7.49	8.46	9.63	10.44	10.93	11.04	10.87	10.40
- O -	4.95	5.01	5.20	5.36	5.73	5.94	6.18	6.30	6.29
O -	6.33	6.33	6.34	6.35	6.36	6.35	6.34	6.32	6.25
- O - *	5.63	5.65	5.75	5.78	6.01	6.09	6.23	6.29	5.96
C	0.51	0.68	1.28	2.07	2.80	3.50	3.82	3.93	4.03
C + H *	0.49	0.75	1.52	2.60	3.46	4.21	4.57	4.74	4.64
C + H	0	0.11	1.06	2.33	3.35	4.20	4.60	4.77	4.66
C + 2H *	0	0.13	1.34	2.77	4.06	4.86	5.37	5.46	5.27
C + 3H	0	0	0.81	2.96	4.74	5.91	6.22	6.19	5.88
N	6.17	6.16	6.16	5.93	5.77	5.58	5.42	5.18	4.76
N + 2 H	4.83	4.91	5.21	5.56	5.95	6.22	6.38	6.42	6.25
H	0	0	0	0	0	0	0	0	0

* (désoxyribose)

TABLEAU N°1

Facteurs atomiques corrigés des différents types d'atomes formant un nucléotide.

II. Choix de l'unité répétitive

Pour un ADN de séquence quelconque mais dont le pourcentage en paires A-T (G-C) est connu, on peut calculer le facteur de structure d'un nucléotide moyen comprenant le groupe désoxyribose phosphate et une base moyenne pondérée suivant le pourcentage de A-T présents. Par contre, dans le cas de polynucléotides alternés, le facteur de structure est calculé en prenant comme unité répétitive deux nucléotides qui se suivent sur une même chaîne (chaque nucléotide étant associé à une base différente). Dans ce cas, l'axe dyade donnant la position de la chaîne antiparallèle doit être placé entre ces deux nucléotides. Un autre cas à envisager pour les

polynucléotides est celui ou chaque chaîne présente la succession d'une même base ; il est alors nécessaire de considérer comme unité élémentaire le bloc des deux nucléotides appariés, l'axe dyade restant interne au bloc. La double hélice sera réalisée par la succession de ces blocs avec les paramètres θ et p précédemment définis. Cette méthode de choix de l'unité répétitive, constituée d'un ou de plusieurs nucléotides, peut donc s'adapter à des structures complexes du type "side by side" par exemple.

III. Intensité calculée

La relation donnant l'intensité calculée sur une strate :

$$I = F^2_{\psi} (R, \frac{\ell}{c}) = \sum_n (A_n^2 + B_n^2)$$

fait donc appel aux coordonnées cylindriques de tous les atomes de l'unité répétitive de la structure affectés d'un facteur atomique modifié par l'effet du solvant. Suivant le type d'unité répétitive choisi (nucléotide d'une seule chaîne ou bloc de deux nucléotides de bases appariés) on a un axe de symétrie entre chaîne ou non, ce qui dans le premier cas simplifie le calcul de I car on peut alors annuler les B_n^2.

De plus, étant donné la résolution des clichés qui ne dépassent pas 3 A, il est superflu de calculer les fonctions de Bessel d'ordre supérieur à 15, ce qui limite souvent à deux fonctions de Bessel la somme sur n dans le calcul d'intensité. En effet, sur une strate la différence entre la fonction de Bessel est u (nombre d'unités répétitives pour la période C), ainsi avec l'ADN en forme B, u = 10 et en forme A, u = 11.

F) FACTEUR D'ACCORD

I. Définition

Le facteur d'accord permet d'évaluer la qualité de la structure proposée. Il dépend de la comparaison entre intensités calculées (I) et observées (I_{obs}). Ce facteur s'exprimer par :

$$R = \frac{\Sigma \mid \sqrt{I} - \sqrt{I_{obs}} \mid}{\Sigma \sqrt{I_{obs}}}$$

Pour les ADN en fibre, R varie entre 20 et 30 %, ce qui n'est pas très bon. Ces mauvais pourcentages sont dûs à plusieurs effets : la désorientation des fibres d'ADN et les nombreux défauts dans la taille et l'organisation des cristallites constituant la fibre. A cela, s'ajoute l'imprécision des différentes mesures. En fait, la précision des meilleures mesures ne dépasse pas 10 %. Une autre difficulté provient de la nécessité de choisir un facteur d'échelle pour comparer les intensités expérimentales aux valeurs calculées.

Enfin, le calcul de l'intensité théorique se fait à partir de plusieurs approximations. La première vient du fait que l'on prend les coordonnées atomiques identiques d'un motif élémentaire à l'autre dans la construction de l'hélice, or la cristallographie de nombreux oligonucléotides révèle une grande diversité de conformation entre motifs élémentaires successifs (47). Une deuxième approximation découle de la difficulté de tenir compte du solvant (eau et cation alcalin).

II. Comparaison entre les courbes des intensités théoriques et les valeurs expérimentales

Une approche commode pour tester la qualité du modèle conformationnel envisagé est de comparer les courbes des intensités calculées et expérimentales. Les intensités calculées pour chaque strate *l* sont représentées par des courbes continues en fonction de la distance R à l'axe du réseau réciproque. Les intensités expérimentales sont positionnées, avec un facteur d'échelle compatible, aux distances R déduites du cliché RX. L'analyse des désaccords sur chaque strate permet, dans certains cas, des corrections sur la conformation proposée. Par exemple, en modifiant le "propeller twist" des bases de la double hélice on change les intensités calculées sur les strates supérieures. Un autre moyen de modifier la distribution des intensités calculées sur toutes les strates est de déplacer l'axe dyade . Il en résulte une modification du "tilt" des bases mais la chaîne sucre phosphate n'est pas perturbée. Ce procédé permet de modifier la conformation étudiée, donc d'améliorer progressivement le facteur d'accord. L'examen des courbes d'intensité calculées permet également d'apprécier comment les intensités du cliché peuvent être modifiées lorsque, pour un type de conformation, les paramètres du réseau cristallin varient en raison des changements de l'humidité relative de la fibre.

G) PREPARATION DES FIBRES

I. Mise en solution de l'ADN

Les ADN et polynucléotides, de poids moléculaire élevé, utilisés pour obtenir des fibres sont achetés (Pharmacia, Sigma...). Ils se présentent sous forme lyophilisée avec une

forte concentration en sel de sodium. Pour obtenir des conditions de préparation de fibre reproductibles, une mise en solution est faite systématiquement ; cela permet de fixer par dialyse un pourcentage précis de sel alcalin par nucléotide.

La mise en solution de l'ADN se fait dans l'eau distillée déionisée à pH 7. Après au moins deux jours à 4°C, la densité optique de la solution est mesurée au spectrophotomètre à 260 nm. On en déduit la concentration en ADN et par le rapport des absorptions à 290 nm et 260 nm, on contrôle le bon appariement des bases en doubles hélices. La connaissance de la concentration permet de fixer la teneur en sel alcalin de la dernière dialyse. C'est également par dialyse que l'on peut remplacer le sel de sodium initialement présent par un autre sel tel le lithium. On obtient en mesurant la densité optique à la fin de la dialyse la concentration exacte de la solution en cation par nucléotide.

II. Obtention du gel d'ADN

Pour passer de l'ADN en solution à la fibre, il est nécessaire de concentrer la solution sans détruire la structure en double hélice et en évitant de couper les très longues chaînes de nucléotides. Le moyen le plus utilisé est la centrifugation de la solution à 40 000 t/mn pendant plusieurs heures. L'ADN est alors rassemblé dans le culot de centrifugation. Séparé du surnageant, il forme un gel dont la viscosité peut être diminuée par l'addition de quelques gouttes d'eau distillée. Ce procédé permet de récupérer tout l'ADN mis en solution même avec de très faibles concentrations en cation alcalin.

Le gel peut aussi être obtenu par précipitation de l'ADN par l'alcool éthylique. Dans ce cas, l'ADN récupéré avec une tige de verre doit subir des lavages successifs à l'acétone avant d'être séché puis ré-humidifié. Il est probable que dans ce cas la teneur finale en sel n'est plus celle de l'ADN précipité. Néanmoins, ce procédé est utile pour les fortes concentrations en sel.

Enfin, un dernier mode de préparation peut être utilisé dans la mesure où la concentration en sel de sodium reste très élevée. Il consiste à prendre une masse connue d'ADN lyophilisé et à la dissoudre directement dans un petit volume d'eau distillée.

III. Etirement et orientation des fibres

Pour obtenir des fibres orientées d'ADN, on opère par étirement du gel tout en augmentant sa viscosité par évaporation de l'eau. Pour ce faire, on dépose goutte à goutte le gel entre deux fines baguettes de verre. Un porte échantillon permet de maintenir fixe une des baguettes et de laisser l'autre mobile. L'ensemble est placé dans une cellule permettant l'observation du gel au microscope polarisant et le maintient d'une humidité relative élevée autour de la fibre ainsi que le déplacement, à l'aide d'une vis micrométrique, de la baguette de verre mobile (48). En plaçant la cellule à 4°C, l'évaporation de l'eau est très lente ; cela permet de procéder à plusieurs étirements successifs. L'étirement est arrêté quand la fibre a tendance à perdre son allure cylindrique. La fibre est ensuite placée à l'humidité

relative ambiante en maintenant sa longueur maximum (on fixe ses extrémités)..

Après un test aux rayons X, il est possible d'améliorer l'orientation de la fibre en exerçant une légère tension mécanique à l'une de ses extrémités tout en augmentant l'humidité relative environnante jusqu'à 93-94 % avant de revenir à l'humidité ambiante .

IV. Contrôle de la concentration en NaCl dans la fibre

Une propriété remarquable des ADN est le fait que leur conformation peut changer lorsque la teneur en eau de la fibre varie. Or ces changements dépendent du type de cation alcalin présent mais également de son pourcentage dans la fibre. Avec le sel de sodium par exemple, le pourcentage relatif du sodium (Na^+) par nucléotide (ou par phosphore) est parfaitement défini en solution. Par contre, pour le passage à l'état de fibre, un contrôle est nécessaire. Ce contrôle a été réalisé par deux techniques différentes pour une série de fibres d'ADN qui présentent les transitions B-C ou B-A. La transition B-C étant obtenue à partir d'une solution à 0,05 NA^+ par phosphore et la transition B-A pour des solutions contenant au moins 0,5 Na^+ par phosphore.

Première technique : la microanalyse par spectre de flamme a été utilisée pour trois types de fibre provenant de trois solutions d'ADN à des concentrations différentes en sodium ; les résultats sont rassemblés dans le *tableau n°II*.
(mesures effectuées au Service Central d'Analyses du CNRS à VERNAISON)

TABLEAU N° II

Solution Na^+/P	Dosage fibre Na^+/p
0,05	0,62
1	1,04
5	1,45

Comparaison des teneurs en sodium par phosphore pour des solutions d'ADN et pour les fibres préparées à partir de ces solutions. (méthode par spectrophotométrie de flamme)

On remarque, avec la solution à très faible taux de sodium, un désaccord d'un ordre de grandeur de 10 avec le dosage réalisé sur la fibre. L'ADN étant un polyélectrolyte on constate bien qu'il y a un minimum de sodium comme cation compensateur qui fait partie de la structure et qui ne peut être éliminé par dialyse. Inversement une grande concentration de sodium en solution n'augmente pas le taux fixé une fois la saturation atteinte. Dans cette approche, on obtient la quantité totale de sodium présent dans la fibre mais pas sa répartition. Pour tenter d'analyser cette répartition, une deuxième technique a été utilisée, à savoir la microsonde électronique.

Pour faire cette analyse, des fibres provenant des préparations d'ADN précédentes sont emprisonnées dans une résine et avec un microtome on découpe des lamelles perpendiculaires à l'axe de la fibre.

En sondant à différents endroits de ces lamelles, le rapport entre sodium et phosphore peut être déterminé. De plus, cette technique permet de visualiser la section complète de la fibre avec sa densité soit de phosphore, soit de Na^+

mais également de Cl^-. Le *tableau III* donne les résultats obtenus par microsonde électronique.

TABLEAU N° III

Solution Na^+/P	Microsonde fibre Na^+/p
0,05	0,27
0,5	0,47
1	0,86
5	0,7 - 0,9

Comparaison des teneurs en sodium par phosphore pour les solutions d'ADN et pour les fibres préparées à partir de ces solutions. (méthode de la microsonde électronique)

A basses concentrations en sodium, on remarque encore à l'intérieur de la fibre un rapport sodium phosphore compatible avec la donnée en solution.

Pour les hautes concentrations de sodium, on constate également une saturation à 0,9 Na^+ par phosphore dans la fibre, ce qui est en accord avec les études théoriques de condensation des contre-ions sur les ADN de petite longueur (49). De plus, pour la plus haute concentration de sodium, l'image de la répartition du sodium dans la fibre montre l'existence d'inclusions de forte densité et une élévation de la densité en périphérie de la fibre. Ce fait explique les écarts d'évaluation avec la méthode de spectrométrie de flamme qui, elle, donne un rapport moyen.

H) DISPOSITIF EXPERIMENTAL

I. Sources RX

Les fibres biologiques étant constituées en majeure partie d'atomes qui diffractent peu les rayons X, la source de ce

rayonnement doit être de la plus grande brillance possible pour éviter d'avoir des temps de pose trop longs.

L'utilisation la plus commode consiste à employer des tubes scellés Philips à foyer fin (0,5 x 8 mm²) de grande brillance. Le rayonnement du tube à anticathode de cuivre est filtré afin d'obtenir la longueur d'onde moyenne du K_α=1,542 A Exceptionnellement, avec des fibres très bien orientées le rayonnement K_α du cuivre a été obtenu à partir d'un tube ouvert à micro foyer (40 μ de diamètre) mais la brillance relativement faible nécessite des temps de pose très importants. Enfin, pour certaines expériences particulières, l'accès au rayonnement synchrotron de LURE a permis d'utiliser une source monochromatique dont la grande brillance réduit les temps de pose d'un ordre de grandeur de 10 par rapport aux temps habituels. Ces dernières expériences ont ainsi permis de mettre en évidence certains artefacts dûs à un rayonnement qui n'est pas parfaitement monochromatique .

II. Chambres RX planes

Les contraintes imposées par la diffraction des fibres constituées de molécules à structure hélicoïdale rendent plus commode l'utilisation de la chambre plane. En effet, la fibre doit être positionnée soit perpendiculairement au faisceau, soit inclinée d'un angle connu. De plus, du fait des modifications de l'humidité relative entourant la fibre, cette dernière se déforme et doit donc être ramenée facilement dans une position correcte dans le faisceau R.X..

Avec la chambre plane, la fibre est placée directement à la sortie du collimateur qui délimite un angle solide très

petit sous lequel on voit la source. Il est constitué d'ouvertures circulaires de diamètre 0,1 à 0,2 mm, espacées de 2 à 8 cm. Pratiquement, pour toutes les chambres planes construites pour différents types d'expériences, un axe, commandé de l'extérieur de la chambre, permet, par des rotations et translations, de positionner correctement la fibre dans le faisceau RX. Le film plan placé perpendiculairement au faisceau direct se trouve à une distance qui peut être fixée entre 15 mm à 70 mm selon le type de la chambre. La distance précise fibre-film est déduite d'un étalonnage réalisé en déposant sur la fibre une poudre de quartz ou de calcite.

Une paroi plane transparente supportant le puits d'arrêt du faisceau direct ferme la chambre. Le film est appliqué contre cette paroi mais à l'extérieur de la chambre. Cette paroi transparente permet d'isoler le volume intérieur de la chambre RX, elle autorise aussi l'observation de la fibre et donc la mesure de ses dimensions à l'aide d'un microscope binoculaire.

Toutes les chambres à RX sont placées sur un banc d'optique dont les réglages permettent de positionner l'axe du collimateur de la chambre dans le faisceau RX. Ce banc permet également un déplacement commode du microscope binoculaire et du porte film.

Un dispositif a été adapté à certaines chambres planes pour permettre d'appliquer une tension mécanique variable à la fibre. Des poids, accessibles dans un "container" extérieur fixé à la chambre, exercent une tension à l'extrémité libre de la fibre par l'intermédiaire d'un fil. Enfin, un dispositif,

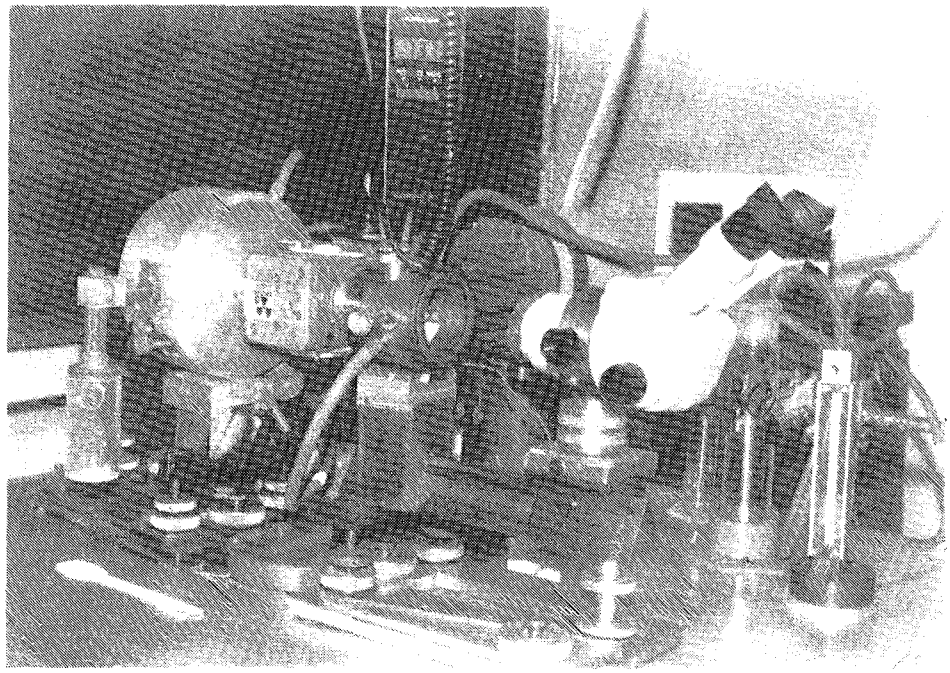

Photo n° 1 : Disposition des chambres planes devant la source RX

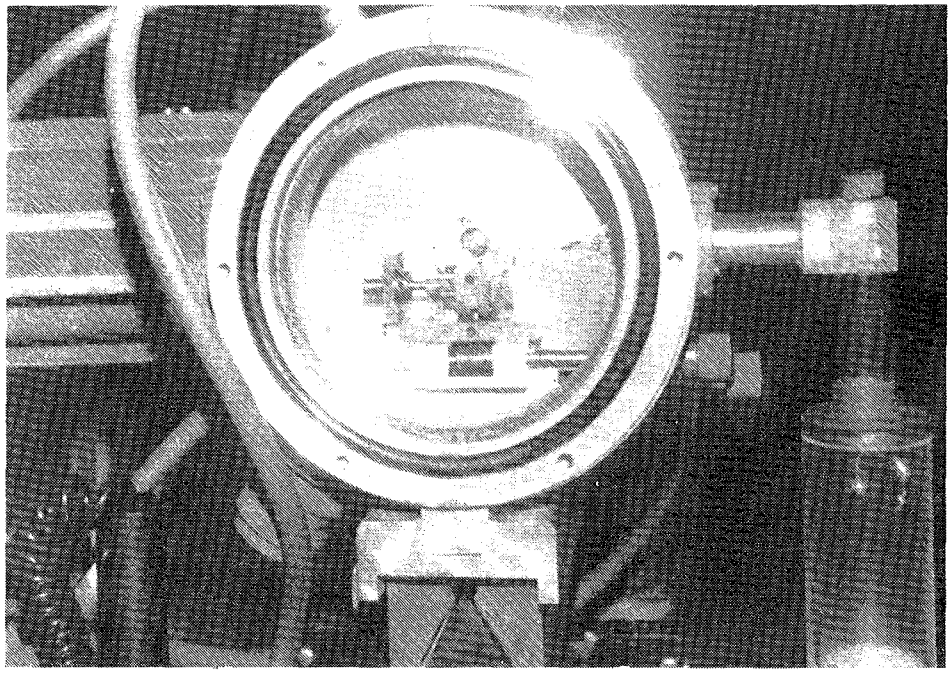

Photo n° 2 : Chambre plane avec ses dispositifs d'orientation de la fibre dans le faisceau RX et d'application d'une tension mécanique

toujours commandé de l'extérieur de la chambre, permet d'orienter la fibre dans le faisceau RX.

III. Fixation et contrôle de l'humidité relative

L'humidité relative entourant les fibres d'ADN est un paramètre important qui conditionne la conformation de ces molécules. Pour réaliser l'humidité relative désirée dans les chambres RX, on fait circuler un courant d'hydrogène chargé d'une vapeur saturante créée par des solutions salines (50). Par ce moyen, des changements progressifs mais également brutaux d'humidité relative, peuvent être obtenus. La stabilité d'une humidité donnée est assurée en ajustant avec un débitmètre le flux d'hydrogène mais aussi en maintenant l'ensemble du dispositif à température constante. La mesure de l'humidité relative est obtenue en plaçant la sonde d'un hygromètre à l'intérieur de la chambre RX.

IV. Mesures des dimensions des fibres

Les fibres d'ADN étirées se présentent sous la forme de cylindre de 0,1 à 0,2 mm de diamètre et de 1 à plusieurs millimètres de longueur et ont, en fait, des dimensions qui dépendent de l'humidité environnante. Pour mesurer ces dimensions, l'emploi d'un microscope binoculaire à zoom variable et possédant un micromètre oculaire s'est révélé le plus commode. De plus, en choisissant un objectif qui donne une distance d'approche supérieure à 30 mm, les mesures sont réalisées sur la fibre à l'intérieur de la chambre RX, sans perturber l'humidité qui l'environne.

CHAPITRE II : COMPARAISON ENTRE LES INTENSITES EXPERIMENTALES ET CALCULEES A PARTIR DE QUELQUES MODELES DE LA FORME B DE L'ADN

A) INTRODUCTION

Les ADN naturels étirés en fibre présentent tous, à haute humidité relative, une conformation de type B (51). Par contre, ces ADN, en présence d'une même concentration en sel de sodium ne présentent pas tous la transition B-A lorsque l'humidité relative de la fibre est diminuée. Ce changement de conformation est d'autant plus empêché que l'ADN est riche en paires de bases A-T (52).

Etant donné ce fait expérimental, il était intéressant de contrôler si sur les clichés RX de fibre de ces ADN en forme B (donc à haute humidité relative), le pourcentage en paires de bases A-T ou G-C a un effet décelable comme cela a du reste été suggéré (53). Cependant les clichés de fibre de ces ADN en forme B présentent peu de taches de diffraction bien définies. Aussi, dans la première publication présentée, les intensités ont été calculées à partir du meilleur modèle en forme B alors proposé (41) mais en modifiant le calcul afin de tenir compte avec précision du pourcentage en bases A-T et G-C. Les quelques intensités expérimentales obtenues avec des fibres d'ADN à taux de A-T très différents ont pu alors être comparées aux intensités calculées pour ces mêmes ADN.

Un autre problème que posent les résultats de la diffraction des fibres d'ADN provient du faible taux d'accord généralement obtenu entre intensités expérimentales et intensités calculées. De ce fait il peut résulter différentes propositions de modèles moléculaires. Cela s'est effectivement présenté pour l'ADN en forme B avec la proposition d'une

conformation dite "side by side" où chaque chaîne est formée alternativement de portions d'hélice droite puis gauche (54). Dans deux publications présentées dans ce chapitre, ce modèle a été étudié. Son intérêt réside surtout dans l'organisation entre hélice droite et gauche avec la contrainte de régularité dans l'espacement des bases. En effet, à l'époque où ce travail a été réalisé,la cristallographie des oligonucléotides avait révélé l'existence d'hélices gauches d'ADN (13) et bien sûr d'hélices droites (55). Les intensités théoriques des modèles proposés ont pu être calculées avec la méthode de calcul de la diffraction par des hélices mais l'unité élémentaire répétitive est dans ce cas, formée d'un bloc de plusieurs nucléotides.

Enfin, dans la dernière publication présentée, ce sont des modèles en hélice gauche, toujours pour l'ADN en forme B, dont on compare les intensités calculées aux intensités expérimentales. Mais pour restreindre le domaine des conformations stéréo-chimiquement possibles, des contraintes sur l'orientation du groupe phosphate sont imposées. Ces contraintes proviennent des résultats obtenus par des mesures de dichroïsme linéaire infrarouge appliqué à des films d'ADN orientés (15,56).

B) ETUDE PAR DIFFRACTION RX DE TROIS ADN DONT LES COMPOSITIONS EN BASES SONT DIFFERENTES

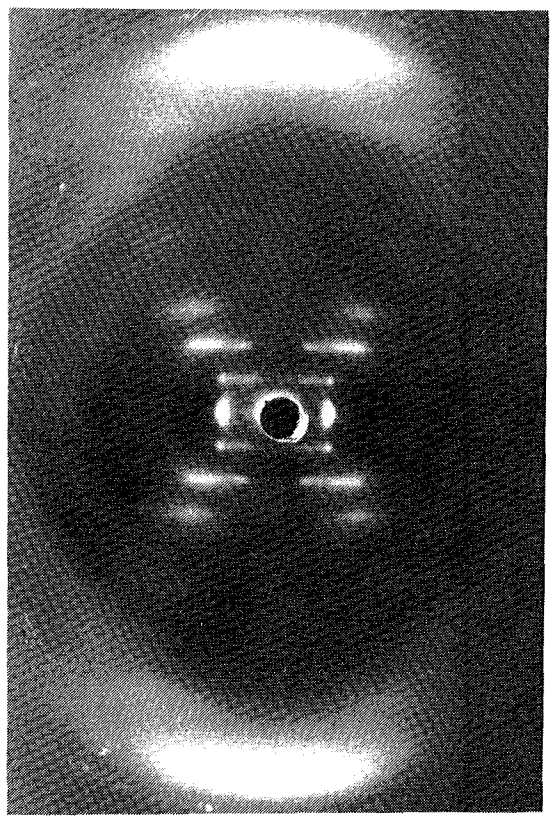

Photo N° 3 : Forme B de l'ADN avec sel de sodium à 92 % d'humidité relative.

J. Mol. Biol. (1975) **99**, 27–36

X-ray Diffraction Study of Three DNA Fibres with Different Base Compositions

S. Premilat and G. Albiser

Université de Nancy I
Laboratoire de Biophysique
Centre de 1er Cycle
Case Officielle 140
54037 Nancy Cedex, France

(Received 26 May 1975)

An X-ray diffraction study on three DNAs with guanine + cytosine contents of 26%, 42% and 72%, respectively has been made in order to establish a possible correlation between base composition and the conformations of double helices.

This work shows that the helical parameters in the *A* and *B* forms in the presence of sodium and lithium salts are independent of the base composition. The experimental intensities are compared to calculated values, taking into account the variations of the parameter *a* in the hexagonal lattice of the *B* form. The three DNAs show no noticeable difference. Theoretical calculations with a ratio of (A + T)/(C + G) varying from 4 to 0·25 confirm that the base composition has a negligible effect on the diffracted intensities, provided the helical parameters remain constant. A complementary calculation made with a tilt of the bases shows that only the intensities corresponding to the higher layers are affected. One may conclude that the conformation of the sugar–phosphate chain is not affected by the base composition, and that the proportion of (G + C) bases cannot be detected by X-ray analysis.

1. Introduction

X-ray diffraction studies on oriented DNA fibres have shown the conformational variations induced by modification of the external conditions (humidity, ionic strength, different alkaline salts). These conditions induce the fundamental and well-determined *B* and *A* forms of DNA double helices. The *B* form appears at high humidity in the presence of different salts; the crystallinity of the fibres is best with lithium salts (Langridge *et al.*, 1960). The *A* form (Fuller *et al.*, 1965) exists when the relative humidity is lower than 75% and a sodium salt is present. DNA in the *A* form has also been observed for calf thymus DNA in the presence of potassium and rubidium salts. With lithium salt, the *A* form of DNA has not been obtained but when the humidity is near 40% a *C* form appears, and this has been described by Marvin *et al.* (1961).

DNA in the *C* form has also been obtained in the presence of sodium salt (Azoulay & Bram, 1973). The influence of humidity on the X-ray patterns has been studied by Franklin & Gosling (1953) and the experimental conditions are known for the *B* to *A* transition of DNA in the presence of sodium salt (Cooper & Hamilton, 1966). The similarity of the X-ray patterns corresponding to a large variety of DNA

species (Hamilton *et al.*, 1958) provided the idea that the DNA conformations do not depend on the base composition. Nevertheless, many studies have been undertaken in order to determine the DNA structure as a function of base composition. For a given sodium salt concentration, the *B* to *A* transition depends on the comparative proportion of (A + T) to (G + C) (Pilet & Brahms, 1972). A polymorphism of the natural DNA has been noted (Bram & Tougard, 1972); more precisely a variation in the X-ray pattern intensities for the *B* form has been correlated with the DNA base composition (Bram, 1973). In this paper we present a more quantitative approach to the problem. The helical parameters of three DNAs very different in base composition are determined, and the experimental diffracted intensities are compared to calculated values using models that include a tilt of the bases and variation of their relative proportions.

2. Materials and Methods

The three DNA molecules studied are: *Spiroplasma citri* DNA obtained from orange trees with the disease (Saglio *et al.*, 1971); this molecule contains 26% (G + C). Calf thymus DNA is the second molecule in our study; it contains 42% G·C base-pairs. The last DNA, extracted from *Micrococcus lysodeikticus*, contains 72% (G + C) and was prepared only with sodium salt.

The oriented DNA fibres were made using the method of Langridge *et al.* (1960) or that of Davies & Baldwin (1963), starting with a few mg of dry DNA. The X-ray photographs were obtained with a flat camera. The specimen-to-film distance was approx. 15 mm and was determined precisely for each fibre lightly dusted with calcite or quartz powder. The relative humidity in the camera was kept constant by passing hydrogen through saturated salt solutions. The photographs obtained from nickel-filtered CuKα radiation (1·542 Å) were enlarged on plastic paper for measurement of the parameters. The values of the diffracted intensities were obtained with a Zeiss microdensitometer. We used the multiple film technique with monolayer films; the ratio of the intensities of one film to the following one is of the order of 1·5. The experimental value of the intensity corresponding to a spot in the X-ray pattern defined by the indices (h,k,l) was calculated according to the following expression (Langridge *et al.*, 1960): $I_{exp}(khl) = AL\zeta/S$, where A is the area measured with a planimeter under the trace densitometered radially across the spot (h,k,l). This value is corrected, taking into account the distances between the diffracting volume and the spots on the flat film. L is the length of the spot-arc and ζ the radial co-ordinate of the (h,k,l) point in reciprocal space. S is the number of points from reciprocal space contributing to the intensity of the spot. The intensities diffracted by a single double-helix in the lattice are determined from the experimental intensities (Langridge *et al.*, 1960), and they are compared with the calculated intensities.

3. Calculation of the Molecular Model

(a) *Building the model*

In order to calculate the Fourier transform of the DNA double-helix structure, it is necessary to determine the cylindrical co-ordinates of the atoms of the molecule. Although one of the two antiparallel helices suffices for calculation of the intensities, it is necessary to build a model of the two complementary helices in order to determine the atomic co-ordinates in a correct reference frame. In such a frame the dyadic symmetry of the system is used so that the co-ordinates (ϕ,Z,R) of a given atom on one helix correspond to the co-ordinates $(-\phi, -Z, R)$ for the homologous atom on the other helix. This is achieved by building with a computer a molecular model of the double helix in one of its precise forms. The geometry of the sugar–phosphate

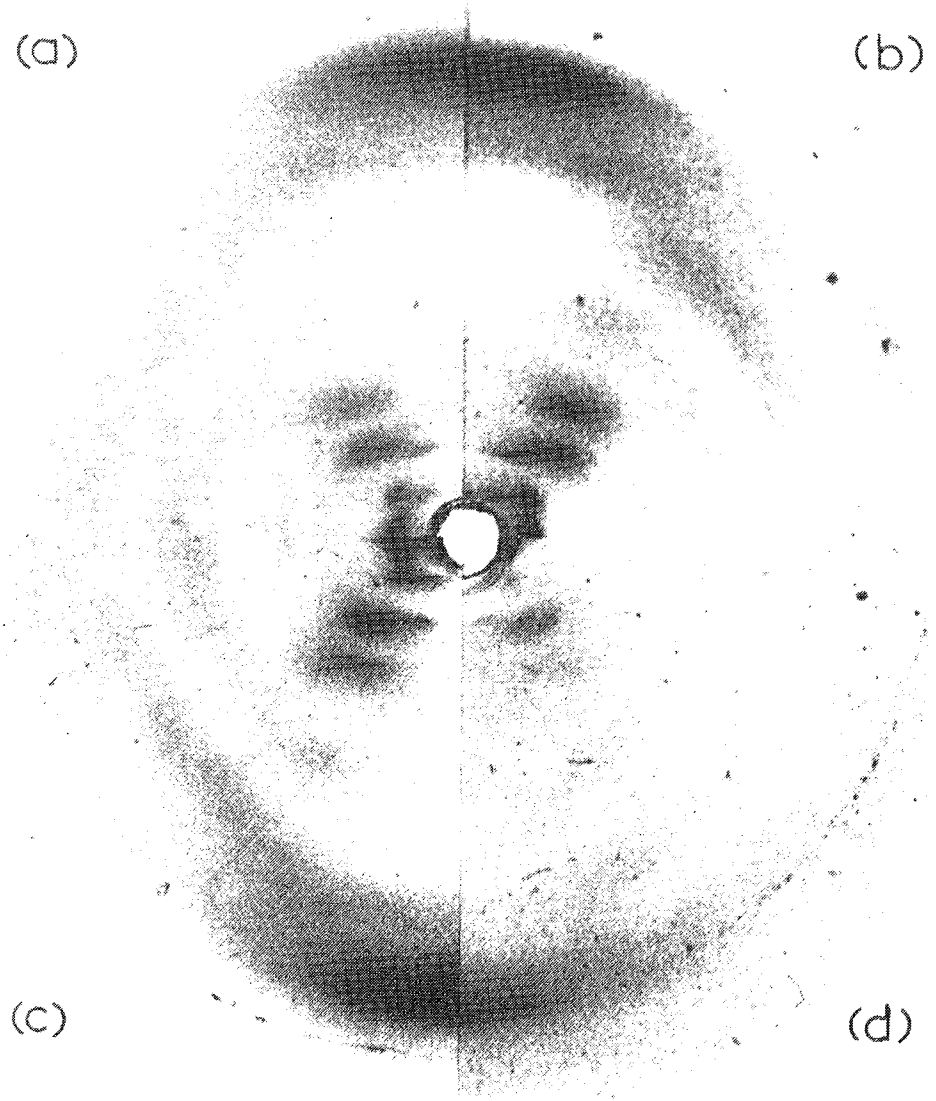

PLATE I. Hexagonal *B* DNA diffraction pattern taken at 92% relative humidity. Sodium salt DNA with (a) 42% (G – C), (b) 26% (G + C) and (d) 72% (G – C). Lithium salt DNA with (c) 42% (G + C).

(Facing p. 50

chain is completely defined by the seven dihedral angles given by Arnott & Hukins (1972). The bond lengths and bond angles are taken from the listing given by Arnott (1970). The calculations relevant to this paper are done on the *B* form, in which the desoxyribose sugar is in the $C_{(3)}$ exo structure. The building programme is based on Eyring's matrices method (Eyring, 1932); it constructs progressively a chain corresponding to a given sequence of bases. The procedure is transposed from that proposed by Hermans & Ferro (1971) for the representation of a protein molecule. The method used allows the conformation to be modified simply and, for instance, makes it easy to introduce a tilt and twist of the bases. When a chain is built in the proper helical form, the complementary, antiparallel one is adjusted to a position that realises the best fit for hydrogen bonds between associated bases. The bases being put at their right levels, the fitting is finished by the rotation of one helix around the common helical axis. Then the cylindrical co-ordinates of the atoms are calculated in a system that uses a dyad axis and the screw-axis; the atom co-ordinates ϕ and Z are related to the dyad axis and the radius R is the distance from the atom to the double-helix axis. Table 1 gives the atomic co-ordinates for the *B* form with no tilt or twist on the bases.

TABLE 1

Cylindrical co-ordinates of the five sets of atoms in B-DNA

Atom	R_j (Å)	$\phi_j^{(0)}$	Z_j (Å)	Atom	R	ϕ	Z
Adenine				Cytosine			
$N_{(9)}$	4·59	−75·88	−0·08	$N_{(1)}$	4·59	−39·85	3·28
$C_{(8)}$	4·85	−92·39	−0·15	$C_{(6)}$	5·04	−55·19	3·20
$N_{(7)}$	3·97	−105·47	−0·14	$C_{(5)}$	4·47	−70·03	3·19
$C_{(5)}$	2·27	−95·25	−0·04	$N_{(4)}$	2·95	−99·75	3·27
$N_{(6)}$	1·97	−154·61	−0·01	$C_{(4)}$	3·07	−74·32	3·27
$C_{(6)}$	1·44	−122·14	0·01	$N_{(3)}$	2·32	−50·02	3·35
$N_{(1)}$	0·70	−42·93	0·10	$O_{(2)}$	3·56	−10·97	3·43
$C_{(2)}$	2·04	−29·33	0·13	$C_{(2)}$	3·40	67·4	0·27
$N_{(3)}$	3·11	−46·15	0·08				
$C_{(4)}$	3·25	−70·50	−0·01				
Guanine				Thymine			
$N_{(9)}$	4·59	−3·83	6·64	$N_{(1)}$	4·59	32·19	9·99
$C_{(8)}$	4·86	−19·65	6·65	$C_{(6)}$	5·02	16·52	9·91
$N_{(7)}$	3·93	−32·09	6·59	Mo	5·61	−10·55	9·82
$C_{(5)}$	2·68	−21·90	6·68	$C_{(5)}$	4·47	1·69	9·91
$O_{(6)}$	1·76	−82·79	6·72	$O_{(4)}$	2·97	−27·34	9·99
$C_{(6)}$	1·37	−38·75	6·74	$C_{(4)}$	3·09	−3·85	9·99
$N_{(1)}$	0·84	33·74	6·82	$N_{(3)}$	2·37	21·20	10·06
$N_{(2)}$	2·90	70·58	6·94	$O_{(2)}$	3·51	60·90	10·15
$C_{(2)}$	2·17	44·72	6·85	$C_{(2)}$	3·37	40·63	10·07
$N_{(3)}$	3·19	26·15	6·80				
$C_{4()}$	3·26	2·34	6·71				
Phosphate				Dooxyribose			
P	8·91	−58·35	1·75	$C_{(1)}$	5·81	−66·24	−0·08
$O_{(1)}$	8·75	−60·55	0·19	$C_{(2)}$	7·04	−72·56	0·69
$O_{(2)}$	10·24	−54·73	1·98	$C_{(3)}$	8·20	−69·05	−0·19
$O_{(3)}$	8·92	−66·42	2·54	$C_{(4)}$	7·58	−69·05	−1·58
$O_{(4)}$	7·73	−51·08	2·00	$C_{(5)}$	7·69	−79·00	−2·30
				$O_{(5)}$	6·23	−64·83	−1·42

(b) *Fourier transform of the double helix*

Owing to the dyad axis in the double helix, the Fourier transform calculation takes a simplified form. One can give the well-known expression (Cochran *et al.*, 1952) for the structure factors:

$$F(l,\psi,\zeta) = \sum_n \sum_j f_j J_n(2\pi R_j \zeta) \exp i \left\{ n\left(\psi - \phi_j + \frac{\pi}{2}\right) + \frac{2\pi l z_j}{c} \right\},$$

where l is the layer line number; R_j, ϕ_j, z_j the cylindrical co-ordinates of the jth atom in the repeating unit and f_j its scattering factor; c is the length of the unit cell along the helix axis; ψ and ζ are, respectively, the angular and the radial co-ordinates of a lattice point in reciprocal space. J_n is the first-order Bessel function of n, and n is defined as the integral solution (positive or negative) of the expression $n/P = (l/c) - (m/p)$, where P is the pitch of the helix, p the axial separation of the repeating units and m any integer. For the DNA in the B form with a hexagonal lattice, one has $P = 34$ Å, $p = 3{\cdot}4$ Å, $c = 34$ Å and so $n = \ell - 10\,m$. For the calculations we made, the values of n were limited by $|n| \leq 13$.

The atomic scattering factors f_j were taken from Langridge *et al.* (1960), which takes into account the water in the structure and includes a temperature factor. For practical reasons, the atoms of the helix are arranged in five sets: in the first set are the atoms of the sugar–phosphate group; the four following sets are composed of the atoms of the bases adenine, cytosine, guanine and thymine, respectively. In this ordering the atoms of group g are numbered from n_g to m_g. As we suppose a statistical repartition of the different base-pairs along the double helix, a coefficient P_g is given to each base group. These factors define the proportion of the base-pairs (guanine and cytosine have the same P_g value, as do adenine and thymine) and $\sum_{g=1}^{4} P_g = 1$. Of course the sugar–phosphate set has $P_g = 1$. The co-ordinates in Table 1 correspond to the atoms of the five groups.

Because of the presence of a dyad axis in the double helix and the fact that the pitch contains ten base-pairs in the B form, the calculated intensities vary when the angle ψ increases from 0 to 18°. Practically, one calculates the diffracted intensities averaged by the rotation ψ; this is well-justified on an experimental level. Therefore, the structure factors can be written:

$$F(l,\psi,\zeta) = \sum_{g=1}^{5} P_g \sum_n \sum_{j=ng}^{mg} f_j J_n(2\pi R_j \zeta) \cos\left(\frac{2\pi l z_j}{c} - n\phi_j\right),$$

and the diffracted intensities are $I(l,\psi,\zeta) = F^2(l,\psi,\zeta)$.

4. Results

(a) *Salt and humidity effects*

With the three sodium salt DNAs, the B to A transition is obtained when the relative humidity is lowered from 92% to 75%. In the B form the lattice is hexagonal and the parameter a is dependent on the humidity. But the main experimental fact that can be drawn from the series of X-ray patterns obtained with a humidity of 92% is: the a parameter is about 49 Å for the 72% (G + C) DNA, it is 45 Å for the 42% (G + C) DNA and 43 Å for the 26% (G + C) DNA (Plate I(a), (b) and (d), Table 2).

For the three DNAs studied in the *B* form, the meridional reflection is at 3·4 Å and the length of the unit cell along the *c* axis is very close to 34 Å (33·8 Å). Consequently, there are ten nucleotides in the pitch of the helix. The patterns corresponding to a relative humidity of 75% present the *A* form with the three DNAs. The meridional reflection is at 2·56 Å, the lattice is triclinic (Fuller *et al.*, 1965) with the parameters $a = 22{\cdot}2$ Å, $b = 40{\cdot}6$ Å, $c = 28{\cdot}15$ Å, $\beta = 97°$, when the quantity of the sodium salt is increased (more than 3·5% w/w), the 26% (G + C) DNA retains the *B* form for relative humidities from 43% to 92% (Albiser *et al.*, 1973). In this case the parameter *a* of the hexagonal lattice varies from 37·6 Å to 49·6 Å.

For the three lithium salt DNAs we have the *B* form with a relative humidity of 92%. The lattice is hexagonal, the parameters *a* and *c* are very close to those for sodium salt DNA (Table 2 and Plate I(c)). When the relative humidity is lowered to about 75%, the *B* form appears in the orthorhombic lattice (Langridge *et al.*, 1960) with $a = 31$ Å and $b = 23$ Å. The pitch does not vary even when the humidity is lowered to 40%. An increase of the lithium salt concentration for the 26% (G + C) DNA stabilizes the *B* form in its hexagonal lattice against the effect of the humidity diminution. The *C* form has been obtained only for the 42% and 72% (G + C) DNA. In this case the lattice is hexagonal or orthorhombic and the pitch of the helix is equal to 31·8 Å.

(b) *The diffracted intensities*

The diffracted intensities have been measured on photographs obtained with DNA fibres in high relative humidity. So the patterns correspond to the *B* form in the hexagonal lattice for the sodium and lithium salt DNA. In Table 2 the intensities that correspond to the strongest spots on the three first layer lines (i.e. (1,1,1), (2,0,2) and (2,1,3)) in the patterns of the three DNAs are compared. The intensity of the spot (2,0,2) is arbitrarily made equal to 100 in each case. The experimental intensities are compared to the calculated values; for these last, the positions of the spots in reciprocal space are taken into account.

The theoretical intensities were calculated for a constant pitch of the helix in the *B* form (Arnott, 1970) but the relative proportion of the base-pairs was included in the computation through the values given to the factors P_g. We used a ratio of

TABLE 2

Maximum relative intensities of the three B-*DNA fibre patterns*

DNA (% G+C)	(A+T)/(G+C)	Relative humidity (%)	Salt	*a* (Å)	*c* (Å)	1st layer line		3rd layer line	
						I_{exp}	I_{cal}	I_{exp}	I_{cal}
Spiroplasma citri	2·8	92	Na	42·8	34	31	26	62	59
26		92	Li	43·5	34	33	30	72	67
Calf thymus	1·35	92	Na	44·5	34	32	30	59·5	63
42		92	Li	46	34	28	32	54	57
Micrococcus lysodeikticus	0·39	92	Na	49	34	38	35	51	47
72									

The intensity of the spot on the second layer line is arbitrarily made equal to 100.

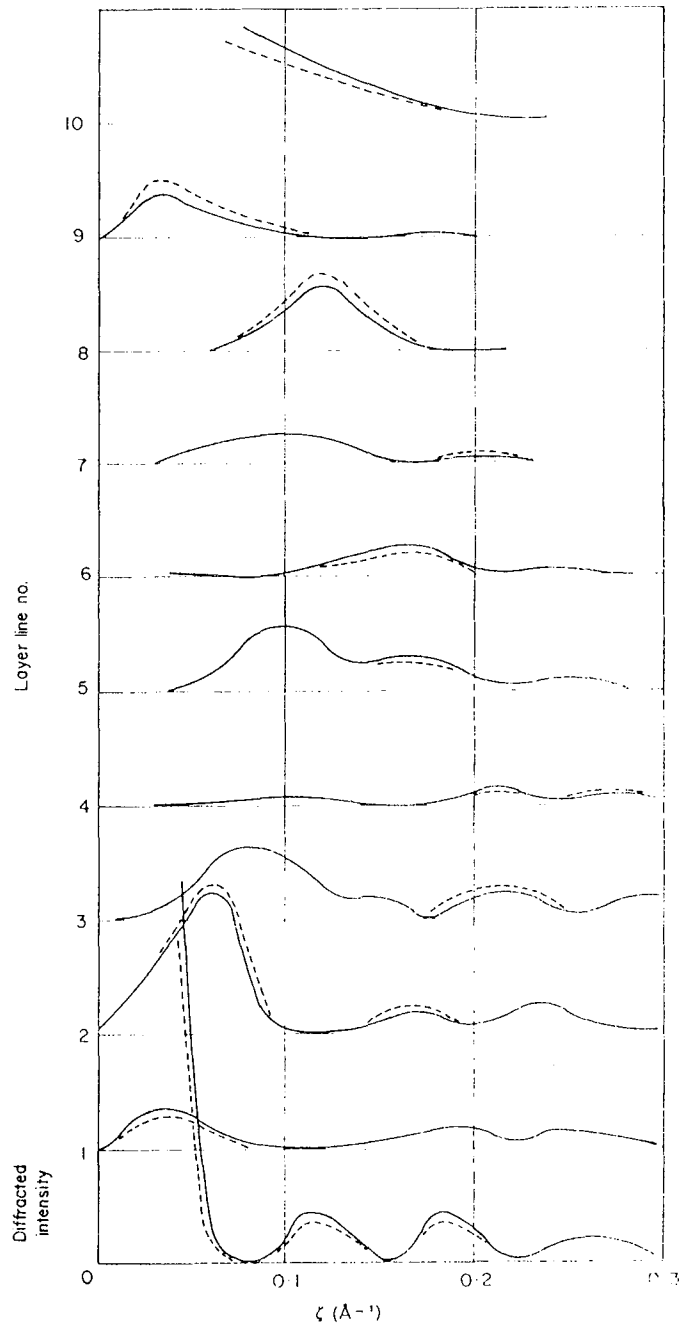

FIG. 1. Curves of the square of the Fourier transform for *B*-DNA with a ratio (A + T)/(G + C) equal to 4 (continuous curve) and 0·25 (broken curve).

bases (A+T/G + C) varying from 4 to 0·25. Analysis of the intensities for each layer, as a function of the radial co-ordinate in reciprocal space, corresponding to the two extreme cases of the base ratio reveals a very light diminution of the intensities of the second, eighth and ninth layer lines and a small increase in the intensity of the tenth layer line (Fig. 1). These calculated effects are less than the experimental errors and therefore cannot be detected on diffraction photographs. It is also a result that would be expected due to the closeness of the total atomic factors for the two possible base-pairs.

Complementary calculations have been made in order to define the effect of the base tilt on the diffracted intensities. For this purpose we vary the dihedral angle χ on the sugar–base bond (Fig. 2). The variations were $+9°$ and $-9°$ with respect to the

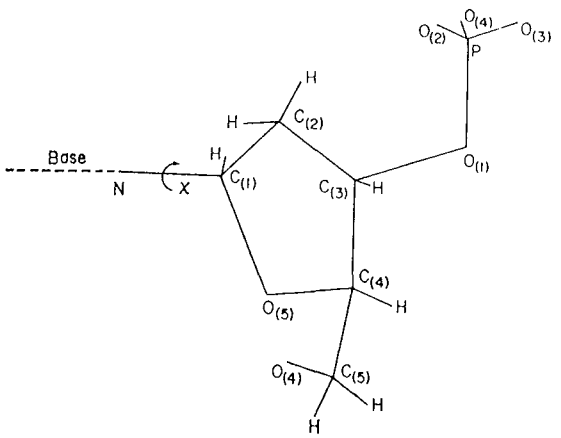

FIG. 2. The dihedral angle χ around the bond between the base and the sugar ring.

original *B* structure. These rotations have the same consequences as a simultaneous tilt from $+4°$ to $-10°$ and a twist from $-4·5°$ to $+11°$ in Arnott (1970) conventions. Such rotations, for the extreme values, correspond to structures with very distorted hydrogen bonds in the base-pairs. Nevertheless, one can only detect an intensity variation on the 8th layer line and very small ones on the 9th and 10th layer lines (Fig. 3). These results are in accordance with a similar study made on the *A* form by Fuller (1961). To be complete, we verified that variation of the base-pair ratio does not modify the preceding results. Thus intensities of the higher layer lines are directly related to the relative orientation of the bases. These data confirm those of Marvin *et al.* (1961) when they examined the DNA *C* form.

5. Discussion

The three DNA helices studied, although they are very different in base composition, do present the same conformation under identical physical conditions (salt concentration and relative humidity); the helical parameters in the *A*, *B* and *C* forms are identical for the three DNA fibres. This is not general behaviour; Bram & Tougard (1972) have studied systems that gave the opposite result. An increase in the lithium or sodium salt concentration favours the stability of the conformation found at

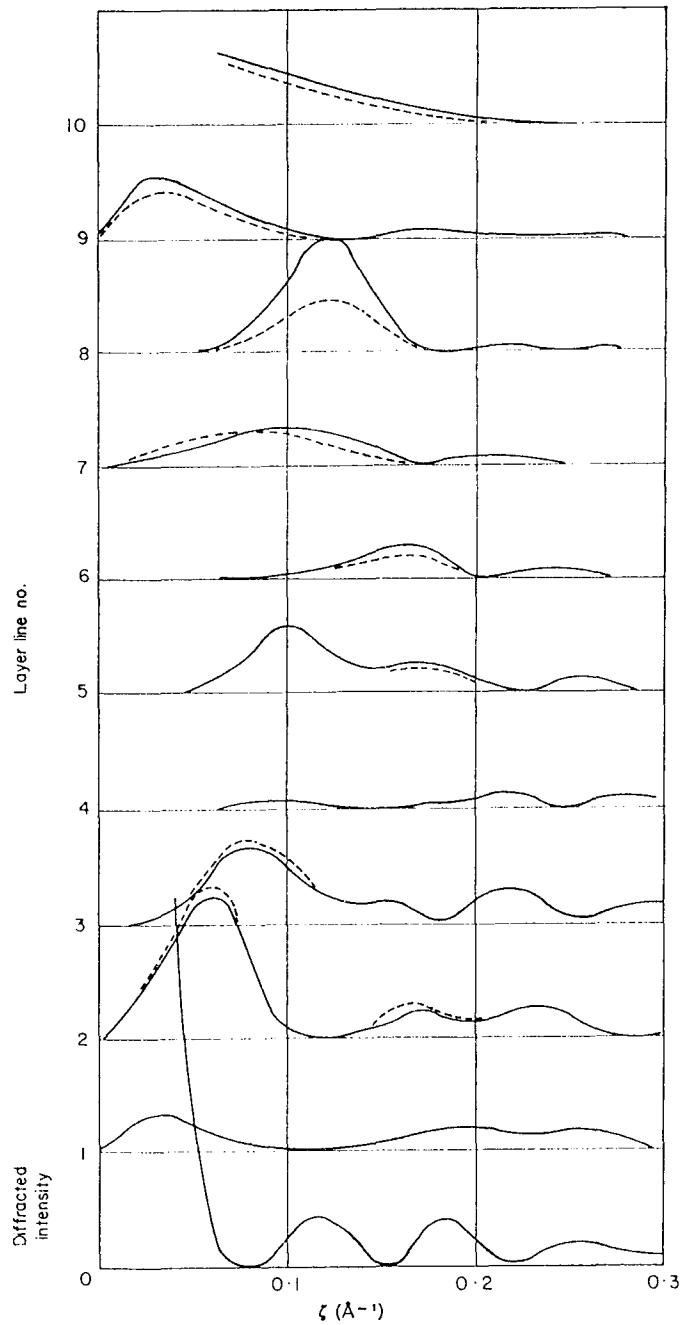

FIG. 3. Curves of the square of the Fourier transform for *B*-DNA. Continuous curve, a variation of the dihedral angle $\Delta\chi = -9°$; broken curve, $\Delta\chi = +9°$.

high humidity (*B* form in the hexagonal lattice). This effect of stabilization against lowering of the relative humidity is more pronounced when the relative number of (G·C) base-pairs in the DNA helix is lower. The experimental differences noted on the diffracted intensities for the three DNAs are related to differences in the hexagonal lattice parameters; if one takes into account the lattice parameter when the intensities are calculated, the experimental values are in good agreement with the theoretical values. Therefore, the hexagonal lattice parameters are different for the three DNA fibres but the helices are the same or, at least, indistinguishable by X-ray diffraction. Moreover, one should expect a correlation between the parameter a of the hexagonal lattice and the relative proportion of the base-pairs.

The calculated intensity curves obtained with DNA in the *B* form are very similar to those given by Langridge *et al.* (1960). The small differences come from the fact that we use the refined dihedral angles proposed by Arnott & Hukins (1972). The intensities calculated with the models of DNA in the *B* form with very different base-pair contents do not reveal any significant variation. The complementary calculations, which introduce a modification in the base orientation added to the variation of the base composition, show that the tilt and twist of the DNA bases has an effect on the 8th layer line intensities. But no differences are noted on the X-ray patterns of the three DNAs; thus the orientation of the base-pairs cannot be related to the base composition of the double helices. Further, one can say that the base composition does not affect the sugar–phosphate chain or the base orientation. Such a conclusion is not obvious; very different chain conformations correspond to given helical parameters because of the number of modifiable dihedral angles in the sugar–phosphate chain. This fact obtains from the hypothesis of a statistical repartition of the base-pairs along the helix. So, one could suppose that the base composition may introduce perturbations in the main chain conformation if the base-pairs are in precise sequences; this has not yet been demonstrated.

From the experimental results presented above, we can draw the conclusion that DNA with a low (G + C) content is characterized by the absence of the *C* form in lithium salt preparations and also of the *A* form when sodium salt is present in concentrations greater than 3·5% (w/w); this behaviour is to be related to the results of Pilet & Brahms (1972). The absence of the transition from the *B* to *C* form for DNA with a low (G + C) content underlines the difficulty of increasing the angle of rotation for succeeding nucleotides. Zimmer & Luck (1974) noted this for long homoligonucleotide sequences, particularly of (A·T) base-pairs.

REFERENCES

Albiser, G., Horn, P., Saglio, P. & Bové, J. M. (1973). *C.R.H. Acad. Sci., Paris*, **276**D, 653–655.

Arnott, S. (1970). *Progr. Biophys. Mol. Biol.* **21**, 261–318.

Arnott, S. & Hukins, D. W. L. (1972). *Biochem. Biophys. Res. Commun.* **47**, 1504–1509.

Azoulay, R. & Bram, S. (1973). *C.R.H. Acad. Sci., Paris*, **276**D, 2977–2979.

Bram, S. (1973). *Proc. Nat. Acad. Sci., U.S.A.* **70**, 2167–2170.

Bram, S. & Tougard, P. (1972). *Nature New Biol.* **239**, 128–131.

Cochran, W., Crick, F. H. C. & Vand, V. (1952). *Acta Crystallogr.* **5**, 581–586.

Cooper, P. J. & Hamilton, L. D. (1966). *J. Mol. Biol.* **16**, 562–564.

Davies, D. R. & Baldwin, R. L. (1963). *J. Mol. Biol.* **6**, 251–255.

Eyring, H. (1932). *Phys. Rev.* **39**, 746–748.

Franklin, R. E. & Gosling, R. G. (1953). *Acta Crystallogr.* **6**, 673–677.

Fuller, W. (1961). Ph.D. Thesis, University of London.

Fuller, W., Wilkins, M. H. F., Wilson, H. R. & Hamilton, L. D. (1965). *J. Mol. Biol.* **12,** 60–80.

Hamilton, L. D., Barclay, R. K., Wilkins, M. H. F., Brown, G. L., Wilson, H. R., Marvin, D. A., Ephrussi-Taylor, H. & Simons, N. S. (1958). *J. Biophys. Biochem. Cytol.* **5,** 397–403.

Hermans, J. & Ferro, D. (1971). *Biopolymers*, **10**, 1121–1138.

Langridge, R., Wilson, H. R., Hooper, C. W. & Wilkins, M. H. F. (1960). *J. Mol. Biol.* **2,** 19–64.

Marvin, D. A., Spencer, M., Wilkins, M. H. F. & Hamilton, L. D. (1961). *J. Mol. Biol.* **3,** 547–566.

Pilot, J. & Brahms, J. (1972). *Nature New Biol.* **236**, 99–100.

Saglio, P., Laflèche, D., Bonissol, C. & Bové, J. M. (1971). *Phys. Veg.* **9**, 569–582.

Zimmer, C. H. & Luck, G. (1974). *Biochim. Biophys. Acta*, **361**, 11–32.

C) COORDONNEES ATOMIQUES ET INTENSITES CALCULEES A PARTIR D'UN MODELE "SYDE BY SIDE" DE L'ADN

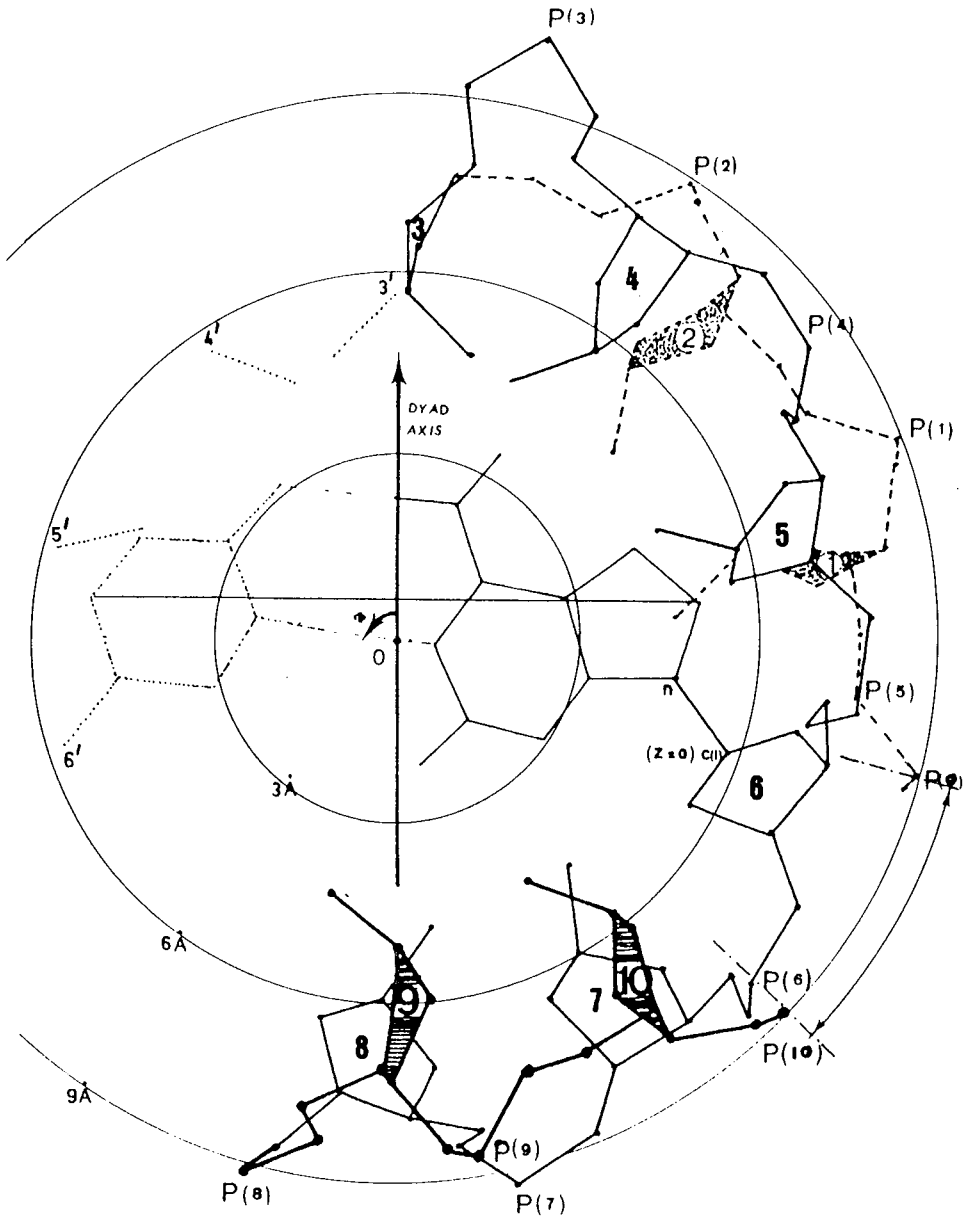

Figure N° 14 : Projection de l'unité de 10 nucléotides sur un plan perpendiculaire à l'axe de la super hélice.

Vol. 95, No. 3, 1980 BIOCHEMICAL AND BIOPHYSICAL RESEARCH COMMUNICATIONS
August 14, 1980 Pages 1231-1237

ATOMIC COORDINATES AND CALCULATED INTENSITIES FOR A SIDE BY SIDE D.N.A. MODEL.

G. Albiser and S. Prémilat

Laboratoire de Biophysique Moléculaire
E.R.A. CNRS N° 828, C.O. N° 140
54037 NANCY CEDEX, France

Received May 6,1980

Summary. A precise conformation of the side-by-side type is proposed for the B-D.N.A. form. In this model the antiparallel chains are related by a dyadic symmetry and binding between complementary bases is realized using Watson-Crick pairing. The elementary unit, comprising 10 nucleotides for one chain, is composed of one segment in a right handed helix, a second segment rotated to the left and two bends. Cylindrical atomic coordinates are given for atoms in the elementary unit and the square of the Fourier transform is calculated for this conformation and compared to the well known double helix and to experimental data.

Introduction.X-ray measurement on crystalized fragments of D.N.A. allowed to propose a new conformation for the D.N.A. double strand. This conformation is very different from the Crick-Watson B-D.N.A. form as it takes the form of a left handed helix (1). Left handed helices seem to be also possible in synthetic D.N.A. fibres (2). These facts increase the interest for D.N.A.conformations presenting simultaneously right and left handed helices e.a side-by-side models. For the two different proposed models (3) (4) the segments of right and left handed helix are each composed by five base pairs which are associated as in Watson Crick model. What differentiates these two conformations is essentially that for type I, sugar rings are C(3) endo for nucleotides in left handed helical segments and C(3) exo for right handed ones, but they are always C(3)exo for the type II. As a consequence in the type I the oxygen atoms of the sugar rings have the same orientation and in type II they are alternatively up and down. Side-by-side models are proposed in very general forms ; no precise atomic coordinates are given and thus comparisons with experimental data as well as with the double helix model can only treat overal features. Moreover the two methods used (3) (5) for calculations of diffracted intensities give results which do not agree. In the present paper a completely defined side-by-side model for D.N.A. is given which allows precise calculations of diffracted intensities.

0006-291X/80/151231-07$01.00/0

As we encountered difficulty when trying to build the type I structure (essentially for nucleotides in helix rotating to the left) we propose atomic coordinates for a D.N.A. conformation similar to the type II. Cylindrical coordinates as well as Fourier transforms are determined for a stereochemically possible conformation of the bicatenary molecule. Curves of the diffracted intensities are therefore calculated and compared to experimental data and to values associated with the double helix model in its B form.

Method. a) Geometrical conditions. In order to define with precision a D.N.A. conformation similar to the type II it is necessary to impose some detailed characteristics of the structure. Firstly, the two antiparallel sugar-phosphate chains and the stacking of the complementary bases must present a good stereochemistry. Sugar rings are put in their C(3) exo conformation which is the admitted one for the B-D.N.A. form (6) but, as sugar rings present great flexibility (7) perturbations of their conformations are allowed during the process of improvement of the chain conformation. The 3.4 Å distance along the axis is a characteristic parameter for the B-D.N.A. revealed by X-ray diffraction. In the proposed conformation the 3.4 Å distance should be found essentially in the interval between successive base-pairs which will be maintened perpendicular to the axis of the structure. Another important feature observed on X-ray patterns is the regular interval between layer lines corresponding to an axial distance of 34 Å. In the double helix model this distance corresponds to the height of 10 pairs of nucleotides. Therefore in the new conformation, the repetitive unit will be constituted by 10 nucleotides per chain. Indeed this conformation will present alternation of three nucleotides on a right handed helix and three nucleotides on a left handed one. These segments will be separated by two types of bends corresponding respectively to the right handed to left handed helix transition and vice-versa. Each bend will be composed of two nucleotides. The 10 nucleotides unit on a chain must be associated with a complementary unit on the antiparallel chain. This condition imposes the existence of a dyad axis perpendicular to the axis of the structure ; moreover, in order for obtaining units of ten nucleotide pairs which exactling repeat through a translation of 34 Å along the main axis, the dyad axis in the right and left segments must have the same direction. For the beginning of the chain, one imposes the geometrical parameter of the B-D.N.A. double helix form (6) to nucleotides in right handed helix. Moreover the axis of the structure must also be the axis for the right handed segments of the chain. Nevertheless, if one retains the dihedral angles of the B-D.N.A. form for the left handed segments of the chain, these latter will present axes with directions very far from the axis of the structure. It will thus be almost impossible to superpose the axes of the successive right handed helical segments. As a consequence, the dihedral angles of nucleotides in left handed segment will be modified taking into account the imposed geometrical conditions.

b) Model building. Computations of atomic coordinates are performed with a procedure previously used (8) ; bond lengths and valence angles used are those listed by Arnott (9). Dihedral angles corresponding to nucleotides in the left handed segments and in the bends are to be determined but one should note that the number of

constraints on the system does not allow an easy computation of these angles. This is why a kind of Kendrew molecular model was built in order to evaluate the unkown dihedral angles. Buth such a model does not permit precise measurements and, moreover as atomic space filling is not materialized it hardly gives a good idea about the stereochemistry of a conformation. Nevertheless this model give approximate values of the dihedral angles which can be used as starting data for computations of the cylindrical coordinates of atoms. With the computed coordinates one can test the conformation as regards the different constraints : if the stereochemistry is good, one has to verify whether the binding of complementary bases is possible. In fact a conformation verifying the imposed constraints and presenting an acceptable stereochemistry, is progressively obtained by going back and forth between the model and the computer and vice-versa.

c) Fourier transform. The computation of the theoretical values of intensities diffracted by the new D.N.A. conformation is performed using the same expressions as for the double helix model (10) (8). Thus, due to the dyadic symmetry between complementary chains, the following simplified expression can be used for the structure factors on the layer line ℓ (11) :

$$F(\ell,\xi) = \sum_n \sum_j f_j J_n(2\pi R_j \xi) \cos\left(\frac{2\pi \ell z_j}{c} - n\Phi_j\right) = \sum_n A_n(\ell,\xi)$$

where ξ is the radial coordinate in reciprocal space and R_j, Φ_j, z_j the cylindrical coordinates of the atoms in the ten nucleotides unit. Order n of Bessel functions J_n are defined according to the rule : $\ell = n t + m u$ with m a positive, negative or null integer. For the present computations n is taken from -13 to + 13 for all values of ℓ because here $\ell = n + m$. Atomic scattering factors f_j are those given by Fraser (12). The diffracted intensities averaged over the orientation angle in reciprocal space is calculated as (8) : $I(\ell,\xi) = \sum_n A_n^2(\ell,\xi)$.

Results. In the best conformation obtained sugar rings in nucleotides 1 and 2 are in the B-D.N.A. double helix form. The first bond is realized between the sugar rings of nucleotides 3 and 4. The nucleotides 5, 6 and 7 are on a pseudo left handed helix. The second bend is formed between the sugar rings of nucleotides 8 and 9. Finally the sugar ring of nucleotide 10 takes the conformation of the B-D.N.A. double helix. It was necessary to modify the conformations of the sugars in the bends in order to maintain the imposed geometry. Hence, the conformations of sugar rings of nucleotides 3 and 8 remain very near to C(3) endo. They correspond respectively to base interval of 3.58 Å for the first bend and 3 Å for the second one ; this last value is due to constraints for association between complementary bases in the two antiparallele strands ; bases complementary to bases of the second bend must be in the conformation of the bases in the first bend (dyadic symmetry). The chain of ten nucleotides constituting a unit present a distance of 34.4 Å along the main axis. Successive units are obtained only by a 34.4 Å translation along this axis and

Table I. Chain dihedral angles for the nucleotides of the unit.

Nucleotide number	DIHEDRAL ANGLES(about atomic bond)						
	$O^{(o)}$ (O_4-C_5)	$\zeta^{(o)}$ (C_5-C_4)	$\sigma^{(o)}$ (C_4-C_3)	$\omega^{(o)}$ (C_3-O_1)	$\phi^{(o)}$ (O_1-P)	$\psi^{(o)}$ $(P-O_4)$	$\chi^{(o)}$ (C_1-N)
1 right handed helix	-146.5	36.4	156.5	154.7	-95.6	- 46.1	150.5
2	-146.5	36.4	156.5	155.7	-93.6	- 70	150.5
3 1st bend	-144	34.4	83	- 174	15	-168	124.6
4	-160	36.4	145	96	-87	- 80	112.6
5	-130	45	149	133	-96	- 84.5	72.2
6 left handed segment	-122	33.4	154.5	140	-100	- 89	71.6
7	-124	32	153.5	140	-111	5	75.5
8 2nd bend	170	- 24.6	107	58.5	-12	-175	16
9	-172	157.5	149.5	169	-77.6	- 67	121
10 right handed helix	-146.5	37.4	156.5	154.7	-95.6	- 46.1	138.9

thus dyadic axis in right and left handed segments have the same orientation. The complementary chain is easily obtained with a Watson-Crick bases association. Pairs of bases are almost perpendicular to the main axis. Dihedral angles along the sugar phosphate chain are given in table I. Progression is done in the 5-3 direction and values correspond to Arnott conventions (9). Cylindrical coordinates for atoms in the unit are given in table II. It can be noted that the mean interval between bases is of the order of 3.4 Å with limiting values of 3 Å and 4.3 Å. In fig. 1 are given curves of the square of the Fourier transform corresponding to this D.N.A. conformation.

Discussion. The proposed conformation has been difficult to realize, it still presents irregularities, mainly in spaces between bases. The total height of 34.4 Å for one unit is very near to the experimental value. The Watson-Crick type of bases association is maintained and dyad axes in same direction for right and left handed segments allow an easy determination of the complementary chain and avoid a superhelical distorsion of the conformation. Interatomic distances are as satisfactory as in the B-double helix model ; one should note that one sugar ring in each bend has to be C(3) endo in order to avoid bad interatomic contacts. Residues 4 and 8 exhibit unusual values for the ω angles (table I). These values are necessary for the bending of the sugar-phosphate chain and are therefore inherent to the present model. Moreover a similar value for ω has

Table II. Cylindrical coordinates for nine nucleotides of an unit. (the coordinates of first nucleotide can be obtained by removing 3.38 Å from z_j and 36 Å from Φ_j of nucleotide 2).

ATOM	NUCLEOTIDE 2			NUCLEOTIDE 3			NUCLEOTIDE 4		
	R_j(Å)	Φ_j(o)	z_j(Å)	R_j(Å)	Φ_j(o)	z_j(Å)	R_j(Å)	Φ_j(o)	z_j(Å)
O_4	7.72	-52.95	2.08	7.70	-17.36	5.48	8.21	-10.60	9.70
C_5	7.68	-44.83	1.14	7.93	- 7.77	4.92	8.35	-16.15	10.89
C_4	7.57	-34.87	1.86	7.64	0.51	5.89	7.60	-25.57	10.82
O_5	6.22	-30.63	2.02	6.33	5.49	5.69	6.23	-24.72	11.28
C_3	8.19	-34.88	3.26	7.75	- 2.11	7.37	7.58	-36.47	9.44
C_2	7.02	-38.40	4.13	6.86	6.26	8.01	6.15	-28.16	8.97
C_1	5.79	-32.06	3.36	5.67	6.91	6.94	5.34	-26.58	10.18
N	4.58	-41.71	3.36	4.46	- 3.07	6.88	4.58	-11.75	10.11
O_1	8.74	-26.36	3.64	9.10	- 1.81	7.81	7.99	-40.49	9.51
P	8.92	-24.25	5.19	9.46	- 4.71	9.30	7.09	-50.55	9.52
O_2	10.23	-20.35	5.40	9.74	2.33	10.15	8.02	-58.12	8.95
O_3	9.0	-32.33	5.96	10.72	- 9.05	9.28	5.86	-49.41	8.70
	NUCLEOTIDE 5			NUCLEOTIDE 6			NUCLEOTIDE 7		
O_4	6.80	-52.13	11.08	6.93	- 93.49	14.43	7.29	-131.44	18.1
C_5	7.88	-55.52	11.93	7.96	- 94.04	15.44	8.23	-132.28	19.18
C_4	7.56	-64.54	12.77	7.80	-102.71	16.35	8.01	-141.01	20.02
O_5	6.62	-61.90	13.83	6.86	-100.48	17.42	7.02	-139.28	21.04
C_3	7.10	-74.40	12.03	7.47	-112.81	15.70	7.70	-150.48	19.27
C_2	5.60	-75.42	12.25	5.96	-114.60	15.83	6.19	-152.13	19.34
C_1	5.36	-67.38	13.53	5.67	-107.26	17.20	5.84	-145.74	20.71
N	4.41	-53.75	13.55	4.56	- 96.05	17.19	4.67	-134.35	20.74
O_1	7.89	-82.65	12.60	8.22	-120.01	16.40	8.43	-157.85	19.91
P	7.34	-93.93	12.89	7.83	-131.02	16.59	8.03	-168.64	19.99
O_2	8.57	-99.53	12.63	9.14	-135.53	16.41	9.26	-173.08	19.50
O_3	6.25	-97.86	12.00	6.87	-135.01	15.59	6.88	-171.59	19.14
	NUCLEOTIDE 8			NUCLEOTIDE 9			NUCLEOTIDE 10		
O_4	7.76	-170.15	21.55	7.44	-169.23	26.14	7.68	-128.95	30.24
C_5	7.75	-161.58	22.40	7.96	-165.04	27.36	7.78	-121.43	29.22
C_4	7.21	-164.21	23.77	7.74	-154.14	27.48	7.57	-111.06	29.78
O_5	6.57	-154.32	24.3	6.48	-150.09	26.97	6.21	-106.89	29.73
C_3	6.38	-175.05	23.83	7.89	-150.02	28.89	8.04	-109.87	31.23
C_2	5.14	-171.45	24.64	6.45	-149.74	29.39	6.77	-112.60	32.01
C_1	5.39	-157.08	25.03	5.61	-147.05	28.04	5.65	-106.76	31.04
N	4.62	-142.41	24.95	4.53	-158.68	28.00	4.43	-116.53	30.99
O_1	7.27	-182.97	24.41	8.67	-141.80	28.90	8.57	-100.96	31.50
P	7.79	-180.85	25.90	8.88	-136.30	30.24	8.61	- 97.38	33.01
O_2	9.26	-181.68	25.94	10.20	-132.31	30.16	9.95	- 93.78	33.26
O_3	7.25	-188.65	26.82	8.94	-142.25	31.40	8.49	-105.03	33.94

Vol. 95, No. 3, 1980 BIOCHEMICAL AND BIOPHYSICAL RESEARCH COMMUNICATIONS

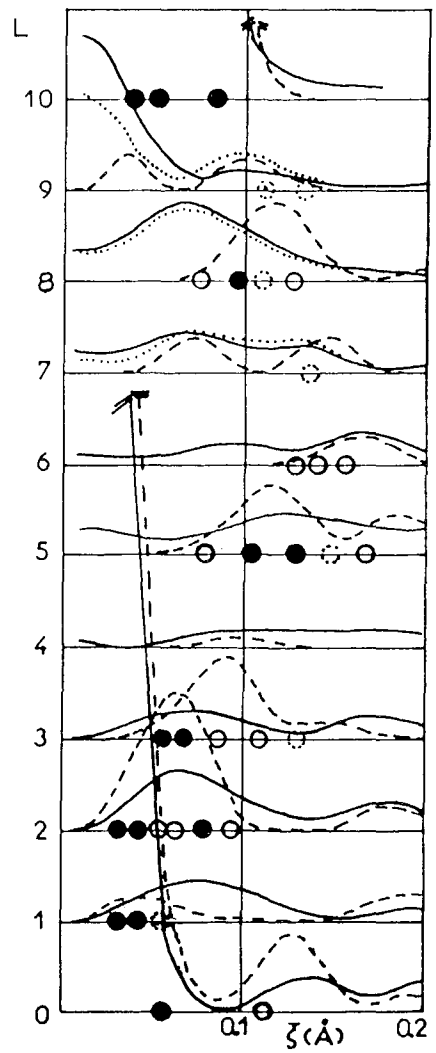

Figure 1. Curves of the square of Fourier transform associated with the new model (——) ; this model with bases perpendicular to the axis (....) ; curves for the B-D.N.A. Watson-Crick double helix (------). Spots indicate experimentally observed intensities. ● strong, O medium and ◌ weak (11).

been found experimentaly (13). Improvements of this conformation could be obtained with refinement methods taking dihedral angles as variables. In that way left handed segments could be given a more regular conformation. Dihedral angles of the right handed segment (helix) could also be modified in order to decrease the interval between bases 7 and 8. Nevertheless it seems difficult to improve spaces between the bases near the bends as long as constraints are maintained on the geometry of the system. Note that the obtained

conformation fits well to the orthorhombic lattice in the space group $P2_1\ 2_1\ 2_1$ e.a. the two molecules in the lattice have their dyad axis in the a direction and one is translated in the c direction with one third of the unit height (ten pairs of bases). Irregularities in the geometry, mainly in spaces between bases, introduce defects in the calculated intensities. Although layer lines 0 and 10 do agree with experiment as the double helix model, layer lines 1,2,6 and 8 presents wide maxima which could permit the existency of intensity spots (taking into account the lattice) which are not indeed observed. Moreover calculated curves present meridian values not equal to zero on layer lines 5,6,7,8 and 9 ; such intensities are not observed with B-D.N.A. These last results agree with conclusions presented recently (5) but the present completely defined side-by-side model furnishes a good starting point for an eventual refinement procedure. Atomic coordinates given for the proposed D.N.A. conformation allow precise calculations and shown that the side-by-side model is a realistic one as concerns the stereochemistry but the calculated intensity curves do not match as well to experimental data as for the double helix. Nevertheless, improvement are possible mainly by increasing the regularity of the present model ; one can already note that the Fourier curves of high order layer lines are improved when bases are maintained perpendicular to the axis of the system (Fig.1).

References

1. Wang,A.H.J., Quigley,G.J., Kolpak,F.J., Crawford, J.L., VanBoom, J.H., Van der Marel,G. & Rich,A.(1979),Nature 282, 680-686.
2. Arnott,S., Chandrasekaran, R., Birdsall, D.L., Leslie, A.G.W. & Ratliff, R.L. (1980), Nature 283, 743-745.
3. Bates, R.H.T., Levitt, R.M., Rowe, C.H., Doy,J.P. & Rodley, G.A. (1977), J.Royal Soc.(New Zeland) 7, 3, 273-301.
4. Sasisekharan, V. & Pattabiraman, N.(1976), Current Sci.,45; 779-783.
5. Greenall, R.J., Pigram,W.J. & Fuller, W.(1979), Nature 282,20-27.
6. Arnott, S. & Hukins, D.W.L. (1972), Biochem.Biophys.Res.Commun., 47, 1504-1509.
7. Levitt, M. & Warshal, A.(1978), J.Amer.Chem.Soc.,100, 2607-2613.
8. Premilat, S. & Albiser, G.(1975), J.Mol.Biol.,99, 27-36.
9. Arnott, S.(1970), In Progress in Biophys.& Mol.Biol.,21,265-319.
10. Cochran, N., Crick, F.M.C.& Vand,V.(1952), Acta Cryst., 5,581-586.
11. Langridge, R., Wilson, H.R., Hooper, G.W. & Wilkins, M.H.F., (1960), J.Mol.Biol., 2, 19-64.
12. Fraser, R.D.B., MacRae, T.P. & Suzuki, E.(1978), J.Appl.Cryst., 11, 693-694.
13. Sundaralingam, M.(1969), Biopolymers 7, 821-860.

D) CONFORMATION ET TRANSFORMEE DE FOURIER D'UN MODELE MOLECULAIRE "SIDE BY SIDE" EXACT POUR L'ADN EN FORME B

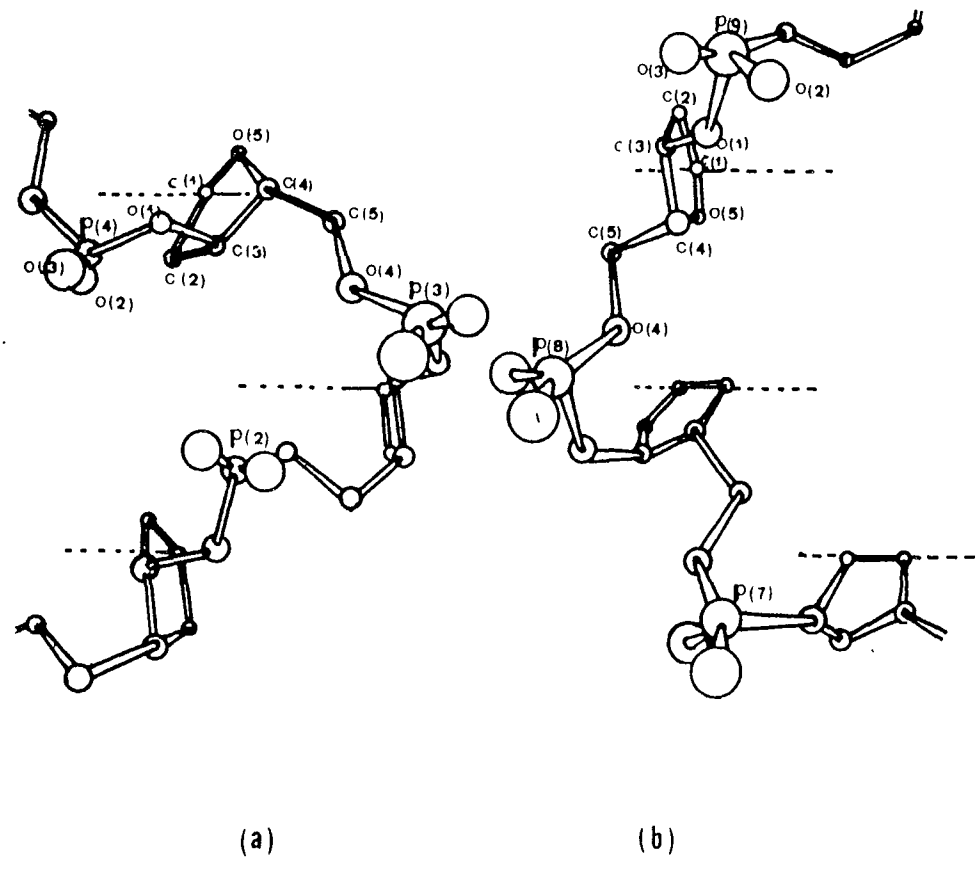

(a) (b)

Figure N° 15 : Les deux régions de changement de sens de la chaîne des nucléotides ; la vue est prise lelong de l'axe dyade.
a) le premier coude entre les désoxyriboses 3 et 4,
b) le deuxième coude entre les désoxyriboses 8 et 9.

Vol. 104, No. 1, 1982 BIOCHEMICAL AND BIOPHYSICAL RESEARCH COMMUNICATIONS
January 15, 1982 Pages 22-29

CONFORMATION AND FOURIER TRANSFORM OF AN EXACT SIDE-BY-SIDE MOLECULAR MODEL OF B-DNA

S. PREMILAT and G. ALBISER

Laboratoire de Biophysique Moléculaire
E.R.A. CNRS N° 828, C.O. N° 140
54037 NANCY Cedex, FRANCE

Received September 24, 1981

Summary. An accurate side-by-side conformation with a good stereochemistry is proposed for the B-DNA. The structure does not present any super helical torsion and its right and left-handed sections, composed of three nucleotides per chain, are connected by two different bends each comprising two nucleotides. Atomic coordinates and a stereo view are given as well as dihedral angles. Diffracted intensities are calculated for this molecular conformation and compared to experimental values and to other DNA models.

Introduction. The DNA in its B-form is generally defined as a right-handed double helix with bases paired according to the WATSON-CRICK scheme. But many experimental facts question the unicity of this model with regard to the conformation of the sugar-phosphate chain. For example, right-handed helices close to the classical B-form have been proposed as models in X-Ray studies on crystals of short sequences of nucleotides (1). But the crystallization of sequences of alternating purines and pyrimidines allowed the determination of a left-handed double helix, the Z-DNA (2) (3), as a new model with a dinucleotide as unit. A polymorphism is also considered for the DNA models used for interpretations of X-Ray results on fibres (4) and left-handed helices were proposed as models for polynucleotides of alternating purines and pyrimidines (5) (6). Besides X-Ray studies, results obtained from solutions are also explained by using the Z-form of DNA (7) (8) or the simultaneous presence of right and left-handed helices (9) (10). In this last case, variations of the physico-chemical conditions induce transition between right and left-handed forms (11) (12) (13). Moreover, theoretical DNA models presenting succession of right and left sections have been proposed (14) (15) as alternatives to the right-handed double helix model of the B-DNA. These side-by-side models are also interesting because they are composed of junctions between helices of opposite screw sense, junctions which should

0006-291X/82/010022-08$01.00/0

be of some importance for the interpretation of experiments on transitions between different DNA conformations. However, most side-by-side conformations are defined with physical models and do not have a good precision in atomic coordinates. Moreover, they generally present a torsion giving to the model of the bicatenary DNA molecule a super helical conformation (15) (16). It is from these imperfect or distorted models that conclusions have been drawn on their relevance for the interpretation of X-Ray measurements on B-DNA fibres (17). In the present paper a precise side-by-side conformation of type II (15) is proposed. It is an improvement of a previous model of the B-DNA (18) which presents a better regularity in the spacing between bases and no super helical torsion. Its stereochemistry is good even for the nucleotides in the junctions between right and left-handed sections. Dihedral angles as well as coordinates of atoms are given and a comparison between calculated and experimental diffracted intensities is presented.

Methods. a) Geometrical conditions. A certain number of constraints are imposed for the realization of the side-by-side model in order to take into account the information deduced from X-Ray measurements. Therefore, the repeat unit must be of 34 Å length and one should have distances near to 3.4 Å between successive bases (ten nucleotide pairs in one unit). The side-by-side model is perfect if there is exactly 360° rotation between the 11th and the first nucleotide in the chain ; units are then exactly superposed along the main axis of the conformation. In the present model, the unit of ten nucleotides is composed of three nucleotides on a right-handed helix followed by two nucleotides for the transition to the left-handed section also constituded of three nucleotides. Then two nucleotides realize the transition to an other right-handed section. The main axis of the conformation is defined by the axis of the section in right-handed helix which is given dihedral angles close to those proposed by Arnott for the B-DNA (19). The model of the bicatenary DNA molecule is composed of two complementary and antiparallel chains, the pairing of bases is made as proposed by WATSON and CRICK. Consequently, the conformation must present a dyadic symmetry and, for the side-by-side model, a dyad axis must be present in each right or left-handed section, in the plan of its central bases. All these axes should have the same direction as no superhelical torsion is permitted. Sugar rings are C_2' endo but variations of their conformation are allowed (20) and do not exclude the C_3' endo form especially for the nucleotides in bends. Right and left sections present opposite orientations of the oxygen in the sugar rings ; up or down depending on the screw sense of the section in which they are included. Bases are always in position anti. The first condition a good conformation must satisfy is the stereochemistry and, therefore, constraints have been imposed in order for contacts between non-bonded atoms to agree with van der Waals radii commonly used for atoms (21) including hydrogen for the present calculations.
b) Model building and calculations. Model building and computation of atomic coordinates are performed according to the procedures used previously (18) (22). Hence a conformation verifying the geometrical constraints and presenting a good stereochemistry is obtained by working simultaneously on a kind of Kendrew molecular model and the computer. From this calculated model, the Fourier transform is computed using the cylindrical coordinates of atoms and values of the diffrac-

ted intensities are then obtained with relations and parameters previously used (22).

Results. For the best conformation presently obtained, the numbering of nucleotides starts with nucleotides 0,1,2 which are on a right-handed helix. The first bend is realized with nucleotides 3 and 4 then, 5, 6 and 7 are on a pseudo left-handed helix. The second bend is formed with nucleotides 8 and 9. Finally, the 10th nucleotide is in the conformation of the B-DNA right-handed helix. As for the preceding model (18) the sugar rings of nucleotides 3 and 8 are in C_3' endo in order to change the direction of rotation of the chain. In the left-handed section, the dihedral angles about C_4'-C_5' in sugars are diminished of some hundred degrees compared to the right-handed section e.a. a transition g-g to t-g. The dihedral angles of nucleotides 5, 6, 7 are somewhat different ; these nucleotides are not exactly on a left-handed helix. The side-by-side conformation presents dyad axes in the base plans of nucleotides 1, 6 and 11... ; these axes are parallel and allow an easy calculation of the coordinates of atoms on the antiparallel and complementary chain. Note that for the determination of the conformation of the nucleotides 7, 8 and 9, one has taken into account the fact they must be paired with nucleotides symmetrical (dyad axis) of 3, 4 and 5. Irregularities in spacing between nucleotides 7, 8, 9 and 10 are mainly due to the constraints of getting the 10th nucleotide in, exactly, the right-handed helix conformation and also of having only a 34 Å translation between this nucleotide and the 0th (no rotation about the main axis). Small tilts and twists have been introduced in view to improve the stacking of the corresponding bases. Dihedral angles corresponding to the best conformation obtained are given in table I ; progression along the chain is 5'-3' and values are expressed with Arnott's conventions (23). Cylindrical coordinates of atoms in the unit are listed in table II and a stereo view is given in figure I. Curves of the square of the Fourier transform corresponding to this side-by-side DNA model are presented in figure II and compared to experimental values and curves associated to the double helix model.

Discussion. The present conformation proposed for the B-DNA is a precise side-by-side model ; each chain is constituted of right and left-handed sections with equal numbers of nucleotides. The length of the repeat unit is 33.7 Å in accordance with experimental values and successive units are just translated along the main axis e.a. the structure is not a super double helix. One can see in table I that changes in the direction of the sugar-phosphate chain is obtained

Table I. Chain dihedral angles for the nucleotides of the unit.

Nucleotide number	DIHEDRAL ANGLES (about atomic bond)						
	θ (o) ($O_4'-C_5'$)	ξ (o) ($C_5'-C_4'$)	σ (o) ($C_4'-C_3'$)	ω (o) ($C_3'-O_1'$)	ϕ (o) ($O_1'-P$)	ψ (o) ($P-O_4'$)	χ (o) $C_1'-N$)
1 right-handed helix	- 146.5	37.4	154	154.5	- 93	- 48	146
2	- 146.5	37.4	154	153.5	- 90	- 65	146
3 1st bend	- 146	34.4	83	- 150	11	- 172	125
4	- 171.5	20	158	- 58	116	- 37	102
5	165	- 80	153	174	- 132	32	58
6 left-handed segment	162	- 60	149	- 168	- 131	33	53
7	161	- 73	158	- 59	123	- 39	58
8 2nd bend	115	- 60.5	100	47	15	- 166	71.5
9	134	167	158	163	- 87	- 61	123
10 right-handed helix	- 146.5	42	154	154.5	- 93	- 48	137

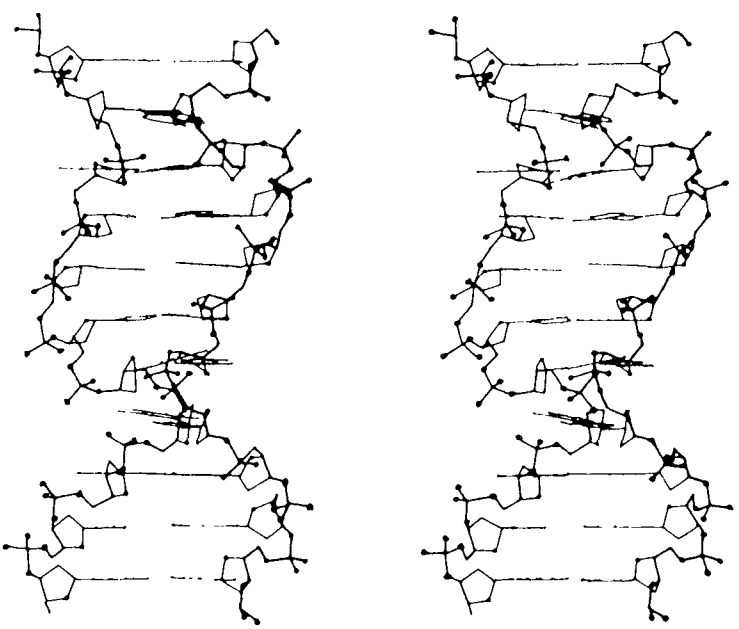

Figure I. Stereoscopic view of 11 pairs of nucleotides of the side-by-side DNA model. (One can see there is no superhelical torsion).

Table II. Cylindrical coordinates for nine nucleotides of an unit. Cartesian coordinates x, y, z, with the x axis along the dyadic direction can be calculated with $x_j = R_j \cos \Phi_j$; $y_j = R_j \sin \Phi_j$; $z_j = Z_j$. (The coordinates of atoms of nucleotide 1 can be obtained by removing 3.36 Å from Z_j and 36° from Φ_j of nucleotide 2).

ATOM	NUCLEOTIDE 2			NUCLEOTIDE 3			NUCLEOTIDE 4		
	R_j (Å)	Φ_j (°)	z_j (Å)	R_j (Å)	Φ_j (°)	z_j (Å)	R_j (Å)	Φ_j (°)	z_j (Å)
O_4'	7.63	-55.00	-14.79	7.56	- 18.84	-11.44	8.39	- 13.81	-7.83
C_5'	7.61	-46.71	-15.72	7.72	- 9.41	-12.12	8.59	- 19.24	-6.67
C_4'	7.48	-36.69	-14.99	7.41	- 0.35	-11.25	7.90	- 28.56	-6.74
O_5'	6.12	-32.59	-14.84	6.07	4.19	-11.45	6.69	- 28.97	-5.93
C_3'	8.08	-36.70	-13.59	7.58	- 2.00	- 9.75	7.52	- 32.27	-8.13
C_2'	6.88	-40.36	-12.77	6.80	7.61	- 9.21	6.13	- 26.95	-8.27
C_1'	5.68	-34.20	-13.50	5.55	8.40	-10.20	5.55	- 29.08	-6.77
N	4.50	-44.41	-13.52	4.26	- 0.05	- 9.99	4.99	- 14.15	-6.58
O_1'	8.66	-28.17	-13.22	8.94	- 1.30	- 9.35	7.69	- 42.92	-8.20
P	8.80	-25.76	-11.67	9.48	- 6.46	- 8.10	9.18	- 46.00	-7.84
O_2'	10.10	-21.65	-11.45	9.72	- 0.97	- 6.96	10.05	- 39.05	-7.57
O_3'	8.88	-33.81	-10.87	10.80	- 9.71	- 8.45	9.80	- 50.30	-8.98
	NUCLEOTIDE 5			NUCLEOTIDE 6			NUCLEOTIDE 7		
O_4'	9.00	-51.82	- 6.55	8.18	- 91.91	- 3.56	8.15	-128.83	0.23
C_5'	7.94	-49.96	- 5.61	7.50	- 87.48	- 2.44	7.15	-126.16	1.21
C_4'	7.82	-58.60	- 4.69	7.44	- 94.99	- 1.30	7.11	-134.78	2.27
O_5'	7.08	-55.79	- 3.49	6.72	- 90.15	- 0.19	6.30	-131.07	3.38
C_3'	7.38	-68.59	- 5.25	6.95	-106.33	- 1.59	6.77	-146.58	1.84
C_2'	5.80	-68.52	- 4.89	5.48	-106.50	- 1.16	5.25	-147.88	2.00
C_1'	5.80	-61.19	- 3.53	5.43	- 95.68	- 0.09	5.08	-138.55	3.38
N	4.84	-48.90	- 3.44	4.49	- 82.25	- 0.16	3.99	-125.65	3.35
O_1'	8.07	-76.21	- 4.65	7.81	-112.89	- 0.83	7.54	-153.44	2.67
P	8.02	-87.32	- 5.01	8.13	-123.85	- 1.20	9.11	-151.31	2.79
O_2'	9.21	-88.77	- 5.87	9.48	-123.60	- 1.82	9.53	-144.05	2.00
O_3'	6.81	-90.85	- 5.73	7.19	-128.57	- 2.16	9.92	-158.05	2.26

Table II (cont'd.)

	NUCLEOTIDE 8			NUCLEOTIDE 9			NUCLEOTIDE 10		
O_4'	9.28	-150.05	4.36	7.76	-164.54	7.96	7.73	-129.29	12.65
C_5'	8.31	-144.96	5.09	8.23	-162.24	9.29	7.85	-121.74	11.65
C_4'	7.58	-151.34	6.07	8.06	-151.92	9.62	7.59	-111.48	12.20
O_5'	6.62	-144.86	6.80	6.78	-147.44	9.26	6.20	-108.05	12.20
C_3'	6.98	-161.33	5.46	8.29	-149.44	11.08	8.09	-110.07	13.63
C_2'	5.75	-163.86	6.33	6.88	-150.87	11.63	6.84	-113.24	14.41
C_1'	5.29	-148.25	6.43	6.03	-144.85	10.43	5.68	-108.29	13.52
N	4.61	-132.83	6.37	4.74	-152.83	10.32	4.54	-119.08	13.52
O_1'	8.02	-168.69	5.57	8.89	-140.89	11.24	8.62	-101.16	13.87
P	8.79	-169.55	6.97	8.95	-136.43	12.68	8.70	- 97.46	15.37
O_2'	10.10	-165.43	6.89	10.25	-132.33	12.80	10.02	- 93.51	15.56
O_3'	9.15	-178.52	7.27	8.94	-143.11	13.73	8.67	-104.93	16.32

with C_3' endo forms of the sugar rings which are C_2' endo elsewhere. Such a simultaneous presence of sugars in C_2' and C_3' endo forms on the same chain has already been proposed for an alternating B-DNA structure in right-handed helix (24). Bases are almost perpendicular to the main axis of the conformation, well oriented and positionned for the WATSON-CRICK pairing of antiparallel and complementary chains. They are in position anti or high anti and the stacking is as good in the left section as in the right one. One can note that bases are at larger distances from the main axis in the left-handed section and that the stacking is less good for the nucleotides in the bends. The larger default in regularity is the 4 Å distance between bases in the second bend which realizes the transition from the left to the right-handed section. It seems to be very difficult to improve the conformation in this region unless some constraints are withdrawn ; one could allow nucleotides of the right-handed section to be on a pseudo helix like those in the left one or accept a super helical torsion or even admit different numbers of nucleotides for the right and the left-handed parts. Such realistic modifications of the present model would render its realization much easier ; the present point was to demonstrate that the most constraint side-by-side conformation is also possible. Junctions between right and left-handed parts present a good stereochemistry. There is no bad atomic

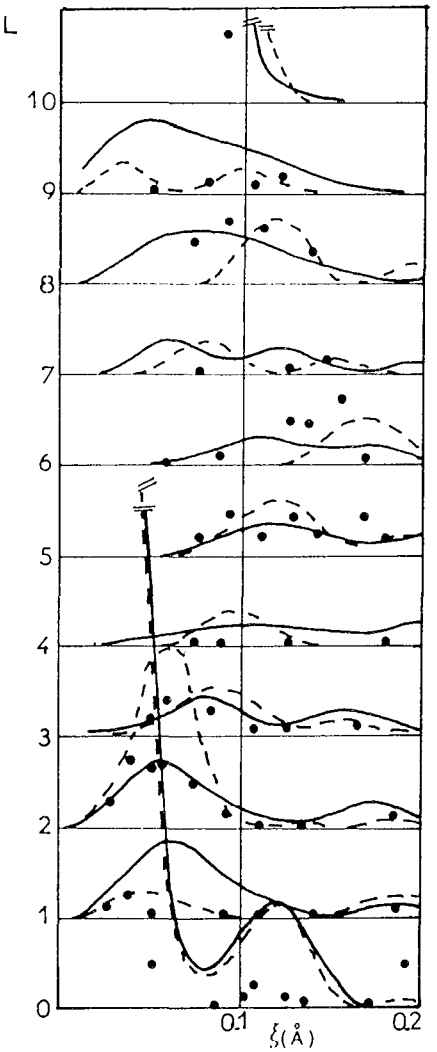

Figure II. Curves of the square of Fourier transform associated with the present model (——) ; curves for the B-DNA double helix (---) ; observed intensities (•).

contact, even between hydrogens, in the nucleotides of the two bends (contacts introduce in the first bend by the dihedral angle (O_1' P) close to the eclipse conformation do increase the van der Waals energy by less than 0.8 KCal/mole). This is also the case for the rest of the conformation and the total van der Waals energy (a 6-12 potential is used) of the present DNA model is as good as that associated to the refined right-handed double helix (19). Calculated diffracted intensities are in a much better agreement with experimental results than values previously obtained with side-by-side models (17) (18). The regular spacing of bases makes the meridian intensi-

ties to disappear except on layer lines 0 and 10. In figure 11, one can see that the comparison with calculated intensities obtained with the double helix does not allow a choice between one or the other model. Besides its importance as an eventual alternative to the B-DNA double helix, the present side-by-side conformation is mainly interesting because of its junctions between right and left-handed helices. These stereochemically acceptable parts of the conformation may be relevant in many other conditions in which the DNA appears to be composed of sections in different forms as it seems to be the case in some experiments on solutions and fibers (25).

References.

1. Drew, H., Wing, R.M., Takano, T., Broka, C., Tanaka, S., Itakura, K. & Dickerson, R.E. (1981) Proc. Nat. Acad. Sci. U.S.A. 78 (4), 2179-2183.
2. Wang, A.H.J., Quigley, G.J., Kolpak, F.J., Crawford, J.L., Van Boom, J.H., Van der Marel, G. & Rich, A. (1979), Nature 282, 680-686.
3. Drew, H., Takano, T., Tanaka, S., Itakura, K.& Dickerson, R.E. (1980), Nature 286, 567-573.
4. Leslie, A.G.W., Arnott, S., Chandrasekaran, R. & Ratliff, R.L. (1980), J. Mol. Biol. 143, 49-72.
5. Arnott, S., Chandrasekaran, R., Birdsall, D.L., Leslie, A.G.W. & Ratliff, R.L. (1980), Nature 283, 743-745.
6. Gupta, G., Bansal, M. & Sasisekharan, V. (1980), Proc. Nat. Acad. Sci. U.S.A. 77 (11), 6486-6490.
7. Patel, D.J., Canuel, L.L. & Pohl, F.M. (1979), Proc. Nat. Acad. Sci. U.S.A. 76 (6), 2508-2511.
8. Mitra, C.K., Sarma, M.H. & Sarma, R.H. (1981), Biochemistry 20, 2036-2041.
9. Stettler, U.M., Weber, H., Koller, Th. & Weissmann, Ch. (1979), J. Mol. Biol. 131, 21-40.
10. Klysik, J., Stirdivant, S.M., Larson, J.E., Hart, P.A. & Wells, R.D. (1981), Nature 290, 672-677.
11. Santella, R.M., Grunberger, D., Weinstein, I.B., & Rich, A. (1981) Proc. Nat. Acad. Sci. U.S.A., 78 (3), 1451-1455.
12. Behe, M. & Felsenfeld, G. (1981), Proc. Nat. Acad. Sci. U.S.A., 78 (3), 1619-1623.
13. Sage, E. & Leng, M. (1980), Proc. Nat. Sci. U.S.A., 77 (8), 4597-4601.
14. Bates, R.H.T., Levitt, R.M., Rowe, C.H., Doy, J.P. & Rodley, G.A. (1977), J. Royal Soc. (New Zeeland), 7 (3), 273-301.
15. Sasisekharan, V. & Pattabiranam, N. (1976), Current Sci. 45, 779-783.
16. Millane, R.P. & Rodley, G.A. (1981), Nucleic Acids Res., 9(7), 1765-1773.
17. Greenall, R.J., Pigram, W.J. & Fuller, W. (1979), Nature 282, 20-27.
18. Albiser, G. & Prémilat, S. (1980), Biochem. Biophys. Res. Comm. 95, 1231-1237.
19. Arnott, S. & Hukins, D.W.L. (1972), Biochem. Biophys. Res. Comm. 47, 1504-1509.
20. Levitt, M. & Warshal, A. (1978), J. Amer. Chem. Soc. 100, 2607-2613.
21. Olson, W.K. & Flory, P.J. (1972), Biopolymers 11, 1-66.
22. Prémilat, S. & Albiser, G. (1975), J. Mol. Biol. 99, 27-36.
23. Arnott, S. (1970), In Progress in Biophys. & Mol. Biol. 21, 265-319.
24. Klug, A., Jack, A., Viswamitra, M.A., Kennard, O., Shakked, Z. & Steitz, T.A. (1979), J. Mol. Biol. 131, 669-680.
25. Sasisekharan, V. & Brakmackari, S.K. (1981), Curr. Sci. 50, 1,10-13.

E) UNE ANALYSE CRITIQUE D'UN MODELE EN DOUBLE HELICE GAUCHE DE L'ADN EN FORME B

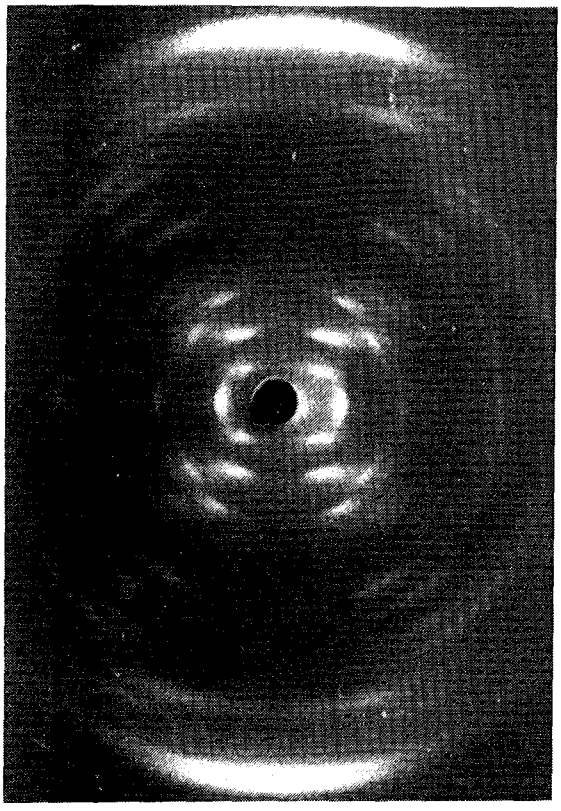

Photo N° 4 : Forme B de l'ADN avec sel de lithium à 75 % d'humidité relative.

Volume 10 Number 13 1982 Nucleic Acids Research

A critical analysis of a left-handed double helix model for B-DNA fibers

G.Albiser and S.Premilat

Laboratoire de Biophysique Moléculaire, E.R.A. CNRS No. 828, Centre ler Cycle, B.P. No. 239, 54506 Vandoeuvre les Nancy Cedex, France

Recieved 17 May 1982; Revised and Accepted 10 June 1982

ABSTRACT

A search for a left-handed double helix model for B-DNA fibers has been undertaken. The model has to present good stereochemistry and also to be in agreement with X-ray and infrared data. Dihedral angles as well as atomic coordinates and calculated intensities curves are given for the best model obtained. Comparison with experimental results shows that this model must be rejected as a candidate for the representation of B-DNA fibers.

INTRODUCTION

It is a well known fact that X-ray on fibers of'DNA can not give the handedness of DNA double helical conformations (1,2). The only evidence used by Watson and Crick for the proposal of a right-handed double helix for the B-DNA was based on stereochemistry (3). Indeed left-handed double helices were built but they presented poor interatomic contacts and thus were rejected. The same scheme of reasoning was used for the proposition of the A form of DNA (4). Even if crystals of nucleotides and t-RNA do present fragments of right-handed helices (5), it is not possible to generalize on the rotational sense of helices of DNA and RNA in fibers or in solutions. New proposed models for the B-DNA, called "side-by-side models" (6,7,8) and constituted from alternating right and left-handed sections of helices have restarted the controversy on this subject (9). The discovery of the left-handed helix (Z-DNA) (10) for crystals of short sequences of purine and pyrimidine nucleotides as well as that of a right-handed double helix of dodecanucleotides (11) demonstrate the polymorphism of DNA molecules.

Besides these experimental studies, theoretical approaches allow one to propose models of left-handed helices having good stereochemistry and parameters corresponding to DNA in its B-

0305-1048/82/1013-4027$ 2.00/0

form (12,13,14,15) and even in its A and C forms (12). Moreover, it has been shown that transitions between Z and B forms are possible in solution (16,17) and fibers (18). As a right-handed double helix which agrees with infrared and X-ray measurements has been proposed for the B-DNA (19), it is interesting to know if a left-handed double helical model can also be accepted or rejected.

In the present work, we have searched for conformations of the DNA in left-handed double helices with a geometry in agreement with the experimental data from infrared spectroscopy (20) as well as from X-ray (2). Dihedral angles of a left-handed double helix conformation are presented together with atomic coordinates and curves of calculated intensities ; comparison with X-ray data enables this kind of conformation as a model for the B-DNA to be rejected.

METHOD

A first step in the determination of a left-handed double helix is the building of a physical model which has the helical parameters of B-DNA, namely a pitch of 33.8 Å and 36° of rotation per base pair. One can also, on this model orientate the phosphate group in order to verify roughly the orientations given by infrared (20) : the direction of the oxygen atoms O_1O_2 has to make an angle of 56° with the helix axis and the bisector of O_1PO_2 an angle of 70° with this axis. This model can hardly be a precise one but it permits the determination of a set of dihedral angles which allows one to compute a well defined conformation. The computational method used to get atomic coordinates of a double helix constrained to agree with geometrical parameters obtained from X-ray and infrared has been previously presented (19) and already used to obtain a right-handed double helical model for B-DNA.

The cylindrical coordinates of the atoms of the helix which give good geometrical parameters and also good stereochemistry are used to calculate the Fourier transform and theoretical diffracted intensities. The same procedure (21) as previously used is followed but the order n of the Bessel functions are now defined by $n = -l + 10m$ for the layer line l (with m an integer).

RESULTS

Table I gives values of the dihedral angles for the best left-handed double helical conformation now obtained (model I). The geometrical parameters of this helix are also given in this table ; the orientation of the base plane is given by the tilt and twist and their position relative to the axis is defined by the distance of the line D joining the atom C_6 (pyrimidine) to C_8 (purine) (22). In table II the directions of O_1O_2 and the bisector of O_1PO_2 relative to the helix axis are presented. In table III atomic coordinates of a nucleotide are given for this model and figure I presents a schematic diagram showing a projection of the left-handed double helix. On figure II curves of the calculated intensities are given and compared with experimental values.

Table I

Chain dihedral angles and parameters of the left-handed double helices.

	model I	model I'
α (o) (P - O5')	58.41	- 160.04
β (o) (O5' - C5')	- 132.88	115.82
γ (o) (C5' - C4')	159.93	24.48
δ (o) (C4' - C3')	138.29	135.88
ε (o) (C3' - O3')	- 71.54	- 7.87
ξ (o) (O3' - P)	179.27	169.66
χ (o) (C1' - N)	- 190	- 159
P (Å)	33.8	34
θ (o)	- 36	- 36
p (Å)	3.38	3.4
tilt (o)	18	- 10
twist (o)	- 4	- 1
D (Å)	- 0.73	1.95

P $\overset{\alpha}{-}$ O5' $\overset{\beta}{-}$ C5' $\overset{\gamma}{-}$ C4' $\overset{\delta}{-}$ C3' $\overset{\varepsilon}{-}$ O3' $\overset{\xi}{-}$ P

χ : O1' - C1 - N1 - C2 for (C,T)
- C4 for (G.A)

Table II

Geometry of the phosphate group compared with infrared results.

Angle with the helical axis	Infra Red Ref (20)	Model I	Model I'
of (O_1O_2)	56°	55° 6	55°
of the bissector of (O_1PO_2)	70°	69°58	68° 5

DISCUSSION

Many different left-handed double helices have already been proposed for B-DNA (12,13,14). Indeed it is not very difficult to obtain such conformations with good stereochemistry and helical parameters in agreement with X-ray data. But if one imposes constraints on the geometry in order to agree also with I.R. data, then almost all these conformations are eliminated. The model

Table III

Atomic cylindrical coordinates for one nucleotide of model I.

Atom	R_j (Å)	ϕ_j (o)	Z_j (Å)	Atom	R_j (Å)	ϕ_j (o)	Z_j (Å)
Phosphate				Guanine			
O3'	7.74	-122.88	2.62	N9	4.40	- 96.58	1.44
P	9.2	-122.86	3.27	C8	4.72	- 80.30	1.40
O1	9.67	-114.64	3.65	N7	3.89	- 67.69	0.95
O2	10.20	-125.81	2.29	C5	2.65	- 77.46	0.70
O5'	9.04	-128.98	4.53	C4	3.12	-102.55	1.00
Desoxyribose				N3	3.03	-127.57	0.90
C5'	8.84	-102.01	0.93	C2	2.07	-145.68	0.45
C4'	7.85	-106.31	1.89	N2	2.80	-172.33	0.29
C3'	7.55	-116.99	1.45	N1	0.80	-129.45	0.13
C2'	6.14	-116.63	0.89	C6	1.44	- 60.46	0.22
C1'	5.51	-106.95	1.88	O6	1.87	- 20.92	-0.10
O1'	6.68	- 99.52	2.04				

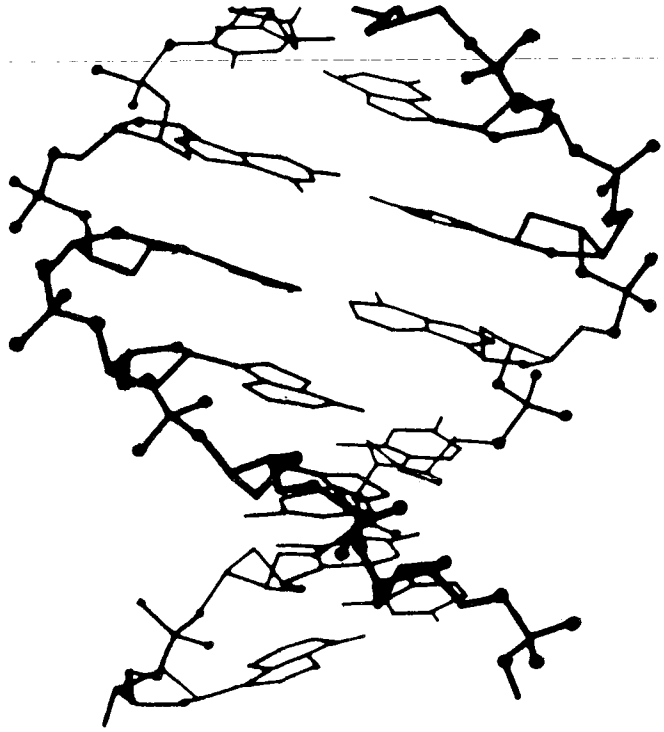

Figure I

Schematic diagram showing the projection of the left-handed double helix (model I).

proposed (model I) is the only one we obtained which fulfills all the geometrical conditions. It presents very good stereochemistry ; the dihedral angles have values in domains commonly allowed for nucleotides (23). The sugar pucker is C_2' endo, its plane is almost perpendicular to the helix axis while it is parallel for right-handed helices (2,19). This last feature induces an important tilt of 18° on the base plane but the small twist of 4° has no effect on their good pairing. The stacking of bases is good (the distance D is small (22) and the phosphorous atom is approximately 9 Å from the helix axis in agreement with X-ray data). The minor groove is narrower for this left-handed conformation than for the right-handed ones (2). When calculated intensities are compared with observed ones, many large disagreements can be seen such that calculated intensities on the layer lines 1, 3, 5, 7 and 10 are much too small when compared with experimental values. Layer lines 4 and 9 also present poor agreement with observed intensities as experimental values are small and the calcula-

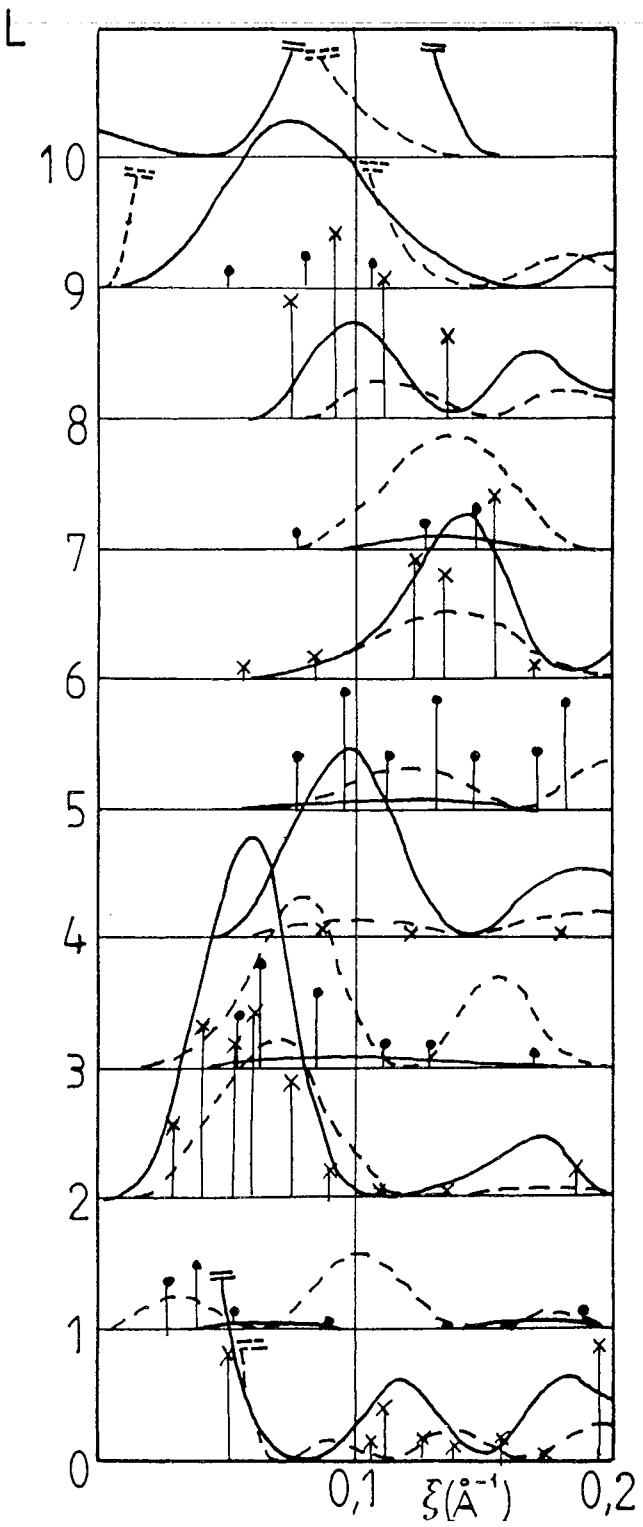

Figure II

Curves of the diffracted intensities, calculated with the model I (——), with the model I' (---), experimentally observed intensities (× •).

ted ones very strong. It was not possible to improve the calculated intensities because the bases cannot be put perpendicular to the axis while the rest of the conformation remains acceptable.

Nevertheless in order to verify that the large tilt of the bases is the main reason for the disagreement between calculated

and observed intensities, another model (I') was determined. This conformation does present good helical parameters (table I) and a good orientation of the phosphate group (table II), the sugar is C_2' endo but the base plane present a tilt of 10° in the opposite sense when compared with model I and near to the tilt found in right-handed helices (2,19,22). The stereochemistry of this conformation is not good ; one can see in table I that many dihedral angles have values far from their permitted regions (23) and cannot be improved when geometrical constraints are maintained. Nevertheless the calculated intensities (fig.II) are better even if large disagreements remain on layer lines 7, 8 and 9.

Thus it seems that the large tilt of bases in the model I is the main reason for the disagreement between the calculated and observed intensities. This geometrical characteristic cannot be modified when one tries to produce a left-handed double helical model of B-DNA which must fit all the geometrical constraints related to X-ray and infrared and also present good stereochemistry. As such a good model has been established for a right-handed double helix of DNA in the B form (19) it appears that a choice can be proposed in favour of this last sense of rotation.

REFERENCES

1. Franklin, R.E. & Gosling, R.G. (1955), Acta Cryst. 8, 151-156
2. Langridge, R., Wilson, H.R., Hooper, G.W. & Wilkins, M.H.F. (1960), J. Mol. Biol., 2, 19-64
3. Crick, F.H.C. & Watson, J.D. (1954), Proc. Roy. Soc. 223, 80-96
4. Fuller, W., Wilkins, M.H.F., Wilson, H.R. & Hamilton, L.D. (1965), J. Mol. Biol. 12, 60-80
5. Rosenberg, J.M., Seeman, N.C., Kim, J.J.P., Nicholas, S.H.B. & Rich, A. (1973), Nature, 243, 150-154
6. Bates, R.H.T., Levitt, R.M., Rowe, C.H., Doy, J.P. & Rodley, G.A. (1977), J. Royal. Soc. (New Zeeland), 7 (3), 273-301
7. Sasisekharan, V. & Pattabiraman, N. (1976), Current Sci. 45, 779-783
8. Prémilat, S. & Albiser, G. (1982), Biochem. Biophys. Res. Comm. 104, 22-29
9. Crick, F.H.C., Wang, J.C. & Bauer, W.R. (1979), J. Mol. Biol. 129, 449-461
10. Wang, A.H.J., Quigley, G.J., Kolpak, F.J., Crawford, J.L., van Boom, J.H. van der Marel, G. & Rich, A. (1979), Nature 282, 680-686
11. Dickerson, R.E. & Drew, H.R. (1981), J. Mol. Biol. 149, 761-786

12. Gupta, G., Bansal, M. & Sasisekharan, V. (1980), Proc. Nat. Acad. Sci. U.S.A. 77, 6486-6490
13. Arnott, S. (1980), Fiber diffraction methods, A.C.S. Symposium series 141 - pp. 1 - 30 A.C.S. Washington
14. De Santis, P., Morosetti, S. & Palleschi, A. (1981), Biopolymers 20, 1727-1739
15. Hopkins, R.C. (1981) Science 211, 289-291
16. Behe, M., Zimmerman, S. & Felsenfeld, G. (1981), Nature 293, 233-235
17. Malfoy, B., Hartmann, B. & Leng, M. (1981), Nucleid Acids Research 21, 5659-5669
18. Sasisekharan, V. & Brahmachari, S.K. (1981), Curr. Sci., 50, 1, 10-13
19. Prémilat, S. & Albiser, G. (1982), C.R. Acad. Sci. Paris, 294, III, 241-244
20. Pilet, J. & Brahms, J. (1973), Biopolymers 12, 387-403
21. Prémilat, S. & Albiser, G. (1975), J. Mol. Biol., 99, 27-36
22. Arnott, S. & Hukins, D.W.L. (1973), J. Mol. Biol., 81, 93-105
23. Sundaralingam, M. (1969), Biopolymers, 7, 821-860

F) DISCUSSION

Les travaux présentés dans ce chapitre font usage de trois conformations très différentes pour interpréter les clichés RX de la forme B de l'ADN à haute humidité relative.

Pour le modèle en double hélice droite classiquement admis, on remarque que les intensités calculées ne sont pas sensibles à la composition en bases de l'ADN. Par contre, sur les clichés à 92 % d'humidité relative, on constate une corrélation entre l'augmentation du pourcentage G-C et l'augmentation de la distance entre axes des hélices (distance déduite du paramètre a du réseau hexagonal). Cette distance est plus grande pour les ADN en présence de lithium que pour ceux associés au sodium.

C'est la variation du paramètre a du réseau qui entraîne une variation des intensités mesurées puisque l'on échantillonne les courbes continues de l'intensité en des endroits différents. D'autre part, l'augmentation de la distance entre les axes des hélices s'explique par une plus grande quantité d'eau associée due à la présence d'une plus grande quantité de cations alcalins. En effet, dans ce cas, les fibres d'ADN ont été préparées à partir de solutions dont la concentration en sel n'a pas été contrôlée. Cependant, dans des expériences ultérieures où les concentrations en sel des solutions sont fixées par dialyse, on ne constate plus de variation de la distance entre molécules d'ADN lorsque le pourcentage en G-C varie (57) à une humidité relative donnée.

L'étude des cristaux d'oligonucléotides a montré que les séquences A-T possèdent une chaîne d'eau structurée dans le petit sillon (58). Cela rigidifie la structure de la forme B

et empêche le passage vers la forme A pour les ADN riches en séquence A-T. Néanmoins, cet effet dépend aussi de la concentration en sel alcalin.

Le modèle "side by side", montre que la diffraction RX de fibre prise comme seul critère n'est pas capable de disqualifier un modèle conformationnel. En effet, le facteur d'accord entre intensités calculées et expérimentales est voisin du modèle en double hélice. Néanmoins, le seul fait de pouvoir construire ce modèle avec une bonne stéréochimie révèle une grande souplesse de la chaîne sucre-phosphate. Cette grande richesse de conformation est bien mise en évidence par les structures d'oligonucléotides déjà établies (47). Avec ceux-ci on n'a pas de régularité conformationnelle d'un nucléotide à l'autre comme cela est logiquement proposé pour la diffraction de fibre. Ainsi, la cristallographie des oligonucléotides a récemment mis en évidence des jonctions entre hélices droite et gauche qui se font sur trois paires de bases (59). Dans le meilleur modèle "side by side" la jonction se fait sur deux paires de bases et c'est pourquoi on obtient un mauvais espacement entre paires de bases pour le passage de la section gauche à la droite.

Enfin, il faut noter que le modèle "side by side" proposé ne donne pas un bon accord comme celui obtenu avec le modèle en double hélice droite, avec les expériences de diffusion RX isotrope par des solutions d'ADN de thymus de veau (60).

Pour construire et tester le troisième modèle envisagé, les contraintes imposées par le dichroïsme linéaire infrarouge ont été utilisées. Dans ce cas, on constate qu'aucun modèle en double hélice gauche ne peut satisfaire à la fois à une bonne

stéréochimie et aux résultats expérimentaux des RX et de l'infrarouge. Il faut remarquer qu'aucun cristal d'oligonucléotide n'a révélé cette double hélice gauche de forme B. Par contre, en solution, des études de dichroïsme circulaire ont montré qu'un hexanucléotide self complémentaire le d(CG-CG-CG) possédait une forme B gauche, mais dans ce cas, le désoxyribose est gauche et non droit comme il est habituellement trouvé dans les ADN naturels (61).

CHAPITRE III:MODELES CONFORMATIONNELS DE L'ADN EN ACCORD AVEC LES DONNEES R.X.,I.R. ET RMN

A) INTRODUCTION

Après la mise en évidence d'une double hélice gauche, appelée z , par diffraction RX d'un cristal d'un hexanucléotide (13), une grande effervescence s'est manifestée pour de nouvelles interprétations des clichés de diffraction de fibre des ADN et des polynucléotides. Les clichés de fibres révèlent en effet un certain polymorphisme avec les formes A, B, C et D dont les paramètres hélicoïdaux sont parfaitement établis mais, jusque là, interprétés à l'aide de conformations en hélices droites. Entre certaines de ces formes des transitions conformationnelles peuvent être induites dans les fibres par des changements d'humidité relative et de concentration de sel.

Tous ces faits, révélant la grande flexibilité conformationnelle de l'ADN, ont entraîné des propositions de modèles aussi bien d'hélices droites que gauches pour les formes A, B et D (14). Les critères justifiant ces modèles conformationnels étant alors limités à leur bonne stéréochimie, à des énergies de conformation acceptables et à un bon accord avec la diffraction RX.

Or, en complétant les critères précédents par la nécessité de vérifier les résultats obtenus par une autre technique, le dichroïsme linéaire infrarouge de films orientés, on a pu établir que la forme B de l'ADN ne pouvait pas être une conformation en double hélice gauche. En poursuivant cette démarche, l'objectif des publications présentées dans ce chapitre est de proposer des modèles conformationnels pour les

formes A, B, C, D qui rendent compte des diverses données expérimentales. Ces dernières étant obtenues de la diffraction RX de fibre, le dichroïsme linéaire infrarouge, parfois la RMN du P^{31}.

B) CONFORMATIONS DE L'ADN A ET B EN ACCORD AVEC LES RX DE FIBRES ET LE DICHROISME INFRAROUGE

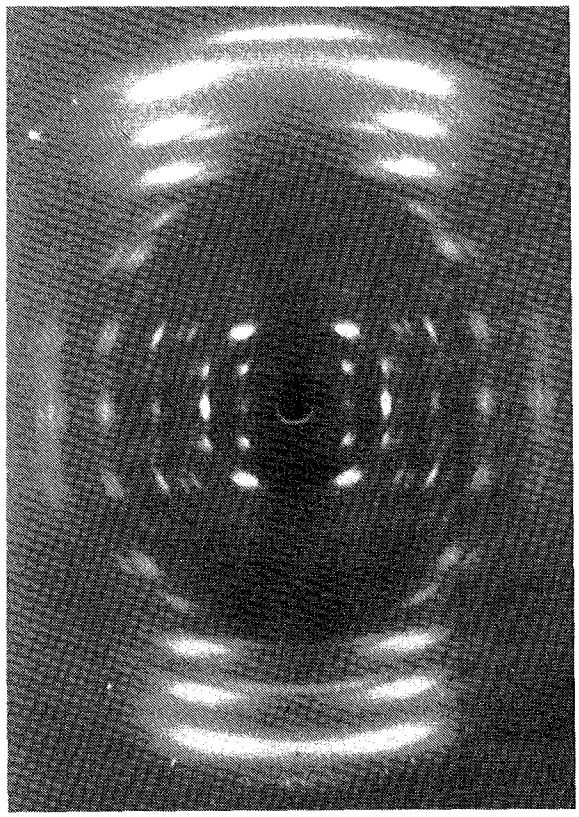

Photo N° 5 : Forme A de l'ADN avec sel de sodium à 75 % d'humidité relative.

Volume 11 Number 6 1983 Nucleic Acids Research

Conformations of A-DNA and B-DNA in agreement with fiber X-ray and infrared dichroism

S.Premilat and G.Albiser

Laboratoire de Biophysique Molèculaire, Université de Nancy I, Faculte des Sciences, ERA CNRS No. 828, Centre 1ER Cycle, B.P. No. 239, 54506 Vandoeuvre les Nancy, France

Received 10 February 1983; Accepted 1 March 1983

ABSTRACT

Two right handed double helices are proposed as models for DNA fibers in respectively the A and the B form. The present conformations have geometrical parameters which agree very well with fiber X-ray and the orientation of their phosphate groups is in good accordance with infrared dichroïsm measurements. Dihedral angles and complete sets of atomic coordinates are given together with stereo-views and curves of the calculated diffracted intensities. Results are compared with experimental data and with preceding DNA models.

INTRODUCTION

X-ray diffraction on DNA fibers provides the helical parameters i.e. the pitch and the number of nucleotides per turn of the double helices. The pattern of the intensity distribution is also an experimental result of main importance as the information it contains must be used as constraints when molecular conformations of DNA are proposed. This is the way A and B models of DNA have been established (1,2) and refined (3,4). Actually, to improve the fit of the calculated diffraction pattern to the observed one, the molecular model has to go through cycles of adjustement. But the structural model so obtained cannot be unique because of the poor precision of the experimental data. Indeed, in this process, even the hand of the double helix must be arbitrarily defined. These limitations on models derived from X-ray data led to many different proposal for the B form of DNA like left handed helices (5) and "side by side" models (6,7,8) and some also for the A form (9).

However, regarding the overall features of the A and B forms and mainly the hand of the DNA double helices, it seems that the ambiguity has been ri..d by the experimental results obtained

from single crystal studies. Actually, the structures of self complementary oligodeoxynucleotides have recently been determined to be right handed helices of the classical type for the A (10) as well as for the B form (11). In these cases, one should note that the determined structures present sequence dependent local irregularities which may disappear in long stretched DNA fibers or, at least, which cannot be defined with X-ray fiber diffraction patterns.

Besides X-ray diffraction, some structural parameters of DNA fibers have been determined by different spectroscopic measurements. Infrared linear dichroïsm, for example, permitted the determination of the orientation of the phosphate group in different DNA conformations (12). However the interpretation of these experimental values led to geometrical parameters which are not in accordance with the models obtained from X-ray fiber diffraction. This disagreement has been interpreted to be due to an incorrect use of the infrared dichroism data (13). But it could also come from structural details of the models presently admitted as the conformations of the A and B forms of DNA. Such a view may be supported by the fact that recent NMR measurements (14) on the A form of poly nucleotides gave a geometry of the phosphate group in good agreement with infrared data and also with the A-DNA model proposed by Fuller et al.

The aim of the present work is to remove this discrepany ; it proposes molecular models for the A and B forms of DNA which agree as well with fiber X-ray data as with infrared measurements. These two DNA conformations are right handed double helices with antiparallel and complementary chains the bases of which are associated according to the Watson-Crick pairing. Dihedral angles corresponding to these structures are presented together with atomic coordinates and stereo-views. For these A and B forms of DNA, the geometry of the phosphate groups and the curves of the calculated diffracted intensities are compared with experimental data.

METHOD

Geometrical constraints are imposed on the calculated molecular conformations in order to define precisely the DNA structures

in the A and B forms. Firstly, one takes into account the information deduced from X-ray measurements : the repeat unit of the A-DNA must be of 28 Å length and 34 Å for the B-DNA, the number of nucleotide pairs per turn is fixed to 11 in the A form (2.56 Å between successive nucleotides) and 10 for the B-DNA (3.4 Å between successive bases).

The computation of the atomic coordinates of a nucleotide sequence placed in a helical conformation is performed with the procedure previously used (15). The geometry of the sugar phosphate backbone is completely defined by the set of values given to the dihedral angles ; bond angles and bond lengths can also be very slightly varied but they are maintained in intervals of values determined by X-ray studies on single crystals (16). The values presently used are near to those listed by Arnott (17).

The bicatenary DNA molecules are composed of two complementary and antiparallel chains, the pairing of bases being realized as proposed by Watson and Crick. Therefore, the DNA conformation must present a dyadic symmetry with corresponding axis perpendicular to the helical axis of the molecular system. When a chain is built in the proper helical form, the complementary and antiparallel one is rotated around the helix axis and adjusted to the position corresponding to the best hydrogen bonds between associated bases. This process permits the determination of the dyadic axis and, therefore, of the correct reference frame for which each atom with the cylindrical coordinate (R,Φ, Z) has an homologous at $(R,-\Phi,-Z)$.

The model building programme allows us to modify progressively the dihedral angles of the molecular chain starting from values taken on physical models which verify roughly the geometrical constraints imposed on the double helices (pitch, number of nucleotides per turn and orientation of the phosphate group). An iterative procedure is used to optimize the orientations of the O_1O_2 direction and that of the bissector of O_1PO_2 relative to the helix axis. The fitting of these orientations to the experimental values (infrared dichroism) is realized maintaining the constraints on the helical parameters of the conformation. At the end of these improvement cycles a molecular model in conformity with X-ray and infrared data is obtained. The stereochemistry

of the model is tested in order to eliminate, by very small variations of the dihedral angles, the possible too short interatomic distances. If the helical or orientation parameters are then too much modified, one comes back to the iterative procedure to refine the structure.

The average Fourier transform and the diffracted intensity curves are computed using the cylindrical coordinates of atoms of the best calculated conformations. Relations and parameters necessary for these calculations are those given by Langridge et al.(1) and used previously (15). The fit of the calculated intensities to the observed values can be improve on the higher layer lines by small variations of the tilt and twist of the base plans. But one also takes into account the fact that such possible movements may have some effect on the position of the dyadic axis and thus on the Fourier transform on all the layer lines. Even if for DNA fibers in A or B forms, the helical parameters do not vary appreciably with the base composition as long as it remains statistical (15) and not regular like in copolymers (18), diffracted intensities are calculated with 58 % of (A-T) base pairs. This percentage corresponds to that of the calf thymus DNA and comparison with the experimental values given by Langridge et al.(1) for the B-DNA and by Fuller et al. (2) for the A form can thus be done.

RESULTS

In table I are listed the dihedral angles corresponding to the best A and B double helical conformations obtained. Characteristic geometrical parameters are also given in this table. The orientation of the base planes is indicated by the tilt and their position relative to the helical axis is given by the distance D to this axis of the line joining the atoms C6 (pyrimidine)and C8 (purine) (4).

The orientations of the directions of O1O2 and of the bissector of O1PO2 relative to the helix axis are presented in table II and compared with infrared dichroism measurements and also with the values corresponding to the conformations nowadays generally accepted as A and B models (3).

Bond angles and bond lengths used for the calculations of

Table I

Chain dihedral angles and parameters of the A and B-DNA double helical conformations.

DIHEDRAL ANGLES (°)	A-DNA	B-DNA
α (P - O5')	- 59.63	- 30.93
β (O5'-C5')	163.55	148.71
γ (C5'-C4')	51.20	37.02
δ (C4'-C3')	81.00	132.32
ε (C3'-O3')	-136.26	-156.80
ζ (O3'- P)	- 87.11	-133.62
χ (C1'- N)	-165.00	-120.00
GEOMETRICAL PARAMETERS	**A-DNA**	**B-DNA**
Helix Pitch (Å)	28.16	33.90
Rotation/Residue (°)	32.73	36.00
Rise/Residue (Å)	2.56	3.39
Base tilt (°)	20.	-3.6
D : Distance to axis of C6(Pyr) C8(Pur) (Å)	4.5	-0.6

P $\underline{\alpha}$ O5' $\underline{\beta}$ C5' $\underline{\gamma}$ C4' $\underline{\delta}$ C3' $\underline{\varepsilon}$ O3' $\underline{\zeta}$ P

χ { O1 - C1' - N1 - C2 for (C,T)
  { O1'- C1' - N9 - C4 for (G.A)

Table II

Geometry of the phosphate group of the A and B-DNA models.

Angle (°) relative to the helix axis of :	A-DNA		B-DNA	
	Infrared *	Model	Infrared *	Model
O1O2	65	64.4 (79)	56	56.7 (75)
the bissector of O1PO2	45	44.8 (15)	70	71.3 (54)

* : ref. 12, 13 ; ( ) models ref. 3, 13

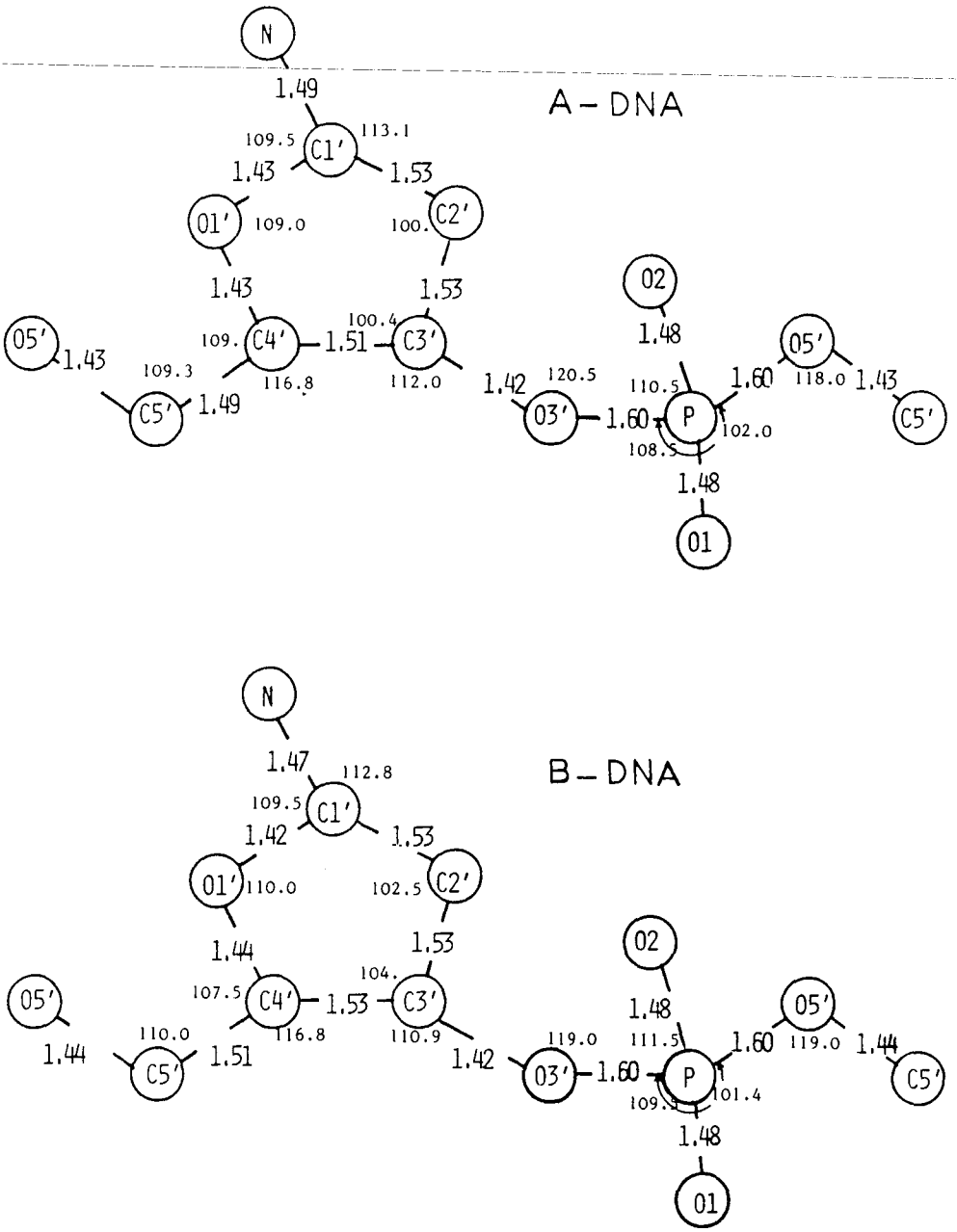

Figure I

Bond angles and bond lenghts of the sugar-phosphate backbones of the A and B-DNA. Lenghts in (Å) and angles in (°).

atomic coordinates are presented in the fig. I. The complete set of cylindrical coordinates of atoms in the A-DNA model is given in table III. The values of the B-DNA are listed in the table IV. These tables contain the coordinates of the atoms of the phosphate-sugar backbone and of the four different bases placed at the same level. The helical and dyadic symmetries

Table III

Atomic cylindrical coordinates of the A-DNA double helix unit.

A - DNA							
ATOM	R_j(Å)	$\Phi^{(o)}$	Z_j(Å)	ATOM	R_j(Å)	$\Phi_j^{(o)}$	Z_j(Å)
Phosphate				Sugar			
O3'	9.74	-35.63	5.06	C5'	9.96	-52.35	3.62
P	8.94	-34.10	6.43	C4'	9.86	-44.23	3.13
O1	9.86	-35.86	7.56	C3'	9.05	-37.99	3.88
O2	7.80	-40.49	6.51	C2'	9.17	-30.86	2.86
O5'	8.71	-23.84	6.31	C1'	8.70	-35.86	1.63
				O1'	9.31	-44.03	1.81
Guanine				Adenine			
N9	7.22	-36.34	1.45	N9	7.22	-36.35	1.45
C8	6.52	-45.48	1.73	C8	6.46	-45.74	1.73
N7	5.22	-44.38	1.45	N7	5.16	-45.26	1.46
C5	5.17	-30.09	0.97	C5	5.14	-30.81	0.99
C4	6.51	-27.14	0.96	C4	6.47	-27.37	0.97
N3	7.22	-18.21	0.58	N3	7.14	-18.09	0.57
C2	6.62	- 9.10	0.16	C2	6.47	- 9.32	0.17
N2	7.48	- 1.46	- 0.27	N1	5.14	- 6.10	0.12
N1	5.29	- 6.35	0.12	C6	4.30	-18.12	0.53
C6	4.33	-17.35	0.51	N6	2.97	-16.98	0.49
O6	3.12	-14.47	0.44				
Cytosine				Thymine			
N1	7.22	-36.35	1.45	N1	7.22	-36.35	1.45
C6	6.67	-46.23	1.79	C6	6.63	-46.32	1.78
C5	5.38	-49.82	1.64	C5	5.36	-50.01	1.65
C4	4.55	-37.66	1.13	CH_3	5.11	-66.43	2.02
N4	3.23	-38.28	0.95	C4	4.49	-38.17	1.14
C3	5.32	-25.26	0.80	O4	3.26	-38.32	0.96
C2	6.66	-26.93	0.96	N3	5.33	-25.88	0.83
O2	7.52	-19.88	0.67	C2	6.70	-27.03	0.97
				O2	7.50	-19.97	0.67

Table IV

Atomic cylindrical coordinates of the B-DNA double helix unit.

B-DNA							
ATOM	R_J(Å)	$\Phi_J^{(o)}$	Z_j(Å)	ATOM	R_J(Å)	$\Phi_j^{(o)}$	Z_j(Å)
Phosphate				Sugar			
O3'	8.42	-61.32	0.28	C5'	8.53	-80.00	-2.13
P	9.31	-59.99	1.59	C4'	7.73	-72.21	-1.48
O1	10.74	-59.47	1.21	C3'	7.99	-70.60	0.01
O2	9.22	-67.05	2.53	C2'	6.68	-73.70	0.69
O5'	8.82	-51.08	2.18	C1'	5.64	-71.28	-0.41
				O1'	6.32	-74.33	-1.62
Guanine				Adenine			
N9	4.49	-81.65	-0.28	N9	4.49	-81.66	-0.29
C8	4.84	-97.48	-0.23	C8	4.83	-98.18	-0.23
N7	3.96	-110.55	-0.11	N7	4.01	-111.83	-0.11
C5	2.67	-102.18	-0.09	C5	2.72	-103.41	-0.09
C4	3.14	- 76.56	-0.19	C4	3.13	- 77.39	-0.19
N3	2.97	- 51.41	-0.21	N3	2.90	- 51.88	-0.21
C2	1.92	- 32.33	-0.11	C2	1.80	- 34.78	-0.10
N2	2.66	- 3.86	-0.11	N1	0.53	- 60.26	0.01
N1	0.64	- 55.09	0.0	C6	1.52	-123.10	0.02
C6	1.50	-122.07	0.02	N6	2.17	-160.23	0.12
O6	2.00	-158.55	0.12				
Cytosine				Thymine			
N1	4.49	- 81.65	-0.28	N1	4.49	- 81.65	-0.28
C6	5.01	- 96.89	-0.25	C6	5.00	- 97.23	-0.24
C5	4.52	-112.0	-0.13	C5	4.52	-112.31	-0.12
C4	3.14	-117.62	-0.05	CH_3	5.71	-123.71	-0.08
N4	3.17	-141.88	0.07	C4	3.18	-119.01	-0.04
C3	2.31	- 95.53	-0.09	O4	3.14	-141.55	0.07
C2	3.26	- 75.15	-0.21	N3	2.35	- 95.72	-0.09
O2	3.40	- 53.84	-0.25	C2	3.25	- 74.12	-0.21
				O2	3.32	- 52.74	-0.24

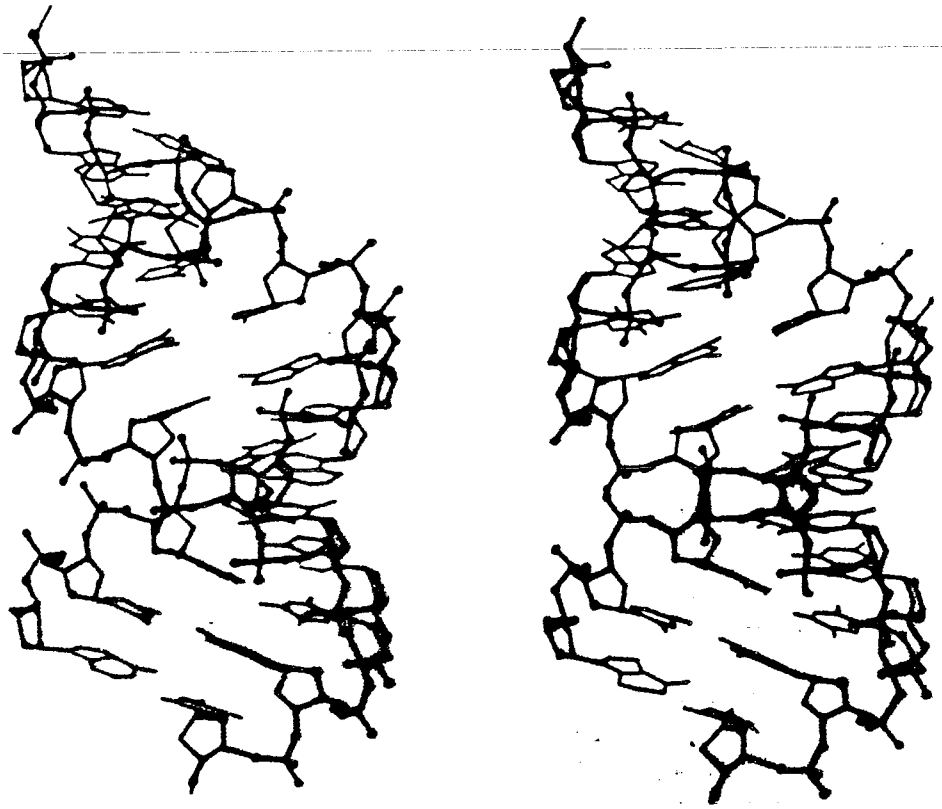

Figure II
Stereo-view of the A-DNA double helix.

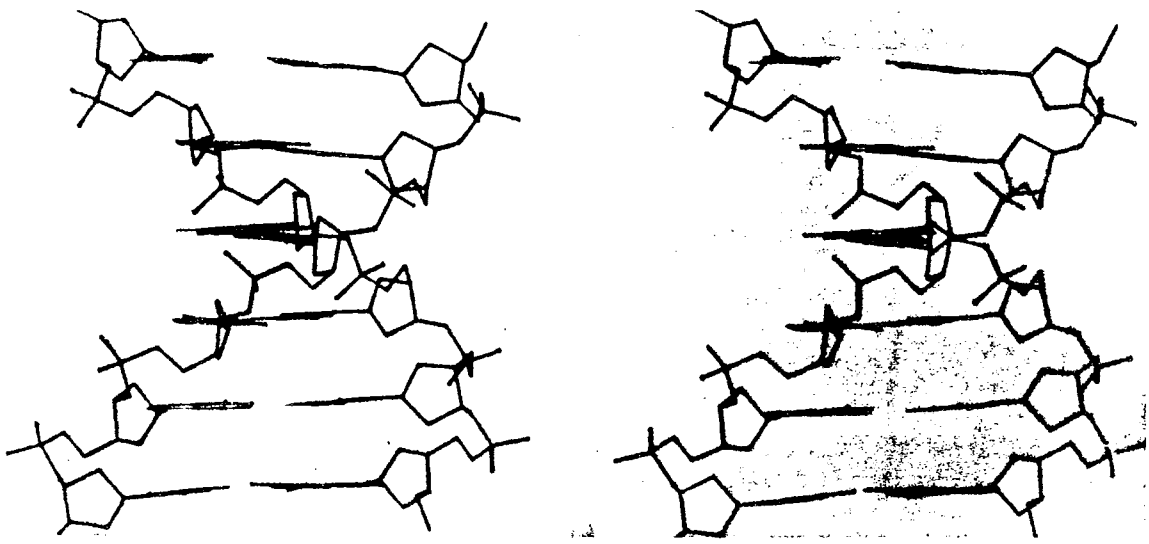

Figure III
Stereo-view of the B-DNA double helix.

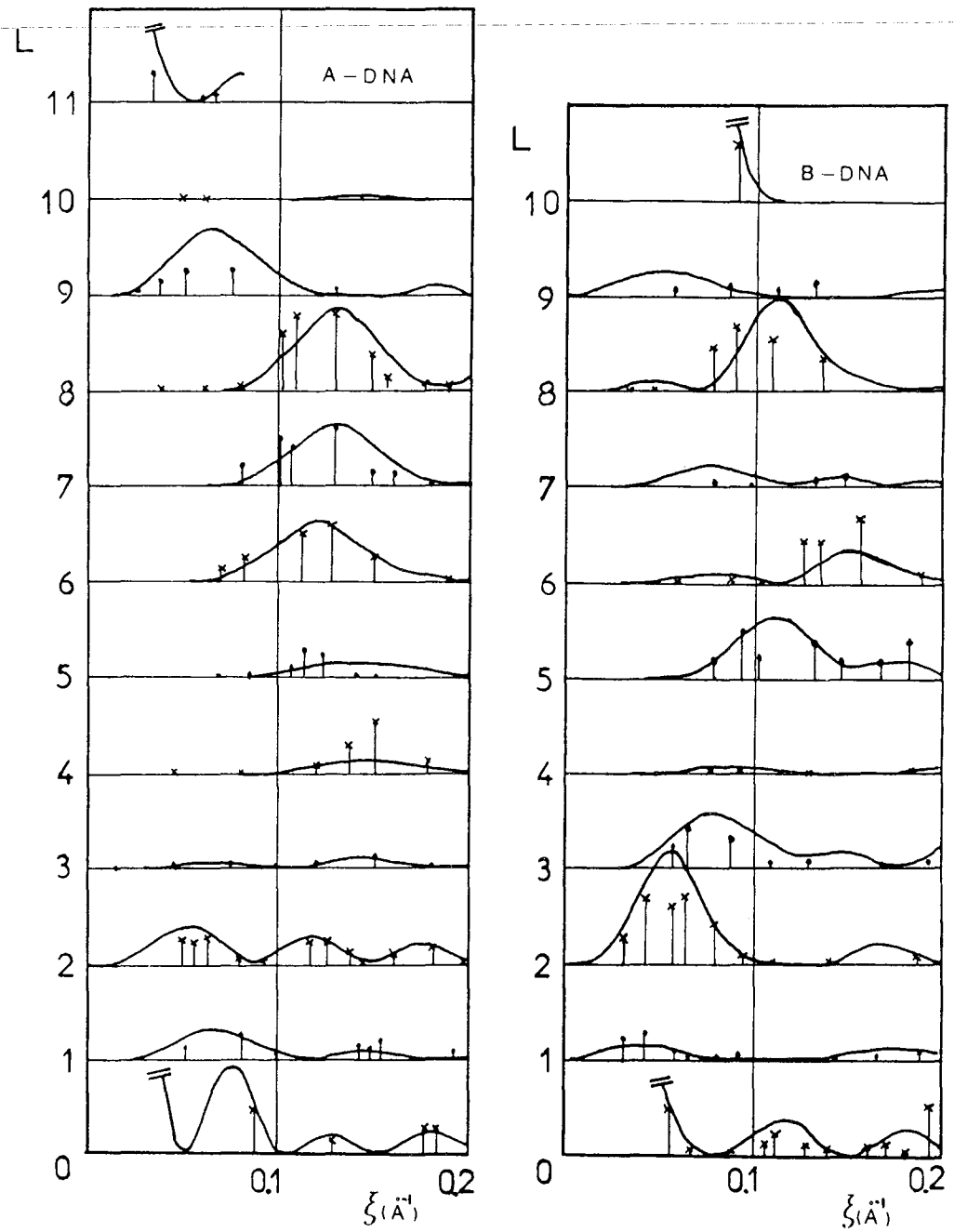

Figure IV

Curves of the diffracted intensities calculated with the A-DNA and B-DNA models. (x, •) experimental values.

allow an easy calculation of the atomic coordinates of any other nucleotide.

On fig.II one can see a stereo-view of the present A-DNA conformation and on fig.III is given the stereo-view of the proposed B-DNA structure. Curves of the calculated intensities

for the two DNA models are presented on fig.IV. Experimental data are also depicted on this figure in order to facilitate the comparison with the calculated values.

DISCUSSION

The present conformations are proposed for the interpretation of different experimental measurements made on long fibers or films of DNA in the A or B form. In such fibers, nucleotides do present a structural regularity (maybe an average) which corresponds very well to the two double helical models. But the proposed molecular structures are not adapted to the more precise and somewhat irregular conformations determined with X-ray on crystals of short polynucleotide chains (10,11).

Constraints imposed on the geometry of the phosphate group which must fit to results from infrared measurements and those related to fiber X-ray data limit considerably the conformational possibilities of the A and B-DNA models and eliminate many possible structures (19). The stereochemistry also must be respected and it is the case for the two proposed helical structures as they do not present any bad atomic contact. Moreover one can note that all the dihedral angles are given values situated in domains commonly allowed for nucleotides (16).

The two double helices are right handed with their bases well oriented and positionned for the Watson-Crick pairing of complementary chains. The helical parameters are in perfect accordance with fiber X-ray data. In the present A-DNA conformation, the sugar pucker is C3-endo and bases are tilted and twisted like in the model proposed by Fuller et al.(2) and refined by Arnott and Hukins (3). In the B-DNA structure which is a very slightly modified and refined version of the previously proposed one (20), the sugar pucker is C1'-exo (it is generally C2'-endo or even C3'-exo in the preceding B-DNA models for fibers) ; this configuration has also been recently found in single crystal X-ray studies (21). The tilt and twist of bases are very small but not abscent ; their slight incline increases the agreement between calculated and experimental diffracted intensities as it does for the B-DNA model of Langridge et al.(1) and for its revised version (4).

Curves of the diffracted intensities calculated with the two present DNA conformations do agree very well with experimental data especially regarding the positions of the maxima and minima of the diffracted intensities (R factors are of the order of 0.3 and even less for the B-DNA). Therefore, the accordance with fiber X-ray is, at least, as good for the present DNA molecular conformations as it is for the structures generally accepted as A and B models (3). In the present case, the agreement with infrared dichroism measurements is also excellent but this advantage is not shared with the preceding models of A and B-DNA fibers.

REFERENCES

1. Langridge, R., Wilson, H.R., Hooper, G.W. & Wilkins, M.H.F. (1960), J. Mol. Biol., 2, 19-64
2. Fuller, W., Wilkins, M.H.F., Wilson, H.R. & Hamilton, L.D. (1965), J. Mol. Biol., 12, 60-80
3. Arnott, S. & Hukins, D.W.L.(1972), Biochem.Biophys.Res. Commun., 47, 1504-1509
4. Arnott, S. & Hukins, D.W.L. (1973), J. Mol. Biol., 81,93-105
5. Gupta, G., Bansal, M. & Sasisekharan, V. (1980), Int. J. Biol. Macromol., 2, 368-380
6. Rodley, G.A., Scobie, R.S., Bates, R.H.T.& Lewitt, R.M. (1976), Proc.Natl.Acad.Sci. USA, 73, 2959-2963
7. Sasisekharan, V. & Pattabiraman, N. (1976), Current Sci., 45, 779-783
8. Prémilat, S. & Albiser, G. (1982), Biochem. Biophys. Res. Comm., 104, 22-29
9. Sasisekharan, V., Bansal, M. & Gupta, G. (1981), Biochem. Biophys. Res.Comm., 102, 1087-1095.
10. Conner, B.N., Takano, T., Tanaka, S., Itakura, K. & Dickerson, R.E. (1982), Nature 295, 294-299
11. Wing, R.M., Drew, H., Takano, T., Broka, C., Tanaka, S., Itakura, K., & Dickerson, R.E. (1980), Nature 287, 755-758
12. Pilet, J. & Brahms, J. (1973), Biopolymers 12, 387-403
13. Beetz, C.P., Ascarelli, G. & Arnott, S. (1979), Biophys. J. 28, 15-26
14. Shindo, H., Wooten, J.B. & Zimmerman, B. (1981), Biochem. 20, 745-750
15. Prémilat, S. & Albiser, G. (1975), J. Mol. Biol., 99, 27-36
16. Sundaralingam, M. (1969), Biopolymers, 7, 821-860
17. Arnott, S. (1970), Progr. Biophys. Mol. Biol. 21, 261-318
18. Leslie, A.G.W., Arnott, S., Chandrasekaran, R. & Ratliff, R.L. (1980), J. Mol. Biol. 143, 49-72
19. Albiser, G. & Prémilat, S. (1982), Nucl. Acid. Res. 10, 4027-4034
20. Prémilat, S. & Albiser, G. (1982), C.R.Acad.Sci.(Paris) 294, 241-244
21. Drew, H.R., Wing, R.M., Takano, T., Broka, C., Tanaka, S., Itakura, K. & Dickerson, R.E. (1981), Proc.Natl.Acad.Sci. USA 78, 2179-2183

C) CONFORMATION DE L'ADN EN FORME C EN ACCORD AVEC LES RX DE FIBRES ET LE DICHROISME INFRAROUGE

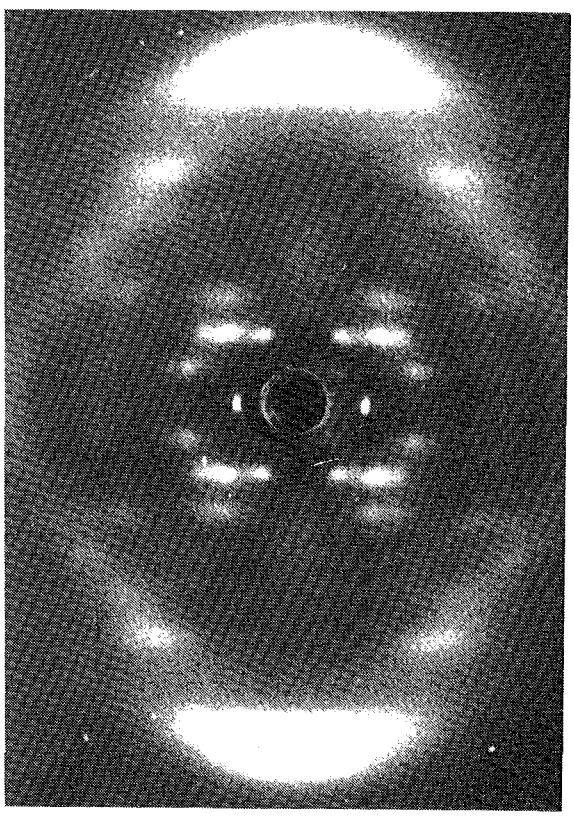

Photo N° 6 : Forme C de l'ADN avec sel de lithium à 66 % d'humidité relative.

Journal of Biomolecular Structure and Dynamics, ISSN 0739-1102
Volume 2, Issue Number 3 (1984), ©Adenine Press (1984).

Conformations of C-DNA in Agreement with Fiber X-ray and Infrared Dichroïsm

S. Premilat and G. Albiser
Laboratoire de Biophysique Moleculaire
Universite de Nancy I, ERA CNRS N° 828
Faculté des Sciences, 1er cycle,
B.P. N° 239, 54506 Vandoeuvre les Nancy
France

Abstract

Different left handed double helices are proposed as models for DNA fibers in the C form. These conformations have geometrical parameters which agree well with fiber X-ray data and the orientations of their phosphate groups are in good agreement with infrared dichroïsm results. A complete set of atomic coordinates and dihedral angles are given together with curves of calculated diffracted intensities. The present results are compared with experimental values and with the other C-DNA models.

Introduction

The C form of DNA is induced in DNA fibers when both humidity and salt levels are relatively low (1,2,3). This conformation, which has been much less studied than the A and B forms, seems now to be of biological importance. The molecular model proposed by Marvin et al. (1) for the C-DNA has been established on the basis of a great similarity between C and B forms, similarity simply deduced from fiber X-ray patterns. But it is a fact that the precision of measurements obtained from DNA fiber X-ray is low and even not sufficient to give the handedness of the double helices. Thus many different conformations can correspond, within the range of precision, to similar fiber X-ray patterns (4). Moreover, recently published results show that the transition from C to B and vice-versa is not very easy. It has been suggested that the A form as intermediate, according to the scheme: C⇒A⇒B (5) and this process can be modified when fibers are maintained under tension (6).

It can be noted that experimental data on C-DNA are much less precise than those obtained from A or B forms. For example, the CD spectrum of C-DNA is not well defined (7,8) and the X-ray studies are only made on fibers and therefore present a poor precision. Besides, the geometrical parameters obtained from infrared dichroism (9) disagree considerably with the X-ray molecular model (10). However, concerning this last point, it has been shown (11) that it is possible to establish DNA

molecular models which are in accordance with X-ray data as well as with infrared measurements. Such A and B-DNA models are more well founded as they refer to two very different experiments.

Methods

The calculation of the DNA structures are performed taking into account the geometrical constraints deduced from X-ray measurements: for the C-DNA, the repeat unit must be of 30.6 A and the rotation per nucleotide is fixed to 38.7° ; there are thus 9.3 nucleotide pairs per turn and 3.03 A between successive bases (1). The geometry of the sugar phosphate backbone is defined by the set of values given to the dihedral angles. Bond angles and bond lengths can also be slightly varied but are maintained in domains of values determined by X-ray studies (12). The procedure followed to compute atomic coordinates of nucleotides placed in a helical conformation is the one previously used (11,13). The model building programme allows us to modify the dihedral angles of the molecular model starting from given rough values obtained form physical models. An interative procedure optimizes the orientation of the phosphate group in order to verify the experimental infrared values. This fitting is realized maintaining the constraints on the helical parameters of the conformation. Moreover, the DNA molecules being composed of two antiparallel and complementary chains with bases paired as proposed by Watson and Crick, the calculated conformations must present a dyadic symmetry and good hydrogen bonds between associated bases. The stereochemistry of the molecular models is also tested and possible too short interatomic distances are eliminated by very small variations of the dihedral angles.

The diffracted intensity curves are computed following the procedure previously described (14) and using the atomic cylindrical coordinates of the best calculated conformations. As the infrared measurements give different values for the orientation of the phosphate group depending on the DNA origin (9), the search for conformations adapted to these different values was realized. But no *a priori* sense was defined for the helices; right as well as left handed conformations were tested.

Results and Discussion

Three sets of dihedral angles are listed in Table I; they correspond respectively to the three different orientations of the phosphate group given by infrared dichroism and associated to DNA of different origins. For these DNA conformations, the helical parameters are maintained at the values characteristic of the C form. Orientations of the base planes are also indicated by the tilt and twist angle values. In this same Table I are also indicated the dihedral angles of the right handed C-DNA helix presenting the best fit with the geometrical constraints.

The orientations of the directions of O1O2 and of the bissector of O1PO2 relative to the helix axis are presented in Table II and compared with values obtained from infrared measurements. A complete set of atomic cylindrical coordinates is listed in

Table I

Dihedral angles of the different C-DNA double helices and helical parameters. Models I, II, III are left handed helices and model VI is a right handed helix

Dihedral Angles (°)	Model N° I Cytophaga sp.	II Salmon sp.	III Calf Thymus	IV Calf Thymus
α (P−O5′)	55.51	54.49	58.78	−28.77
β (O5′−C5′)	−143.06	−144.26	−139.61	146.53
γ (C5′−C4′)	157.38	160.45	157.38	35.14
δ (C4′−C3′)	151.92	153.36	146.64	138.92
ϵ (C3′−O3′)	−67.56	−68.62	−69.52	−156.46
ξ (O3′−P)	−178.79	179.53	176.18	−139.93
χ O1′−C1′ < N1−C2(Pyr) / N9−C4(Pur)	175	179.5	177	−121.5
θ°, Rotation/Residue	−38.7	−38.69	−38.7	38.7
Rise/Residue (A)	3.28	3.28	3.29	3.30
Base tilt (°)	8.6	7.3	8.1	−9.5
twist (°)	−0.7	−3.9	−1.3	0
D=distance to axis of C6(Pyr) C8(Pur)(A)	−1.4	−1.3	−0.8	−1

Table II

Geometry of the phosphate group of the different C-DNA models compared to experimental values (I.R.)

DNA Origin	Cytophaga sp.		Salmon sp.		Calf Thymus			
Angle (°) relative to the helix axis of:	I.R.	Model I	I.R.	Model II	I.R.	Model III	Model IV	Model (ref. 3-10)
O1O2	48±3	48.1	48±2	48.4	51±2	50.9	50.9	73
the bissector of O1PO2	62±3	62.0	67±2	66.8	64±2	63.8	75.4	56

Table III. The presented coordinates correspond to the Calf-thymus DNA which is taken as an example; the three left handed conformations are indeed very similar. The different bases are placed at the same level and the dyadic and helical symmetries allow the calculation of the coordinates of any other nucleotide.

Figure 1 shows, as an example, a representation of one of the proposed C-DNA conformations. For this left handed helix one can see the perfect pairing of the bases in *anti* position and the good stereochemistry of the molecular model; figure 2 shows a stereo view of this model. In figure 3 curves of the calculated diffracted intensities for the right and a left handed C-DNA models are presented together with experimental data.

The orientation of the phosphate group imposed by the infrared results associated to the helical parameters deduced from fiber X-ray studies constitute a set of

Table III
Cylindrical atomic coordinates of a unit of the left handed C-DNA helix (model III)

	R(A)	ϕ(°)	Z(A)		R(A)	ϕ(°)	Z(A)
Phosphate				Desoxyribose			
O3'	7,52	−125,35	1,12	C5'	8,59	−102,89	−0,62
P	9,01	−126,04	1,70	C4'	7,76	−107,82	0,46
O1	9,60	−118,04	2,11	C3'	7,33	−118,49	0,03
O2	9,80	−129,26	0,56	C2'	5,87	−117,06	−0,40
O5'	8,86	−132,45	2,94	C1'	5,45	−108,00	0,77
				O1'	6,66	−101,06	0,88
Guanine				Adenine			
N9	4,34	− 96,46	0,60	N9	4,34	− 96,47	0,59
C8	4,75	− 80,46	0,61	C8	4,74	− 79,75	0,60
N7	3,96	− 66,54	0,42	N7	4,01	− 65,33	0,42
C5	2,63	− 72,97	0,29	C5	2,69	− 71,86	0,29
C4	2,97	−100,34	0,40	C4	2,97	− 99,46	0,39
N3	2,73	−127,07	0,33	N3	2,66	−126,47	0,32
C2	1,65	−147,07	0,14	C2	1,53	−144,02	0,13
N2	2,39	−179,29	0,05	N1	0,37	− 91,48	0,00
N1	0,44	−104,83	0,02	C6	1,60	− 48,28	0,08
C6	1,58	− 49,10	0,09	N6	2,39	− 16,79	0,04
O6	2,22	− 17,97	−0,03				
Cytosine				Thymine			
N1	4,34	− 96,47	0,60	N1	4,34	− 96,46	0,60
C6	4,92	− 81,18	0,63	C6	4,91	− 80,81	0,63
C5	4,51	− 65,59	0,48	C5	4,52	− 65,27	0,48
C4	3,17	− 58,50	0,28	Me	5,76	− 54,68	0,52
N4	3,32	− 35,18	0,13	C4	3,22	− 57,18	0,28
N3	2,25	− 78,79	0,26	O4	3,30	− 35,44	0,13
C2	3,09	−102,00	0,41	N3	2,28	− 78,69	0,26
O2	3,16	−124,87	0,40	C2	3,07	−103,06	0,42
				O2	3,07	−125,96	0,38

constraints to which we couldn't adapt any right handed C-DNA conformation. The best right handed helix obtained presents very good helical parameters and a good stereochemistry. The corresponding calculated intensities are acceptable (fig. 3b) but, the model is not totally consistent with the infrared data. Although the angle of O1O2 with the helix axis in the right-handed model is close to that obtained from infrared studies, the orientation of the bisector O1PO2 is not in agreement with the infrared data (Table II).

Conversely it was relatively easy to get left handed helices satisfying perfectly all the geometrical constraints and presenting very good stereochemistry. This was possible, for the three values of the orientation of the phosphate group proposed by the infrared data, by just varying progressively the dihedral angles. The perturbations hence introduced can always take into account the necessary fit to the C-DNA helical parameters and to a good pairing of complementary bases. One can add that

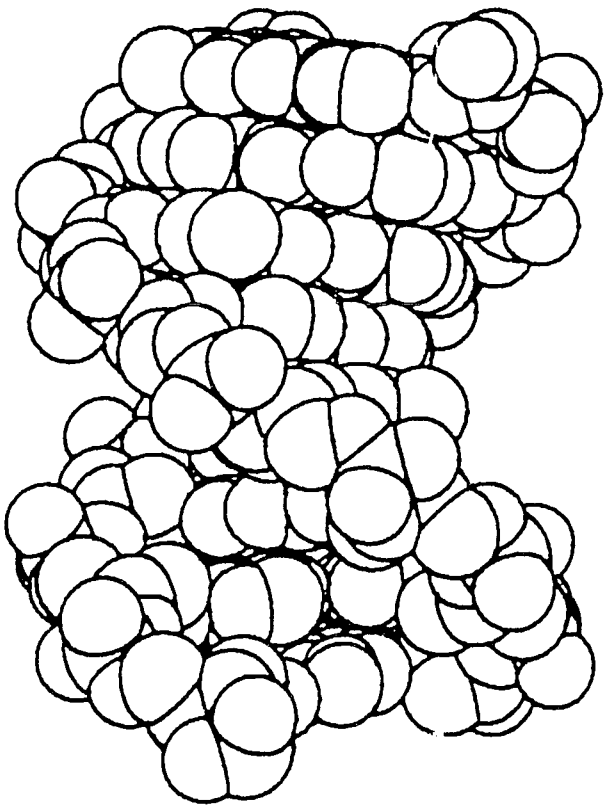

Figure 1. Molecular model of left handed C-DNA double helix (model N° III).

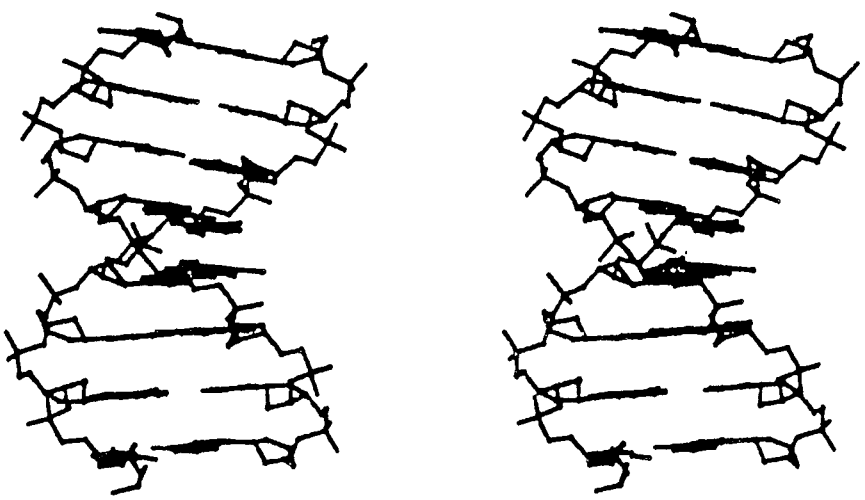

Figure 2. Stereo view of the model n° III.

all the dihedral angles of these conformations are given values very well situated in domains generally allowed for nucleotides (15) and sugar pucker is C2′ endo. This confirms the good stereochemistry of the present molecular models of left handed C-DNA which are in the same family as already proposed left handed DNA conformations (16,17).

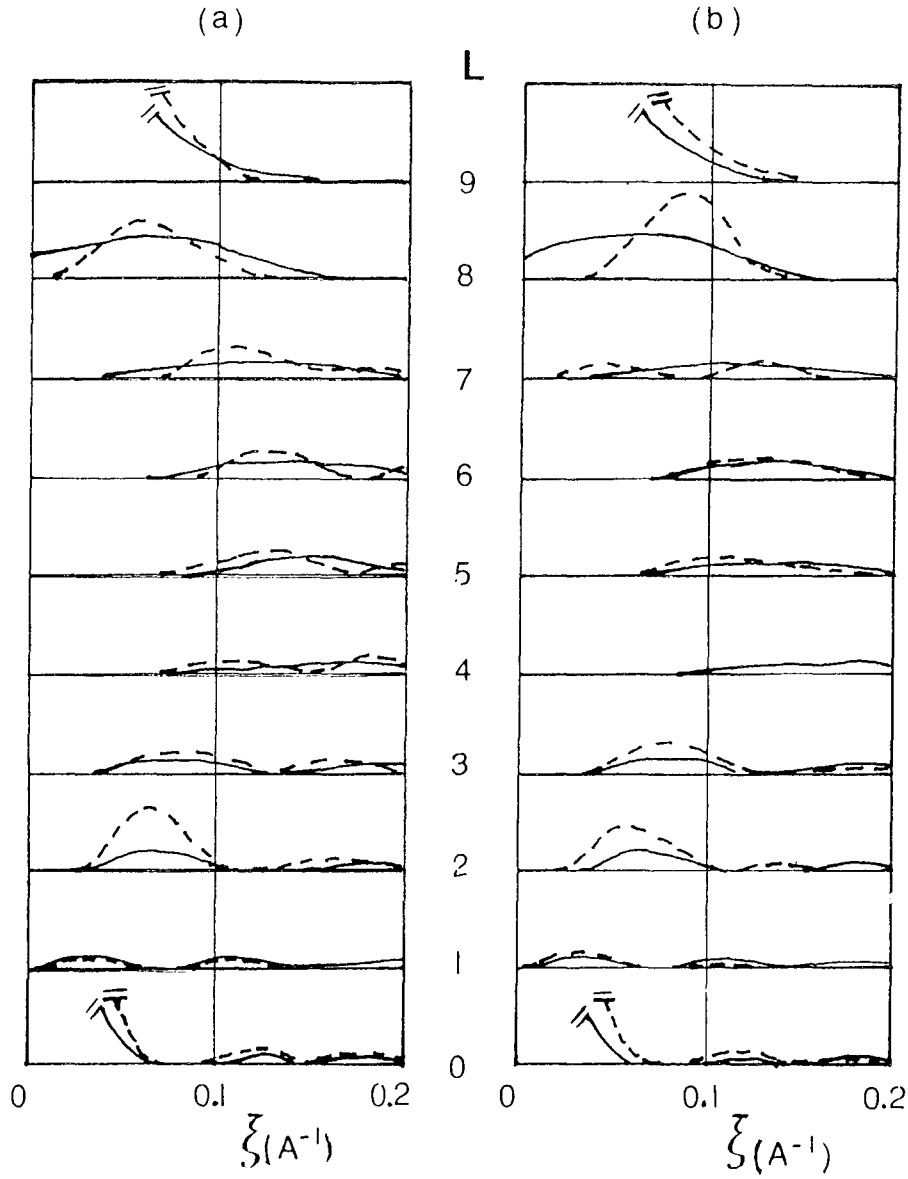

Figure 3. Curves of the diffracted intensities calculated (------) with the left handed model III (a) and the right handed model IV (b) compared to experiments (——).

Concerning the diffracted intensities, one can see that calculated curves do agree very well with experiments (fig. 3). This agreement is at least as good as that obtained with the preceding C-DNA models (1,3). It is interesting to note that the present right and left handed C-DNA models give indeed very similar calculated intensities (fig. 3ab); this behavior confirms a fact already remarked for fibre X-ray studies (4).

On the other hand the agreement between the present left handed molecular models and values deduced from infrared dichroïsm is perfect. At last, it can be noted that the present C forms of DNA, being left handed helices with $\theta = -38.7°$, are closer to the A form ($\theta = 32.7°$) than to the B form ($\theta = 36°$); this fits very well and could explain the C→A→B transition.

References and Footnotes

1. Marvin, D. A., Spencer, M., Wilkins, M.H.F. and Hamilton, L.D., *J. Mol. Biol. 3*, 547 (1961).
2. Zimmerman, S. B. and Pheiffer, B. H., *J. Mol. Biol. 142*, 315 (1980).
3. Arnott, S. and Selsing, E. J., *J. Mol. Biol. 98*, 265 (1975).
4. Gupta, G., Bansal, M. and Sasisekharan, V., *Int. J. Biol. Macromol. 2*, 368 (1980).
5. Rhodes, N.J., Mahendrasingam, A., Pigram, W. J., Fuller, W., Brahms, J., Vergne, J. and Warren, R.A.J., *Nature 296*, 267 (1982).
6. Fornells, M., Campos, J. L. and Subirana, J. A., *J. Mol. Biol. 166*, 249 (1983).
7. Chen, C. Y., Pheiffer, B. H., Zimmerman, S. B. and Hanlon, S., *Biochem. 22*, 4746 (1983).
8. Fisch, S. R., Chen, C. Y., Thomas, G. J. and Hanlon, S., *Biochem. 22*, 4751 (1983).
9. Brahms, J., Pilet, J., Tran, T. P. L. and Hill, L. R., *Proc. Nat. Acad. Sci. USA 70*, 3352 (1973).
10. Beetz, C. P., Ascarelli, G. and Arnott, S., *Biophys. J. 28*, 15 (1979).
11. Premilat, S. and Albiser, G., *Nucl. Acid Res. 11*, 1897 (1983).
12. Voet, D. and Rich, A., *Prog. Nucleic Acid. Res. Mol. Biol. 10*, 183 (1970).
13. Albiser, G. and Premilat, S., *Nucl. Acid. Res. 10*, 4027 (1982).
14. Premilat, S. and Albiser, G., *J. Mol. Biol. 99*, 27 (1975).
15. Sundaralingam, M., *Biopolymers 7*, 821 (1969).
16. Gupta, G., Bansal, M. and Sasisekharan, V., *Proc. Nat. Acad. Sci. USA 77*, 6486 (1980).
17. Gupta, G., Sarma, M. H., Dhingra, M. M., Sarma, R. H., Rajagopalan, M., and Sasisekharan, V., *J. Biomole. Str. Dyns 1*, 395 (1983).

Date Received: November 2, 1984

D) MODELES DE L'ADN POUR LES CONFORMATIONS A, B, C ET D EN RELATION AVEC LES MESURES RX DE FIBRE, L'INFRAROUGE ET LA RMN.

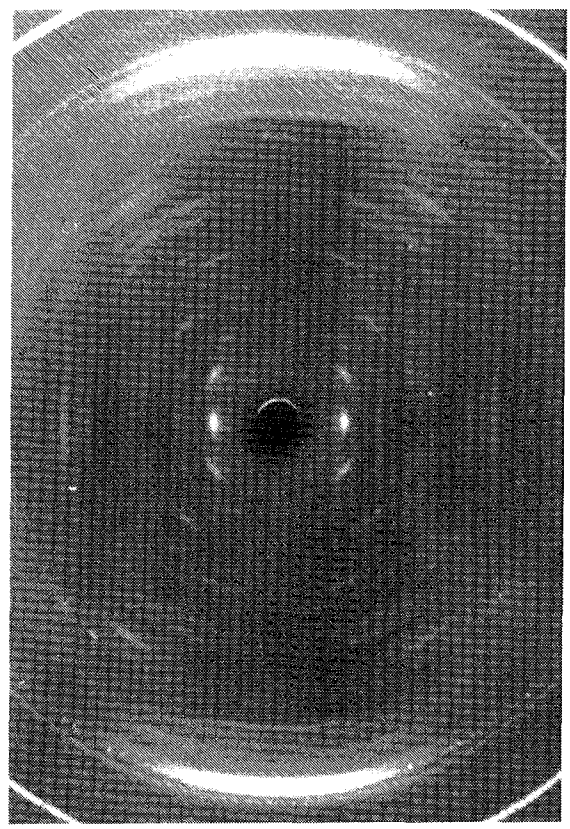

Photo N° 7 : Forme D du poly (dA-dT).poly (dA-dT) avec sel de sodium à 50 % d'humidité relative.

Journal of Biomolecular Structure and Dynamics, ISSN 0739-1102
Volume 3, Issue Number 5 (1986), © *Adenine Press (1986)*.

DNA Models for A, B, C and D Conformations Related to Fiber X-ray, Infrared and NMR Measurements*

S. Premilat and G. Albiser
Laboratoire de Biophysique Moléculaire, U.A. CNRS 497
Faculté des Sciences, Université de Nancy I, B.P. N° 239
54506 Vandoeuvre les Nancy, France

Abstract

A conformational analysis of the A, B, C and D DNA forms was made in order to establish molecular models presenting a good agreement with experimental data obtained from fiber X-ray, infrared linear dichroism and ^{31}P NMR. The proposed models have been refined and do present good stereochemistry and optimized H-bond distances between bases associated with the Watson-Crick pairing. The DNA conformations proposed are a left handed double helix for the C form and right handed helices for A, B and D. Relations to conformational transitions between these forms are discussed.

Introduction

The conformational variations of DNA induced by modifications of humidity and salt concentration are well established by X-ray diffraction studies on oriented fibers. By using this technique the fundamental A, B, C and D forms of DNA or polynucleotides were determined (1,2,3,4). The A form appears in the presence of sodium salt when the relative humidity is lower than 75%. The B form exists for high humidity when different salts are present. The C-DNA form was studied by X-ray diffraction on fibers immersed in different solvents (5). A recent experimental study (6) has shown in great detail how the C form of DNA can be obtained when both water and salt contents are low. Moreover the C→A⇌B transitions were shown to occur as a function of the increase of the amount of sodium salt and relative humidity. The same kind of study devoted to the poly(dA-dT)•poly(dA-dT) established the transitions which can be observed from or to the D form (7). Nevertheless, even if X-ray is indeed a powerful tool which permits to differentiate between DNA conformations without any ambiguity the extremely poor resolution of the diffraction measurements does not allow one to get a unique molecular model from a fiber X-ray pattern. Therefore, it is important to take into account any information coming from other experimental methods in order to establish reliable DNA models.

*Paper presented at the Fourth Conversation in Biomolecular Stereodynamics, SUNY at Albany, June 04-08 1985.

Among the different spectroscopic technics used, NMR gives very fine structural details on the sugar and the bases (8,9) and recently ^{31}P NMR has been shown to be able to give geometrical parameters on the phosphate group of DNA in the A and B forms (10,11). Besides, infrared linear dichroism is used to determine the orientation of the phosphate group and experimental values are available for A, B and C forms (12,13,14). In recent publications (15,16) it was shown that one can establish A, B, and C-DNA molecular models which agree with X-ray and infrared measurements and moreover, the A and B models proposed by this method are also in accordance with ^{31}P NMR data (11).

In the present work refined A, B and C conformations are presented together with a D conformation of poly(dA-dT)·poly(dA-dT). For this last form one should note that no infrared or NMR data is available and therefore the present D model was only constrained to agree with its fiber X-ray pattern (4) and to remain in the vicinity of the present right handed B form. The variations of the dihedral angles introduced on the earlier models (15,16) are indeed very small and improvements on the A, B and C conformations are mainly obtained on the distances of H-bonds between paired bases and on the inter chain stereochemistry. For all these DNA conformations dihedral angles, helical parameters, the base pairing are given together with views of the different models. Comparison with infrared and ^{31}P NMR data are indicated and the consistency of the present DNA models is related to the experimental observations made on transitions between these different DNA conformations.

Methods

Helical parameters derived from fiber X-ray patterns associated with the known geometry of the nucleotide units permit to determine molecular models which can be used to compute diffracted intensities and different structural features. Owing to the dyad axis, only one of the two antiparallel helices suffices to calculate the diffracted intensities but it is necessary to determine a model of the two complementary molecular chains in order to define the atomic coordinates in a correct reference frame based on the helical and the dyadic axes.

Bond lengths and bond angles are taken from the listing given by Arnott (17); they can be very slightly modified but must be maintained in intervals of values determined by X-ray studies on single crystals (18,19,20). The geometry of the sugar phosphate chain is completely defined by its dihedral angles. The computation of the atomic coordinates of a nucleotide sequence placed in a helical conformation is performed with the same procedure as previously used (21). The program is based on a method transposed from that proposed by Hermans and Ferro (22) for the representation of a protein molecule. This procedure allows one to modify very easily the calculated structure and makes it simple to introduce the tilt and twist of bases. An iterative procedure is used to optimize the helical conformation and the orientation of the phosphate group namely the O1O2 direction and that of the bissector of O1PO2 relative to the helix axis (angles φ_1 and φ_2 respectively). The fitting of these orientations to the experimental values of infrared dichroism is realized maintaining

the helical parameters as constraints on the conformation. At the end of improvement cycles, in good cases a molecular model in conformity with X-ray and infrared data emerged. When a polynucleotide chain is built and placed in its proper helical system (23), the antiparallel and complementary one is adjusted so that good hydrogen bonds are realized between bases paired according to Watson and Crick. This last building step permits also to determine the dyad axis. Cylindrical coordinates of atoms are then calculated in the reference system defined by the helical and dyadic axes. The average Fourier transform and the diffracted intensity curves are computed using the atomic cylindrical coordinates of the best calculated conformations. Relations and parameters necessary for these calculations are those given by Langridge et al (2) and used previously (15,16). As one supposes a statistical repartition of the different bases along the helix, except for the D form, the percentage of base pairs is included in the computation procedure (21). The molecular model is modified or rejected if it does not give a good calculated X-ray pattern. The stereochemistry (intra and inter chain atomic distances, H-bond geometry . . .) of satisfactory molecular models can be improved by small variations of the dihedral angles or of the geometry (bond angles). If this leads to modifications of the helical parameters, the model goes through new improvement cycles or must sometimes be rejected.

Regarding the calculation on molecular models of the angles β and γ deduced from ^{31}P NMR measurements, one can show that they are related to φ_1 and φ_2 (infrared). In fact let us consider in figure 1 the angles β and γ given by Shindo et al (11) and the orthogonal system (a,b,c) with the c axis along the helix axis (or fiber axis). The orthogonal system (x,y,z) corresponds to the line O1O2 (oxygens of the phosphate group) for the z axis and to the bissector of O1PO2 for y. Angles φ_1 and φ_2 are shown in figure 1. The axis b is along the intersection of planes (a,b) and (x,y).

One can introduce another orthogonal system (b,d,z) by using the axis d situated in the plane (x,y) and perpendicular to b. One can see that $\varphi_1 = \beta$ and introducing the

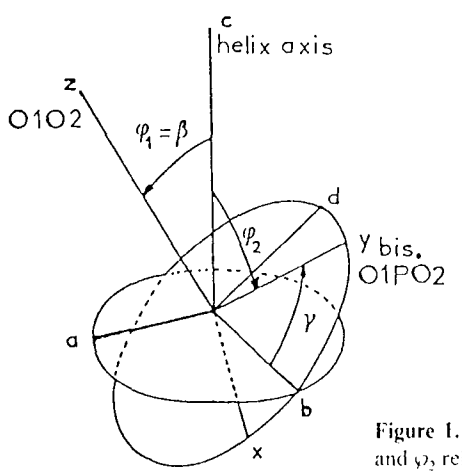

Figure 1. Orientation angles β and γ related to ^{31}P NMR. φ_1 and φ_2 related to infrared.

angles θ_1 = (x,c), θ_2 = (y,c) and θ_3 = (z,c) (magnetic field along c; see ref. 11), one gets $\varphi_1 = \beta = \theta_3$, $\varphi_2 = \theta_2$ and with scalar products expressed in (b,d,z) one obtains:

$$\cos\theta_1 = -\sin\beta\cos\gamma;\ \cos\theta_2 = \sin\beta\sin\gamma.$$

Note also that θ_1 can be obtained from $\cos^2\theta_1 + \cos^2\theta_2 + \cos^2\theta_3 = 1$ and $\theta_3 = \varphi_1$; $\theta_2 = \varphi_2$.

So when β and γ are known from NMR one can calculate φ_1 and φ_2 (infrared). Conversely from φ_1 and φ_2 one gets $\beta = \varphi_1$ and

$$\operatorname{tg}\gamma = -\frac{\cos\theta_2}{\cos\theta_1} = -\frac{\cos\varphi_2}{(1-\cos^2\varphi_1-\cos^2\varphi_2)^{1/2}}$$

Finally, these angles are defined between lines and their values are in the interval $\left(0, \frac{\pi}{2}\right)$.

Results

The set of dihedral angles corresponding to the different molecular models of DNA presently studied are given in table I. In this same table all the relevant conformational parameters are also indicated. One should note that the DNA conformations are ordered according to the increase of the rotation angle per residue. The sign of this angle indicates the handedness of the double helix model. Thus for the presently proposed conformations C is left handed and A, B and D are right handed helices. This handedness of A and B forms do agree with results obtained from X-ray measurements on oligonucleotide crystals (24,25).

The A, B, and C-DNA molecular models are depicted in figure 2 together with details on the geometry of paired bases. The modifications made on these models compared to those already proposed (15,16) have been done mainly to improve the H-bond distances between bases. Such variations did not affect the dihedral angles but only the internal geometry of the A and B forms and just very slightly the angles of the C-DNA models. The corresponding atomic coordinates and Fourier transform diagrams remain very close to previously published values (15,16) and therefore are not presented. Finally, table II and figure 3 present respectively the atomic coordinates of the D form of poly[d(A-T)] and a view of the model as well as curves of calculated diffracted intensities. For this molecular model the dyad axis is located between base planes and the unit is a (A-T) nucleotide pair on one chain. Therefore the double helix presents 4 units in one turn and the relation used for the calculation of the Fourier transform is $l = n + 4m$. Another point concerning the D form is that A and T bases are given slightly sifferent twist and tilt angles (see table I) in order to improve H-bond distances; it also gives better agreement with diffraction curves.

In table III are indicated the orientation angles of the phosphate group in the

Table I
Chain dihedral angles and geometrical parameters of the C, A, B, D double helical conformations

DNA form	C		A	B	D
DNA origin	Calf Thymus	Salmon sp.	Calf Thymus	Calf Thymus	poly(dAdT)poly(dAdT)
$\theta(°)$	−38.70	−38.70	32.73	36.00	45.00
P(A)	30.60	30.60	28.16	33.90	24.20
p(A)	3.29	3.29	2.56	3.39	3.03
$\alpha(°)$	60.78	53.50	−59.63	−30.93	−34.00
$\beta(°)$	−139.89	−143.27	163.55	148.71	144.60
$\gamma(°)$	155.38	161.45	51.20	37.02	43.46
$\delta(°)$	146.64	152.38	81.00	132.32	153.77
$\epsilon(°)$	−69.72	−68.67	−136.26	−156.80	−157.04
$\zeta(°)$	176.06	179.51	−87.11	−133.62	−154.70
$\chi(°)$	177.00	177.00	−165.00	−123.00	−106(A) −102(T)
Tilt (°)	7.00	12.60	20.00	−6.00	−16 (A); −13 (T)
Twist (°)	−1.00	−0.50	10.00	2.30	−2.6 (A); 3.9 (T)
D (A)	−1.10	−1.00	4.60	−0.60	−2.60

$P \overset{\alpha}{-} O5' \overset{\beta}{-} C5' \overset{\gamma}{-} C4' \overset{\delta}{-} C3' \overset{\epsilon}{-} O3' \overset{\zeta}{-} P$; $\chi \begin{cases} O1' - C1' - N1 - C2 \text{ for (C,T)} \\ O1' - C1' - N9 - C4 \text{ for (G,A)} \end{cases}$

different models. Experimental infrared values are available for A, B and C forms and can be compared with angles calculated from the models. Only A and B-DNA conformations can be compared with ^{31}P NMR measurements. Nevertheless in table III the calculated values are given for all the present models. One should note that all these values for the angles can be more or less changed because the O1 and O2 bond angles of the molecular models can be chosen in an interval of values defined by X-ray studies on nucleotide crystals (19,20). Examples of such variations are indicated in table III for the D form.

Discussion

The conformations proposed here correspond to models in accordance with different experimental measurements made on long fibers of DNA in A, B, C or D form. In these double helical models, nucleotides do present a structural regularity which is not adapted to the more precise and irregular conformations determined by X-ray on crystals of short polynucleotide chains (24,25).

The geometry of the phosphate group which must fit to values derived from infrared measurements and to fiber X-ray data limits considerably the conformational possibilities and eliminates many good structures. For all the models presented, one can note that the dihedral angles are in the domains commonly allowed for nucleotides (18). Helical parameters are in perfect agreement with fiber X-ray data and bases are in the anti conformation.

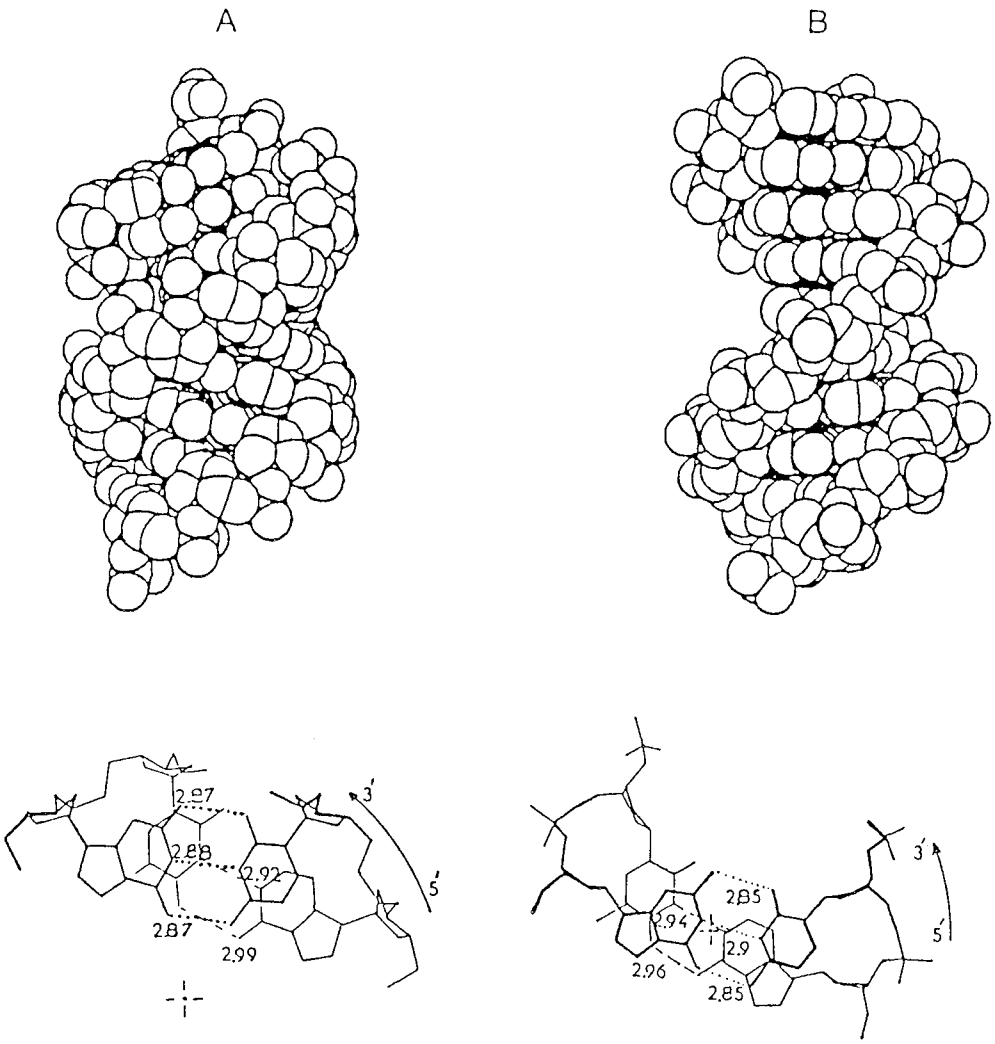

Figure 2. Molecular models of A, B, C forms of DNA.

In the A-DNA conformation, the sugar pucker is C3′-endo and bases are tilted and twisted like in the model proposed by Fuller et al (1). In the refined B-DNA structure, the sugar pucker is C1′-exo and the slight incline of bases increases the agreement between calculated and experimental diffracted intensities. These two conformations are indeed very near to those previously proposed (15) but they do present better H-bond distances for the paired bases. The agreement with fiber X-ray remains very good and the structures are in accord with infrared and ^{31}P NMR.

For the C-DNA, no right-handed helix (16, see also ref. 14) could be obtained which agreed with the infrared angles for the phosphate group and the helical parameters from the X-ray patterns. On the contrary, left handed helices satisfying perfectly all

C

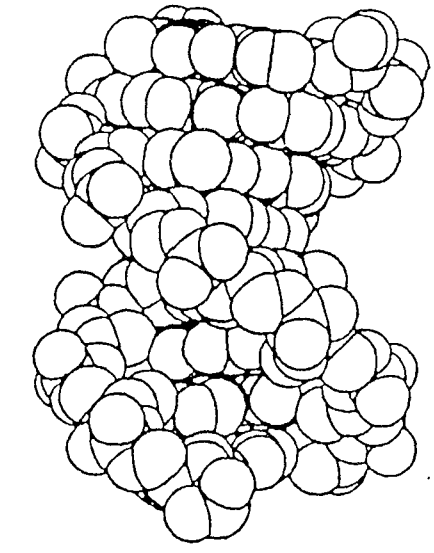

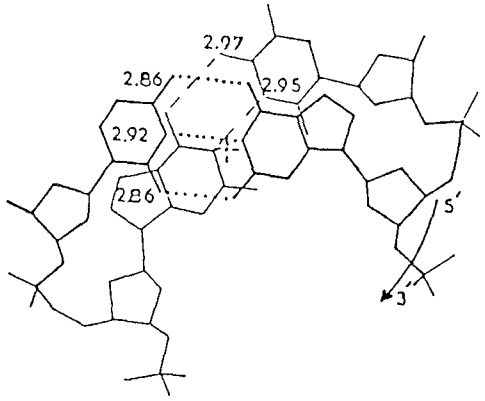

Figure 2 continued

these constraints presenting a very good stereochemistry can easily be obtained. Here also all dihedral angles have values well situated in the domains allowed to nucleotides and the sugar pucker is C2′-endo for one model and C3′-exo for the other. These facts guarantee the good stereochemistry of these left handed models for C-DNA. The present C-DNA left handed helices which are very close to our previous models (16) are in very good agreement with fiber X-ray patterns and infrared data. No comparison with ^{31}P NMR can be made as no precise experimental values have been proposed up to now.

The generally accepted similarity in the handedness of the B and C forms of DNA does not fit well with the physiochemical conditions to which these forms relate. Actually, C is a very low humidity and low salt form of DNA while B is adapted to

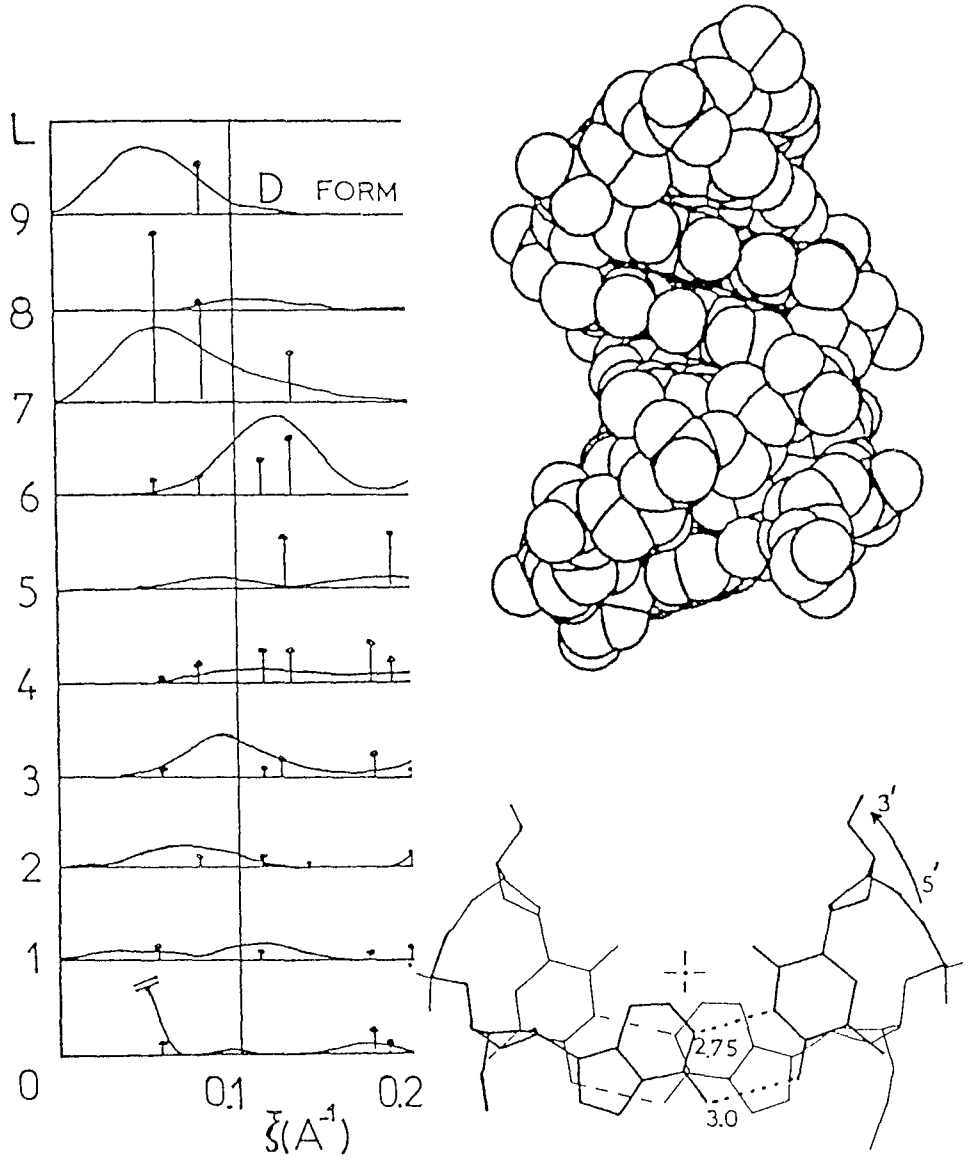

Figure 3. Molecular model of D form, H-bond distances in A and curves of diffracted intensities: calculated (——); experimental values (•), ref. 4.

high humidity and higher amount of salt. The precise study of the transitions between A, B and C forms (6) has shown that X-ray patterns corresponding to mixtures of A and C or A and B are observed according to the C⇒A⇒B reversible transitions. The conformational proximity of B and C has not been demonstrated. The helical parameter values of the different DNA forms can be well explained if one supposes a left handed helical model for C-DNA, A and B being right handed.

Table II
Atomic cylindrical coordinates of the D form unit

D form	R(A)	ϕ(°)	Z(A)		R(A)	ϕ(°)	Z(A)
Phosphate				Adenine			
O3′	7.06	267.45	−2.97	N9	4.37	231.46	−2.72
P	8.17	270.86	−1.90	C8	5.27	219.14	−2.83
O1	9.48	271.52	−2.57	N7	5.03	205.23	−2.55
O2	8.32	263.84	−0.83	C5	3.70	202.35	−2.23
O5′	7.73	281.34	−1.39	C4	3.16	223.33	−2.33
Deoxyribose				N3	2.06	240.18	−2.09
C5′	7.26	243.98	−5.34	C2	1.12	207.75	−1.73
C4′	6.51	253.16	−4.63	N1	2.02	170.06	−1.59
C3′	7.09	256.17	−3.26	C6	3.25	181.17	−1.84
C2′	6.33	248.08	−2.32	N6	4.33	169.32	−1.70
C1′	4.95	247.85	−2.96				
O1′	5.14	249.90	−4.35				
Phosphate				Thymine			
O3′	7.06	312.44	0.06	N1	4.37	276.45	0.31
P	8.17	315.85	1.12	C6	5.39	265.69	0.23
O1	9.48	316.51	0.46	C5	5.46	251.71	0.45
O2	8.32	308.83	2.20	Me	6.85	246.47	0.37
O5′	7.73	326.34	1.64	C4	4.46	240.21	0.77
Deoxyribose				O4	4.95	226.64	0.99
C5′	7.26	288.97	−2.31	N3	3.15	246.72	0.83
C4′	6.51	298.15	−1.60	C2	3.07	272.00	0.61
C3′	7.09	301.16	−0.23	O2	2.31	292.67	0.69
C2′	6.33	293.07	0.71				
C1′	4.95	292.84	0.07				
O1′	5.14	294.89	−1.33				

Table III
Geometry of the phosphate group in the different DNA models related to IR and ^{31}P NMR data

DNA form	C			A			B		
DNA origin	Calf Thymus (Salmon sp.)			Calf Thymus			Calf Thymus		
Angle (°)	$\varphi_1(\beta)$	φ_2	γ	$\varphi_1(\beta)$	φ_2	γ	$\varphi_1(\beta)$	φ_2	γ
I.R.*	51±2 (48±2) 48-50	64±2 (67±2) 61-64		65±2	45±3 46-50		56±2 52-55	70±3 62-65	
^{31}P NMR†				71±2	37	58±3	55±5	66.8	30±15
Model	51.5 (48.8)	63.7 (67.4)	34.4 (30.8)	65.1	44.9	51	56.7	71.3	21.8

For D form poly(dA-dT)·poly(dA-dT); Model: $\varphi_1 = 43.8$; $\varphi_2 = 76.5$; $\gamma = 19.8$
If O1 and O2 bond angles values are in (103°-110°) it comes:
$40 < \varphi_1 < 48$; $75 < \varphi_2 < 84$; $9 < \gamma < 21$

†From ref. 10,11. *From ref. 12-14

In that case the A form is between C and B and one has the order C,A,B with increasing values of the angle of rotation per nucleotide. (This angle is negative for C and positive for A and B).

The model presently proposed for D-DNA is right handed and has dihedral angle values near to those of the B form (see table I), the sugar pucker is C3′-exo. Note that bases are on the outside part of the conformation, far from the helix axis. This situation corresponds to a better stereochemistry for it improves atomic contacts between bases on the antiparallel and complementary chains. This conformation is similar to models already proposed (4,26,27). As far as we know, neither infrared nor ^{31}P NMR data are available for D-DNA and left handed as well as right handed helices have been proposed as models for poly[d(A-T)] (28). However conformational transitions recently observed (7) in poly[d(A-T)] fibers show that the transition between B and D forms is indeed reversible and the A to D is not. That can be interpreted as being due to the relative position of these conformations which should be ordered A,B,D and thus D is placed beyond B compared to A. For a left handed D form the order would be D,A,B or even D,C,A,B and could not fit to the observed transitions.

References and Footnotes

1. Fuller, W., Wilkins, M.H.F., Wilson, H.R., and Hamilton, L.D., *J. Mol. Biol. 12*, 60 (1965).
2. Langridge, R., Wilson, H.R., Hooper, C.W., and Wilkins, M.H.F., *J. Mol. Biol. 2*, 19 (1960).
3. Marvin, D.A., Spencer, M., Wilkins, M.H.F., and Hamilton, L.D., *J. Mol. Biol. 3*, 547 (1961).
4. Arnott, S., Chandrasekaran, R., Hukins, D.W.L., Smith, P.J.C., and Watts, L., *J. Mol. Biol. 88*, 523 (1974).
5. Zimmerman, S.B., and Pheiffer, B.H., *J. Mol. Biol. 142*, 315 (1980).
6. Rhodes, N.J., Mahendrasingam, A., Pigram, W.J., Fuller, W., Brahms, J., Vergne, J., and Warren, R.A.J., *Nature 296*, 267 (1982).
7. Mahendrasingam, A., Rhodes, N.J., G dwin, D.C., Nave, C., Pigram, W.J., Fuller, W., Brahms, J., and Vergne J., *Nature 301*, 535 (1983).
8. Dhingra, M.M., and Sarma, R.H., in *Stereodyn. of Mol. Syst.*, Ed., Sarma, R.H., Pergamon, New York, p. 3 (1979).
9. Altona, C., in *Meth. in Struct. Mol. Biol.*, Ed., Davies, B., Saenger, W., Danyluk, S.S., Plenum Press, London, p. 161 (1981).
10. Shindo, H., Wooten, J.B., Pheiffer, B.H., and Zimmerman, S.B., *Biochemistry 19*, 518 (1980).
11. Shindo, H., Fujiwara, T., Akutsu, H., Matsumoto, U., and Kyogoku, Y., *Biochemistry 24*, 887 (1985).
12. Pilet, J., and Brahms, J., *Biopolymers 12*, 387 (1973).
13. Brahms, J., Pilet, J., Tran, T.P.L., and Hill, L.R., *Proc. Nat. Acad. Sci. USA 70*, 3352 (1973).
14. Pohle, W., Zhurkin, V.B., and Fritzsche, H., *Biopolymers 23*, 2603 (1984).
15. Premilat, S., and Albiser, G., *Nucl. Acid. Res. 11*, 1897 (1983).
16. Premilat, S., and Albiser, G., *J. Biomol. Str. Dyns. 2*, 607 (1984).
17. Arnott, S., and Hukins, D.W.L., *Biochem. J. 130*, 453 (1972).
18. Sundaralingam, M., *Biopolymers 7*, 821 (1969).
19. Seeman, N.C., Rosenberg, J.M., Suddath, F.L., Kim, J.J.P. and Rich, A., *J. Mol. Biol. 104*, 109 (1976).
20. Rosenberg, J.M., Seeman, N.C., Day, R.O., and Rich, A., *J. Mol. Biol. 104*, 145 (1976).
21. Premilat, S., and Albiser, G., *J. Mol. Biol. 99*, 27 (1975).
22. Hermans, J.J., and Ferro, D., *Biopolymers 10*, 1121 (1971).
23. Sugeta, H., and Miyazawa, T., *Biopolymers 5*, 673 (1967).

24. Conner, B.N., Takano, T., Tanaka, S., Itakura, K., and Dickerson, R.E., *Nature 295*, 294 (1982).
25. Wing, R.M., Drew, H., Takano, T., Broka, C., Tanaka, S., Itakura, K., and Dickerson, R.E., *Nature 287*, 755 (1980).
26. Arnott, S., Chandrasekaran, R., Puigjaner, L.C., Walker, J.K., Hall, I.H., Birdsall, D.L., and Ratliff, R.L., *Nucl. Acid. Res. 11*, 1457 (1983).
27. Gupta, G., Bansal, M., and Sasisekharan, V., *Int. J. Biol. Macromol. 2*, 368 (1980).
28. Rajagopalan, M., Gupta, G., and Sasisekharan, V., *Febs Letters 159*, 285 (1983).

Date Received: June 04, 1985

Communicated by the Editor V. Sasisekharan

E) DISCUSSION

La méthode employée pour proposer des conformations des formes A et B de l'ADN en fibre s'est révélée efficace. Les contraintes imposées par l'orientation du groupe phosphate, déduites des mesures de spectroscopie infrarouge, limitent les conformations possibles de la chaîne sucre-phosphate (62). Une sélection est rapidement opérée quand on cherche le meilleur accord entre ces modèles conformationnels et les données expérimentales de RX. Pour les formes A et B, ce sont des doubles hélices droites qui satisfont au mieux les données expérimentales. Ces conformations ont des caractéristiques très voisines des premiers modèles proposés (28,30). Il est intéressant de remarquer que les valeurs des angles dièdres établis par cette méthode ont été progressivement proposés par Arnott à la suite de raffinements successifs des clichés RX de fibre (Tableau n° IV)

Angles dièdres moyens (°) déterminés à partir de cristaux d'oligonucléotides comparés à ceux déduits des fibres d'ADN.

A.D.N. FORME A	α	β	γ	δ	ε	ζ	χ
	P —— O5'—— C5'—— C4'—— C3'—— O3'—— P						
d(GCCCGGGC)•	- 71	177	55	85	- 165	- 64	- 160
d (GGGTACCC)x	- 69	172	64	79	- 151	- 77	- 165
d(ACCGGCCGGT)o	- 65	166	51	80	- 157	- 66	- 158
d(CCCCCGCGGGGG) *	- 75 (16)	182 (22)	53 (14)	79 (8)	- 168 (28)	- 71 (20)	- 163
Fibre+(Prémilat,Albiser)	- 59	163	51	81	- 136	- 87	- 165
Fibre++ (Arnott)	- 52	175	42	79	- 148	- 75	- 157

• U. Heinemann & al.,Nucl. Acid. Res. 19, 427 (1991)

x Z. Shakked & al., Nucl. Acids Res. 18, 3185 (1990)

o A. Rich & al., Eur. J. Biochem. 181, 259 (1989)

* J. Subirana & al., J.Mol.Biol. 221, 623 (1991)

\+ S. Prémilat & G. Albiser, Nucl.Acids Res. 11, 1897 (1983)

++ S. Arnott & al., J.Biomol.Struct.Dyn. 6, 1189 (1989)

TABLEAU N° 4

A.D.N. FORMÉ B	α	β	γ	δ	ε	ζ	χ
	P —— O5'—— C5'—— C4'—— C3'—— O3'—— P						
d(CGCGAATTCGCG)•	- 63	171	54	122	-169	-108	- 117
d(CCAGGCCTGG)x	- 61	165	42	131	-144	-130	- 98
d(CCAACGTTGG)o	- 64	166	49	128	-156	-121	- 103
Fibre+(Prémilat,Albiser)	- 31	148	37	132	-156	-133	- 122
Fibre++ (Arnott)	- 33	138	33	142	-141	-157	- 99

• R. Dickerson et al. Proc.Nat.Acad.Sci.USA 78, 2179 (1981)

x U. Heinemann & C. Alings, J.Mol. Biol. 210, 369 (1989)

o R. Dickerson & al. J.Mol.Biol. 217, 177 (1991)

+ S. Prémilat & G. Albiser, Nucl.Acids. Res. 11, 1897 (1983)

++ S. Arnott & al. Nucl.Acids. Res. 11, 4151 (1983)

TABLEAU N° 4

D'autre part, la confrontation entre les valeurs des angles dièdres trouvées par diffraction RX sur des fibres et les valeurs moyennes de ces angles déduites de la cristallographie d'oligonucléotides montre un bon accord (47). Mais dans les cristaux d'oligonucléotides on remarque une grande dispersion des valeurs de ces angles d'un nucléotide à l'autre (perturbations dues aux effets d'extrémité).

L'étude de la forme C de l'ADN s'est révélée plus délicate étant donné la faible définition des clichés de diffraction RX due aux fibres semi cristallines. Il faut également remarquer que les paramètres hélicoïdaux retenus, P = 30,6 A et p =3,30 A pour définir cette forme correspondant en fait à un pas P, dont les valeurs expérimentales sont comprises entre 31,2 A et 29,2 A (31).

Néanmoins, dans la publication consacrée à cette forme C, plusieurs modèles sont proposés, qui, à nouveau, satisfont aux données RX de fibre et au dichroïsme linéaire infrarouge. Mais à la suite de travaux expérimentaux réalisés ultérieurement sur les transitions conformationnelles des ADN et des polynucléotides, les conclusions pour le choix d'un modèle conformationnel en double hélice gauche ne nous semblent pas correctes. En effet, la transition B-C a lieu, avec des ADN en présence de lithium ou avec un très faible pourcentage de sodium, quand on abaisse progressivement l'humidité relative. Or, durant cette transition, les clichés de diffraction RX révèlent une modification très progressive des paramètres hélicoïdaux et, en associant des mesures des dimensions de fibre, le caractère non coopératif de cette transition a été prouvé (Chap. V, B). Le caractère non coopératif de cette transition a également été remarqué par spectroscopie infrarouge sur les films d'ADN (63). La conformation de la forme B étant une double hélice droite, celle de la forme C reste donc dans cette famille d'hélices. Dans la publication présentée, c'est le modèle IV qui doit être retenu bien qu'il correspond à un moins bon accord avec les résultats infrarouge. On remarque que les angles dièdres de ce modèle sont très proches de ceux proposés pour la forme B (Tableau N°IV).

Il faut également préciser que les caractéristiques attribuées classiquement aux clichés de la forme C (P = 31 A, p = 3,3 A avec la présence d'une tache de Bragg à R = 0,1 A^{-1} sur la première strate) ne sont réunies que transitoirement lorsque l'humidité relative varie.

Un argument qui également avait été décisif pour le choix d'une conformation gauche pour la forme C résidait dans l'analyse de la transition C-A-B expérimentalement observée sur des fibres d'ADN à faible concentration en sodium. En effet l'angle de rotation entre nucléotides successifs est voisin de 38,7° pour la forme C, pour la forme A, il est de 32,7° et de 36° en forme B. Ce changement de sens de la torsion de l'hélice lorsque l'humidité relative croît semble s'expliquer difficilement si l'hélice reste droite. Or, après de nombreux essais effectués pour reproduire ces transitions, on s'est rendu compte que cela n'était réalisable que dans des conditions particulières.En effet, une tension mécanique appliquée à la fibre à haute humidité empêche la transition vers A quand l'humidité est réduite, on a alors une déformation de la forme B en C. La tension étant supprimée, une élévation très lente de l'humidité fait disparaître la forme C au profit de la forme A. On peut également retrouver les transitions C-A-B avec des fibres ayant une concentration assez faible en sel de sodium en opérant des variations brutales d'humidité (de 92 % à 40 %) et en élevant à nouveau progressivement l'humidité relative.

Un autre argument renforce également l'impossibilité de passer d'une hélice gauche à une hélice droite lors de la transition C-A provient des études d'hydratation (Chap. V,C). En effet on évalue en moyenne, à 4 ou 5 le nombre de molécules d'eau associé à chaque nucléotide en formes C ou A. Cela conduit à un assemblage compact des molécules et empêche tout mouvement dans la fibre et donc tout changement de sens de la double hélice.

La dernière publication de ce chapitre présente également une conformation en double hélice droite pour la forme D présentée par certains polynucléotides tel que le poly (dA-dT)-poly (dA-dT). Dans ce cas les seules mesures sont faites par diffraction RX. C'est donc l'analyse des transitions de forme qui permet de justifier le sens hélicoïdal retenu. L'analyse des transitions réalisées ultérieurement avec ce polynucléotide conduit à la même conclusion à savoir que la forme D est une double hélice droite.

CHAPITRE IV : CONFORMATION DE L'ADN EN PRESENCE DE CATIONS METALLIQUES ET EFFET DE LA TENSION MECANIQUE SUR DEUX TYPES DE TRANSITIONS CONFORMATIONNELLES

A) INTRODUCTION

Dans la première publication proposée, c'est l'étude d'un cation métallique (Ag^+) fixé sur l'ADN qui est abordée, le cation compensateur étant toujours le sodium. Les résultats donnés par de nombreuses techniques physico-chimiques permettent de classer en trois catégories les métaux qui se fixent sur l'ADN. On distingue ceux qui se lient au phosphate, entre bases et phosphate ou simplement sur les bases (Tableau N° V) (64).

TABLEAU N° V

Sites	Ions métalliques
Phosphate	$Li^+, Na^+, K^+, Rb^+, Cs^+, Mg^+, Ca^{2+}, Sr^{2+}, Ba^{2+}, Fe^{3+}$
Phosphate et base	$CO^{2+}, Ni^{2+}, Mn^{2+}, Zn^{2+}, Cd^{2+}, pb^{2+}, Cu^{2+}, Fe^{2+}$
Base	Ag^+, Hg^{2+}

Classification des ions métalliques en fonction de leur site de liaison sur l'ADN.

Certains de ces cations sont présents naturellement dans les ADN et ARN extraits des cellules, ils participent également dans des fonctions biologiques (effet mutagène) ou encore, ils permettent des réactions enzymologiques (65). Il est également connu que des cations peuvent bloquer certaines conformations de l'ADN ou encore favoriser certaines transitions entre doubles hélices droites (66), mais aussi

entre doubles hélices droites et gauches et cela, pour certaines séquences de bases (67).

Le cation Ag^+ fixé sur les bases G-C de l'ADN est soupçonné de provoquer un changement de conformation. Ainsi, le spectre dichroïque de l'ADN en solution à haute teneur en argent fait apparaître une bande négative très intense vers 2 700 A qui n'est attribuée à aucune conformation connue (17). La diffraction R.X. de fibre semble donc indiquée afin d'analyser ce changement de conformation et, éventuellement, sélectionner le site de chélation de l'argent sur les bases. En effet, cette étude est semblable à la méthode de "l'atome lourd" classiquement utilisée en cristallographie. Néanmoins, la distribution non périodique du cation rend l'interprétation des clichés R.X. de fibre plus délicate.

La deuxième publication présentée s'intéresse à un facteur souvent occulté dans la diffraction R.X. de fibre, la tension mécanique appliquée aux fibres. En effet, la méthode empirique d'orientation des fibres d'ADN à partir de gel fait appel à l'action d'une tension mécanique. Le maintient de cette tension sur la fibre peut éventuellement contrarier l'évolution de la fibre lorsque, par exemple, l'humidité relative environnante change. Pour déterminer l'influence de ce facteur, une étude de diffraction R.X. a été entreprise sur des fibres qui présentent les transitions A-B ou B-C lorsque l'humidité relative est modifiée. D'autre part, il faut remarquer que la tension n'est pas sans intérêt biologique puisque dans la cellule l'ADN peut subir ce type de contraintes mécaniques.

B) RX DE FIBRE ET ETUDE CONFORMATIONNELLE DE L'ASSOCIATION D'IONS METALLIQUES A L'ADN

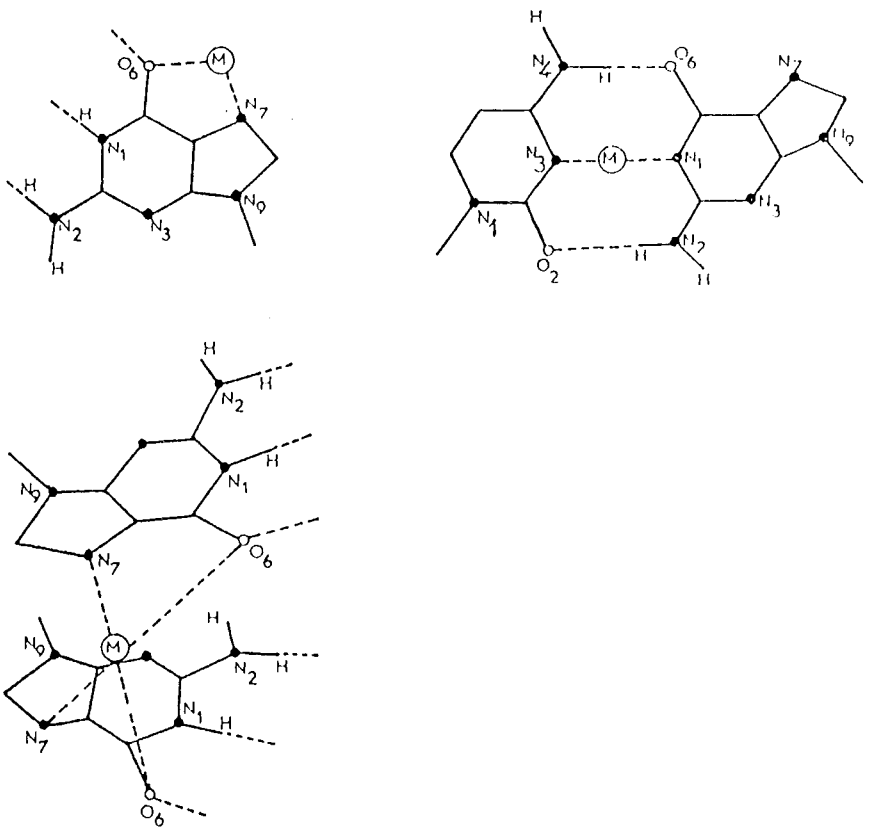

Figure N° 16 : Les sites envisagés pour l'association de Ag^{+} sur l'ADN.

Journal of Biomolecular Structure and Dynamics, ISSN 0739-1102
Volume 2, Issue Number 4 (1985), ©Adenine Press (1985).

Fibre X-Ray and Conformational Study of the Binding of Metal Ions on DNA

G. Albiser and S. Premilat
Laboratoire De Biophysique Moleculaire
Universite De Nancy I
ERA CNRS N° 828
Centre 1ER Cycle, B.P. N° 239
54506 Vandoeuvre Les Nancy (France)

Abstract

Results obtained from X-ray diffraction as well as from conformational analysis of Ag-DNA fibres are presented. For small percentages of Ag^+ bound and high humidity, the B-DNA form is maintained. As the percentage of Ag^+ is increased, the helical parameters of the B-DNA are modified. These modifications are directly related to the percentage of G−C bases. The periodicity of the DNA fibres are perturbed as Ag^+ is mainly bound to G−C pairs and, thus, only the equatorial diffracted intensities can be compared to values calculated from molecular models. It is shown, by this way, that the first binding site is located on N7 of G. A second site is situated between N3 and N1 of the G−C pair, at the place of a hydrogen bond. A molecular model of the Ag-DNA complex is proposed and shown to be in agreement with experimental data. Results obtained allow to get some information on the binding of other ions such as Cu^{2+} and Hg^{2+} which give very little modification of the fibre X-ray patterns.

Introduction

Effects of metallic ions on the conformations and functions of nucleic acids are the subjects of many experimental studies (1-5). They clearly show that the different experimental technique used (such as spectrophotometry, potentiometry, etc. . . .) provide information on the binding sites of ions. Nevertheless, in some cases, different sites remain possible and no molecular model has actually been presented in order to take into account the modifications of the DNA structures induced by the ions. The present study is devoted to this last problem particularly in the case of the binding of the monovalent cation Ag^+ on DNA. As a matter of fact, with the spectroscopic techniques, silver does not present any absorption in the scale of the investigated wavelengths and thus does not hide the modifications of the spectrum due to conformational changes (6-13). So, it has been shown that the binding of the cation Ag^+ on the DNA in solution is realized in two successive steps corresponding to the existence of two different binding sites (6,7,8,9). In a first step, for a ratio of

cation Ag^+ per nucleotide below 0.2, the binding site could be located on N7 of the guanine or between O6 and N7 of the guanine or also in chelate between two successive bases one of which, at least, is a guanine (7). Then, for a ratio of silver above 0.2, a second site appears in the middle of a pair of bases, at the place of a hydrogen bound, between N1 of a purinic base and N3 of a pyrimidinic one (6,7). Binding on this second site must lead to a disruption of the macromolecular conformation.

Studies in solution can hardly give fundamental information on DNA conformations and the lack of crystallographic results on single crystals renders X-ray diffraction on oriented fibres an interesting approach (14). In the present work, X-ray diffraction by oriented fibres associated to silver ions is used as a method of conformational analysis. Moreover, it appears that the binding of Ag^+ on DNA gives more pronounced and clear effects of fibre X-ray patterns than other metal ions (Cu^{2+} and Hg^{2+} for example). Hence, the binding of Ag^+ can also be used as an example permitting to get some information on these other ion-DNA systems which are more important on a biological level.

Materials and Methods

Two different DNA molecules have been used in the present study: the calf thymus DNA which contains 42% of guanine-cytosine bases and the micrococcus lysodeikticus DNA which has 72% of guanine-cytosine bases. These DNA were purchased from Miles Laboratories in lyophilised form. For the X-ray studies, the DNA must be stretched in fibres and the different samples are realized as follows: a DNA solution in sodium acetate 10 to 20 mM is realized after dialysis and precipitation. The pH of the solution is either 5.4, to get only one binding site with a small value of r (the average number of cations per nucleotide) or 8 to bind simultaneously Ag^+ on the two sites (6). Measurement of the optical density of the solution allows to determine the DNA concentration. To a definite volume of this DNA solution, an appropriate volume of silver nitrate solution is added so as to get the defined r value which varies, in the present work from 0.05 to 0.5. Precipitation with alcohol and centrifugation gives a gel from which fibres are streched (15,16). The process is realized sheltered from light in order to avoid oxydo-reduction.

The procedure followed for the determination of the molecular models of the different DNA double helices is the one used before (17). It takes into account the helical parameters, the Watson-Crick pairing of complementary bases associated to antiparallel sugar-phosphate chains and the stereochemical constraints. In the present case, distances between silver and nitrogen or between silver and oxygen, have been given values of respectively 2.1 Å and 2.3 Å and the distance between the two nitrogens of a base pair, bound to a silver ion, is 3.8 Å (18).

The calculations of the theoretical diffracted intensities from a DNA molecular model are performed following the procedure previously described and used (19). But this method is not presently totally valid because it has been established that silver ions bind essentially to guanine (for small r) (20,21). Thus, the fact that the

silver bound has an atomic scattering factor much higher than those of the DNA atoms perturbs the periodicity of the molecular structure and makes the concept of average nucleotide inapplicable (19). This loss of periodicity does not allow any more to calculate correctly the diffracted intensity on the different layer lines. However, the calculation remains possible for the equatorial line. As a matter of fact, the rule of selection, in this last case, gives essentially for n, the order of the Bessel functions, the value 0. This eliminates the phases in the structure factor and the equatorial intensities are only dependent on the radial positions of the atoms of the repetitive unit. In this case, the average nucleotide which is a function of the percentages of G−C and A−T bases can still be used; one shall just add to the list of atoms, the silver ion with its percentage. The structure factor F and the expression of the calculated diffracted intensity, for the equatorial layer line, can be written as:

$$F(O,\xi) = \sum_j f_j J_o(2\pi R_j \xi);$$

$$I(O,\xi) = F^2(O,\xi)$$

where:

ξ = radial coordinate of a lattice point in reciprocal space,

R_j = radial coordinate of the J^{th} atom in the repeating unit in real space.

f_j = scattering factor of the J^{th} atom.

J_o = Bessel function of first kind of order zero.

Consequently, only the equatorial intensities are compared to the calculated ones and by this way, the radial positions of silver atoms in the DNA double helical conformation are determined.

Results

In order to make possible a comparison between the present results and those from studies on solutions, the DNA fibres have been prepared with ratio r of silver per nucleotide varying from 0.05 to more than 0.5. For ratio r up to 0.2 with the DNA containing 72% of G−C bases and less than 0.15 for the DNA with 42% of G−C, at high relative humidity, the B-form is obtained. The double helical parameters are not modified: the pitch is 34 Å, the rotation per nucleotide is near to 36° and the rise per nucleotide is near to 3.4 Å. The crystal lattice is hexagonal or orthorhombic (Fig. 1(A,B,D,E)). For some fibres prepared with a low concentration of sodium salt, the lowering of the humidity allows to obtain the A-form. The patterns of the equatorial intensity diffracted by the DNA in B-form associated to silver ions, show the same positions and relative amplitudes of the intensity maxima as those observed classically for the B-DNA. Nevertheless some stretched fibres obtained from solution at pH 8 with a ratio r higher than 0.1 do present the B-form but the

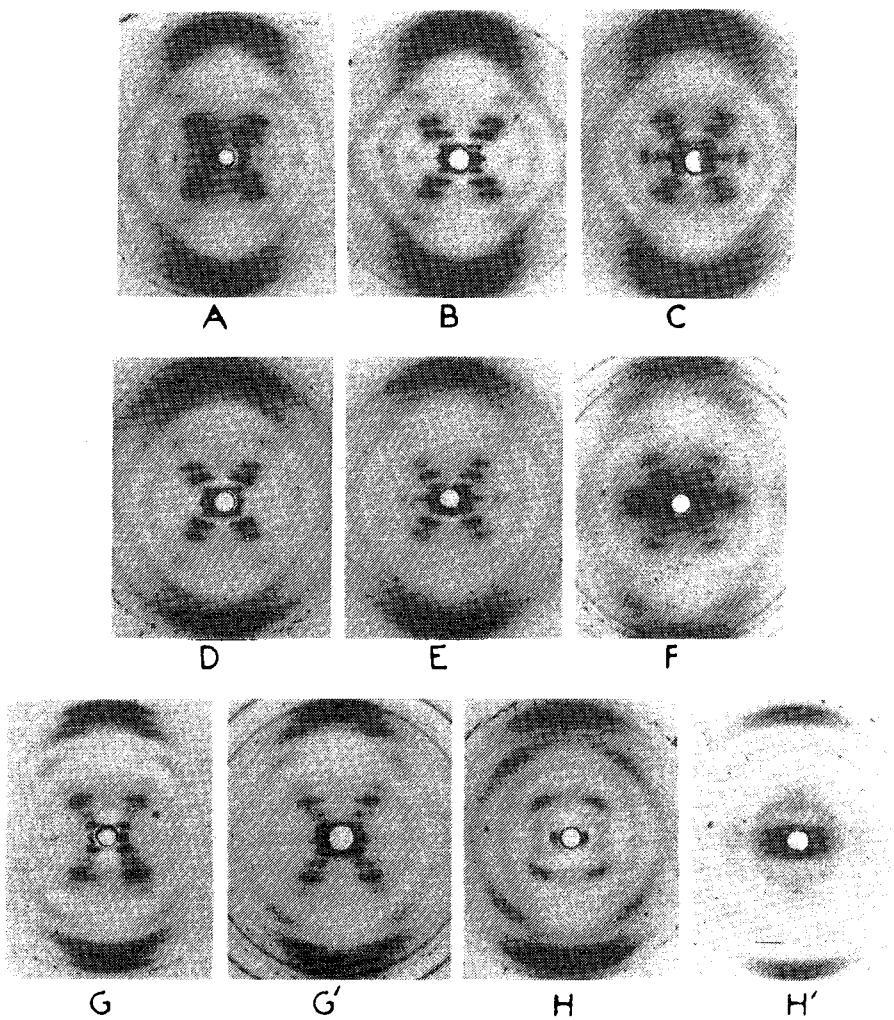

Figure 1. X-ray fibre patterns obtained at 92% relative humidity. DNA (42% G + C). A) without Ag^+; B) $r = 0.1$; C) $r \sim 0.15$. DNA (72% G + C): D) without Ag^+; E) $r = 0.1$; F) $r \sim 0.2$. G) Poly dA - poly dT without Ag^+; G') $r \sim 0.4$; H) poly dG - poly dC without Ag^+; H') $r \sim 0.5$.

intensity minimum near $\xi = 0.08$ Å^{-1}, on the equator, has disappeared and the relative intensities of the maxima at 0.12 and 0.18 Å^{-1} have been inverted compared to the B-DNA.

For r higher than 0.15 and up to 0.5 one can note, on the diffraction patterns, modifications of the helical parameters of the DNA with 42% of C = G; the meridional reflection is located at 3.27 Å and the layer-line spacing has a value of 31.7 Å (Fig. 1(C)). There are 9.7 nucleotide pairs per turn and the rotation per nucleotide

is thus 37°. With the DNA containing 72% of G−C bases the modification of the helical parameters is even more pronounced (Fig. 1(F)); the pitch gets near to 28.8 Å, the meridional reflection is then at 3.2 Å; that corresponds to an average rotation per nucleotide of 40° (with 9 units per turn). On figure 2, one can see the representation of the behavior of these two DNA, with a ratio r of silver bound higher than 0.2. The helical parameters of these two DNA keep these values when the relative humidity is even much lower than 92%. Moreover, the diffraction pattern does not change when the tension on the fibre is removed (one end of the fibre is free).

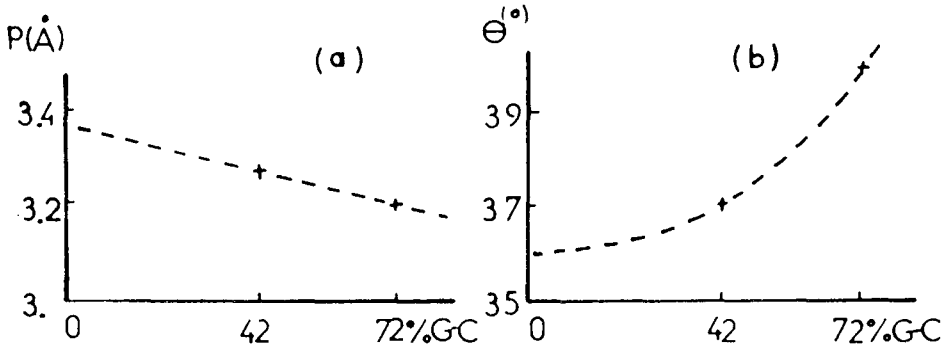

Figure 2. DNA saturated with Ag^+. Experimental values in function of the (G−C) percentage, of: a) the position p of the meridian spot; b) the mean rotation θ per nucleotide.

The measurements of the equatorial intensities for these two DNA with r = 0.2 (Fig. 3) show an increase of the diffracted intensity at $\xi = 0.08$ Å^{-1}, a position which corresponds to a very pronounced minimum for the B-DNA. The increase of the diffracted intensity is also very important at the usual maximum of 0.12 Å^{-1}. Conversely, the maximum at 0.18 Å^{-1} disappears totally. This last fact is more pronounced when the percentage of G−C bases is lower (fig. 3b,c).

In order to determine the limiting behavior of DNA in B-form associated to Ag^+ cations, the binding of AG^+ on poly dA−poly dT and poly dG−poly dC has been studied. With the poly dA−poly dT no modification of the diffraction pattern is observed when r varies from 0.1 to 0.5 (relative humidity of 92%) (fig. 1 (G'))(22). But one can see, even with small value of r, diffraction spots due to the silver salt which is not included in the DNA structure.

For the poly dG−poly dC, at 92% of relative humidity, the presence of silver ions does not introduce any modification of the helical parameters (23) except a spreading of the spots due to a disorganization of the fibre is observed even with low percentages of silver (fig. 1(H')). For a r value near to 0.5, the only reflection which is observable is the meriodional one.

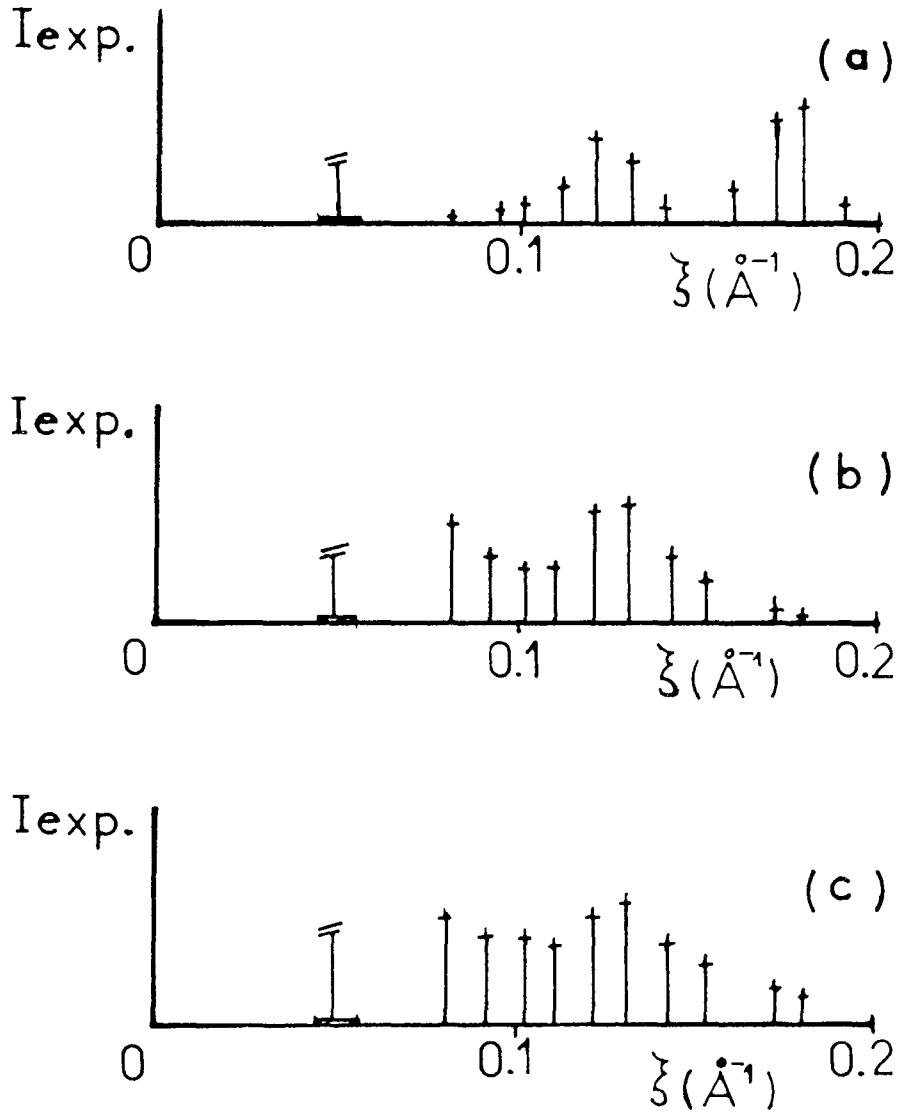

Figure 3. Experimental diffracted intensities—arbitrary scale—the lattice is hexagonal (parameter a). a) DNA (42% G−C) without Ag^+, a = 43 Å; b) DNA (42% G−C) with Ag^+, r = 0.2, a = 44 A°; c) DNA (72% G−C) with Ag^+, r = 0.4, a = 44 A.

— Calculated intensities for r smaller than 0.2

For the molecular model of B-DNA (17), the distance to the axis of a silver ion bound to N7 of guanine is 5.2 Å. This distance becomes 3.6 Å when the ion Ag^+ is bound to O6 and N7 of the same guanine. For a Ag^+ ion situated between two successives bases of one chain, its distance to the helix axis is still near to 5 Å.

With silver percentage in DNA solution corresponding to r smaller than 0.2, the stretched fibres do present the classical B-form at a high relative humidity. But if one admits that the cation Ag^+ is essentially bound on the guanine, the saturation of the first site corresponds to a maximum ratio of 0.2 for the DNA with 42% of

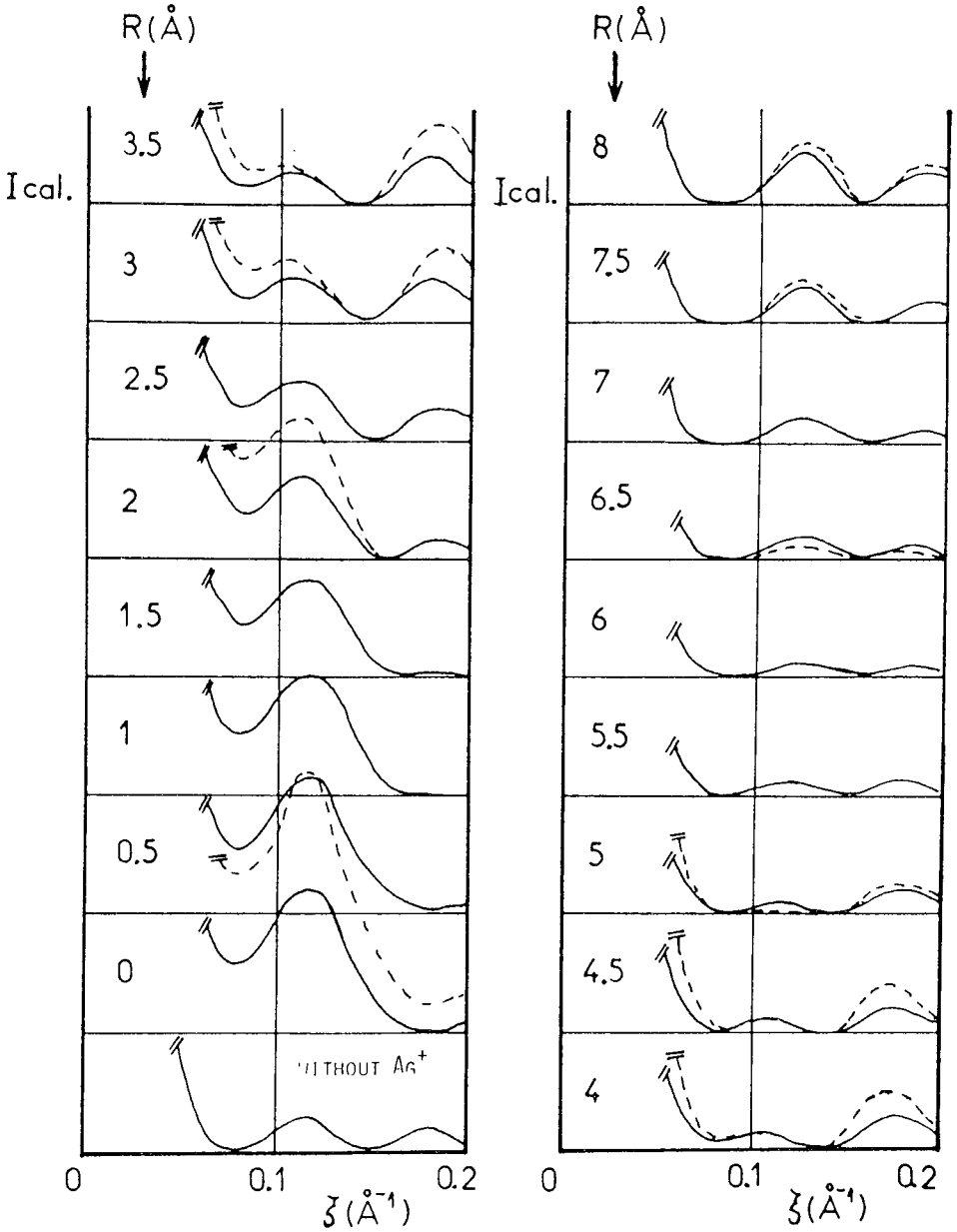

Figure 4. Equatorial intensity calculated from the B-DNA, the radial position of Ag^+ is given values from 0 to 8 Å with 42% (G−C), r = 0.24 (——) and with 72% (G−C), r = 0.36 (·····).

G−C and a maximum ratio of 0.36 for the DNA with 72% of G−C. The figure (4) presents calculated equatorial intensities for the B-form of DNA with radial positions of bound silver atoms varying from 0 to 8 Å and that for the two DNA with the first site saturated. These curves of calculated intensities show large modifications of the positions and amplitudes of the maxima and minima when the distance to the axis of the cation Ag^+ varies from 0 to 4 Å. Conversely, above 4 Å the positions of maxima and minima remain identical to those of the DNA without silver (the amplitudes are slightly reduced).

— Calculated intensities for r higher than 0.2

When the percentage of bound silver is higher than 0.2, the DNA fibres give diffraction patterns of helices with parameters different from those of the B-DNA and with equatorial intensities very much increased. It is thus necessary to determine a new molecular model which must agree with the new experimental parameters of the double helix (fig. 2).

As poly dA−poly dT is not modified by Ag^+ and as the 72% G−C DNA is more perturbed by Ag^+ than the 42%, one can suppose that the G−C bases are still involved in the binding of the ion to the second site. Moreover, the behavior of the poly dG−poly dC which presents, in solution, a binding ratio near to 0.25 seems to confirm the hypothesis of the binding of silver between two successive guanines of the same chain (first site). Fibres of this polynuceotide, with a higher silver percentage, do present mainly a desorganization of the conformation which can be explained by the presence of a second binding site on the G−C base pairs. This second binding site has already been proposed (6,7) and is situated between N3 of C and N1 of G at the place of a H-bond (with the release of the proton). The resulting 3.8 Å distance between the 2 nitrogens (instead of 2.8 Å) introduces a distorsion of the G−C paired bases. Since one observes an increase of the average rotation per nucleotide together with a lowering of the pitch of the helix, one can suppose this to be due to an increase of the dihedral angle δ of the sugars associated with the G and C bases. These modifications cause the bases G and C to be moved towards the large groove.

To determine this new conformation, it is logical to take, as structural unit, a dinucleotide constituted by a nucleotide with modified dihedral angles (for bases G or C) and a nucleotide near to the B-form (bound to a base A or T). For the determination of the antiparallel chain, one can define a dyad axis, either in the G−C plane, or in the A−T one. The table (1) gives the dihedral angles of a double helical structure verifying the geometrical conditions. These angles allow to calculate the atomic coordinates of a dinucleotide corresponding to a DNA having 50% of G−C bases an average of 3.25 Å between successive bases and a mean rotation of 37.8° (evaluated from the figure (2)). Actually for the dinucleotide, the rise along the axis is 3.39 Å (for A or T) + 3.19 Å (for G or C) and the rotation is 36° (for A or T) + 39.6° (for G or C). This conformation corresponds to a Watson-Crick pairing of the A−T bases, it verifies the geometrical constraints on the distances

Table I
Chain dihedral angles for the dinucleotide of the molecular model with Ag^+
(χ: O1′−C1′−N1−C2 for C or T; O1′−C1′−N9C4 for G or A.)

Dihedral Angles (°)	Dinucleotide A or T	G or C
α (P−O5′)	−31.40	−31.82
β (O5′−C5′)	150.11	151.03
γ (C5′−C4′)	35.34	35.56
δ (C4′−C3′)	132.34	143.67
ϵ (C3′−O3′)	−157.41	−158.75
ζ (O3′−P)	−136.01	−134.48
χ (C1′−N): A,T	−115.60	
χ (C1′−N): G,C		−105.60

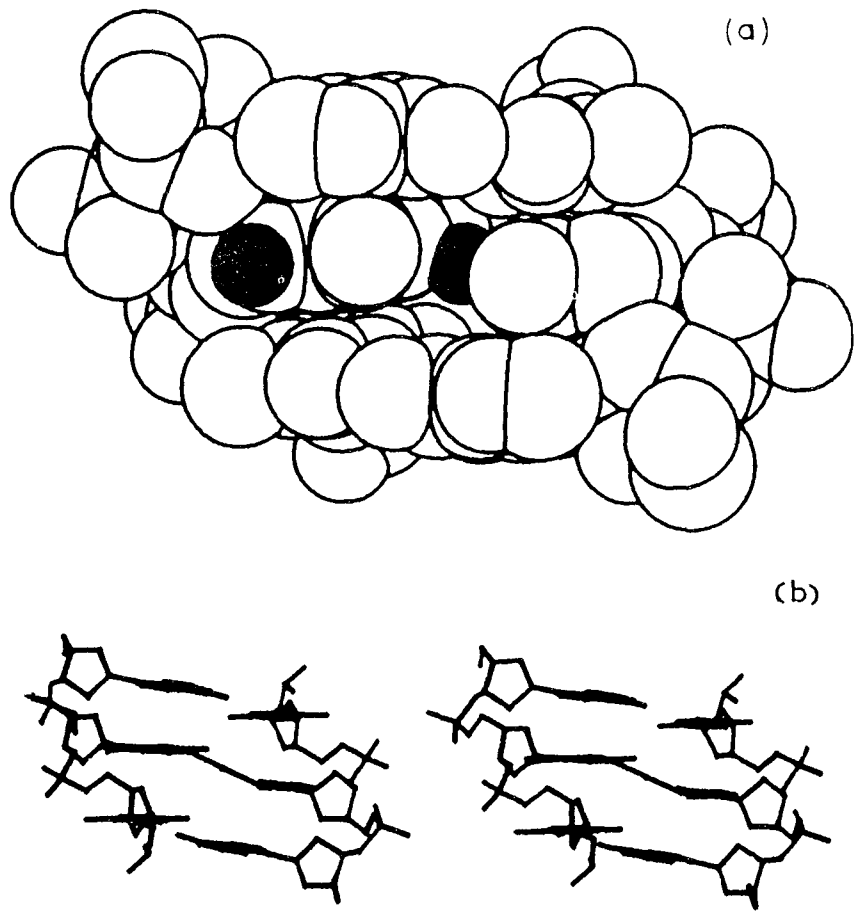

Figure 5. a) Molecular model of the perturbed B-DNA with the two binding sites of Ag^+ on a (G−C) pair b) a stereo view of this model.

between G and C and presents a very good stereochemistry. In this DNA conformation, the silver bound in the first site on N7 of the guanine is situated at a distance of 5.8 Å to the axis (for the B form it is 5.2 Å) and the other binding position between N7 and O6 becomes 4.7 Å instead of 3.6 Å. The distance to the axis is then 1.2 Å for the silver ion in the second site between the bases of a G−C pair. The figure (5) shows a description of this DNA molecular model with the two bound silver ions.

In the figure (6a,b), the equatorial intensities, calculated with the atomic coordinates of this molecular structure are represented for different distances of the ion, close to the helix axis. In the figure (6a), the first binding site is situated on N7 of guanine. The ratio r is 0.2 and 0.3 respectively for the DNA with 42% of G−C and for the 72% one. In this case, the second site between the G and C bases is also

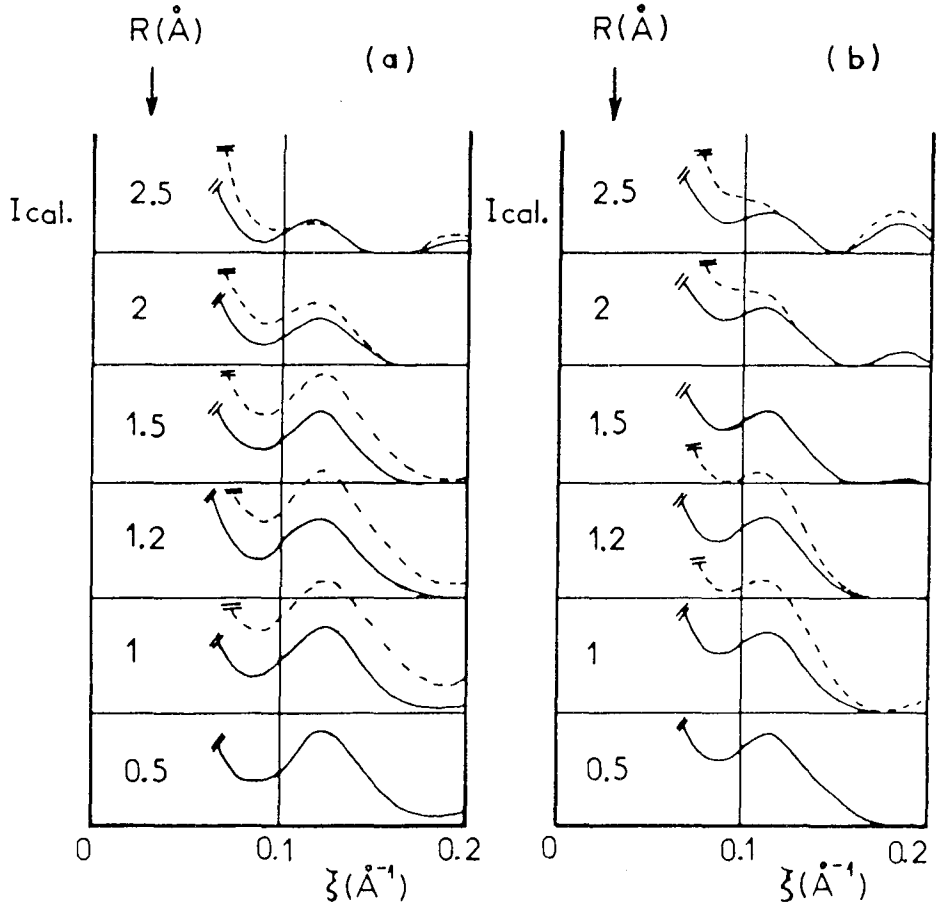

Figure 6. Calculated equatorial intensity obtained with the molecular model satured with Ag^+. Values of the radial distance R of Ag^+ in the second site vary from 0.5 to 2.5 Å. DNA 42% (G−C) (——); DNA 72% (G−C) (·····) a) Ag^+ in the first site is fixed on N7 of G with R = 5.8 A°. b) Ag^+ in the first site is fixed between O6 and N7 of G with R = 4.7 Å.

occupied as there is saturation. On the figure (6b) the equatorial intensity is represented for the model with the same position of Ag^+ in the second site, near to the axis; the two sites are saturated for the two DNA. But in this last case, the first binding site is located between N7 and O6 of the guanine. These curves of the diffracted intensity obviously show the absence of minimum for $\xi = 0.08$ Å^{-1}, an increase of the intensity at 0.12 Å^{-1} and the absence of a maximum at 0.18 Å^{-1}.

Discussion

The measurements of X-ray intensities diffracted by DNA fibres with silver ions associated to a molecular conformational analysis are complementary to the experimental methods used for the study of DNA solutions. Although the binding of cations is not realized in a regular and periodic way, the modifications of the helical parameters and the perturbations of the equatorial intensities are experimental facts which allow to determine the radial distances of the cations in the DNA conformations. The method presently used permits to define the existence, on the DNA, of two different binding sites for the cation Ag^+. More precisely, a small percentage of silver per nucleotide (r below 0.15 for the DNA with 42% of G−C and 0.2 for the one with 72% of G−C) leaves the DNA in the B-form at high humidity and, in some cases, the decrease of the relative humidity can induce the A-form. This situation corresponds to the binding of Ag^+ on a site which perturbs just a little bit the conformation of the double helix. But note that for Ag^+ distances to the axis smaller than 4 Å, the curves of the calculated intensity are very much different from the observed ones. Hence the comparison between the experimental equatorial intensities and the calculated ones, as a function of the distance of the silver ion to the helix axis, allows to determine that the first binding site is located at a distance larger than 4 Å. So, the binding site of Ag^+ on the N7 of the guanine, located at a distance of 5.2 Å to the axis, seems to be very likely (24). Conversely, the binding site between N7 and O6 of the guanine at a distance of 3.6 Å to the axis, which creates non linear connections between the three atoms, is less probable. Another proposed site, which forms a complex with two or four ligands between successive bases from which at least one is a guanine (7), still gives, for silver ions, distances to the axis of respectively 3.6 Å and 5.2 Å. The distance of 3.6 Å can again be excluded but the position at 5.2 Å remains possible. Moreover, the existence of this complex seems to be justified by the behavior of the poly dG−poly dC which presents a percentage of bound silver (in solution) limited to 0.25.

The increase of silver ions bound modifies the helical parameters and one can see on X-ray diffraction patterns a clear increase of the equatorial intensities. These experimental facts confirm the existence of a second binding site for the silver and a modification of the DNA structure. The behaviors presented by the two DNA different in base composition, allow to suppose that again the G−C base pairs are perturbed by Ag^+ in the second site. The results obtained with the poly dA−poly dT and the poly dG−poly dC in presence of silver, confirm this hypothesis. The ion site between the nitrogens of G and C bases is well determined by the present study and the distance to the helix axis of this silver atom is near to 1.2 Å.

Moreover, the proposed conformation of DNA with silver ions has a good stereochemistry; it maintains the Watson-Crick pairing of the A−T bases with nucleotides in a form very close to B. This conformation presents pairs of G−C bases "open" in the large groove allowing the access of the silver ion to the internal site. The curves of the equatorial intensities calculated from this model are in good agreement with the experimental data.

It can be noted that the amount of silver bound on the fibres is not very well defined and that the same preparation can give different helical parameters for DNA samples. This fact is mainly due to a non homogenous fixation of the ions along the DNA fibres. Consequently a more precise estimation of the percentage of the bound cations, by flame photometry for example as recently used for Li-DNA (25), would not change significantly the present results.

The present method of conformational analysis based on fibre X-ray have also been applied to other metal ion-DNA systems. The binding of Cu^{2+} and Hg^{2+} were studied by this way and information in these cases are more relevant for biological studies. However these ions give modifications of the X-ray patterns which are much less pronounced than with Ag^{+}. Nevertheless results obtained from the Ag^{+}-DNA system permit to arrive at some conclusions concerning the binding of these cations. For example, Cu^{2+} bound to DNA leads to almost no perturbation of the diffracted intensities when r is small; the B form is maintained at high humidity and no increase in the equatorial reflexions can be noted (14). One can conclude that, in this case, the binding site is situated at a distance to the helix axis larger than 4 Å. When the value of r is larger, the X-ray pattern becomes hardly analysable; the DNA double helix is too much desorganized. One gets almost the same kind of results with Hg^{2+}, hence this cation is also fixed at a distance to the axis larger than 4 Å and its binding site can be on N7 of purinic bases (4,20).

References and Footnotes

1. Zimmer, C., *Z. Chem. 12*, 441-458 (1971).
2. Izatt, R.M., Christensen, J.M. and Rytting, J.H., *Chem. Rev.* 1972, 5, 439-481 (1971).
3. Daune, M., *Metal ions in biological systems*. Edit. Sigel, H., V.3, 1-37 (1974).
4. Sissoëff, I., Grisvard, J., and Guillé, E., *Prog. Biophys. Molec. Biol. 31*, 165-199 (1976).
5. Eichhorn, G.L., Adv. in *Inorg. Biochem. 3*, 2-46 (1981).
6. Jensen, R.H., and Davidson, N., *Biopolymers 4*, 17-32 (1966).
7. Daune, M., Dekker, C.A., and Schachman, H.K., *Biopolymers 4*, 51-76 (1966).
8. Eichhorn, G.L., Butzow, J.J., Clark, P., and Tarrien, E., *Biopolymers 5*, 283-296 (1967).
9. Wilhelm, F.X., and Daune, M., *Biopolymers 8*, 121-134 (1969).
10. Luk, K.F.S., Maki, A.H., and Hoover, R.J., *J. Am. Chem. Soc. 97*, 1241-1242 (1975).
11. Arya, S.K., and Yang, J.T., *Biopolymers 14*, 1847-1861 (1975).
12. Dattagupta, N., and Crothers, D.M., *Nucl. Acid. Res. 9*, 2971 2985 (1981).
13. Matsuoka, Y., and Norden, B., *Biopolymers 22*, 601-604 (1983).
14. Albiser, G., and Premilat, S., *C.R. Acad. Sci. Paris 282*, D, 1557-1560 (1976).
15. Langridge, R., Wilson, H.R., Hooper, C.W., and Wilkins, M.H.F., *J. Mol. Biol. 2*, 19-64 (1960).
16. Davies, D.R., and Baldwin, R.L., *J. Mol. Biol. 6*, 251-255 (1963).
17. Premilat, S., and Albiser, G., *Nucl. Acid. Res. 11*, 1897-1908 (1983).

18. Swaminathan, V., and Sundaralingam, M., *C.R.C. Crit. Rev. in Biochem.*, 245-336 (1979).
19. Premilat, S., a,d Albiser, G., *J. Mol. Biol. 99*, 27-36 (1975).
20. Walter, A., and Luck, G., *Nucl. Acid. Res. 4*, 539-550 (1977).
21. Ding, D., and Allen, F.S., *Biochem. Biophys. Acta 610*, 64-71 (1980).
22. Arnott, S., and Selsing, E., *J. Mol. Biol. 88*, 509-521 (1974).
23. Arnott, S., and Selsing, E., *J. Mol. Biol. 88*, 551-552 (1974).
24. Zavriev, S.K., Minchenkowa, L.E., Vorlickova, M., Kolchinsky, A.M., Volkenstein, M.V., and Ivanov, V.I., *Biochim. Biophys. Acta 564*, 212-224 (1979).
25. Parrack, P.K., Datta, S., and Sasisekharan, V., *J. Biomol. Str. Dyns.* 2, 149-157 (1984).

Date Received: August 1, 1984

C) INFLUENCE D'UNE TENSION MECANIQUE SUR LES TRANSITIONS CONFORMATIONNELLES B-A ET B-C DES ADN EN FIBRES

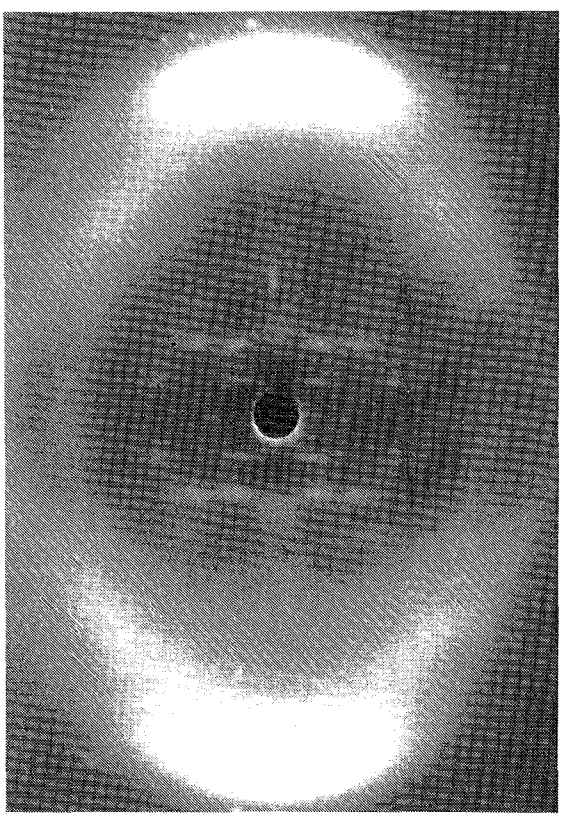

Photo N° 8 : Pour l'ADN à très faible concentration de sel de sodium la tension mécanique appliquée à la fibre permet l'obtention d'un cliché de la forme C à 0 % d'humidité relative.

Journal of Biomolecular Structure & Dynamics, ISSN 0739-1102
Volume 6, Issue Number 2 (1988), ©Adenine Press (1988).

Influence of a Mechanical Tension on the B-A and B-C Conformational Transitions in DNA Fibres

G. Albiser, M. Harmouchi and S. Premilat
Laboratoire de Biophysique Moléculaire, U.A. C.N.R.S. N° 494
Faculté des Sciences, Université de Nancy, I, B.P. N° 239
54506 Vandoeuvre les Nancy, France

Abstract

In the present fibre X-ray study we attempt to quantify the effect of a mechanical tension on the conformations, and transitions between the structural forms of DNA. A simple experimental device has been realized in order to apply precise mechanical forces on DNA fibres during X-ray exposure. It is shown that, as the applied tension is increased, the B→A transition can be prevented as well as with a decrease of the sodium salt content. A kind of distorted B form is then observed the helical parameters of which change with the relative humidity. On the contrary, the mechanical tension does not prevent the B→C transition; it only slows down the form change and improves the X-ray patterns up to a relative humidity of 0%.

Introduction

The structural polymorphism of the DNA macromolecule has been well established by X-ray fibre diffraction studies which have shown that the A, B and C forms (1-5) can be present in natural DNA while many other forms such as D, E, S (4) and P (6) are possible for synthetic polynucleotides. It is well known that the DNA polymorphism is influenced by, at least, three different physico-chemical factors namely the base sequence, the amount of salt in DNA preparations and the relative humidity of the fibre. The primary structure or sequence of nucleotides is an important characteristic of natural DNA and it has been shown that transitions between different helical forms are dependent on base composition (7,8). The type and amount of alkaline cation associated with the DNA may prevent the transitions of a double helical conformation (9,10); hydration or the relative humidity of fibres is also a main parameter which influences the transition between DNA conformations (2,11).

Although these different factors are generally well taken into account in preparing and studying X-ray fibre diffraction of DNA, many authors have noted that fibres obtained from the same preparation do sometimes present, during conformational transitions, very different behaviors which were hypothetically explained as due to some hysteresis effect (3). Moreover, one should note that a mechanical tension may be applied by the holder which maintains the sample extended during X-ray exposure (2). In order to avoid this effect, experimental studies have been made on

fibres free of tension placed in capillary tubes (12,13). Conformational changes due to stretching of DNA fibres or applied tensions have been mentioned (14) and confirmed recently (15) but only in a qualitative way. The aim of the present work is to get quantitative information on the effects of this supplementary parameter. The present study is limited to natural calf thymus DNA which is composed of almost as many A-T base pairs as C-G ones and also to only one alkaline cation, namely Na^+, used in low concentrations in order to observe the effect of the tension on the three forms A, B and C.

The behavior and form transitions of DNA are presently observed and followed by X-ray fibre diffraction. Samples are submitted to precise mechanical tensions (weights) during X-ray exposure and the relative humidity in the camera is varied in order to realize conformational transitions. It is shown that, starting from the B form at high relative humidity, the tension may forbid the transition to the A form and more generally modify the conditions normally associated to transitions between stable DNA forms.

Material and Methods

DNA samples were prepared from solutions of low concentration in sodium salt of calf-thymus DNA purchased from Pharmacia. The lyophilized material is dissolved in distilled water; the concentration of DNA in solution is determined from optical density measurement. The NaCl concentration is fixed by dialysis and a gel is obtained from centrifugation of the DNA solutions. In order to apply a precise tension on the fibre, it is mounted between two glass rods. One glass rod is fixed to the fibre holder and a thin thread is attached to the other rod which can slide on the holder so that tensions can be applied by hooking weights to the other thread extremity. The X-ray camera has been adapted to the holder and its thread so that one can change easily the weights without modifying the fibre position and orientation relatively to the collimator. Precise values of the relative humidity (r.h.) from 95% to 0%, are obtained by using different satured salt solutions (16). When the r.h. is changed, one waits for at least 24 hours for the equilibrium to be realized in the fibre environment.

Results

All the X-ray diffraction photographs have been obtained from two series of DNA fibres pulled from gel of calf thymus DNA. The two preparations differ in their sodium salt content; we used two different NaCl concentrations, namely a low salt concentration of 0.005 M and a very low salt concentration of 0.0005 M NaCl for DNA concentrations of 3 mg/ml.

DNA Fibres from 0.005 NaCl Solutions

The diameters of the different fibres used to obtain X-ray patterns were of the order of 0.1 mm and their lengths of a few mm. Samples mounted without mechanical tension do present the classical B and A forms at the respective relative humidity of 95% and 75%. When the r.h. is lower than 92%, the X-ray pictures are mixtures of the A

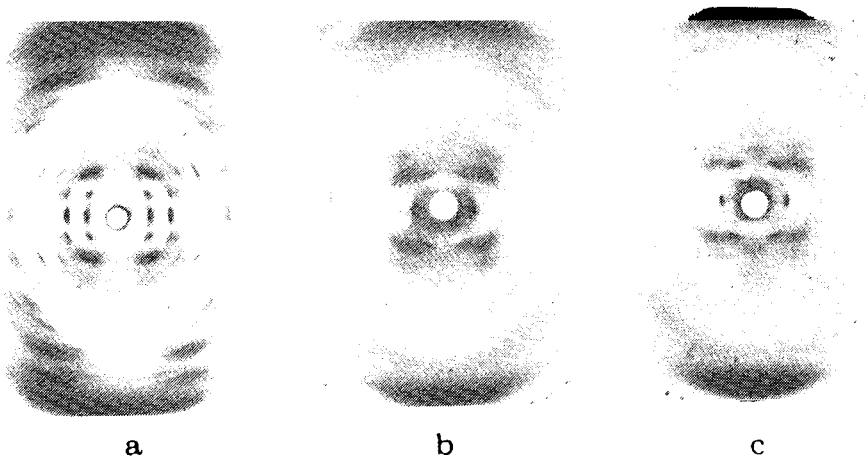

Plate 1: DNA fibre X-ray patterns (fibres from 0.005 M NaCl solutions).
a) relative humidity (r.h.) 75%. Tension of 10 g; mixture of A and B forms.
b) r.h. = 95%. Tension of 10 g; B form.
c) r.h. = 75%. Tension of 15 g; B* form.

and B patterns. The transition from B to A is reversible but we noted that the change from A to B takes a much longer time than the B to A transition. With these samples we could not obtain the C form even at very low r.h.

The mechanical tension is generally applied to the fibre at high r.h. (95%) and only then, one can lower the humidity. Fibres mounted with a tension of 5 g do not present any modification in their behavior as compared to the same samples mounted free of tension. When the tension is 10 g, the B form (plate 1b) is always observed at high r.h. but we obtained X-ray patterns of mixtures of A and B forms when the r.h. is lowered (plate 1a). Under these conditions of tension, we could not obtain the A form alone at any relative humidity.

Under a tension of 15 g, the classical B form is observed at high relative humidity and one cannot get the A form or mixtures of A and B when the r.h. is reduced. For r.h. lower than 92% the X-ray patterns (plate 1c) look like those of the B form but with helical parameters (Table I) varying depending on the r.h. The B form is thus progressively distorted and becomes a helical conformation we designate by B*. When the r.h. is lower than 63%, X-ray spots are not more discernible and it becomes impossible to determine helical parameters.

Tension being maintained on the fibre, the transition between B and B* is reversible with a change of the relative humidity. On the contrary, when the tension is withdrawn from fibres in the B* form at 75% r.h., the DNA remains under this form while it classically adopts the A form at this humidity. To get back the ordinary DNA

Table I

Helical parameters of DNA. Fibres from 0.005 M NaCl solutions. r.h. = relative humidity; P = Helix Pitch; ρ = rise per nucleotide pair; $\frac{P}{\rho}$ number of base pairs per helix turn; $\Delta\theta$ = rotation per nucleotide; d_{eq} = position of the 1th equatorial spot.

	No tension applied				Tension of 15 g		
r.h.%	95	90	86	75	95	75	63
P(A)	33.7	28.4 32.74	28.06 -	27.5	33.5	32	31
ρ(A)	3.37	2.59 3.37	2.57 3.34	2.54	3.35	3.33	3.32
$\frac{P}{\rho}$	10	10.96 9.7	10.92 -	10.8	10	9.6	9.36
$\Delta\theta^{(\circ)}$	36	32.8 37	32.9 -	33.3	36	37.5	38.4
d_{eq}(A)	22.4	-	-	-	20.65	18.2	16.54
DNA form	B	A B	A B	A	B	B*	B*

behavior from B*, when tension is removed, the relative humidity must be put to 95% and the fibre maintained under these conditions (corresponding to the B form) for 24 hours before the humidity can be lowered in order to obtain again the A form at 75% r.h.

DNA Fibres from 0.0005 M NaCl Solutions

The diameters of the fibres we studied were of the order of 0.1 mm as for the preceding series. When samples are mounted without any additional tension, the B form is observed at high r.h. (95%) and the C form appears at a r.h. of 86% (plate 2a). It can be noted that the X-ray pattern of the C form is different from the B* one even if these two forms do present similar helical parameters. The main difference is in the presence of a diffraction spot at R = 0.1 A^{-1} in the C pattern. When the r.h. is lowered, the helical parameters of the C form present large variations (Table II) and for r.h. lower than 75% the X-ray pattern is so poor that the measurement of parameters becomes impossible. The B to C transition is reversible with an increase of the relative humidity for fibres free of tension. But we never obtained the A form, nor did we observe the C-A-B transitions (10) with these DNA fibres drawn from preparations very low in salt content.

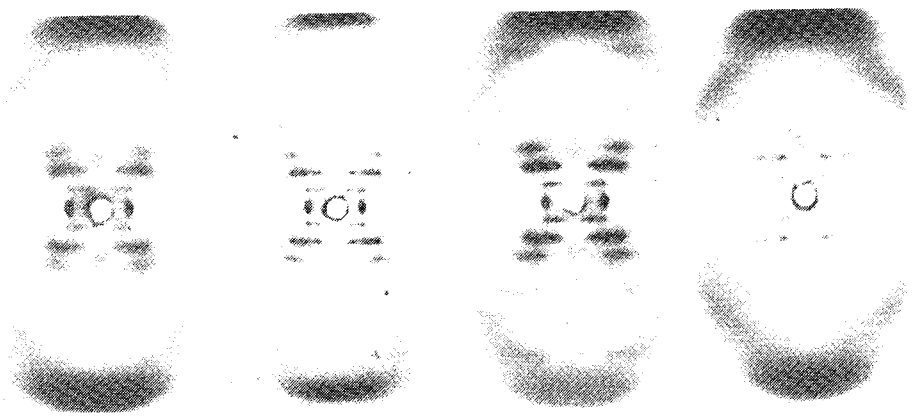

a b c d

Plate 2: DNA fibre X-ray patterns; (fibres from 0.0005 M NaCl solutions).
a) r.h. = 86%. No tension applied; C form.
b) r.h. = 95%. Tension of 5 g; B form.
c) r.h. = 86%. Tension of 5 g; C form.
d) r.h. = 0%. Tension of 5 g; C form

Table II

Helical parameters of DNA. Fibres from 0.0005 M NaCl solutions. No tension applied. See Table I for the definitions of parameters.

r.h.%	95	87	82	79	75
P(A)	33.5	32	31	29.4	28.9
p(A)	3.35	33.3	3.32	3.31	3.30
$\frac{P}{p}$	10	9.6	9.3	8.8	8.7
$\Delta\theta^{(\circ)}$	36	37.5	38.6	40.5	41.1
d_{eq}(A)	20.4	19.1	18.7	18.3	17.6
DNA form	B	C	C	C	C

When a 5 g tension is applied on a sample placed in a high r.h. environment, the B form is observed (plate 2b). By lowering the humidity, the C form appears and we got very good X-ray pictures even up to 0% r.h. (plate 2d). Thus one can distinguish, for r.h. in the range of 86% to 75%, that the higher layer lines of the X-ray patterns correspond to a multiplicity of 10 while the lower ones are associated to another multiplicity

Table III
Helical parameters of DNA. Fibres from 0.0005 M NaCl solutions. Applied tension of 5 g. See Table I for the definitions of parameters.

r.h.%	95	87	85	75	66	53	43	36	22	0
P(A)	33.7	33	32.7	32	31	30.4	30	29.5	29.1	28.3
p(A)	3.37	3.36	3.36	3.35	3.34	3.33	3.32	3.32	3.31	3.29
$\frac{P}{p}$	10	9.82	9.73	9.55	9.28	9.13	9.03	9.88	8.79	8.60
$\Delta\theta(^\circ)$	36	36.6	37	37.7	38.8	39.4	39.8	40.5	40.9	41.8
d_{eq}(A)	20.4	18.7	18	17.6	17.2	16.7	16.3	16	15.9	15.8
DNA form	B	C	C	C	C	C	C	C	C	C

(plate 2c). This corresponds very well to non-integral values for the number of base pairs per helical turn of the C helix (Table III). The reversibility of the B to C transition for samples held with a tension of only 5 g is well observed when the relative humidity is varied. One can see in Table II and III that the applied tension slows the variation of the C helical parameters P (helix pitch) and *p* (rise per base pair) with the lowering of the r.h. For instance, we got, with a tension applied on the fiber, a ratio $\frac{P}{p}$ (number of nucleotide pairs per helix turn) equal to 8.8 at 22% r.h. although this value is already obtained at 75% r.h. without tension. Moreover, we observed that an extreme value of 8.6 can be obtained for this ratio of the C form at 0% r.h. with a tension of 5 g (Table III).

When tensions greater than 5 g are applied on fibres at high humidity, the B form is maintained and relatively good X-ray patterns are obtained. But when one lowers the r.h., the X-ray patterns of the C form become very poor.

Discussion

The present experimental study gives quantitative insight on the effects of a mechanical tension on DNA conformations. This parameter seems to be as important as the amount of salt or the relative humidity. We also noticed that time is an important factor for the B to A transition; at high relative humidity and without any tension, a fibre initially in the A form, returns always to the B form if one lets it enough time depending on the fibre diameter (more than 24 hous in the present case); so one can hardly suppose that the A form can exist, under ordinary conditions, in cells.

One should note that when the B form is observed, at high r.h., the tension has no effect on the DNA helical parameters and fibres which are not well oriented without tension do not improve when a tension is applied. But fibres well oriented without an applied tension do give better X-ray pictures when submitted to a tension.

Comparison between experimental results obtained at a fixed relative humidity,

75% for example, show that, without any applied tension, the A form is observed with samples drawn from solutions 0.005 M NaCl (Table I). When a tension of 15 g is applied, the form B* is observed at the place of A which can no longer be obtained (Table I). The C form is obtained at 75% r.h. (Table II) with fibres prepared with a lower salt concentration. In this case, an applied tension slows down the transition from B to the C (Table III) as the number of base pairs per helix turn is 9.6 compared to 8.8 when no tension is applied. Moreover one should note that this same value of 9.6 base pairs per turn (at 75% r.h.) is obtained with tensions three times higher when the DNA fibres are drawn from preparations with a salt concentration ten times higher (the fibres dimensions are very similar).

In Tables I, II and III, the position of the equatorial X-ray spot is given. It allows us to determine the parameter of the hexagonal lattice i.e., the distance between double helices. One can see that the position of the equatorial spot depends on the value of the relative humidity but it appears, by comparison between the data presented in Tables II and III that the tension has no effect on the position of the equatorial spot in the range of 95% to 75% r.h.

When a mechanical tension is applied (at high r.h.) on DNA samples presenting normally the B to A transition, the A form can no longer be obtained and one gets a B* form when the r.h. is lowered. So the tension can clearly prevent the change of DNA to the A form (15). It is important to remark that for fibres presenting the B and A forms when free of mechanical tension, the tension has an effect on the form transition only if it is applied at high relative humidity. We could not for example realize the transition from A to B* by applying a tension on a fibre already in the A form.

We have also remarked that the transition from B to A can be opposed by decreasing the amount of NaCl salt in the DNA preparation. The r.h. being maintained constant, this gives the same effect as the application of a mechanical tension on the fibre. Therefore one should note that to put DNA samples under a mechanical tension or to fix the two ends of stretched fibres may have the same effect. It is thus important, for X-ray fibre studies of the B-A transition in DNA associated to different cations or polypeptide chains, to let, at least, one end of the fibre free during X-ray exposures.

Fibres drawn from low NaCl concentration gels to present only the (B-C) transition. Applying a tension in this case does not forbid this change of DNA form; on the contrary a slight tension allows a very progressive evolution of the helical parameters until 0% r.h. Nevertheless too high applied tensions disorganize the system and give poor X-ray patterns. With samples from very low salt preparations, the A form is never observed; the form change occur between B and C according to the r.h. But, contrary to the preceding case, if one applies a tension on a fibre in the C form at 86% r.h. a change to the B form can be induced (the r.h. being maintained at 86%). So the reversibility of the B to C transition can be obtained with a mechanical tension as well as with a variation of the relative humidity at least for relatively high humidities. In this case, the effect of the tension on the DNA conformation is exactly opposed to that of the relative humidity.

References and Footnotes

1. Fuller, W., Wilkins, M.H.F., Wilson, H.R. and Hamilton, L.D., *J. Mol. Biol. 12*, 60 (1965).
2. Langridge, R., Wilson, H.R., Hooper, C.W., Wilkins, M.H.F. and Hamilton, L.D., *J. Mol. Biol. 2*, 19 (1960).
3. Marvin, D.A., Spencer, M., Wilkins, M.H.F. and Hamilton, L.D., *J. Mol. Biol. 3*, 547 (1961).
4. Leslie, A.G.W., Arnott, S., Chandrasekaran, R. and Ratliff, R.L., *J. Mol. Biol. 143*, 49 (1980).
5. Premilat, S. and Albiser, G., *J. Biomol. Struct. Dyn. 3*, 1033 (1986).
6. Coll, M., Frederick, C.A., Wang, A.H.-J. and Rich, A., *Proc. Natl. Acad. Sci. (USA) 84*, 8385 (1987).
7. Pilet, J. and Brahms, J., *Nature New Biol. 236*, 136 (1972).
8. Dickerson, R.E., *J. Mol. Biol. 166*, 419 (1983).
9. Cooper, P.J. and Hamilton, L.D., *J. Mol. Biol. 16*, 562 (1966).
10. Rhodes, N.J., Mahendrasingam, A., Pigram, W.J., Fuller, W., Brahms, J., Vergne, J. and Warren, R.A.J., *Nature 296*, 267 (1982).
11. Franklin, R.E. and Gosling, R.G., *Acta Crystal 6*, 673 (1953).
12. Zimmerman, S.B. and Pheiffer, B.H., *J. Mol. Biol. 135*, 1023 (1979).
13. Parrack, P.K., Dutta, S. and Sasisekharan, V., *J. Biol. Struct. Dyn. 2*, 149 (1984).
14. Wilkins, M.H.F., Gosling, R.G. and Seeds, W.E., *Nature 167*, 759 (1951).
15. Fornells, M., Campos, J.L. and Subirana, J.A., *J. Biol. Mol. 166*, 249 (1983).
16. O'Brien, M.A., *J. of Sci. Inst. 25*, 73 (1948).

Date Received: March 30, 1988

Communicated by the Editor R. H. Sarma

D) DISCUSSION

Les deux séries d'expériences réalisées par diffraction R.X. de fibres démontrent l'intérêt de cette technique pour suivre l'évolution de la conformation de l'ADN lorsque son environnement est modifié. En particulier, pour obtenir des résultats qualitatifs, on peut, sur la même fibre, faire des ajouts successifs de cation et, pour chaque concentration, prendre des clichés R.X. en fonction de l'hygrométrie et de la tension appliquée.

L'étude de la fixation de l'argent sur l'ADN est un modèle type puisque l'analyse des clichés R.X. de fibre permet de déterminer les sites de fixation de ce type "d'atome lourd" malgré une distribution non périodique. En effet, pour la strate équatoriale du cliché, la fonction de Bessel contribuant essentiellement à cette strate est d'ordre zéro. Cela entraîne que l'intensité ne dépend que de la distribution radiale des atomes de l'unité répétitive de la structure. Avec l'ADN en présence d'argent, l'intensité équatoriale est modifiée et le calcul de l'intensité théorique montre que cet atome doit être au voisinage de l'axe de la double hélice. Le site retenu se trouve dans ce cas entre les bases G et C appariées. La distorsion créée sur les bases G-C entraîne une modification des paramètres hélicoïdaux d'autant plus prononcée que l'ADN est riche en ce type de bases. Le spectre dichroïque de l'ADN en solution avec l'argent rend compte de cette nouvelle conformation dont les paramètres hélicoïdaux sont proches de ceux de la forme C droite mais ce spectre dichroïque est différent de celui de la forme C et, en fait, ce nouveau spectre a été interprété en termes de "tilt" et de

"propeller twist" des bases (68). La comparaison de ces paramètres, entre la forme C (Chap.III,D) et la conformation proposée pour l'ADN avec l'argent, montre effectivement une variation de "tilt" de - 9° à + 4° et de "propeller twist" de 0 à - 7°. A ces variations s'ajoute l'ouverture des bases vers le grand sillon. Par contre, les angles dièdres de la chaîne sucre-phosphate ont des valeurs très voisines dans les deux conformations. .

De l'étude expérimentale par diffraction R.X. de l'action de la tension mécanique sur le comportement des fibres d'ADN, on peut remarquer que ce paramètre est aussi important que la proportion de sel ou l'humidité relative. A haute humidité relative et quelle que soit la teneur en sel de la fibre, la conformation de type B n'est pas modifiée par la tension. Par contre, si l'humidité relative est abaissée, la tension peut empêcher la transition B-A pour les fibres dont la teneur en sel de sodium est au moins de 2 % (mais alors les paramètres d'hélice de la forme B sont modifiés).

Pour les fibres dont la teneur en sel est beaucoup plus faible, la transition B-A n'a plus lieu mais on observe une transition de type B-C. Dans ce cas, la tension sur la fibre n'empêche pas cette transition mais la rend très progressive jusqu'à 0 % d'humidité relatives (Photo N°8). Ces quelques résultats montrent que la tension mécanique est un facteur qui permet à la molécule d'ADN, de séquence quelconque, de rester dans une conformation de type B malgré les fluctuations de son environnement (quantité d'eau, taux de sel...). Ce facteur peut donc être important dans le processus d'association protéine-acide nucléique. Les études structurales montrent en

effet, que les principes de reconnaissance sont surtout spécifiques de la séquence des bases avec l'ADN stabilisé en forme B (69).

CHAPITRE V : ETUDES DES DIFFERENTES TRANSITIONS CONFORMATIONNELLES DE L'ADN ET DES POLYNUCLEOTIDES EN FIBRE

A) INTRODUCTION

Le polymorphisme de l'ADN et des polynucléotides, dont quelques conformations ont déjà été étudiées, est un fait établi par de nombreuses techniques aussi bien pour des solutions, des films ou fibres orientés et pour des cristaux d'oligonucléotides. Ce polymorphisme dépend de nombreuses causes : taux et type de cation alcalin associé, pourcentage en bases A-T, et séquence, tension mécanique appliquée, torsion mais aussi du taux d'hydratation.

Les variations de ces paramètres peuvent donc induire des changements de conformations. La diffraction RX de fibre est une méthode de choix, comme cela a été présenté dans le chapitre précédent, pour suivre ces changements de conformation puisque les fibres peuvent être soumises à différents facteurs variables. Néanmoins, dans le cas de superpositions de formes sur un même cliché lors d'une transition, il est impossible de quantifier le taux respectif des formes en présence comme semble pouvoir le réaliser la spectroscopie infrarouge (70,71)

De plus, afin d'étudier expérimentalement la cinétique des transitions et l'évolution de la structure moléculaire de l'ADN durant ces transitions, une technique simple et complémentaire de la diffraction RX est nécessaire. La technique utilisée consiste à mesurer les dimensions de la fibre avant chaque prise de cliché RX.

La méthode qui permet de relier la longueur de la fibre au paramètre cristallographique p est présentée dans la première

publication de ce chapitre. Ainsi, la comparaison entre longueur de la fibre et paramètre moléculaire permet d'établir, avec précision, des courbes expérimentales pour les transitions. Les transitions A-B et B-C de l'ADN sont ainsi analysées en fonction de l'humidité relative et des conditions de sel alcalin précises.

Dans une deuxième publication, la méthode qui associe la diffraction RX et l'observation des dimensions de la fibre est à nouveau employée pour montrer que les variations de l'état d'hydratation de la fibre peuvent être évaluées lors de chaque transition. Avec les exemples des transitions A-B et B-C de l'ADN, il est ainsi montré que le nombre minimum de molécules d'eau nécessaire pour stabiliser chaque structure peut être déduit des dimensions de la fibre et de l'analyse des clichés RX.

Enfin, les deux dernières publications de ce chapitre analysent, avec cette même méthode, les transitions particulières rencontrées avec les polynucléotides de séquences alternées A-T et G-C. En effet, avec le poly (dA-dT). poly (dA-dT) on peut obtenir les conformations de types A, B mais également D. Cette dernière conformation étant encore une double hélice droite dont les angles dièdres de l'unité répétitive ont été précisés au chapitre (III,D). Par contre, avec le poly (dC-dG). poly (dC-dG), on rencontre une nouvelle conformation appelée S ou Z en double hélice gauche. Ce polynucléotide peut présenter également des conformations de types A et B, les transitions qui réalisent un changement de sens de la double hélice sont donc particulièrement intéressantes à étudier dans ce cas.

B) UNE METHODE POUR L'ETUDE EXPERIMENTALE DES TRANSITIONS CONFORMATIONNELLES DE L'ADN EN FIBRE

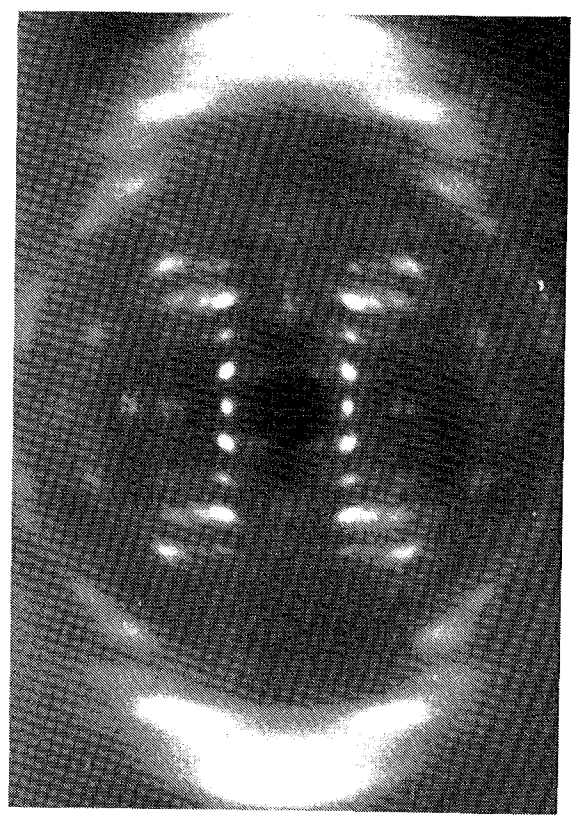

Photo N° 9 : Forme B' du poly dA-poly dT avec sel de sodium à 85 % d'humidité relative (Pas P = 32,6 A et p = 3,2 A)

Biophysical Chemistry, 35 (1990) 37–45
Elsevier

BIOCHE 01399

A method for the experimental study of DNA conformational transitions in fibers

S. Premilat, M. Harmouchi and G. Albiser

Laboratoire de Biophysique Moléculaire, U.A. CNRS 494, Faculté des Sciences, Université de Nancy I, BP 239, 54506 Vandoeuvre les Nancy, France

Received 1 May 1989
Revised manuscript received 8 September 1989
Accepted 11 September 1989

DNA; Conformational transition; Fiber dimensions; X-ray diffraction

The method proposed for the study of DNA conformational transitions is based on the proportionality, experimentally observed, between the length of a DNA fiber and the axial rise per nucleotide characterizing the molecular helix. Precise curves for the A-B and B-C transitions as a function of the relative humidity are obtained by using X-ray fiber data and measurements of fiber dimensions. It is thus shown that the A-B transition is a cooperative process between two different states, whereas the B-C transition can be considered as a progressive change of conformation. The present method is applied on two natural DNAs differing in base composition so that the effect of the nucleotide content on the conformational changes can be estimated.

1. Introduction

Recent single-crystal analyses [1–4] of oligonucleotides with well-defined nucleotide sequences have confirmed, in a more detailed way, the regular helical structures of DNA already established by X-ray fiber diffraction [5–8]. The local variations thus observed in the conformation of oligonucleotides depending on their precise base composition have given an accurate and perhaps more functional view of the DNA molecules. Moreover, single-crystal studies of oligonucleotides allowed the determination of new conformations, the Z double left-handed helices which are obtained from poly(C-G)-poly(C-G) in very high ionic content preparations [9,10]. We can add that results deduced from fiber or single-crystal studies of polynucleotides are frequently completed by the use of different spectroscopic techniques, mainly NMR [11–15] and infrared [16–20], which permit conformational information to be obtained on these same molecules in film and also in solution.

However, the dynamical aspects of the conformational transitions of DNA can hardly be studied by using single crystals. Fibers or films of DNA are actually more valuable for such approaches because they allow changes of the molecular conformation when subject to external variable and reversible constraints. Although they are well known in their general features, the conformational transitions of DNA are far from being well-determined experimentally [21–23] even if the main causes of these changes are firmly established. So, among the factors inducing transitions in DNA conformations, knowledge of the relative humidity of the fiber surroundings is surely essential, at least as concerns the type and content of salt associated to the DNA molecule [5,24–27]. The nucleotide composition and more precisely its

Correspondence address: S. Premilat, Laboratoire de Biophysique Moléculaire, U.A. CNRS 494, Faculté des Sciences, Université de Nancy 1, BP 239, 54506 Vandoeuvre les Nancy, France.

sequence are also important for the dynamics of conformational transition [8,28,29]. We could also include mechanical forces which can modify or even prevent conformational changes when applied to fibers [30,31].

Nevertheless, information on molecular structures and conformational transitions of DNA can also be obtained by the simple and direct observation of the fiber dimensions. Indeed, a parameter which characterizes very well the double helix form of DNA is the axial rise per nucleotide (or rise per base-pair), p. It represents the increase in length along the helix axis due to one pair of nucleotides in the antiparallel and complementary molecular chains. One should note that this relevant parameter is directly related to the length of DNA molecules. These long molecules can be well organized (by stretching a gel) into fibers where they are mainly lengthened and placed on end or side-by-side. The length of such a fiber should in principle be directly related to that of the DNA molecules it contains and hence to the type of helix they form. Moreover, changes of the molecular conformation, i.e., of the helix form, induced, for example, by variations of the relative humidity, can be performed keeping the structure of the fiber intact. Such changes modify the length of the DNA molecules and thus that of the fiber. Note that DNA helices could slide past one another during form transitions and the fiber length variations could therefore practically result from these movements. However, if such eventual molecular sliding is very small it should be possible to estimate changes of the molecular parameter p by simple measurements of variations of the sample length and to study, by this direct procedure, conformational changes. In the present work, it is shown that we can actually establish such an approach which allows us to propose accurate experimental curves for the A-B and B-C transitions in DNA.

2. Materials and methods

In order to gain information about the effect of base composition on the DNA conformational transitions, two different natural DNAs were used. Namely, DNA from calf thymus containing 42% of G-C bases was purchased from Pharmacia and *Micrococcus lysodeikticus* DNA which contains 72% of G-C, was obtained from Sigma. The following method was used to realize, in a reproducible way, well oriented fibers from DNA gels: a few milligrams of dry DNA is put in solution in water at pH 7; its concentration is measured from the absorbance at 2600 Å and the NaCl content of the solution is fixed by dialysis. Two different preparations were made depending on the transition considered. For the A-B transition, an NaCl concentration of 0.005 M is achieved with DNA solutions of 3 mg/ml. However, to observe the B-C transition, a 10-fold lower NaCl concentration is necessary. These solutions are centrifuged at 40000 rpm and with the DNA gel thus obtained, fibers are obtained by stretching the gel between two glass rods. X-ray fiber diffraction patterns are obtained following the now classical method [5]. Details on the procedure we use have been given elsewhere [32] and, as before, a slight flux of hydrogen, passing through appropriate saturated salt solutions, allows us to obtain fixed relative humidities [33] in the X-ray camera where the fiber is placed.

The measurement of the fiber length is made using a binocular microscope. The sample is placed in a cell through which a small flux of humidified air is passed. This set-up, devised in order to maintain or modify the relative humidity in the fiber environment, is fixed on the microscope stage; it comprises two transparent bases through which the dimensions of the fiber can be measured. In the cell, the fiber is placed under the objective of the microscope with one end fixed to the holder while the other one remains free or is maintained by a very light tension (of the order of 1 g) which has no effect on the conformational changes [31] but permits one to avoid small deformations of the sample when it lengthens. An ocular micrometer is used for the determination of the fiber dimensions, i.e., its length (distance between two arbitrarily chosen points on the fiber) and diameter. It should be noted that for X-ray fiber diffraction as well as for measurements performed with the microscope, enough time must be allowed to ensure attainment of equilibrium of the

system at a given relative humidity [34]. This time depends on the thickness of the sample and also on the value of the fixed humidity. We noted that it takes less time to reach equilibrium when the relative humidity is reduced rather than when it is increased.

3. Results

3.1. The A-B transition

3.1.1. X-ray fiber diffraction

Samples of the two different DNAs, prepared from 0.005 M NaCl solutions, were studied by X-ray diffraction. The X-ray patterns thus obtained present the following features in common: the classical parameters of the B double helix are observed at a relative humidity (R.H.) of 95% and one obtains the A form at 66% R.H. (see tables 1 and 2). Between these two values of the relative humidity, a mixture of the two DNA conformations is observed on the X-ray patterns; this superposition is very clearly visible at 90 and 86% R.H. (an example of X-ray photographs is given in fig. 1). For lower values of the R.H. the more crystalline A form of DNA is preponderant on the X-ray patterns whereas the presence of the B form becomes gradually less observable. The A conformation disappears in turn at R.H. $< 60\%$. It is obviously difficult to obtain from X-ray patterns an estimation of the exact proportion of A and B forms in the mixture during the transition between the forms although their simultaneous presence is certain.

3.1.2. Fiber dimensions

Measurements of fiber dimensions, performed at fixed values of the relative humidity, with a binocular microscope, allowed us to draw the curves shown in fig. 2. These measurements of the length and diameter of fibers were made on the samples previously studied by X-ray diffraction under the same conditions of relative humidity. We can clearly ascertain that the length of DNA samples changes with the relative humidity according to sigmoidal curves, characteristic of cooperative effects, whereas the fiber diameter undergoes a steep diminution when the relative humidity is at about 95%. Thereafter, it decreases very slightly with lowering of the relative humidity. It should be noted that the large variation in fiber diameter appears before any change in its length can be observed. Moreover, a series of

Table 1

A-B transition: geometrical parameters of helical conformations; fiber length (L) and diameter (D) for calf thymus DNA

	R.H. (%)					
	95	92	90	86	75	66
Pitch P (A)						
B-form	33.7	33.6	33.0			
A-form			28.4	28.06	27.8	27.4
p(A)						
B-form	3.37	3.36	3.36	3.34		
A-form			2.58	2.57	2.56	2.55
P/p						
B-form	10.00	10.00	9.82			
A-form			11.00	10.92	10.86	10.74
L (mm)	3.775	3.700	3.425	3.175	2.975	2.875
D (mm)	0.375	0.317	0.307	0.293	0.281	0.275
L/p ($\times 10^{-7}$)	1.12	1.10			1.16	1.12
X(B-form)	1	0.92	0.61	0.33	0.11	0
m (A)	3.37	3.30	3.05	2.82	2.64	2.55
L/m ($\times 10^{-7}$)	1.12	1.12	1.12	1.12	1.12	1.12

Table 2

A-B transition: geometrical parameters of helical conformations; fiber length (L) and diameter (D) for micrococcal DNA

	R.H. (%)					
	95	92	90	86	75	66
Pitch P (A)						
B-form	33.7					
A-form			28.08	27.9	27.7	27.2
p(A)						
B-form	3.37		3.35	3.34		
A-form			2.58	2.57	2.56	2.55
P/p						
B-form	10					
A-form			10.88	10.86	10.82	10.70
L (mm)	3.531	3.203	3.028	2.921	2.771	2.689
D (mm)	0.357	0.299	0.289	0.277	0.266	0.260
L/p ($\times 10^{-7}$)	1.05				1.08	1.05
X (B-form)	1	0.61	0.40	0.28	0.10	0
m (A)	3.37	3.05	2.88	2.78	2.63	2.55
L/m ($\times 10^{-7}$)	1.05	1.05	1.05	1.05	1.05	1.05

At 93% R.H., $L = 3.460$ mm, $D = 0.309$ mm.

dimension measurements, performed in the two senses of variation of the relative humidity, indicates the perfect reversibility of the transition. It is important, however, to observe that we actually obtain the same fiber length at a given relative humidity irrespective of the sense of variation, provided that enough time has been taken to establish a good equilibrium (stability of the fiber length). We noted that such equilibrium conditions take longer to reach when the transition goes from A to B as compared to the reverse direction. Fig. 3 shows, as an example, a DNA fiber at 95 and 75% R.H. The length variation is obvious as well as the modification of the sample volume.

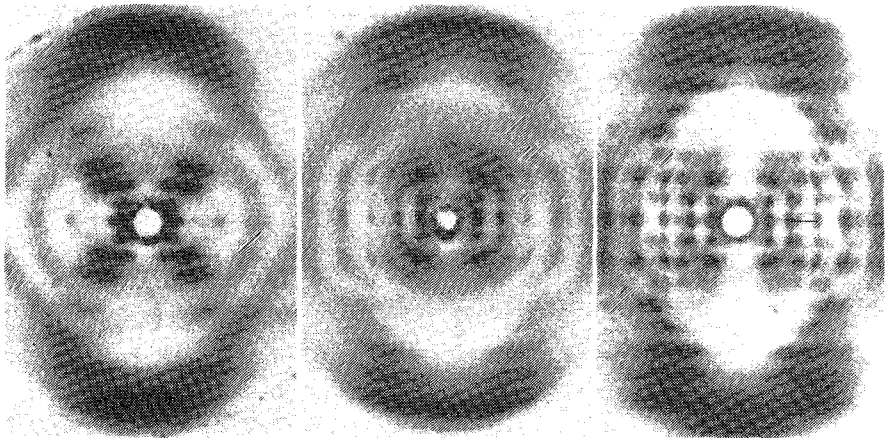

Fig. 1. X-ray fiber patterns obtained at (B) 95% R.H. (B-form), (B-A) 90% R.H. (mixture of A- and B-forms) and (A) 75% R.H. (A-form).

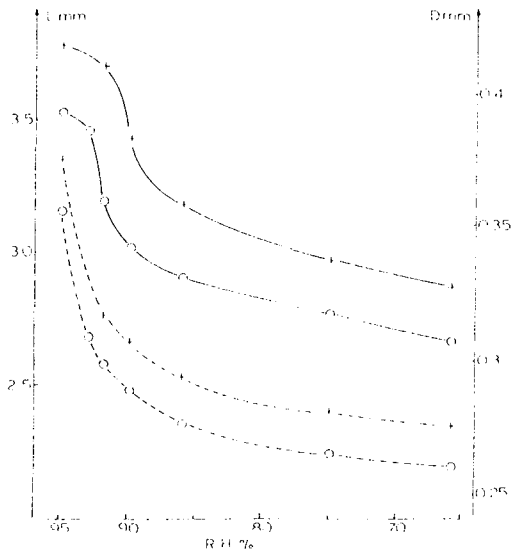

Fig. 2. A-B transition: DNA fiber dimensions as a function of the relative humidity. Length (+———+) and diameter (+- - - - - +) for calf thymus DNA; length (○———○) and diameter (○- - - - - ○) for micrococcal DNA.

For instance, we observed that the ratio between the volumes of the fiber at 95 and 66% R.H., respectively, is about 2.5 (values of length and diameter listed in table 1).

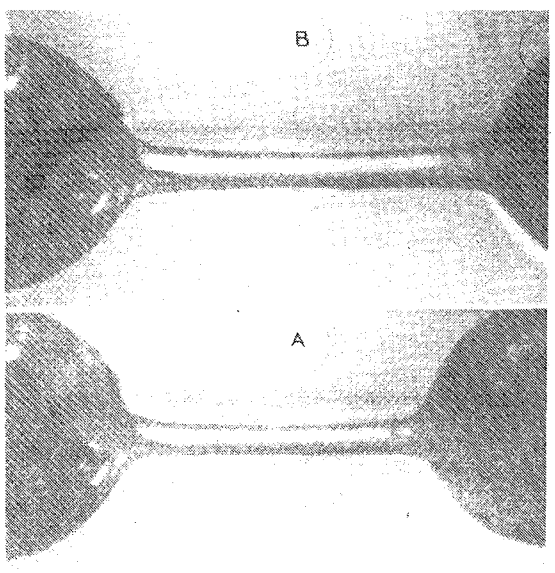

Fig. 3. Example of a DNA fiber at 95% R.H. (B) and 75% R.H. (A).

3.2. Relation between X-ray results and fiber dimensions

In tables 1 and 2, examples of values of the length L and diameter of fibers made from the two different DNAs are listed as a function of the relative humidity. In these tables are also indicated values of the parameter p (axial rise per nucleotide) obtained from X-ray diffraction of the same samples under identical conditions. We can note that the ratio L/p has the same value at 95 and 66% R.H. Between these relative humidity values, this ratio cannot be well defined because of the low precision of the X-ray data obtained when conformations A and B coexist in DNA fibers. Note that the ratio L/p represents the constant number of base pairs located along the fiber axis, between the two points chosen for the length measurement. Therefore, we can estimate the percentage of nucleotides respectively in the A or B conformation by simple measurement of the fiber length. Indeed, with one among these fibers taken as an example, we obtained X-ray patterns of the B form at 95% R.H. and then determined a value of $p(\mathrm{B}) = 3.37$ Å for the parameter p whereas at 66% R.H., we found the corresponding value for conformation A to be $p(\mathrm{A}) = 2.55$ Å. The values of the fiber length corresponding to these two situations were respectively $L(\mathrm{B}) = 3.775$ mm and $L(\mathrm{A}) = 2.875$ mm. Therefore, we have $L(\mathrm{B})/L(\mathrm{A}) = 1.31$ and $p(\mathrm{B})/p(\mathrm{A}) = 1.32$; hence, we can practically write $L(\mathrm{B})/L(\mathrm{A}) = p(\mathrm{B})/p(\mathrm{A})$, i.e., there is a very good proportionality between the length of the fiber and the helical parameter p.

Note that such behavior is actually general and perfectly reversible; it is observed with any homogeneous and well-oriented DNA fiber (i.e., giving the A and B X-ray patterns according to the relative humidity). Consequently, it appears that the fiber length variations are practically only due to changes of the DNA helical form. Molecular sliding may exist in the fiber but has no perceptible effect and can thus be neglected in the present case. For intermediate values of the relative humidity a mixture of A and B forms is present in the fiber. Very recently, it has been shown that the A and B forms can also coexist in a single crystal [35]. However, the values then determined must be

understood as being averages which could result from a mixed population of molecules of each form as well as from DNA molecules containing fractions of the two forms. The distinction between these two possibilities is of little importance and can scarcely be made experimentally. We, therefore proceed in the following to deal with the situation according to the second hypothesis which is generally used in theoretical approaches to the problem of conformational transitions in polypeptides [36] and DNA [37]. Accordingly, the length L, measured at any given value of the relative humidity between 66 and 95%, can be written as follows. $L = X(B)L(B) + X(A)L(A)$, where $X(B)$ and $X(A)$ denote the fractions of nucleotides in conformation B and A, respectively. So, with $X(B) + X(A) = 1$, we have $X(B) = (L - L(A))/(L(B) - L(A))$. An example of $X(B)$ values thus obtained with calf thymus DNA (42% of G-C) is given in table 1 and corresponding values for micrococcal DNA (72% of G-C) are listed in table 2. In these tables, we can also see that, when the mean parameter $m = 3.37X(B) + 2.55X(A)$ is used in a complementary way, the ratio L/m remains practically constant in the relative humidity interval between 66 and 95%. In contrast, we observe in table 1, that at 92% R.H., the ratio L/p has a value of 1.10 instead of 1.12; this means that a small fraction of nucleotides already have adopted conformation A. In a symmetrical way, the excessively high value of 1.16 obtained for L/p shows that some fraction of the DNA is still in the B conformation at 75% R.H.

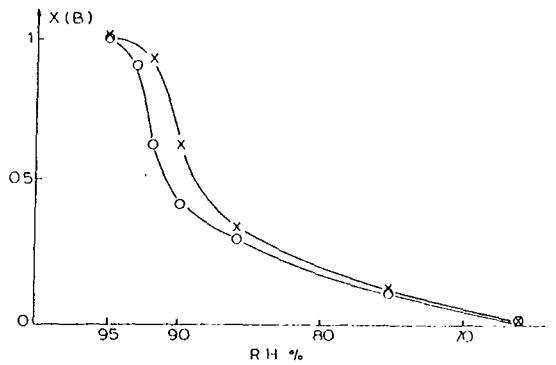

Fig. 4. A-B transition: fraction of nucleotides in the B form as a function of the relative humidity. (× ——— ×) Calf thymus DNA (42% C-G); (○ ——— ○) micrococcal DNA (72% C-G).

The same kind of behavior is observed with samples derived from the micrococcal DNA. However, we can see, in table 2, that such variations appear at shifted values of the relative humidity, expressing the effect of the base composition on the transition.

More precisely, in fig. 4 are shown, for the two DNA types presently studied, the curves of the fraction $X(B)$ of nucleotides in the B-form vs. relative humidity. We can observe that a higher percentage of G-C facilitates the transition to the A-form when the relative humidity decreases [28]. So at 90% R.H., the DNA containing 42% of G-C is at 40% in the A conformation (mid-point at 89% R.H.) whereas, under these conditions, 60% of the DNA which contains 72% of G-C is already in that form (mid-point at 92% R.H.).

We pointed out above that the ratio of the volumes of the fiber in respectively the B- and A-forms can be deduced directly from measurements of dimensions made with a microscope. However, the ratio of the volumes actually occupied by the DNA molecule in these two conformations can also be determined from X-ray data. Indeed, the equatorial spot permits one to determine the average distance between helices in the lattice (22.3 Å in the B-form and 18 Å in the A-form) and thus with values of $p(B)$ and $p(A)$, we can evaluate the order of magnitude of the volumes occupied in the crystal lattice by the DNA and the water associated with the molecular conformations. The volume ratio thus obtained is about 2 as compared to 2.5 determined by using fiber dimensions. The difference is mainly due to the fact that the sample is swollen with water at high relative humidity; it then contains highly hydrated disorganized parts [34] between crystallized regions where DNA molecules are well positioned.

3.3. The B-C transition

3.3.1. X-ray fiber diffraction

We continued as described above but samples were prepared from DNA solutions with a salt content 10-fold lower than in the preceding case. Only results obtained with DNA from calf thymus are presented, since, under these conditions, no

Table 3

B-C transition: geometrical parameters and DNA fiber length (L) and diameter (D)

	R.H. (%)						
	95	92	87	82	79	75	64
Pitch							
P (A)	33.5	33.0	32.0	31.0	29.4	28.9	
p (A)	3.35	3.34	3.33	3.32	3.31	3.30	
P/p	10.00	9.90	9.60	9.33	8.88	8.75	
L (mm)	3.375	3.341	3.285	3.228	3.195	3.150	3.087
D (mm)	0.214	0.178	0.160	0.152	0.149	0.143	0.142
L/p ($\times 10^{-7}$)	1.007	1.000	0.986	0.972	0.965	0.955	
DNA form	B	B	C	C	C	C	

difference in the behavior of the two DNAs can be clearly discerned. Fiber X-ray diffraction therefore gives patterns which, according to the relative humidity, correspond to the B-C transition of DNA. The results thus obtained, with the relative humidity fixed at values between 75 and 95%, are presented in table 3. For R.H. < 75%, DNA fibers are disorganized and X-ray patterns are so poor that the determination of helical parameters becomes practically impossible.

In the present case, variations in the helical parameters of the DNA molecules do not have the same features as those of the A-B transition; the conformational change is now rather progressive and slow. Characteristic X-ray patterns of the C-form, with a supplementary spot at 0.1 A-1 on the first layer line, are obtained at R.H. $\leqslant$ 87%. Moreover, the crystal lattice remains hexagonal and the helical parameter p (see table 3) decreases linearly with the relative humidity.

3.3.2. Fiber dimensions

Measurements of fiber dimensions, at different fixed values of the relative humidity, made with the binocular microscope, allowed us to draw the experimental curves presented in fig. 5. We can observe linear variations of the fiber length with a change of slope at 75% R.H. (no X-ray pattern can then be used). Moreover, it can be noted that the fiber diameter decreases very rapidly as far as 75% R.H., subsequently decreasing more slowly. This latter fact can be used to explain, qualitatively at least, the change in slope of the plot for length vs. relative humidity. Indeed, it appears that up to 75% R.H., there is sufficient water around the DNA helices to facilitate changes being induced in their conformation than at lower relative humidity where almost all excess water has been removed. A series of length and diameter measurements have shown the perfect reversibility of this progressive process of DNA conformational change which, now, does not show any cooperative effect.

3.4. Relation between X-ray results and fiber dimensions

The ratio of the sample length L divided by the helical parameter p, determined at different relative humidities (in the interval 75–95%), is listed in table 3. This ratio which represents, as stated

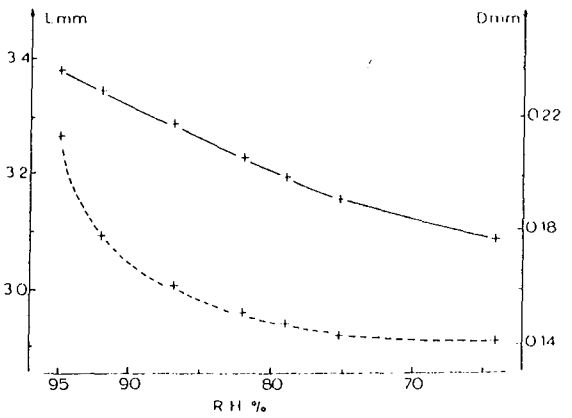

Fig. 5. B-C transition: variations of the length (+ ——— +) and diameter (+ - - - - - +) as a function of relative humidity.

above, the constant number of base-pairs along the fiber axis, does not remain exactly constant; it diminishes by a few percent when the relative humidity decreases.

Furthermore, we also observed that the ratio of the fiber volume divided by the mean volume occupied by a DNA double helix in the crystal lattice (X-ray data) becomes constant at R.H. $\leqslant 82\%$. Therefore, in the present case, as in that of the A-B transition, the DNA fiber is swollen at high values of the relative humidity when in the B form; it then includes disorganized and highly hydrated parts. At the other limit of relative humidity, the very small decrease in length when R.H. $< 75\%$ (see table 3) corresponds to the disorganization of DNA helices as concluded from the very poor X-ray patterns we obtained under these conditions.

4. Discussion

Fiber X-ray diffraction results compared to values obtained from measurements of dimensions made on the same samples at the same relative humidity allowed us to establish a simple and precise method for the study of DNA conformational transitions. We observed experimentally that the main factor responsible for the fiber length variations is the change, with relative humidity, of the DNA helical parameters. We therefore used the proportionality actually existing between the length of a DNA fiber and the helical parameter p (axial rise per base-pair) of the DNA molecular conformation.

Consequently, a most significant variation in the fiber length can easily be observed during the perfectly reversible A-B transition. The presence of cooperative effects in this conformational change is well characterized by the sigmoidal form of the transition curve of the length (or the fraction of nucleotides in the B-form) vs. the relative humidity. In contrast, the B-C transition shows very progressive variations of the fiber length, indicating a continuous deformation of the B conformation of DNA which takes the C-form when the relative humidity is diminished. The latter conformational transition is also perfectly reversible. However, in this case, the proportionality between the fiber length and the helical parameter p is somewhat perturbed by disorganization of the fiber (X-ray patterns become poor when the relative humidity is lowered). The excessively large diminution in fiber length thereby observed (table 3) may be due to slight sliding of DNA helices past one another or to some undulations of DNA molecules which are superimposed on conformational changes as described previously in oligonucleotide single-crystal studies [38].

Moreover, it is interesting to note that even with samples made from very low salt concentration solutions, we were unable to observe any transitions of the type C-A-B [25] which should be characterized by a significant decrease followed by an almost equal increase in fiber length when the relative humidity undergoes a steady decrease.

The determination of variations in fiber diameter and hence of the volume also provides valuable information on the importance of water in the process of DNA conformational changes. The particularly large decrease in fiber diameter during the B-A transition, a decrease which takes place before any variation of the fiber length occurs, may be due to the loss of a significant amount of water located between the organized parts of the fiber as well as around the double helices. It is only after this release of excess water has been achieved that a decrease in relative humidity induces changes of the DNA conformation by removing water molecules from the inside of the molecular structure. For the reverse A-B transition, we observed that, from an increase of the relative humidity, it firstly results in a change of the DNA conformation due to the penetration of water into the molecular structure. This is clearly associated with lengthening of the fiber. The swelling of the lattice of helices and thus of the sample is only observed after.

During the B-C transition, the fiber diameter also diminishes very rapidly with a decrease in the relative humidity. In this case, however, the fiber length decreases slightly and regularly at the very beginning of the process. We can thus suppose that the withdrawal of water from the DNA environment induces constraints on organized parts of the fiber which modify the double helix confor-

mation. The low NaCl content of the DNA preparations does not allow, in this case, the transition to the A-form.

To conclude, let us add that we also began the study of the B-Z transition, i.e., the change between a right-handed and a left-handed helix [39,40]. Such a transition which is observed with samples of poly(G-C)-poly(G-C) made from solutions under unusual chemical conditions [9] may also correspond to variations in the fiber dimensions. Observations with the microscope are, however, very difficult in this case because the conformational change occurs at relative humidities between 100% (for B) and 95% (for Z). For such values of the relative humidity, the fibers are unstable and become distorted when the slightest tension is applied. We are currently attempting to modify these unfavorable conditions in order to be able to apply the present experimental method to the study of this singular conformational transition.

References

1 R.M. Wing, H.R. Drew, T. Tanako, C. Broka, S. Tanaka, K. Itakura and R.E. Dickerson, Nature 287 (1980) 755.
2 Z. Shakked, D. Rabinovich, W.B.T. Cruse, E. Egert, O. Kennard, G. Sala, S.A. Salisbury and M.A. Viswamitra, Proc. R. Soc. Ser. B 213 (1981) 479.
3 B.N. Conner, T. Tanako, J. Tanaka, K. Itakura and R.E. Dickerson, Nature 295 (1982) 294.
4 A.H.J. Wang, S. Fujii, J.H. van Boom and A. Rich, Proc. Natl. Acad. Sci. U.S.A. 79 (1982) 3968.
5 R. Langridge, H.R. Wilson, C.W. Hooper, M.H.F. Wilkins and L.D. Hamilton, J. Mol. Biol. 2 (1960) 19.
6 W. Fuller, M.H.F. Wilkins, H.R. Wilson and L.D. Hamilton, J. Mol. Biol. 12 (1965) 60.
7 D.A. Marvin, M. Spencer, M.H.F. Wilkins and L.D. Hamilton, J. Mol. Biol. 3 (1961) 547.
8 A.G.W. Leslie, S. Arnott, R. Chandrasekaran and R.L. Ratliff, J. Mol. Biol. 143 (1980) 49.
9 A.H.J. Wang, G.J. Quigley, F.J. Kolpak, J.L. Crawford, J.H. van Boom, G. van der Marel and A. Rich, Nature 282 (1979) 680.
10 A.H.J. Wang, G.J. Quigley, F.J. Kolpak, G. van der Marel, J.H. van Boom and A. Rich, Science 211 (1981) 171.
11 H. Shindo, J.B. Wooten, B.H. Pheiffer and S.B. Zimmerman, Biochemistry 19 (1980) 518.
12 D.J. Patel and L. Shapiro, Annu. Rev. Biophys. Biophys. Chem. 16 (1987) 423.
13 M.H. Sarma, G. Gupta and R.H. Sarma, Biochemistry 27 (1988) 3423.
14 R. Brandes, R.R. Vold, D.R. Kearns and A. Rupprecht, Biopolymers 27 (1988) 1159.
15 C.A.G. Haasnoot, H.P. Westerink, G. van der Marel and J. van Boom, J. Biomol. Struct. Dyn. 2 (1984) 345.
16 W. Pohle and H. Fritzsche, Nucleic Acids Res. 8 (1980) 2527.
17 J. Pilet and J. Brahms, Biopolymers 12 (1973) 387.
18 J. Pilet and M. Leng, Proc. Natl. Acad. Sci. U.S.A. 79 (1982) 26.
19 J.A. Taboury and E. Taillandier, Nucleic Acids Res. 13 (1985) 4469.
20 E. Taillandier, S. Adam, J.P. Ridoux and J. Liquier, Nucleic Acids Res. 16 (1988) 5621.
21 W. Saenger, in: Principles of nucleic acid structure, ed. C.R. Cantor (Springer-Verlag, New York, 1984) p. 228.
22 S.C. Erfurth, P.J. Bond and W.L. Peticolas, Biopolymers 14 (1975) 1245.
23 V.N. Potaman, Yu.A. Bannikov and L.S. Shlyachtenko, Nucleic Acids Res. 8 (1980) 635.
24 P.J. Cooper and L.D. Hamilton, J. Mol. Biol. 16 (1966) 562.
25 N.J. Rhodes, A. Mahendrasingam, W.J. Pigram, W. Fuller, J. Brahms, J. Vergne and R.A.J. Warren, Nature 296 (1982) 267.
26 J. Portugal and J.A. Subirana, EMBO J. 4 (1985) 2403.
27 P.K. Parrack, S. Dutta and V. Sasisekharan, J. Biomol. Struct. Dyn. 2 (1984) 149.
28 J. Pilet and J. Brahms, Nat. New Biol. 236 (1972) 136.
29 R.E. Dickerson, J. Mol. Biol. 166 (1983) 419.
30 M. Fornells, J.L. Campos and J.A. Subirana, J. Mol. Biol. 166 (1983) 249.
31 G. Albiser, M. Harmouchi and S. Premilat, J. Biomol. Struct. Dyn. 6 (1988) 359.
32 S. Premilat and G. Albiser, J. Mol. Biol. 99 (1975) 27.
33 M.A. O'Brien, J. Sci. Instrum. 25 (1948) 73.
34 S.M. Lindsay, S.A. Lee, J.W. Powell, T. Weidlich, C. Demarco, G.D. Lewen, N.J. Tao and A. Rupprecht, Biopolymers 27 (1988) 1015.
35 J. Doucet, J.P. Benoit, W.B.T. Cruse, T. Prange and O. Kennard, Nature 337 (1989) 190.
36 D. Poland and H.A. Scheraga, Theory of helix-coil transition in biopolymers (Academic Press, New York 1970).
37 T.M. Birshtein and O.B. Ptitsyn, Conformations of macromolecules (Interscience, New York, 1966).
38 R.E. Dickerson, D.S. Goodsell, M.L. Kopka and P.E. Pjura, J. Biomol. Struct. Dyn. 5 (1987) 557.
39 S. Arnott, R. Chandrasekaran, D.L. Birdsall, A.G.W. Leslie and R.L. Ratliff, Nature 283 (1980) 743.
40 V. Sasisekharan and S.K. Brahmachari, Curr. Sci. 50 (1981) 10.

C) CHANGEMENT DE L'HYDRATATION DURANT LES TRANSITIONS CONFORMATIONNELLES DE L'ADN

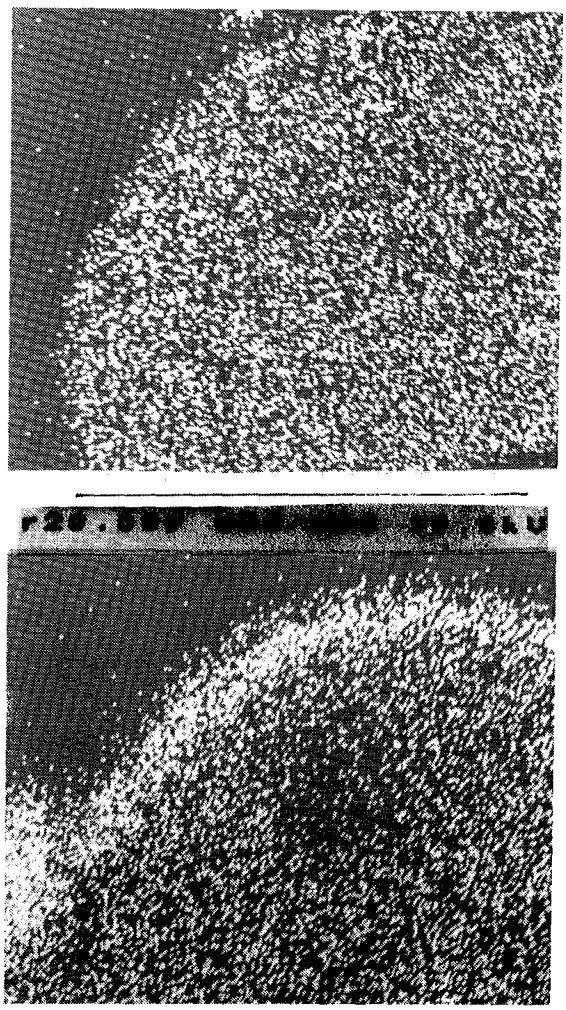

a

b

Photo N° 10 : Distribution du sodium détecté par microsonde électronique dans la section
a) d'une fibre d'ADN (42 % G-C)
b) d'une fibre de poly (dC-dG).poly (dC-dG) présentant la transition Z-B, on remarque l'accumulation de sodium en périphérie.

Eur Biophys J (1990) 19:87–92

European Biophysics Journal

Changes of hydration during conformational transitions of DNA

M. Harmouchi, G. Albiser, and S. Premilat

Laboratoire de Biophysique Moléculaire, UA CNRS 494, Faculté des Sciences, Université de Nancy I, BP 239, F-54506 Vandoeuvre les Nancy, France

Received May 22, 1990/Accepted in revised form August 31, 1990

Abstract. Fiber X-ray diffraction and measurement of fiber dimensions yields information about the hydration of DNA in fibers. The results obtained give us the fraction of nucleotides in the B form for the A → B transition or the rate of progression for the B → C transition as functions of the number of water molecules per nucleotide. The present experimental results confirm the importance of cooperativity in the A → B transition and the progressive change of the DNA double helix conformation during the C–B transition. At least twenty additional water molecules per nucleotide are necessary to stabilize the B form for DNA molecules in fibers following the A to B transition whereas only ten are sufficient when the B conformation is obtained starting from the C form.

Key words: DNA – Conformational transitions – Hydration – Fiber X-ray

Introduction

It is well known that water is of major importance for the stabilization of secondary and tertiary structures of biological macromolecules (Tanford 1968; Kuntz et al. 1974; Eldelhoch and Osborne 1976). In the case of DNA, hydration of the molecules is an important factor (Drew et al. 1981; Conner et al. 1984; Lee et al. 1987) which determines the form of the more or less stable double helix conformations. For DNA in fibers, we obtain the B-form at a high r.h. (relative humidity) (Langridge et al. 1960) and when the r.h. is lowered, the A form (Fuller et al. 1965) or the C one (Marvin et al. 1961) is obtained, depending on the type and content of salt. This is also the way one can observe the D (Davies and Baldwin 1963) or the Z form (Leslie et al. 1980), depending on the primary structure of the polynucleotide chains.

Many different experimental methods such as equilibrium sedimentation (Hearst and Vinograd 1961; Cohen and Eisenberg 1968; Tunis and Hearst 1968a, b; Wolf and Hanlon 1975), gravimetry (Falk et al. 1962), isopiestic measurements (Hearst 1965), spectroscopy (Falk et al. 1963, 1970; Hanlon et al. 1975; Semenov et al. 1988); X-ray diffraction (Saenger et al. 1986; Westhof 1987) have clearly shown that DNA molecules are generally highly hydrated. The average number of water molecules bound to or in the near vicinity of nucleotides determines the DNA helical structure (Dahlborg et al. 1980; Lindsay et al. 1988; Forsyth et al. 1989; Tao et al. 1989; Grimm and Rupprecht 1989). These water molecules contribute to the primary and secondary hydration shells.

In a previous study (Premilat et al. 1990) it was shown how one can follow conformational transitions of DNA by coupling X-ray diffraction with measurements of fiber dimensions. We recently found in the literature that variations of DNA fiber length, characteristic of form transitions of DNA, can also be observed in water-ethanol mixtures (Rupprecht and Piskur 1983). In the present approach, precise evaluation of the water content and its variation with the r.h. during conformational changes associated with the A → B and B → C transitions of natural DNA are presented. It is shown that the minimum number of water molecules necessary to stabilize different DNA structures can be deduced from measurements of fiber dimensions and analysis of X-ray patterns. The present approach shows that the B form can be realized with very different numbers of water molecules, depending on the salt used for the preparation of DNA fibers.

Material and methods

In the present study, preparations of calf thymus DNA, purchased from Pharmacia, were used without further purification. The lyophilized DNA was dissolved in distilled water at pH 7 and the salt concentration was defined by dialysis. The DNA gel from which fibers were drawn was obtained from centrifugation of the solutions at 40 000 rpm. Two different salt concentrations were

Offprint requests to: S. Premilat

used for NaCl solutions of DNA; one with 0.05 Na^+ per nucleotide and the other one with 0.5 Na^+ per nucleotide. The same concentrations of salt were used for Li DNA preparations.

The behaviour of the different DNA fibers submitted to variations of the r.h. was analysed by X-ray diffraction measurements and direct observation with an optical microscope. Details concerning the experimental methods used are given elsewhere (Premilat et al. 1990). One should only note that a small tension was applied to the fiber. This is because measurement of the fiber length can be complicated by slight fluctuations of the fiber which may appear when the r.h. is varied. As shown previously (Albiser et al. 1988), such a tension has no effect on the conformational transition of the DNA.

In order to determine the number of water molecules associated with a nucleotide in a given DNA conformation, one has to know the total number of nucleotides in the fiber. The number, N, of nucleotides situated along the fiber axis is given by the ratio of the fiber length to the rise per base pair in the DNA helix. This ratio remains constant with changes of the r.h. (Premilat et al. 1990). We also need to determine the number, n, of nucleotide pairs in a section of the DNA fiber. This number is equal to the ratio of the section, S, of the fiber to the section, s, of a DNA double helix. The fiber section was obtained from a direct measurement of its diameter and the section of the DNA helix can be deduced from the lattice parameters determined from X-ray patterns obtained at very low relative humidities. Hence, because in the hexagonal lattice there are three DNA molecules in a unit cell and only two in the monoclinic lattice (Langridge et al. 1960; Marvin et al. 1961; Fuller et al. 1965), we obtain, with the unit cell parameters a and b in a plane perpendicular to the helix axis:

$$s = a^2\sqrt{3}/6 \quad \text{(hexagonal)}$$

and

$$s = a\,b/2 \qquad \text{(monoclinic; } \alpha = \gamma = 90°;\ \beta = 97°\text{)}.$$

The number of moles of nucleotides in the fiber is thus given by $2N \cdot n/\mathcal{N}$ ($\mathcal{N}$ is Avogadro's number).

The number of water molecules associated with the DNA in the fiber varies during conformational changes and was determined from measurements of the variations of the fiber volume following modifications of the relative humidity. We assume that the volumes of DNA and water can be simply added to obtain the total volume, V_f, of the fiber at a given r.h. So, $V_f = V_w + V_0$, where V_w is the water volume and V_0 the DNA volume at 0% r.h. The number of water moles in the fiber is then given by $m \cdot V_w/M_w$, with m the density and M_w the molecular weight of water. Hence, the number, G, of water molecules per molecule of nucleotide in the fiber is:

$$G = (m \cdot V_w/M_w)/(2N \cdot n/\mathcal{N})$$

$$= (m \cdot \mathcal{N}/2M_w)(V_w/N \cdot n) = K \cdot V_w/N \cdot n$$

with V_w given in mm^3, the constant $K = 1.67 \cdot 10^{19}$ mm^{-3}). Note that water molecules bound to DNA at 0% r.h. (Tao et al. 1989) are not included.

Table 1. A - B transition of Na DNA. Fiber length (l), diameter (D) and geometrical parameters of helical conformations, p (rise per nucleotide), unit cell constants a, b

r.h. %	l (mm)	D (mm)	p (Å)	a (Å)	b (Å)	Lattice	DNA form
95	4.000	0.214	3.37	44.6		hexag.	B
92	3.920	0.182	3.36	41.0		hexag.	B
90	3.629	0.173	3.36	22.8	41.3	mono.	B A
			2.58				
86	3.364	0.168	3.34	22.6	41.2	mono.	B A
			2.57				
75	3.152	0.158	2.56	22.2	41.0	mono.	A
66	3.046	0.154	2.55	21.8	39.8	mono.	A
58	2.980	0.152		21.4	39.2	mono.	
45	2.864	0.151		21.4	38.2	mono.	
0	2.543	0.148					

Estimated standard deviations:

l, D: $3 \cdot 10^{-3}$ mm; p: 0.01 Å; a, b: 0.1 Å; r.h.: 1%

Results

1. The A - B transition

DNA fibers used for the study of the A - B transition were prepared from solutions with 0.5 Na^+ per nucleotide. The cooperativity of the A - B transition in DNA is well established; it is therefore interesting to analyze, in this case, the variations of the parameter G with the fraction X_B of nucleotides in the B form. We have shown (Premilat et al. 1990) that the variation of X_B with the r.h. can be determined by measurements of the fiber length and we have:

$$X_B = (l - l_A)/(l_B - l_A)$$

where l_B, l_A and l represent, respectively, the length of the fiber in the conformations B, A and intermediate states appearing during the conformational change (mixtures of A and B).

As an example of experimental results, note that the fiber under study adopts the B form at 95% r.h. and the A form at 66% with the corresponding rises per nucleotide $p_B = 3.37$ Å and $p_A = 2.55$ Å. For these well defined conformational states of the DNA, the fiber lengths $l_B = 4.000$ mm and $l_A = 3.046$ mm were measured (Table 1). The number N of base pairs along the fiber axis is then given by:

$$N = l_B/p_B = l_A/p_A = 1.19 \cdot 10^7$$

We noted that the ratio S/s of the fiber section to the section of a DNA double helix remains constant for r.h. lower than 80% (Fig. 1). This constant value represents the average number, n, of pairs of nucleotides contained in a section of the fiber and is, for the present fiber, equal to $43 \cdot 10^8$. This set of data allows us to determine values of G as a function of the relative humidity (Fig. 2). The present results are in accordance with previous observations (Tao et al. 1989). By using the set of values of X_B as a function of the r.h. (Premilat et al. 1990) and the data for G as a function of r.h. (Fig. 2) one can establish the curve

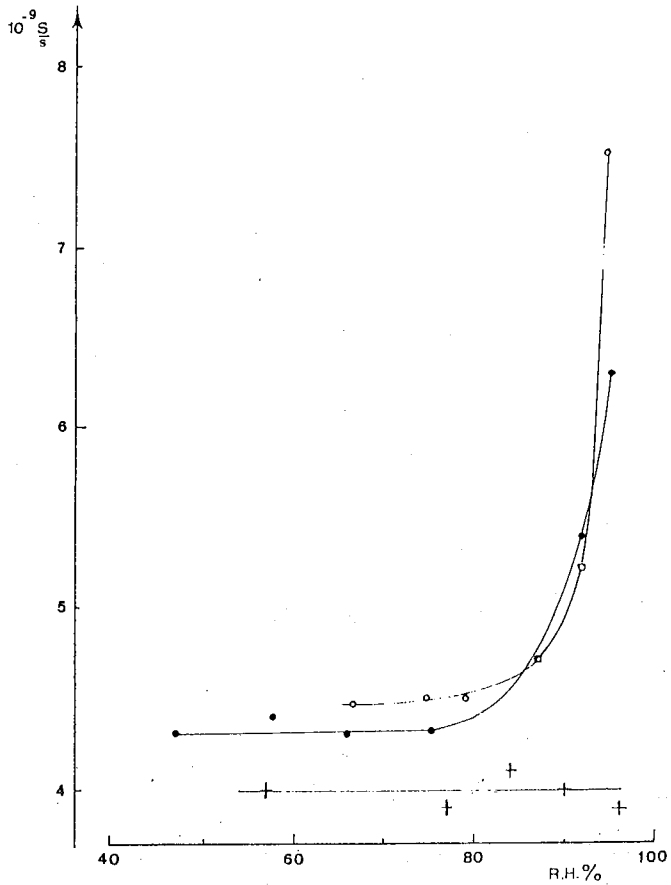

Fig. 1. Ratio of the fiber section, S, to a section, s, of the DNA double helix as a function of the relative humidity. A - B transition with Na DNA (•); B - C transition: Na DNA (o); Li DNA (-+-)

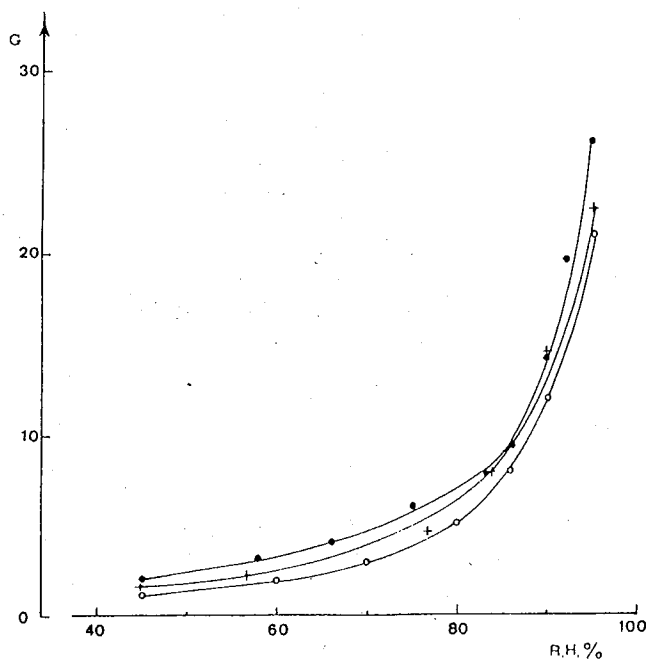

Fig. 2. The number, G, of water molecules per nucleotide as a function of the r.h. for Na DNA: A - B transition (- • -); B - C transition (o). Li DNA: B C transition (+)

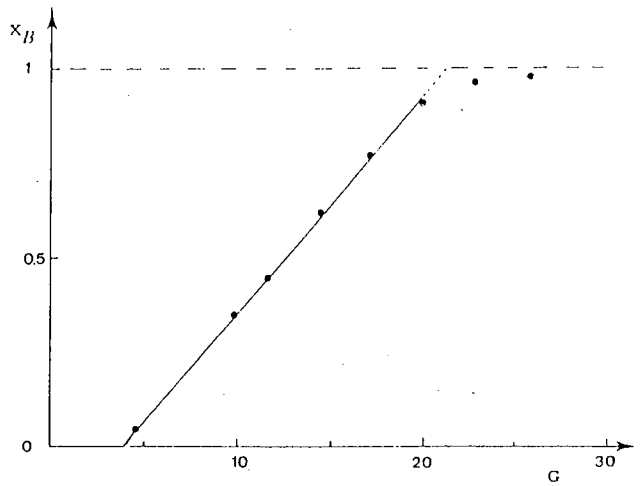

Fig. 3. A B transition: fraction X_B of nucleotides in the B form versus G

of X_B versus G given in Fig. 3 where linear variations of X_B are observed until $G=20$. This last value is obtained at 92% r.h. (Fig. 2) and corresponds to $X_B=0.92$. When G is larger than 20, a saturation effect appears and X_B is no longer proportional to G. Practically, the extrapolation of the linear part of the curve $X_B=f(G)$ until its intersection with the line $X_B=1$ (Fig. 3) gives a number $G_B=21$ molecules of water per molecule of nucleotide necessary to get the DNA completely in its B form. When G is larger than G_B, the DNA helices remain in the B form but the lattice dimensions are increased. In addition, the linear part of the curve $X_B=f(G)$ intersects the line $X_B=0$ at $G_A=4$ (Fig. 3) and this value represents the number of water molecules per molecule of nucleotide in the A form. Between these two extreme values of G, we have the fraction X_B of nucleotides in the B form and $(1-X_B)$ in A. The linear variation of G with X_B can therefore be expressed by:

$$G = X_B(G_B-G_A)+G_A \ .$$

II. The B C transition

The B-C transition of DNA was studied with Na and Li DNA fibers. In order to get the B C rather than the A-B transition with Na DNA, one has to use very low salt concentrations. We prepared solutions with 0.05 Na^+ per nucleotide in the DNA solution. With LiCl there is no such limitation as only the B-C transition is observed with that salt.

NaDNA fibers. X-ray fiber diffraction shows clearly the B or C conformation adopted by the DNA helices depending on the value of the relative humidity. We also noted that for r.h. lower than 75%, DNA fibers are largely disorganized. The experimental curve corresponding to the B-C transition as a function of the r.h. is linear and shows a change of slope in the vicinity of 75% r.h. (Premilat et al. 1990). It corresponds to a progressive and not a cooperative change of conformation: we thus deter-

90

Table 2. B-C transition of Na DNA. Fiber length (l), diameter (D) and geometrical parameters of helical conformations, p (rise per nucleotide), hexagonal unit cell a

r.h. %	l (mm)	D (mm)	p (Å)	a (Å)	DNA form
95	3.375	0.214	3.35	40.8	B
92	3.341	0.178	3.34	39.8	B
87	3.285	0.160	3.33	38.2	C
82	3.228	0.152	3.32	37.4	C
79	3.195	0.149	3.31	36.6	C
75	3.150	0.143	3.30	35.2	C
64	3.087	0.141			
58	3.062	0.139			
45	3.017	0.137			
0	2.870	0.135			

Estimated standard deviations:

l, D: $3 \cdot 10^{-3}$ mm; p: 0.1 Å; a: 0.1 Å; r.h.: 1%

Table 3. B-C transition of Li DNA. Fiber length (l), diameter (D) and geometrical parameters of helical conformations, p (rise per nucleotide), hexagonal unit cell a

r.h. %	l (mm)	D (mm)	p (Å)	a (Å)	DNA form
95	1.160	0.186	3.37	49.0	B
90	1.125	0.161	3.36	41.9	B
84	1.085	0.143	3.35	35.8	B
77	1.050	0.136	3.33	35.1	C
57	1.005	0.128	3.31	33.2	C
45	0.990	0.126	3.30	32.5	C
34	0.980	0.125	3.28	32.0	C
0	0.950	0.121			

Estimated standard deviations:

l, D: $3 \cdot 10^{-3}$ mm; p: 0.1 Å; a: 0.1 Å; r.h.: 1%

mined a progression rate R for the transition from C to B as a function of the number of water molecules per nucleotide. Values of this factor R at different r.h. were obtained from measurements of the fiber length l. We actually have:

$$R = (l - l_c)/(l_B - l_C),$$

where l_B and l_C are the lengths of the fiber in the B (r.h. higher than 95%) and the C (75% r.h.) forms. Different parameters characterizing the DNA fiber during the conformational change are given in Table 2. We determined

$$P_B = 3.35 \text{ A} \quad \text{and} \quad P_C = 3.30 \text{ A}$$

from X-ray patterns.

As for the A-B transition, the ratio S/s remains practically constant during the transition as long as the r.h. is lower than or equal to 80%. We can see in Fig. 1 that the variations of this ratio are very similar to those observed for the A-B transition.

By using the values of l as a function of the r.h. (Table 2) and combining them with the variations of G with the r.h. (Fig. 2) one can establish a curve representing R as a function of G. We can see in Fig. 4, that the relation between these two quantities corresponds to a saturation effect as the function associated with the curve can be written as:

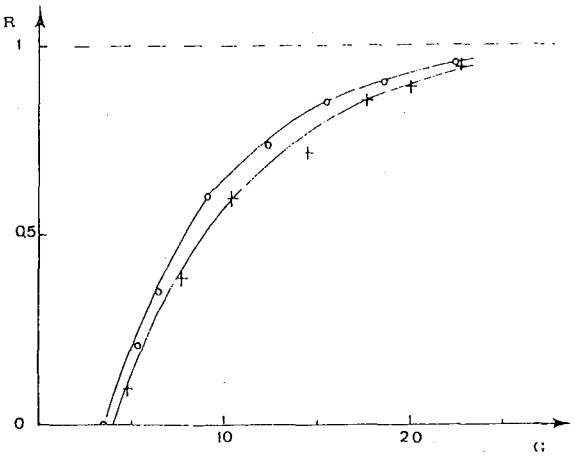

Fig. 4. Progression rate R for the B C transition as a function of the number G of water molecules per nucleotide. Na DNA (o); Li DNA (+)

$$R = 1 - \exp(-u(G - G_c)) \quad \text{or} \quad \ln(1 - R) = -u(G - G_c)$$

with a positive constant u; $G \to G_c$ when $R \to 0$ and G_c the number of water molecules per molecule of nucleotide necessary to get the DNA completely in the C conformation (at 75% r.h.). The experimental curve presented in Fig. 4 corresponds to $u = 0.16$ and $G_c = 3.5$.

Li DNA fibers. DNA fibers prepared from Li DNA solutions give better defined X-ray patterns than those obtained from NaDNA fibers. The fibers are homogeneous and very well organized. The crystal lattice remains hexagonal with practically the value of the a parameter obtained with Na DNA at r.h. lower than 80%. For higher values of the r.h. the lattice parameter a increases much more with Li DNA fibers than with Na DNA (Tables 2, 3).

We also noted that the X-ray reflection on the first layer line at 0.1 A $^{-1}$, which is characteristic for the C conformation, disappears when the r.h. is in the range of 80 to 86%. It is important to observe that it takes much more time to stabilize a Li DNA fiber at a given r.h. than a Na DNA one; the withdrawal of water is more difficult to achieve when the Li salt is present. Nevertheless the same kind of curve of R versus G is obtained (Fig. 4) with $u = 0.14$ and $G_c = 4.0$.

In Table 3 different fiber data are given to show their variations during the B C transition of Li DNA. An important difference in the behaviour of the Li DNA compared to the Na DNA is that the ratio S/s remains constant when the r.h. is varied (see Fig. 1). This may be related to a better organization of Li DNA molecules in the fibers and also to the higher conformational stability given to the DNA by the Li salt. This is the reason why the B-C transition is the only possible one with the Li salt; it actually represents a relatively slight change of conformation compared to the more substantial A B transition.

Discussion

Measurements of DNA fiber dimensions associated with X-ray fiber diffraction give precise information on the polymorphism of the DNA and on the role of water during conformational transitions (Premilat et al. 1990). The determination of the fiber volume and its variation with r.h. also allows one to determine the evolution of the number of water molecules associated with a nucleotide during the A - B and B - C transitions.

For the A – B transition of DNA, the results presently obtained show that every nucleotide in the A form is associated with an average of 4 water molecules (water molecules still present at 0% r.h. are not included) whereas 20 are necessary to stabilize the B conformation (Saenger et al. 1986; Tao et al. 1989). Mixtures of these two stable forms correspond to intermediate states of the DNA which can be defined by the fraction X_B of nucleotides in the B form. We observed that this fraction varies linearly with the average number of water molecules per nucleotide. This experimental fact confirms that no other conformation (different from A or B) appears during the A – B transition. Moreover, we can note that a nucleotide remains in the A form as long as the number of water molecules in its vicinity is lower than $G_B = 20$.

For the B – C transition, obtained with Li as well as with Na DNA, we observed exponential variations of the progression rate of the transition as a function of G. Such an effect of saturation shows clearly the progressive deformation of the DNA conformation which changes from the C to the B form by addition of water molecules to the double helices. When the average number of water molecules per nucleotide is larger than 9, the B form is stabilized. This happens for relative humidities equal to or higher than 85%.

Moreover, we observed that only four water molecules are associated with one nucleotide when the DNA is in the C form at 75% r.h.; surprisingly, this is the same amount as for the A form. However, as noted before, whereas 20 water molecules per nucleotide are necessary in order to get all the DNA in the B form during the A – B transition, only 10 are sufficient to obtain it from the C - B transition (with Na or Li salt). These minimum amounts of water stabilizing the B form are obtained at 92% r.h. (A – B transition) and 86% r.h. (B – C transition).

The ratio of the fiber section to the section occupied by a DNA double helix in the lattice is constant when the r.h. is lower than 80%. At higher values of the r.h., this ratio increases for Na DNA fibers whereas it remains constant during the B – C transition of Li DNA. Note that similar results, showing differences in the behaviour of Na and Li DNA, have recently been presented (Lindsay et al. 1988). The swelling of Na DNA fibers thus observed indicates the enlargement of highly hydrated and disorganized parts of the fiber. As Li DNA fibers do not show such behaviour, it seems that the presence of Li salt induces a good organization of the DNA in the fiber (X-ray patterns are better defined) and also a stabilization of the B-form as only the small conformational changes necessary for the B – C transition are then possible.

References

Albiser G, Harmouchi M, Prémilat S (1988) Influence of a mechanical tension on the B - A and B - C conformational transition in DNA fibres. J Biomol Struct Dyn 6:359 366

Cohen G, Eisenberg H (1968) Deoxyribonucleate solutions: sedimentation in a density gradient, partial specific volumes, density and refractive index increments, and preferential interactions. Biopolymers 6:1077 1100

Conner BN, Yoon C, Dickerson JL, Dickerson RE (1984) Helix geometry and hydration in an A-DNA tetramer: C-C-G-G. J Mol Biol 174:663 695

Dahlborg U, Dimic V, Rupprecht A (1980) Study of the hydration of oriented DNA by the neutron scattering technique. Phys Scripta 22:179 187

Davies DR, Baldwin RL (1963) X-ray studies of two synthetic DNA copolymers. J Mol Biol 6:251 - 255

Drew HR, Dickerson RE (1981) Structure of a B-DNA Dodecamer III. Geometry of hydration. J Mol Biol 151:535 - 556

Edelhoch H, Osborne JC Jr (1976) The thermodynamic basis of the stability of proteins, nucleic acids and membranes. Adv Protein Chem 30:183 250

Falk M, Hartman KA, Lord JR, Lord RC (1962) Hydration of deoxyribonucleic acid I. A gravimetric study. J Am Chem Soc 84:3843 3846

Falk M, Hartman KA, Lord JR, Lord RC (1963) Hydration of deoxyribonucleic acid II. An infrared study. J Am Chem Soc 85:387 394

Falk M, Poole AG, Goymour CG (1970) Infrared study of the state of water in the hydration shell of DNA. Can J Chem 48:1536 1542

Forsyth VT, Mahendrasingam A, Pigram WJ, Greenall RJ, Bellamy K, Fuller W, Mason SA (1989) Neutron fibre diffraction study of DNA hydration. Int J Biol Macromol 11:236 240

Fuller W, Wilkins MHF, Wilson HR, Hamilton LD (1965) The molecular configuration of deoxyribonucleic acid IV. X-ray diffraction study of the A form. J Mol Biol 12:60 80

Grimm H, Rupprecht A (1989) Hydration structure in natural DNA observed by thermal neutron scattering. Eur Biophys J 17:173 186

Hanlon S, Brudno S, Wu TT, Wolf B (1975) Structural transitions of deoxyribonucleic acid in aqueous electrolyte solutions. Reference spectra of conformational limits. Biochemistry 14:1648 1660

Hearst JE (1965) Determination of the dominant factors which influence the net hydration of native sodium deoxyribonucleate. Biopolymers 3:57 68

Hearst JE, Vinograd J (1961) The net hydration of deoxyribonucleic acid. Proc Natl Acad Sci USA 47:825 830

Kuntz ID Jr, Kauzmann W (1974) Hydration of proteins and polypeptides. Adv Protein Chem 28:239 345

Langridge R, Wilson HR, Hooper CW, Wilkins MHF, Hamilton LD (1960) The molecular configuration of deoxyribonucleic acid I. X-ray diffraction study of a crystalline form of the Lithium salt. J Mol Biol 2:19 37

Lee SA, Lindsay SM, Powell JW, Weidlich T, Tao NJ, Lewen GD, Rupprecht A (1987) A Brillouin scattering study of the hydration of Li and Na-DNA films. Biopolymers 26:1637 - 1665

Leslie AGW, Arnott S, Chandrasekaran R, Ratliff RL (1980) Polymorphism of DNA double helices. J Mol Biol 143:49 72

Lindsay SM, Lee SA, Powell JW, Weidlich T, Demarco C, Lewen GD, Tao NJ, Rupprecht A (1988) The origin of the A to B transition in DNA fibers and films. Biopolymers 27:1015 - 1043

Marvin DA, Spencer M, Wilkins MHF, Hamilton LD (1961) The molecular configuration of deoxyribonucleic acid III. X-ray diffraction study of the C form of the Lithium salt. J Mol Biol 3:547 - 565

Premilat S, Harmouchi M, Albiser G (1990) A method for the experimental study of DNA conformational transitions in fibers. Biophys Chem 35:37 - 45

Rupprecht A, Piskur J (1983) A simple mechanochemical method for studying structure and dynamics of biopolymer fibers in various media. Acta Chem Scand B 37:863–864

Saenger W, Hunter WN, Kennard O (1986) DNA conformation is determined by economics in the hydration of phosphate groups. Nature 324:385–388

Semenov MA, Starikov EB, Bolbukh TV (1988) Hydratation isotherms and structural state of nucleotides and polynucleotides. Stud Biophys 123:217–224

Tanford C (1968) Protein denaturation. Adv Protein Chem 23:121–282

Tao NJ, Lindsay SM, Rupprecht A (1989) Structure of DNA hydration shells studied by Raman spectroscopy. Biopolymers 28:1019–1030

Texter J (1978) Nucleic acid-water interactions. Prog Biophys Mol Biol 33:83–97

Tunis MJB, Hearst JE (1968a) On the hydration of DNA. I. Preferential hydration and stability of DNA in concentrated trifluoroacetate solution. Biopolymers 6:1325–1344

Tunis MJB, Hearst JE (1968b) On the hydration of DNA. II. Base composition dependance of the net hydration of DNA. Biopolymers 6:1345–1353

Westhof E (1987) Hydration of oligonucleotides in crystals. Int J Biol Macromol 9:186–192

Wolf B, Hanlon S (1975) Structural transitions of deoxyribonucleic acid in aqueous electrolyte solutions. II. The role of hydration. Biochemistry 14:1661–1670

D) TRANSITIONS CONFORMATIONNELLES ET HYDRATATION DU POLY D(A-T). POLY D(A-T) EN FIBRE

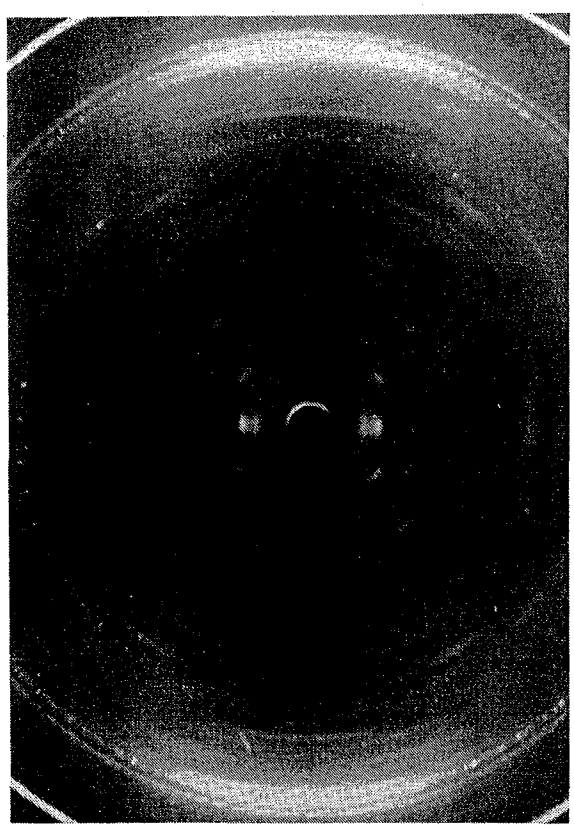

Photo N° 11 : Mélange des formes B et D avec sel de sodium du poly (dA-dT).poly (dA-dT) à 64 % d'humidité relative. (Le cliché a été obtenu au cyclo synchrotron de LURE)

Eur Biophys J (1991) 20: 109 - 114

European Biophysics Journal

Conformational transitions and hydration of poly d(A-T) · poly d(A-T) in fibers

A. Abouelkassimi, G. Albiser, and S. Premilat

Laboratoire de Biophysique Moléculaire, UA CNRS 494, Université de Nancy I, Faculté des Sciences, BP 239, F-54506 Vandoeuvre Les Nancy, France

Received February 11, 1991/Accepted in revised form May 7, 1991

Abstract. Conformational transitions of poly d(A-T) · poly d(A-T) have been studied by fiber X-ray diffraction and measurement of fiber dimensions. Results obtained for the D-A-B and D-B transitions are presented and analyzed. For all these form transitions, cooperativity effects are observed for the variation of the rise per nucleotide versus the relative humidity. Detailed information about hydration of the polynucleotide during form transitions and the numbers of water molecules per nucleotide necessary to stabilize the different helical conformations are presented.

Key words: poly d(A-T) · poly d(A-T) – D-A-B and D-B helical transitions – DNA hydration – X-ray fiber diffraction

Introduction

Polynucleotides do present, as revealed by X-ray diffraction (Leslie et al. 1980), a polymorphism equivalent to that of natural DNA. Recent studies on oligonucleotides using different approaches such as NMR (Patel et al. 1987) and I. R. spectroscopy (Adam et al. 1986; Pilet et al. 1975) or crystallography (Kennard and Hunter 1989) have confirmed this polymorphism, which is observable for the family of right handed double helices (Wing et al. 1980) as well as for the left handed Z form (Wang et al. 1979).

The polymorphism of DNA and polynucleotides is associated with different conformational transitions which can be revealed by the study of well organized fibers (Lindsay et al. 1988; Mahendrasingam et al. 1983; Premilat et al. 1990). Actually, helical transitions depend on many physico-chemical parameters such as the type and concentration of salt, the relative humidity and also on the tension applied on fibers (Albiser et al. 1988). It should be noted that DNA conformations and form transitions are also dependent on the base composition or, more precisely, on the base sequence of polynucleotides (Arnott et al. 1974; Arnott et al. 1980; Leslie et al. 1980).

A recently proposed method for the experimental study of DNA conformational transitions in fibers allowed us to follow and analyze the A-B and B-C transitions by using, in a complementary way, fiber X-ray diffraction and measurement of fiber dimensions (Premilat et al. 1990). Moreover, it has been shown (Harmouchi et al. 1990) that one can also determine, by using results obtained from this method, the variations of the number of water molecules associated with the DNA base pairs during the form transitions.

In the present study, we used this experimental method in order to gain information on the conformational transitions in poly d(A-T) · poly d(A-T) which presents fiber X-ray patterns of the A, B or D double helical forms according to the sodium salt concentration and the relative humidity (Arnott et al. 1974; Davies et al. 1963; Mahendrasingam et al. 1983 and 1986; Leslie et al. 1980). Results of a detailed study of the D-B and D-A-B transitions which could have some biological importance in A+T rich sequences of DNA (Moreau et al. 1982), are presented.

Material and methods

Lyophilized poly d(A-T) · poly d(A-T) associated with sodium chloride was purchased from Pharmacia and used without any further purification. Fibers were obtained from the stretching of a gel of polynucleotide humidified with water at pH 7 following a method already described (Fuller et al. 1967).

As the type of the helical transition observed depends mainly on the salt concentration, an empirical procedure was applied in order to get the appropriate amount of NaCl in the fiber. We proceeded as follows: the fiber was firstly tested by getting an X-ray pattern; the type of conformation and the degree of organization of the fiber was therefore determined. Then we added successive small

Offprint requests to: S. Premilat

110

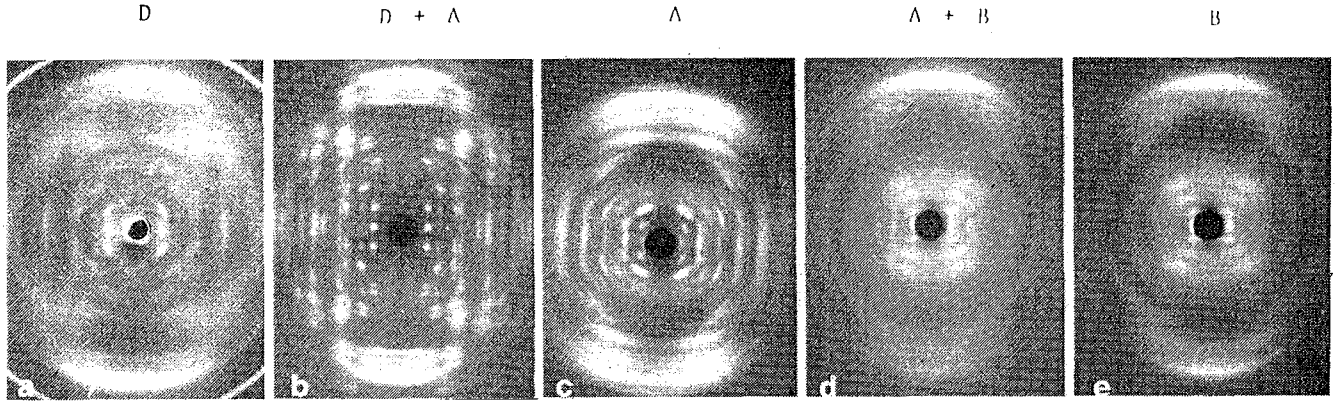

Fig. 1. X-ray patterns obtained at a 40% r.h. (D-form); b 60% r.h. (mixture of A and D forms); c 68% r.h. (A form); d 78% r.h. (mixture of A and B forms); e 88% r.h. (B form)

Table 1. D-A-B transition: geometrical parameter of helical conformations: p (rise per nucleotide), P (pitch)

R.H. (%)	DNA form	Lattice type[a]	a (Å)	b (Å)	c (Å) ($=P$)	p (Å)	P/p
40	D	T	17.4	17.4	24.2	3.00	8.07
56	D	T	17.8	17.8	24.9	3.02	8.25
60	D	T	18.1	18.1	25.1	3.00	8.40
	A	M	21.4	40.2	27.6		
68	A	M	21.8	40.6	27.8	2.54	10.96
74	A	M	22.5	41.0	28.1	2.56	10.98
78	A	M	23.1	41.9	28.5	2.56	11.05
	B	H	39.2		32.4	3.32	9.76
88	B	H	44.2		33.5	3.35	10
90	B	H	45.0		33.6	3.36	10

[a] T: Tetragonal; M: Monoclinic; H: Hexagonal

amounts of a solution 0.01 M NaCl on the humidified fiber the extremities of which were fixed to the holder. It is in this way that one can observe the D-B transition whereas the D-A-B transitions are obtained from fibers at lower salt concentrations. Conversely, fibers containing an excess of salt, as revealed by characteristic spots of NaCl powder on X-ray patterns, can be slightly "washed" by taking off the salt on the fiber surface (at low r.h.) with a few drops of water. Moreover it can be noted that a better organization of the fiber is obtained after it has been submitted to variations of the relative humidity (r.h.) while its extremities are maintained fixed to the holder. However, for the actual X-ray and dimension measurements, one extremity of the fiber is freed from the holder and this is done when equilibrium at low r.h. is realized (the diameter of the fiber then has its smallest value).

A special X-ray camera was realized in order to get the same physico-chemical conditions when X-ray or fiber dimension measurements are performed. The camera side facing the collimator is a transparent plastic sheet with a well on its centre to stop the direct X-ray beam. It allows us to observe the DNA fiber, with a binocular microscope, before and after every X-ray exposure. The photographic plate can be positioned at distances from the fiber equal or superior to 18 mm. One can also, without any opening the camera (the fixed value of the r.h. is not perturbed), modify the position of the fiber relative to the incident X-ray beam. The fiber is maintained vertical and the very slight tension applied by the glass rod fixed to its extremity prevents undulations of the fiber during form transitions. The r.h. in the fiber surroundings is given precise values according to the method already described (Premilat et al. 1990).

The evaluation of the number of water molecules associated with a nucleotide as well as its variation during a conformational transition is made following the method previously used for the study of the A-B and B-C transitions (Harmouchi et al. 1990).

Results

A. The D-A-B transitions

X-ray fiber diffraction. At 40% r.h. the poly d(A-T) poly d(A-T) presents the D helical conformation (Fig. 1a) with parameters given in Table 1. These experimental data show some variations of the unit cell with increasing r.h. We note that the unit cell parameters at low r.h. do not differ from values given in recent X-ray diffraction studies of the D form (Millane et al. 1984; Forsyth et al. 1989). The A form is observed at 68% r.h. (Fig. 1c) and a mixture of D and A forms is obtained for r.h. values between 40 and 68% (Fig. 1b). When the r.h. is increased from 68%, a mixture of A and B forms is observed (Fig. 1d) on X-ray patterns (easily observable at 78% r.h.). At 88% r.h. X-ray patterns of the B-form alone are obtained (Fig. 1e). By decreasing the r.h. from 88%, we could only observe the reversible B-A transition; the transition from A to D could not be realized (Mahendrasingam et al. 1983) when the r.h. was lowered in the range of 68 to 40% and the poor X-ray patterns then obtained indicate the disorganization of the A form of the polynucleotide in the fiber. However, transitions from the D (or F) to A and then to the B form of poly d(A-T) poly d(A-T) were already observed from X-ray diffraction studies (Fuller et al. 1984) and actually, one can get the D form again by a complete rehydration of the fiber

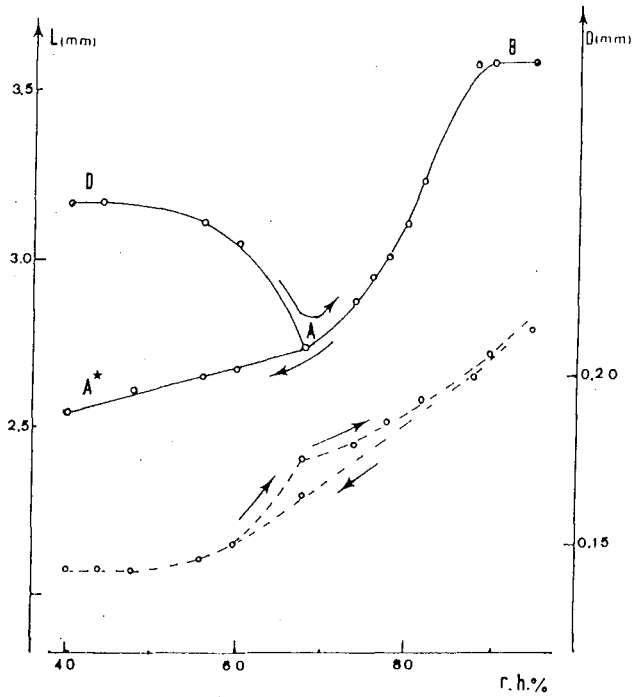

Fig. 2. D-A-B transition: variations of the length ( ) and diameter (- - -) as a function of the r.h.

(we then have the B form) followed by a decrease of the r.h. until 40%. However, it is necessary to keep the two ends of the fiber fixed to the holder during this last operation. Therefore the important effect of a tension applied to the fiber (Albiser et al. 1988) must be taken into account in order to realize reversible transitions. The present result confirms, in a complementary way, those given in a recent study (Loprete and Hartman 1990) of non-oriented gels of poly d(A-T) · poly d(A-T) where the D form could not be observed.

Fiber dimensions. Results of measurement of the fiber dimensions, made as explained above, are presented in Fig. 2. We can thus see that the variations of the fiber length with the r.h. is characterized by cooperative effects for the D-A and A-B transitions. The D-A transition is not reversible under the present conditions but the A-B transition is perfectly reversible as noted before for natural DNA (Lindsay et al. 1988; Premilat et al. 1990). The part A-A* of the transition curve (Fig. 2), corresponding to the non-cooperative disorganization of the A form, is linear with the r.h. (values of the helical parameters can then no longer be obtained from X-ray patterns).

We noted that when the r.h. is increased starting from a low value (D form), the fiber diameter presents two types of variations corresponding respectively to the D-A and A-B transitions (Fig. 2) with a marked point of inflexion between these two transitions. When the r.h. is decreased from the high value corresponding to the B form, the route followed by the diameter value is not reversible as for the fiber length; the diameter decrease is then uniform even in the A-A* portion of the curve.

Table 2. D-B transition: geometrical parameters of helical conformations: p (rise per nucleotide), P (pitch)

R.H. (%)	DNA form	Lattice type[a]	a (Å)	b (Å)	c (Å) ($=P$)	p (Å)	P/p
40	D	T	17.3	17.3	24.0	2.97	8.08
48	D	T	17.5	17.5	24.3	2.97	8.18
56	D	T	17.8	17.8	24.6	2.99	8.22
60	D	T	18.2	18.2	24.7	3.00	8.23
64	D	T	19.2	19.2	25.3	3.00	8.43
	B	H	37.4		31.6	3.33	9.49
68	D	T	20.2	20.2	27.1		
	B	H	37.7		32.3	3.33	9.70
76	B	H	40.2		33.4	3.33	10.03
80	B	H	41.0		33.4	3.34	10
86	B	H	43.0		33.5	3.35	10

[a] T: Tetragonal; H: Hexagonal

B. The D-B transition

We proceeded as for the preceding study but salt was added to the fiber progressively until the A form could no longer be observed on X-ray patterns. The perfectly reversible B-D transition can then be analysed from X-ray patterns. Note that it is not necessary in the present case to maintain the fiber fixed to the holder in order to get the D form.

Results thus obtained are given in Table 2. One can see that for r.h. lower than 60%, the D form is obtained (Fig. 3a); its helical parameters vary very slightly with the relative humidity. As soon as the r.h. is 76%, only the B form appears on X-ray patterns (Table 2 and Fig. 3c).

Between 60% and 76% r.h. (i.e. the range of D-B transition) no continuous variation of the parameter p (rise per nucleotide) is observed as was the case for the B-C transition (Premilat et al. 1990). A mixture of D and B forms is rather clearly observed on the X-ray patterns (Fig. 3b). Measurements of fiber dimensions give values presented in Fig. 4. The fiber length remains practically constant for r.h. lower then 60% (D form) and a steep increase of length is then observed until 80% r.h. The length variations with the r.h. are perfectly reversible and in complete agreement with observations made on X-ray patterns. Actually, we noted that the ratio of the length values at 80 and 56% r.h. is indeed equal to the ratio of the corresponding values of the parameter p measured at the same r.h.; this is in accordance with the direct relation existing between the fiber length and the rise per base pair in the molecular double helix (Premilat et al. 1990).

C. Hydration of poly d(A-T) · poly d(A-T)

The important role played by water during form transitions of the poly d(A-T) · poly d(A-T) can be well appreciated in Figs. 2 and 4 where the variation of the fiber diameter is represented as a function of the r.h.

The double helical conformations adopted by natural DNA as well as by synthetic polynucleotides are directly

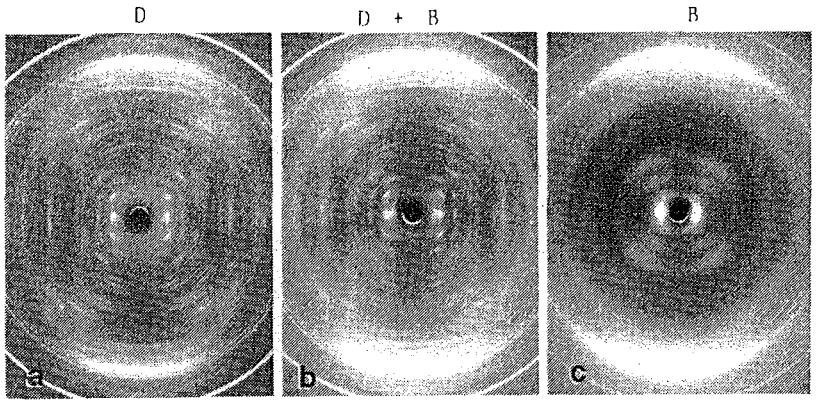

Fig. 3. X-ray patterns obtained at a 54% r.h. (D-form), b 64% r.h. (mixture of D and B forms) and c 76% r.h. (B form)

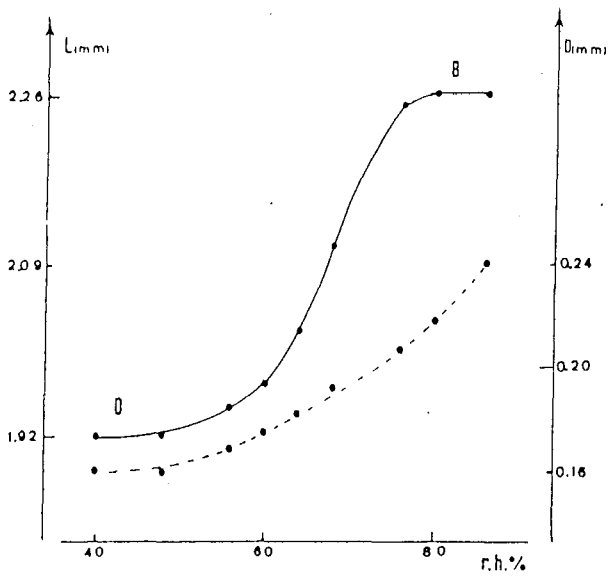

Fig. 4. D-B transition: variations of the fiber length (—) and diameter (- - -) as a function of the r.h.

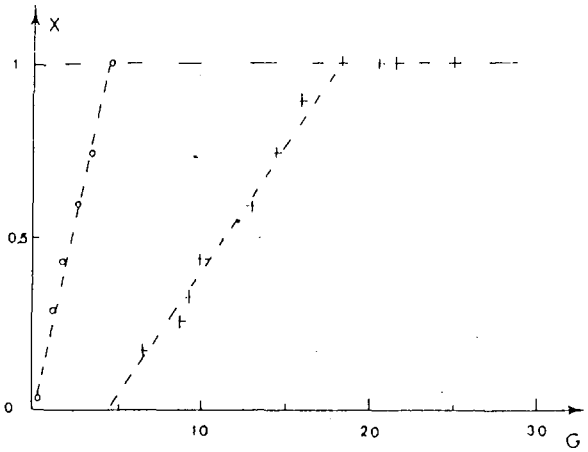

Fig. 5. D-A-B transition: (o) fraction X_A of nucleotides in the A form, (+) fraction X_B of nucleotides in the B form versus the number G of water molecules per nucleotide

related to the degree of hydration of the molecules. Hydration can be defined by the averaged number of water molecules associated with a nucleotide of the molecular helix. This number, G, can be determined by the following expression previously established (Harmouchi et al. 1990):

$$G = K(V_f - V_0)/N \cdot n$$

where V_f is the volume of the fiber at a given r.h., V_0 that volume at 40% r.h.; N is the number of nucleotides situated along the fiber axis, n is the number of nucleotide pairs in a section of the fiber and K is a constant equal to $1.67 \cdot 10^{19}$ mm^{-3}.

1. Variations of G during the D-A transition. By using the values of the fraction X_A of nucleotides in the A form as a function of the r.h. as well as the values of G corresponding to the D to A transition, we established the curve of X_A versus G presented in Fig. 5. The linear variation of X_A until $G = 5$ (r.h. of 68%) corresponds to the transition D-A. Results thus obtained show that only one water molecule (an average) is associated with a nucleotide in the D form at 56% r.h. while 5 water molecules per nucleotide stabilize the A form.

2. Variations of G during the A-B transition. The variation of the fraction X_B of nucleotides in the B form versus G is given in Fig. 5. Here also, the variation is linear until $G = 18$ (r.h. of 88%). This last value of G is the average number of water molecules necessary to transform all the poly d(A-T) · poly d(A-T) into its B form. For larger values of G, there is a saturation which mainly affects the fiber diameter.

3. Variations of G during the D-B transition. In Fig. 6 one can see the variation of X_B as a function of G. The variation is linear until $G = 13$, a value corresponding to $X_B = 1$. This value of G represents the average number of water molecules associated with every nucleotide in the B form during the D to B transition. The present results show that there are now 3 water molecules per nucleotide in the D form at 60% r.h. (Forsyth et al. 1989). This

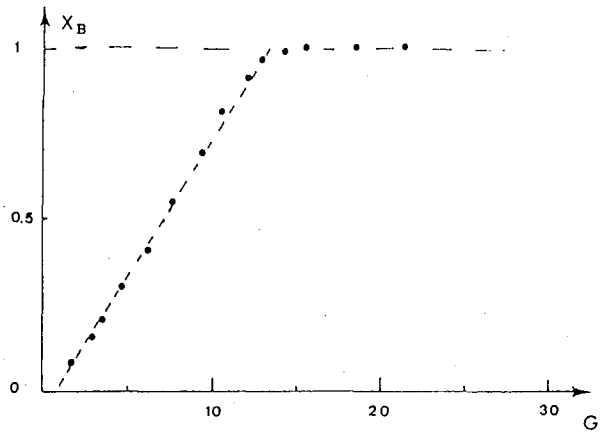

Fig. 6. D-B transition: fraction X_B of nucleotides in the B form versus the number G of water molecules per nucleotide

figure, much larger than that for the D-A transition, could be a consequence of the larger amount of salt used, in the present case, in order to avoid the A form.

Discussion

The experimental method which associates fiber dimension measurements with X-ray diffraction, allows one to gain information on the role played by water during the different conformational transitions of poly d(A-T) · poly d(A-T). Actually, the present study gives the evolution of the average number of water molecules associated with a nucleotide during the D-A-B and D-B transitions. It is also shown that the A form is stabilized with an average of 5 water molecules per nucleotide when the D to A transition is performed in the poly d(A-T) · poly d(A-T) (one should note that water present in the fiber at 40% r.h. is not included in these estimations). For the A-B transition, an average of 18 water molecules per nucleotide is necessary to get the polynucleotide in the B conformation. This figure is indeed very near to the value obtained for natural DNA (Saenger 1984; Brandes et al. 1989; Harmouchi et al. 1990). However, when the B form is obtained from the D-B transition, an average of 13 water molecules per nucleotide are then sufficient to stabilize the B form. This value is intermediate between that obtained ($G=9$) for the C-B transition in natural DNA (Harmouchi et al. 1990) and the value of 18 presently observed for the B form resulting from the A to B transition. One should note that these different numbers of water molecules necessary to stabilize the B form result from the different salt concentrations used in order to obtain specific DNA transitions.

The present method of analysis does not allow one to determine the precise position of water molecules in the double helical structure as it is realized in single crystal X-ray studies on oligonucleotides (Drew et al. 1981, Conner et al. 1984). Nevertheless, our approach permits one to discriminate between helical deformations and actual transitions between distinct structural families of double helices. For instance, one can draw important information from the observation of the linearity of the curves representing the fraction X of nucleotides in a given helical form as a function of the water content G (Figs. 5 and 6). Such behaviour is characteristic of transitions between different forms of the double helices while a progressive deformation of one conformation would result in non-linear variations of X versus G (Harmouchi et al. 1990). This linearity, clearly observed for the D-B as well as for the D-A-B transitions, is in accordance with the sigmoidal variations of the fiber length as a function of the r.h. (Figs. 2 and 4); this indeed characterizes cooperative conformational transitions between distinct helical forms of polynucleotides or natural DNA (Premilat et al. 1990). Moreover, mixtures of X-ray patterns corresponding respectively to A, B and D forms are actually observed when the r.h. is given values located in the transition intervals. It appears therefore that the D form of poly d(A-T) · poly d(A-T) is not an element of the B family but rather a stable distinct conformation of polynucleotides or DNA.

Acknowledgements. We thank Drs. J. Doucet and J. P. Benoit for assistance in conducting experiments with Synchrotron radiation at L.U.R.E. (Orsay) where X-ray patterns of mixtures of D and B forms were obtained.

References

Adam S, Liquier J, Taboury JA, Taillandier E (1986) Right and left-handed helixes of poly d(A-T) · poly d(A-T) investigated by infrared spectroscopy. Biochemistry 25:3220–3225

Albiser G, Harmouchi M, Premilat S (1988) Influence of a mechanical tension of the B-A and B-C conformational transition in DNA fibres. J Biomol Struct Dyn 6:359–366

Arnott S, Chandrasekaran R, Hukins DWL, Smith PJC, Watts L (1974) Structural details of a double helix observed for DNAs containing alternating purine and pyrimidine sequences. J Mol Biol 88:523–533

Arnott S, Chandrasekaran R, Birdsall DL, Leslie AGW, Ratliff RL (1980) Left-handed DNA helices. Nature 283:743–745

Brandes R, Rupprecht A, Kearns DR (1989) Interaction of water with oriented DNA in the A and B form conformations. Biophys J 56:683–691

Conner BN, Yoon C, Dickerson JL, Dickerson RE (1984) Helix geometry and hydration in an A-DNA tetramer: C-C-G-G. J Mol Biol 174:663–695

Davies DR, Baldwin RL (1963) X-ray studies of two synthetic DNA copolymers. J Mol Biol 6:251–255

Drew HR, Dickerson RE (1981) Structure of a B-DNA dodecamer. J Mol Biol 151:535–556

Forsyth VT, Mahendrasingam A, Pigram WJ, Greenall RJ, Bellamy K, Fuller W, Mason SA (1989) Neutron fibre diffraction study of DNA hydration. Int J Biol Macromol 11:236–240

Fuller W, Hutchinson F, Spencer M, Wilkins MHF (1967) Molecular and crystal structures of double-helical RNA. J Mol Biol 27:507–524

Fuller W, Pigram WJ, Mahendrasingam A, Forsyth VT, Naye C, Greenall RJ (1984) X-ray diffraction studies of the polynucleotides poly d(A-T) · poly d(A-T) and poly d(G-C) · poly d(G-C). Biological Systems Structure and Analysis, Proceedings of the study weekend at Daresbury Laboratory, DL/SCI/R22:106–108

Harmouchi M, Albiser G, Premilat S (1990) Changes of hydration during conformational transitions of DNA. Eur Biophys J 19:87–92

Kennard O, Hunter WN (1989) Oligonucleotide structure: a decade of results from single crystal X-ray diffraction studies. Q Rev Biophys 22:327–379

Leslie AGW, Arnott S, Chandrasekaran R, Ratliff RL (1980) Polymorphism of DNA double helices. J Mol Biol 143:49–72

Lindsay SM, Lee SA, Powell JW, Weidlich T, Demarco C, Lewen GD, Tao NJ, Rupprecht A (1988) The origin of the A to B transition in DNA fibers and films. Biopolymers 27:1015–1043

Loprete DM, Hartman KA (1990) Conditions for the stability of the alternative structures of duplex poly (dA-dT). Biopolymers 30:753–761

Mahendrasingam A, Rhodes NJ, Goodwin DC, Nave C, Pigram WJ, Fuller W, Brahms J, Vergne J (1983) Conformational transitions in oriented fibres of the synthetic polynucleotide poly d(A-T)·poly d(A-T) double helix. Nature 301:535–537

Mahendrasingam A, Forsyth VT, Hussain R, Greenall RJ, Pigram WJ, Fuller W (1986) Time resolved X-ray diffraction studies of the B-D structural transition in the DNA double helix. Science 233:195–197

Millane RP, Walker JK, Arnott S, Chandrasekaran R, Birdsall DL, Ratliff RL (1984) Structure of a pleomeric form of poly d(A-T)·poly d(A-T). Nucl Acids Res 12:5475–5493

Moreau J, Marcaud L, Maschat F, Kejzlarova-Lepesant J, Lepesant JA, Scherrer K (1982) A+T-rich linkers define functional domains in eukaryotic DNA. Nature 295:260–262

Patel DJ, Shapiro L, Hare D (1987) Nuclear magnetic resonance and distance geometry studies of DNA structures in solution. Ann Rev Biophys Chem 16:423–454

Pilet J, Blicharski J, Brahms J (1975) Conformations and structural transitions in polydeoxynucleotides. Biochemistry 14:1869–1875

Premilat S, Harmouchi M, Albiser G (1990) A method for the experimental study of DNA conformational transitions in fibers. Biophys Chem 35:37–45

Saenger W (1984) In: Cantor CR (ed) Principles of nucleic acid structure. Springer, New York Berlin Heidelberg, p 370

Wang AHJ, Quigley GJ, Kolpak FJ, Crawford JL, Van Boom JH, Van der Marel G, Rich A (1979) Molecular structure of a left handed double helical DNA fragment at atomic resolution. Nature 282:680–686

Wing R, Drew H, Takano T, Broka C, Tanaka S, Itakura K, Dickerson RE (1980) Crystal structure analysis of a complete turn of B-DNA. Nature 287:755–758

E) LA TRANSITION CONFORMATIONNELLE B-Z ET HYDRATATION DU POLY (DC DG). POLY (DC DG) EN FIBRE

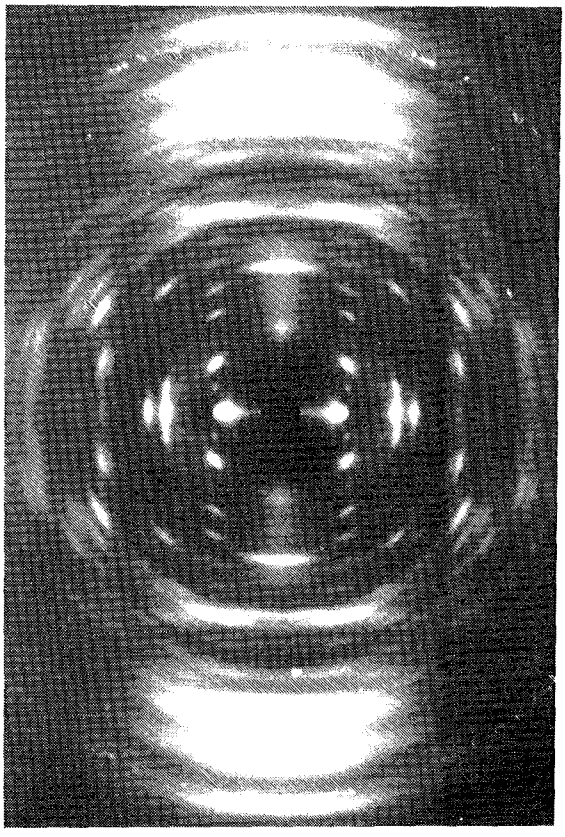

Photo N° 12 : Forme Z du poly (dC-dG).poly (dC-dG) avec sel de sodium à 77 % d'humidité relative.

The B-Z conformational transition and hydration of poly (dC-dG). poly (dC-dG) in fibers

G. Albiser and S. Prémilat

Laboratoire de Biophysique Moléculaire, U.A.CNRS 494, Faculté des Sciences, Université de Nancy I, B.P. N° 239, 54506 Vandoeuvre les Nancy, France

Abstract

The B-Z transition of poly (dC-dG).poly (dC-dG) has been studied by fiber X-ray diffraction and mesurement of fiber dimensions. The polymorphism of the Z form is well observed as a function of variations of the r. h. (relative humidity). The Z to B transition is obtained at very high r.h. values The cooperative transition from B to Z is associated with a disorganization of the fiber. Details about the hydration of the polynucleotide during conformational transitions are presented and it is shown that a nucleotide in Z form can be associated with up to 16 water molecules and to 22 when in the B form.

Keywords : poly (dC-dG).poly (dC-dG) ; B-Z helical transitions ; hydration ; X-ray diffraction ; fiber dimensions.

Running headline : B-Z conformational transitions

Introduction

The left handed double helical conformation of oligonucleotides composed of sequences of alternating cytosine and guanine have been precisely determined by X-ray crystallography[1]. This Z form of polynucleotides has also been observed in solutions[2] and in fibers by X-ray diffraction of poly (dC-dG). poly (dC-dG)[3-7]. Note that in these last cases, the left handed helical conformation is frequently named the S form[8].

Besides its interesting physico-chemical properties, the biological importance of the Z conformation has been put into evidence by in vivo experiments on different plasmids[9]. The left handed helical form of DNA intervenes in genetic recombination[10] and in the transcription process[11]. It has also been shown that some proteins and ligands[12] can be more tightly bound to polynucleotide sequences when they are in the Z form rather than when in B conformation. Supercoiling, generated by biological processes, is a factor which can also stabilize stretches of Z-DNA in vivo as demonstrated in a recent work[13].

In order to gain information about the effects of variations of external parameters on the form transitions, the study of poly (dC-dG). poly (dC-dG) molecules in fibers is particularly interesting as it can adopt left handed as well as right handed helical conformations depending on the physico-chemical conditions[6]. Moreover, the transition between

these two families of double helixes can be followed by fiber X-ray diffraction associated with measurements of fiber dimensions, according to an experimental method previously established[14] and applied to the analysis of the hydration[15] of DNA during conformational transitions. This method is used in the present study and it allowed us to establish experimental curves for the B-Z transitions of poly (dC-dG). poly (dC-dG) and to determine the changes of hydration during the conformational modifications of the polynucleotide.

Material and Methods

Lyophilized samples of poly (dC-dG). poly (dC-dG), purchased from Pharmacia, were used without any further purification to get, by addition of distiled water at pH 7, a gel from which fibers were drawn. As the salt concentration is of main importance for the type of helical conformation adopted by the polynucleotide molecules, the following empirical procedure was applied in order to get the appropriate amount of NaCl in the fiber : X-ray patterns were firstly obtained to test the fiber and, according to the type of helix pattern observed, a small amount of a solution 0.01 M NaCl was added to the fiber which was then tested again by getting another X-ray pattern. This was made again until the desired helical conformation was obtained.

The organization of the fibers is improved when they are submitted to cycles of variations of the r.h. (relative humidity) from very high values (95 %) to low ones. During theses cycles, the fiber is maintained vertical with a light

tension applied on its free extremity[16] . This tension is withdrawn when actual measurements are performed. The side of the X-ray camera facing the collimator has been made of a transparent plastic sheet which allows us to measure, before and after every X-ray exposure, the fiber dimensions with a binocular microscope. Fiber X-ray patterns associated to the different fiber lengths are therefore obtained under the same well controlled conditions of r.h. as for fiber dimension measurements[14].

The determination of the number G of water molecules located in the vicinity of every nucleotide as well as its variations during conformational transitions is made according to the procedure described previously[15]. We therefore applied the following relation :

$$G = K \frac{V}{Nn} \qquad \text{with } K = 1.67\ 10^{19}\ mm^{-3}$$

and where V is the difference between the fiber volume measured at a given r.h. and at 0 % r.h.; N and n are the numbers of nucleotides respectively located along the fiber axis (between two points chosen for the length measurement) and in a section of the fiber. Values of N and n are obtained from the determination of the crystallographic parameters following the method already used[13].

Results

X-ray diffraction

Fibers of poly (dC-dG). poly (dC-dG) used for the present study are well organized and they do not present the A helical form when at 75 % r.h. but rather the Z conformation.

In table 1 are given the different characteristic parameters of the double helical conformations determined from X-ray diffraction patterns obtained at different r.h.. One can see that measurement is possible even on patterns obtained at very low r.h. values. Actually, the X-ray patterns do present a good definition for r.h. between 35 and 85 % (Plate 1 a,b); we then get the Z form of the polynucleotide. When the r.h. is risen at values between 85 and 95 %, the diffraction spots become more diffused (Plate 1 c) and the pattern obtained at values of the r.h. higher than 95 % is characteristic of the B form (Plate 1 d) with the classical helical parameters P = 33.8 A and p = 3.39 A. One should note that the present experimental observations are in agreement with results already obtained on fibers of poly (dC-dG). poly (dC-dG) with synchrotron radiation[7].

We noted an evolution of the parameters P and p (table 1) of the Z form presently observed, while the r.h. was increased. But the ratio P/p remained almost constant with a value very near to 6. During these modifications of the Z form, one gets the helical parameters corresponding to the two forms defined as Z_1 (or S_1) and Z_2 (or S_2)[7,17]. These conformations observed at 40 % and 88 % r.h. respectively, correspond to P = 43 A and P = 45 A .

When the polynucleotide is in its Z form, the meridian spots observed on X-ray pattern are characteristic of a dinucleotide as the repeating unit. These spots are modified with increasing r.h. and finally disappear for r.h. values higher than 95%. We then have a change of conformation ; the meridian spot which corresponds to 7.5 A disappears and the one associated to a distance of 6.4 A is observed on X-ray patterns. When the B form is obtained at 97,5 % r.h., only one meridian spot at 3.4 A is present ; the repeating unit is then one nucleotide in one helical conformation. The curve on figure 1 represents the variations with the r.h. of the value Pm of the mean axial projection of a nucleotide. We can see that this parameter presents increasing values when the r.h. is risen from 0 to 95 % and it decreases very steeply for r.h. higher than this last value.

Moreover, we can note that when the Z form is observed, the parameter a of the hexagonal unit cell varies from 17 to 23.8 A. The unit cell comprises then only one double helix[7] and the value of a represents therefore the distance between the axes of nearest neighbour helixes. When the transition from Z to B appends, the distance between axes of helixes in the fiber varies from 24 to 27 A and the cell, with a = 47 A, contains then three double helixes.

To study the reverse transition from B to Z, the r.h. was lowered very slowly from the value of 97 %. When the r.h. is near to 90 % a mixture of B and Z forms is still observed on X-ray patterns (Plate 2 a). Actually, one can see a meridian spot at 3,4 A (B form), a meridian at 6.46 A associated with the alternating sequence of dinucleotides and only one

meridian spot at 3.74 A characterizing the Z form. At 88 % r.h. the meridian spot at 7.27 A (Z form) reappears on the patterns (Plate 2 b) and at 80 % the Z form alone is observed on X-ray photographs (Plate 2 c).

We noted that when the r.h. is lowered suddenly from 97.5% (the polynucleotide is then in the B form) to 30 %, one then obtains a poor X-ray pattern with a meridian spot at 3.32 A and an important second layer line which allows us to determine a helical pitch of 30 A (see Plate 2 d). This distorted B conformation (or C form)[14] which corresponds to 9 nucleotide pairs per helical turn, is modified when the r.h. is increased and one gets again the Z form at 80 % r.h. but the fiber is then very much disorganized.

Fiber dimensions

Measurements of fiber dimensions during the Z to B and B to Z transitions have given values presented in figures 1 and 2. These measurements are performed under the same conditions of r.h. as those realized for X-ray diffraction. On figure 1, we can see how the fiber length increases until 95 % r.h. and it then suddenly decreases when the r.h. is higher than 95 %. At 97.5 % r.h. the fiber length is even lower than at 0 %. Conversely the fiber diameter (figure 2) increases slightly until 80 % r.h. and steeply thereafter.

When the r.h. is decreased from 97.5 %, the fiber length remains almost constant (figure 1) until 88 % r.h. (note that at such a value of r.h., X-ray patterns show mixtures of B and Z forms). For r.h. lower than 80 % the fiber length decreases

but one do not obtain the length values we had at the beginning of the process (the fiber length is 5% smaller). Nevertheless, the fiber diameter takes again its initial value (as the crystallographic cell parameter). An additional cycle of r.h. variations gives the same effect and the fiber length is lowered again when the r.h. is at 0 %. Moreover, when the r.h. is suddenly decreased from 97.5 to 30 % such a loss of the fiber length is even larger (near to 10 %).

Hydration of poly (dC-dG). poly (dC-dG)

Results obtained simultaneously from X ray diffraction and measurements of variations of the fiber dimensions with the r.h., allowed us to follow the changes of the number of water molecules associated with a nucleotide during the conformational transitions[15]. We therefore determined (Table 1) that there are 2 water molecules per nucleotide when the poly (dC-dG). poly (dC-dG) is in the Z_1 form. This number increases regularly during the evolution from Z_1 to Z_2 and there are 16 water molecules per nucleotide in this last conformation (just before the transition to the B form). Note that these figures do not take into account water which remains in the fiber at 0 % r.h.[18]. The complete transition from Z_2 to B necessitates the addition of 6 water molecules per nucleotide which have then 22 water molecules in their vicinity ; this last number is even increased when the r.h. is larger than 97.5 %. Results presently obtained are in agreement with data deduced from studies on poly (dC-dG). poly (dC-dG) films by infrared spectroscopy[19] and with

Table 1. Z-B-Z transitions as functions of the relative humidity. Crystallographic parameters : a=b parameter of the hexagonal cell ; c=P helix pitch ; p axial separation of the repeating unit (dinucleotide) ; p_m axial separation of the repeating unit (one nucleotide) u=P/p number of repeating units per helical turn ; G number of water molecules per nucleotide.

R.H. %	Form	a = b (Å)	C = P (Å)	p (Å)	p_m (Å)	u	G
6	Z_1	17.0	42.0	6.85	3.42	6.1	
25	Z_1	17.3	42.5	6.92	3.46	6.1	0.3
47	Z_1	18.0	43.5	7.13	3.51	6.1	1.5
75	Z_1	18.7	43.8	7.25	3.62	6.0	3.5
85	Z_2	19.5	44.2	7.32	3.66	6.0	6.1
90	Z_2	21.6	44.2	7.36	3.68	6.0	9.8
95	Z_2	23.8	46.5	6.46	3.78		16.6
97.5	B	47.0	33.8		3.39	10.0	22.7
90.5	B	42.0	33.8	6.46	3.37	10.0	15.3
	Z_2		45.2		3.75		
88	B	40.0	33.8	6.40	3.37	10.0	10.8
	Z_2		44.4	7.27	3.63	6.1	
65	Z_1	18.5	43.4	7.20	3.60	6.0	3.0
18	Z_1	17.5	42.0	6.90	3.45	6.0	0.1

values obtained from studies on solutions by dielectric relaxation [20]. Moreover, the present observations concerning the variations of the number of water molecules during the B-Z conformational transition are complementary to those obtained from X-ray crystallography where the precise position of water in the Z double helix can be estimated[21-23] .

The comparison of results obtained from X-ray diffraction with the measurement of variations of the fiber dimensions puts into evidence a proportionality between the inter helical distance and the fiber diameter (see figure 2). This fact is observed when poly (dC-dG). poly (dC-dG) is in its Z form as well as when the transition to the B form occurs. We also noted that the change of conformation from Z to B appears when the distance between helix axes has a value of least 23.8 A and that distance increases to 27 A for the B form. Besides, we know[1] that the diameter of the double helixes of poly (dC-dG). poly (dC-dG) in Z form is near to 18 A and that it is 20 A in the B conformation[24]. We therefore see that relatively large inter helical distances are necessary in order to allow the important molecular movements inducing the transition between left and right handed helical conformations of poly (dC-dG). poly (dC-dG). Such enlargement of the packing distances of the double helixes is due to water molecules and is obtained by rising the r.h. until values very near to 100 %.

Discussion

The present experimental results, obtained simultaneously from X-ray diffraction and measurement of dimensions of poly (dC-dG). poly(dC-dG) fibers, clearly show the reversibility of the B-Z transition. However, we noted that the form transition is realized at very high and in a narrow interval of r.h. values (mainly for the Z_2 to B transition). At very low r.h., the polynucleotide is in the Z_1 form and it progressively evolves, as the r.h. is risen, toward the Z_2 form until it changes steeply to the B form. The application of the present experimental method[14] allowed us to determine that the Z form of poly (dC-dG). poly (dC-dG) can be associated with up to 16 water molecules per nucleotide and that 6 more are necessary to achieve the Z to B transition.

An almost perfect proportionality between the fiber length and the helical parameter p (an average value for Z) is observed (see figure 1) for the transitions Z_1-Z_2-B. This fact clearly indicates the polymorphism of the Z form[25] of poly (dC-dG). poly (dC-dG). But it should be noted that, even if p varies with the r.h., the number of dinucleotides per helical turn remains equal to 6 .Moreover, the Z_1 helical conformation corresponds to very low r.h. while Z_2 is obtained at very high r.h., just before the transition to the B form. We can add that the continuous Z_1-Z_2 change of form is perfectly reversible.

Conversely, the reverse transition from B to Z, observed when the r.h. is lowered, is much slower as already noted in studies on solutions[26] or on fibers[19]. Moreover, under the

present experimental conditions, this change of form is obtained in a larger interval of r.h.. We firstly observed a mixture of B and Z_2 forms when the r.h. is decreased and thereafter, a progressive change from Z_2 to Z_1. The transition from B to Z is always associated to a disorganization of the fiber and that effect is more important when the r.h. is suddenly lowered . As a consequence, we observed that, even for very slow variations of the r.h., there is no proportionality between the fiber length and the helical parameter p. Larger lengths of the fiber should correspond to the transition from B to Z_2, but the disorganization of the fiber is superposed on that transition and any observation of the fiber length variation becomes impossible when the r.h. is lowered from the value of 97 %. We can add that a tension applied on the fiber[16] improves the B-Z transition and actually maintains the fiber organization. But it also induces sliding of the polynucleotide helixes past one another and that makes the fiber length measurements irrelevant.

Nevertheless, it appears that the change from B to Z conformation remains cooperative because no well organized form, different from B or Z, can actually be observed on X-ray patterns during the transition. That is in agreement with results obtained from studies on solutions[27-29] and also on films[19] of poly (dC-dG). poly (dC-dG).

References

1 Wang, A.H.J., Quigley, G.J., Kolpak, F.J., Crawford, J.L., Van Boom, J.H., Van der Marel, G. and Rich, A. *Nature* 1979, **282**, 680

2. Pohl,F.M. and Jovin, T.M. *J. Mol. Biol.* 1972, **67**, 375

3. Arnott, S., Chandrasekaran, R., Birdsall, D.L., Leslie, A.G.W. and Ratliff, R.L. *Nature* 1980, **283**, 743

4. Behe, M., Zimmerman, S. and Felsenfeld, G. *Nature* 1981, **293**, 233

5. Sasisekharan, V. and Brahmachari, S.K. *Curr. Sci.* 1981, **50**, 10

6. Mahendrasingam, A., Pigram, W.J., Fuller, W., Brahms, J. and Vergne, J. *J. Mol. Biol.* 1983, **168**, 897

7. Manhendrasingam,A., Denny, R.C., Forsyth, V.T., Greenall, R.J., Pigram, W.J., Papiz, M.Z. and Fuller W. *Inst. Phys. Conf.*1990, **101**, 225

8. Leslie, A.G.W., Arnott, S., Chandrasekaran, R. and Ratliff, R.L. *J. Mol. Biol.* 1980, **143**, 49.

9. Jaworski, A., Hsieh, W.T., Blaho, J.A., Larson, J.E. and Wells, R.D. *Science* 1987, **238**, 773

10. Kmiec, E.B. and Holloman, W.K. *Cell* 1986, **44**, 445

11. Vasicek, T.J., McDevitt, B.E., Freeman, M.W., Fennick, B.J., Hendy, G.N., Potts, J.T., Rich, A. and Kronenberg, H.M. *Proc. Natl. Acad. Sci.USA* 1983, **80**, 2127

12. Fishel, R.A., Detmer, K. and Rich, A. *Proc. Natl. Acad. Sci. USA* 1988, **85**, 36

13. Rahmouni, A.R. and Wells, R.D. *Science* 1989, **246**, 368

14. Premilat, S., Harmouchi, M. and Albiser,G. *Biophys. Chem.* 1990, **35**, 37

15. Harmouchi, M., Albiser, G. and Premilat, S. *Eur. Biophys. J.* 1990, **19**, 87

16. Albiser, G., Harmouchi, M. and Premilat, S.J. *Biomol. Structure and Dynamics* 1988, **6**, 359

17. Wang, A.H.J., Quigley, G.J., Kolpak, F.J., Van der Marel, G., Van Boom, J.H. and Rich, A. *Science* 1981, **211**, 171

18. Tao, N.J., Lindsay, S.M., and Rupprecht, A. *Biopolymers* 1989, **28**, 1019

19. Pilet, J. and Leng, M. *Proc. Natl. Acad. Sci. USA* 1982, **79**, 26

20. Umehara, T., Kuwabara, S., Mashimo, S. and Yagihara, S. *Biopolymers* 1990, **30**, 649

21. Westhof, E. *Int. J. Biol. Macromol.* 1987, 9, 185

22. Saenger, W., Hunter, W.N. and Kennard, O. *Nature* 1986, **324**, 385

23. Gessner, R.V., Frederick, C.A., Quigley, G.J., Rich, A. and Wang,A.H.J. *J. Biol. Chem.* 1989, **264**, 7921

24. Premilat, S. and Albiser, G. *Nucl. Acids Res.* 1983, **11**, 1897

25. Drew, H.R. and Dickerson, R.E. *J. Mol. Biol.* 1981, **152**, 723

26. Goto, S. *Biopolymers* 1984, **23**, 2211

27. Soumpasis, D.M., Robert-Nicoud, M. and Jovin, T.M. *F.E.B.* 1987, **213**, 341

28. Preisler, R.S., *Biochem. Biophys. R. Comm.* 1987, **148**, 609

29. Hamori, E. and Jovin, T.M. *Biophys. Chem.* 1987, **26**, 375

FIGURE CAPTIONS

Figure 1. Variations of the fiber length L (•—•) for the Z-B-Z transitions and of the rise per nucleotide p_m (■- -■) for the Z-B transition as functions of the relative humidity.

Figure 2. Variations of the fiber diameter D (•—•) and the distance between helix axes d_{aa} (■- -■) for the Z-B transition as functions of the relative humidity.

Plate 1. Z-B transition. X-ray patterns obtained at : (a) 23 % r.h.- Z_1 form ; (b) 86 % r.h. - Z_2 form ; (c) 95 % r.h. - limite of Z_2 form ; (d) 97,5 % r.h. - B form.

Plate 2. B-Z transition. X-ray patterns obtained at : (a) 90 % r.h. - B-Z forms ; (b) 85 % r.h. - Z_2 form ; (c) 40 % r.h.- Z_1 form ; (d) result of a sudden decrease of r.h. from 97 % to 50 %.

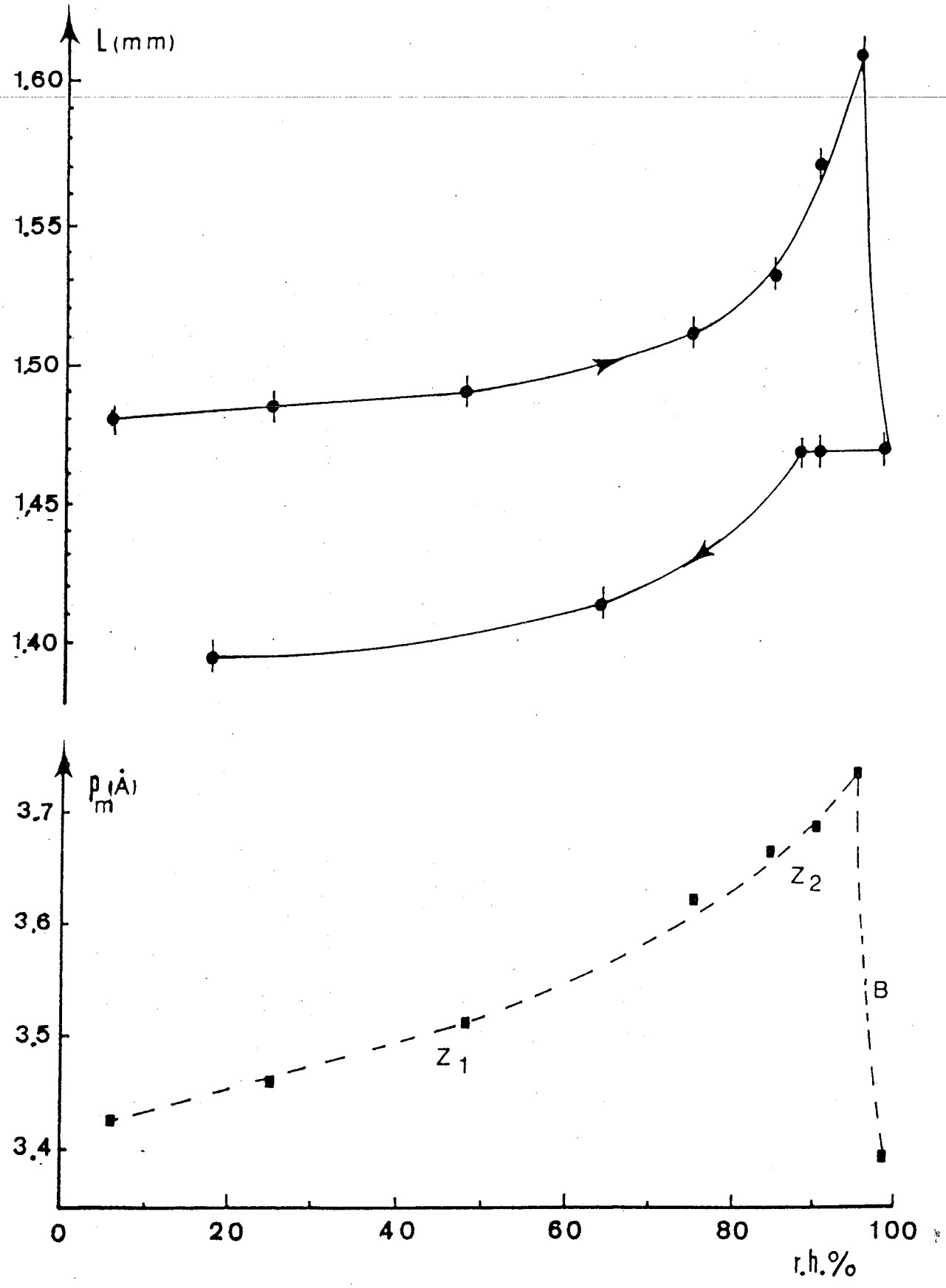

Fig. 1

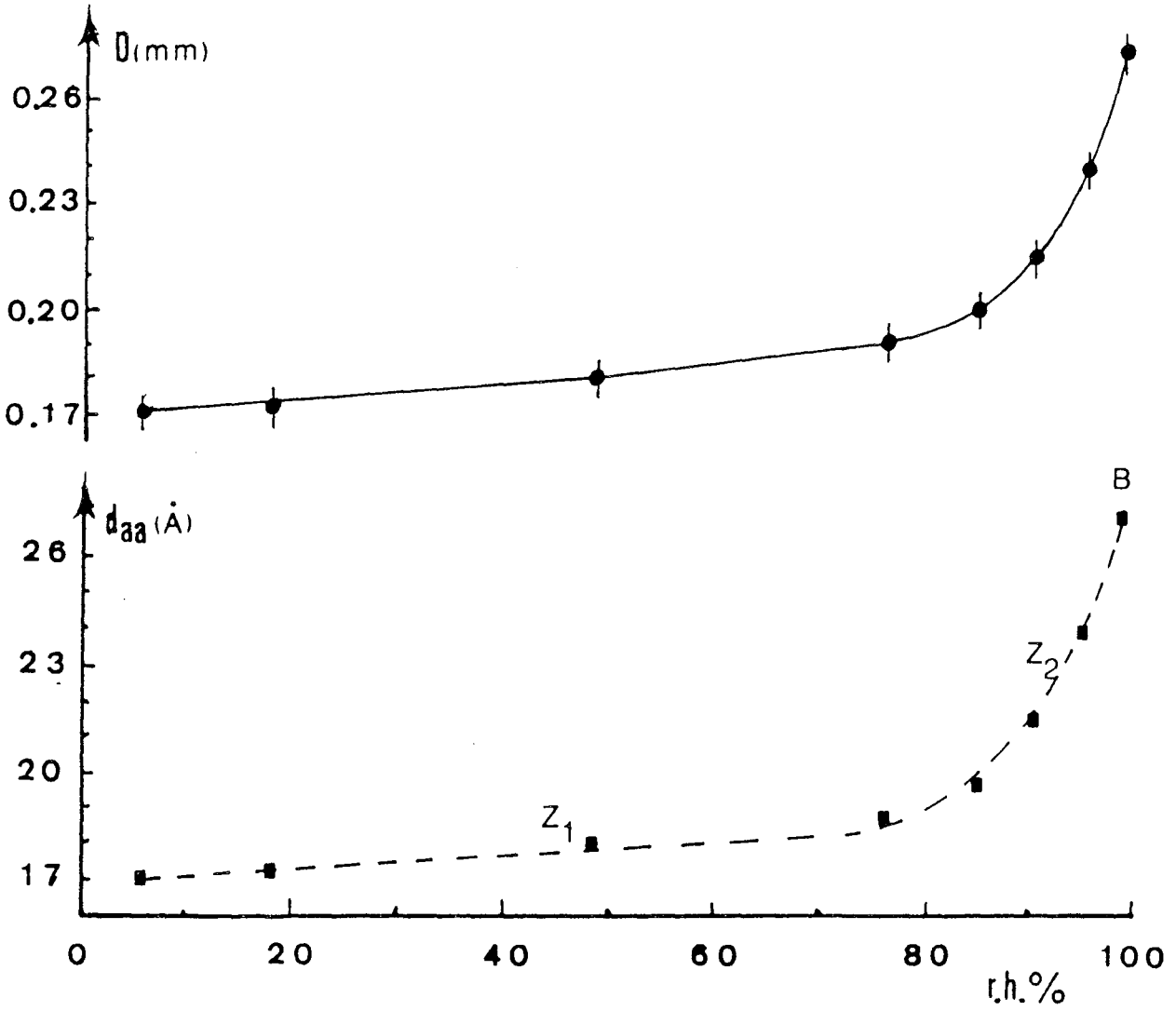

Fig. 2

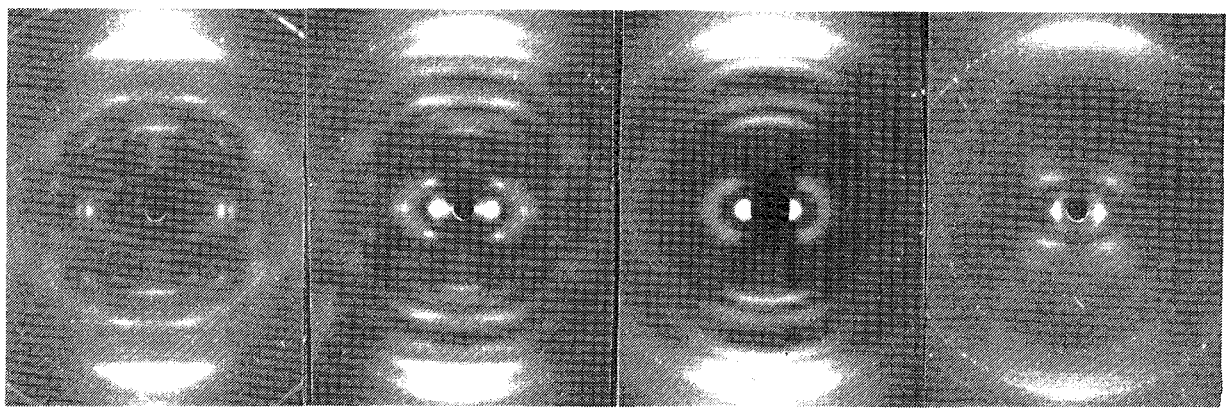

(a) (b) (c) (d)

Plate I

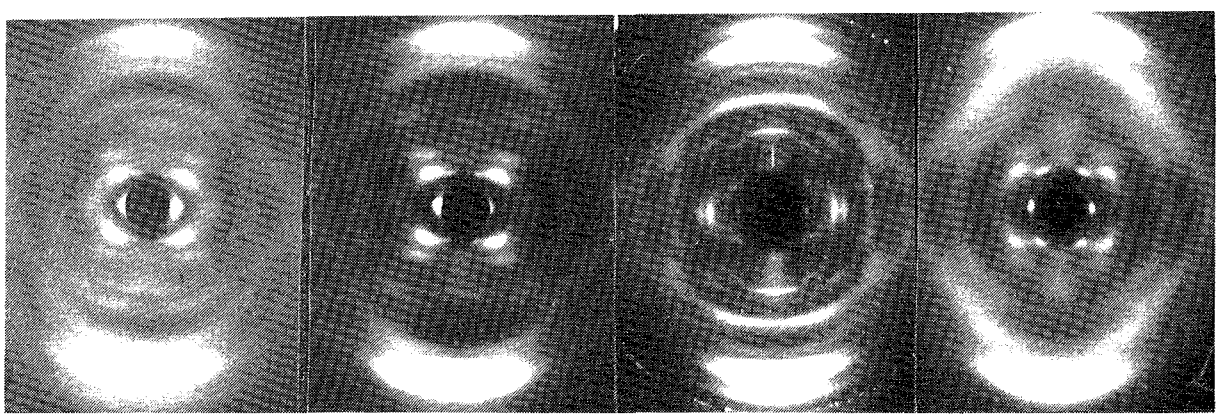

(a) (b) (c) (d)

Plate II

F) DISCUSSION

L'ensemble des résultats expérimentaux recueillis sur les différentes transitions de l'ADN, par la méthode qui associe la diffraction RX et l'observation directe de la fibre, montrent l'intérêt de cette méthode. Les facteurs qui agissent sur les transitions peuvent être mis en évidence ainsi que la subtilité de leurs interactions. Les résultats obtenus sans ambiguïté par cette méthode peuvent être comparés à ceux déduits des autres techniques. On remarque que la proportionnalité entre la longueur de la fibre et le paramètre p n'est vérifié que dans la mesure où les transitions sont lentes et dans le domaine où il y a un ordre acceptable des molécules d'ADN à l'intérieur de la fibre. On peut noter que les fibres, surtout dans un environnement à faible humidité relative (souvent en-dessous de 50 %) ne donnent généralement plus de clichés R.X. exploitables, étant donnée la désorganisation des molécules que l'on remarque également par une diminution de la longueur de la fibre. De même, une diminution brutale et rapide, sur un grand intervalle d'humidité relative, entraîne une plus grande diminution de la longueur de la fibre qui masque souvent la transition attendue et, de plus, crée un désordre irréversible dans la fibre. Ce phénomène se rencontre particulièrement avec le poly (dC-dG). poly (dC-dG) où une diminution brutale de l'humidité relative de 97 % (le polynucléotide est en forme B) à 35 % crée une diminution relative de longueur de 10 %, alors que la diminution de p n'est que de 2,5 %. Le cliché R.X. dénote alors une forme B déformée et pas la forme Z attendue.

La proportionnalité entre longueur de la fibre et le paramètre p n'est pas respectée dans un autre cas avec le poly (dC-dG). poly (dC-dG) : par diminution lente de l'humidité relative de 97 % (forme B) à 88 %, la longueur de la fibre reste constante alors qu'avec la coexistence des formes B et Z, p augmente. Dans ce cas, on a encore perte de l'ordre initial de la fibre, ce que révèlent du reste les clichés RX de moins bonne qualité. Le retour de la fibre à basse humidité fait apparaître un déficit de longueur de 6 % qui peut être attribué au désordre résultant de la transition B-Z. En fait, on constate que la longueur des fibres d'ADN ne peut que décroître ou être à la limite stationnaire lorsque l'humidité relative diminue. Ce principe explique également le caractère irréversible des transitions D-A du poly (dA-dT). poly (dA-dT) ou C - A de l'ADN. En effet, les transitions inverses exigent une augmentation du paramètre p, donc de la longueur de la fibre, lorsque l'humidité relative décroît à partir de 75 %. Cela ne peut se réaliser à ces faibles humidités étant donné les contraintes dues à l'imbrication des molécules. Il faut également mentionner que c'est par l'application d'une tension mécanique sur les fibres que les formes D et C sont obtenues avant d'initier ces transitions irréversibles.

Des résultats obtenus, on déduit le caractère coopératif des transitions A-B, D-B et Z-B. Pour ces transitions, on peut souvent évaluer le pourcentage des formes en présence. Le mélange des formes A et B a du reste été obtenu, non seulement avec un duplex d'oligonucléotides en solution concentrée de sel, mais aussi dans des cristaux d'oligonucléotides (72) et le pourcentage des deux formes en présence a pu être évalué

par spectroscopie infrarouge pour un tel type de cristal (73,74). Le passage de la forme B à la forme C est, par contre, très progressif. Il est dû à la déformation de la forme B.

Un autre intérêt de la méthode utilisée vient de la possibilité que l'on a de suivre les variations du nombre de molécules d'eau associées à chaque nucléotide et d'évaluer le nombre exact de ces molécules pour obtenir un changement de conformation. Le tableau N° VI montre les résultats ainsi obtenus. Il est bien entendu que le nombre de trois molécules d'eau à l'état déshydraté de l'ADN (75) n'est pas pris en compte puisqu'il ne peut pas être évalué par la présente méthode.

Duplex	[Poly (dC dG)$_2$]	ADN 72 % CG	ADN 42 % CG	ADN 42 % CG	[Poly (dA dT)]$_2$	[Poly (dA dT)$_2$]
$Na^+/_p$ %	0,8	0,5	0,5	0,28	0,5	0,66
Transition / H.R.%	Z_1-Z_2-B	A-B	A-B	C-B	D→A-B	D-B
97.5	B(23)					
95	Z_2(16)	B(22)				
92			B(20)	B(20)		
90					B(18)	
96						
80				B* C(10)		B(13)
75	Z_1(3)			C(4)		
70					A(5)	
66		A(5)	A(4)			
50						
40					D(1)	D(1)

TABLEAU N° 6

Nombre de molécules d'eau associées à un nucléotide pour les différentes transitions rencontrées avec les ADN et polynucléotides. Les transitions étant réalisées en fonction de l'humidité relative entourant la fibre.

Le nombre de cation Na^+ par nucléotide, donné dans ce tableau, provient de l'analyse par microsonde électronique sur des sections de fibres desséchées. Il représente le nombre de sodium effectivement lié à la structure de la molécule d'ADN mais non celui présent dans toute la fibre. Dans cette analyse, avec les photos de répartition du sel, on constate que pour le poly (dC-dG). poly (dC-dG), une forte quantité de sel est rejetée sur la surface de la fibre et élève donc la teneur en sel de la fibre à haute humidité (Photo n°10 b).

Les résultats rassemblés dans le tableau N° VI permettent de faire quelques constatations. La forme B est d'autant mieux maintenue lorsque l'humidité relative diminue, que l'ADN est riche en paires de bases A-T ou encore pour un ADN donné, que la teneur en sel est plus élevée. Inversement, la transition A-B se fait à d'autant plus hautes humidités que le pourcentage en bases G-C de l'ADN est élevé et que la teneur en sel est basse.

On remarque également que l'augmentation de la teneur en sel de sodium empêche la forme C mais par contre favorise l'obtention de la forme Z du poly (dC-dG). poly (dC-dG).

Pour la forme Z on constate que les paramètres hélicoïdaux évoluent avec l'humidité relative et que la transition vers la forme B ne peut se faire qu'à très haute humidité car les modifications de structure imposées par le changement de sens de l'hélice deviennent alors possibles.

CONCLUSION GENERALE

L'analyse des clichés de diffraction RX obtenus avec des fibres d'ADN permet d'évaluer, sans ambiguïté, les paramètres moléculaires des doubles hélices et de constater le polymorphisme de ces molécules. Parmi les facteurs conditionnant ce polymorphisme on relève le pourcentage en type de bases, la séquence, le type et le pourcentage du cation alcalin associé, le taux d'hydratation, la tension mécanique et l'association avec d'autres ligands.

Etant donnés la limite de résolution des clichés à 3 A et le faible nombre de taches de diffraction, associé souvent à une mauvaise cristallinité, il est difficile de proposer un modèle conformationnel unique. Un exemple de cet état de fait est donné avec le modèle conformationnel "side by side", formé de portions d'hélices droites et gauches et présentant les paramètres hélicoïdaux de la forme B de l'ADN. Ce modèle présente une bonne stéréochimie et un facteur d'accord entre intensités expérimentales et théoriques proche du modèle en double hélice droite.

Pour remédier à cette indétermination, on a fait appel aux résultats provenant d'autres techniques : le dichroïsme linéaire infrarouge et la RMN du P^{31}. Le critère imposé par l'orientation du groupe phosphate pour différentes formes de l'ADN permet alors de sélectionner un modèle conformationnel en accord avec toutes les données expérimentales.

Ainsi, pour la forme B de l'ADN, il a pu être montré qu'un modèle en double hélice gauche n'est pas correct. La même méthode a permis de proposer pour les formes A, B, C de l'ADN

et D du poly (dA-dT). poly (dA-dT), des modèles conformationnels satisfaisants.

L'analyse des transitions réalisées entre ces différentes formes permet de conclure que toutes ces conformations sont en doubles hélices droites. Les valeurs des angles dièdres qui définissent ces conformations sont proches, en général, des angles dièdres moyens déduits de la cristallographie des oligonucléotides. Bien sûr, la méthode utilisée ne permet pas d'accéder à la disparité topologique dans l'empilement des paires de bases, ce qui semble très important pour la reconnaissance ADN-protéine

Les conformations A, B et C de l'ADN doivent essentiellement leur existence aux conditions de l'environnement, à savoir le type et le pourcentage du cation alcalin présent ainsi que le taux d'hydratation. En effet, dans le cas de l'ADN en forme B, le pourcentage en base A-T ou G-C n'a aucune incidence sur les intensités calculées. Les disparités d'intensité expérimentales entre fibres d'ADN étant alors dues à des assemblages des molécules dans des réseaux différents en fonction de l'environnement eau-sel.

La fixation d'un ligand supplémentaire à l'ADN, comme un cation métallique (type argent) est un exemple intéressant pour déduire d'un cliché de diffraction RX perturbé les sites de fixation du cation sur l'ADN. On remarque alors que malgré une distribution non périodique du cation sur l'ADN il est possible de situer les sites de fixation et cela d'autant plus facilement que ceux-ci se trouvent proches de l'axe de la double hélice. Il est alors possible de proposer une conformation de l'ensemble ADN-cation. L'analyse de cette

conformation permet éventuellement d'expliquer les anomalies spectrales observées en solution. Il faut aussi remarquer que ce genre d'étude peut être menée avec d'autres types de ligands.

C'est par l'étude des transitions entre les formes A-B et B-C de l'ADN que l'influence de la tension mécanique a été prise en considération. L'importance de ce facteur, du reste souvent mentionné dans les études de diffraction RX de fibre, est mis en évidence par le fait qu'il peut empêcher la transition de la forme B vers la forme A. De plus il étale sur un plus grand domaine la variation de l'humidité relative, le passage de B vers C. Ce facteur a un effet comparable à celui de l'augmentation de sel dans la fibre car il maintient la forme B malgré une diminution de l'hydratation.

Pour analyser les transitions entre les différentes formes des ADN et polynucléotides, une méthode originale est proposée. Cette méthode associe étroitement la diffraction RX de fibre et l'observation des dimensions de la fibre. Elle est fondée sur des relations de proportionnalité entre paramètres moléculaires et macroscopiques. Les différentes courbes de transition établies, lorsque l'humidité relative varie, permettent d'établir le caractère coopératif des transitions A-B, D-B et Z-B. Par contre la transition C-B est progressive et dénote une déformation continue de la double hélice. Les caractéristiques de la forme C ne sont atteintes qu'à basse humidité.

On constate également un polymorphisme pour la forme Z car cette forme existe sur un grand domaine de variation de l'humidité relative. La présente méthode d'étude des

transitions permet d'évaluer le nombre de molécules d'eau associées à chaque nucléotide et de quantifier le nombre de molécules d'eau nécessaire à chaque forme en fonction du taux de cation alcalin présent mais aussi du pourcentage en bases A-T ou G-C.

L'existence de transitions irréversibles des formes C vers A ou de D vers A, à basse humidité, s'explique par le faible apport d'eau nécessaire entre ces formes mais aussi par le fait qu'un facteur comme la tension mécanique intervient pour obtenir l'état initial C ou D.

La transition réversible Z-B qui entraîne un changement de sens de la double hélice, ne se fait qu'à haute humidité. En effet, l'éloignement des molécules entre elles laisse alors la place aux déformations nécessaires. On constate par contre que le passage de la forme B à la forme Z est plus difficile et qu'il s'accompagne d'une désorientation de la fibre si aucune tension n'est exercée.

Pour tout ADN, lors d'une transition, on remarque donc des interactions subtiles entre l'eau, les cations alcalins et la tension mécanique. Les fluctuations locales de l'environnement peuvent donc entraîner des modifications de conformation de l'ADN dans les nombreuses situations à l'intérieur même des cellules vivantes.

BIBLIOGRAPHIE

1 J.D. WATSON, Biologie Moléculaire du Gène, InterEditions,Paris (1978)

2 F. GROS, Les Secrets du Gène, Seuil, Paris (1986)

3 W. GUSCHLBAUER, Nucleic Acid Structure, Springer Verlag, New York (1976)

4 G. CHAMPETIER, Chimie Macromoléculaire, Herman, Paris (1972)

5 J.D. WATSON, La double Hélice, Laffont, Paris (1984)

6 T.A. STEITZ, Quart. Reviews of Biophys. 23, 3, 205 (1990)

7 S.C. SCHULTZ, G.C. SHIELDS et T.A. STEITZ, Science 253, 1001 (1991)

8 A.R. RAHMOUNI et R.D. WELLS, Science 246, 368 (1989)

9 S. NEIDLE, L.H. PEARL et J.V. SKELLY, Biochem. J. 243, 1 (1987)

10 M. GELLERT, K. MIZUUCHI, M.H. O'DEA, H. OHMORI et J. TOMIZAWA, Coll. Spring. Harbor, Symp. Quant. Biol. 43, 35 (1979)

11 A. BHATTACHARYYA, A.I.H. MURCHIE, E. VON KITZING, S. DIEKMAN, B. KEMPER et D.M.J. LILLEY, J. Mol. Biol. 221, 1191 (1991)

12 W. SAENGER, Principles of Nucleic Acid Structure, Springer Verlag, New York (1984)

13 A.H.J. WANG, G.J. QUIGLEY, F.K. KOLPAK, J.L. CRAWFORD, J.H. VAN BOOM, G. VAN DER MOREL et A. RICH, Nature 292, 680 (1979)

14 G. GUPTA, M. BANSAL et V. SASISEKHARAN, Int. J. Biol. Macromol. 2, 368 (1980)

15 J. PILET et J. BRAHMS, Biopolymers 12, 387 (1973)

16 H. SHINDO, J.B. WOOTEN, B.H. PHEIFFER et S.B. ZIMMERMAN, Biochemistry 19, 518 (1980)

17 F.X. WILHELM et M. DAUNE, Biopolymers 8, 121 (1969)

18 I. SISSOËFF, J. GRISVARD et E. GUILLE, Progr. Biophys. Molec. Biol. 31, 165 (1976)

19 F.H.C. CRICK et J.D. WATSON, Proc. Royal Soc. A 223, 80 (1954)

20 W. COCHRAN, F.H.C. CRICK et V. VAND, Actal Crystall. 5, 591 (1952)

21 B.K. VAINSHTEIN, Diffraction of X-rays by Chain Molecules, Elsevier, Londres (1966)

22 M. KAKUDO et N. KASAI, X-Ray Diffraction by Polymers, Kodansha, Tokyo (1972)

23 P. HORN, Chimie Macromoléculaire II, Hermann, Paris, 670 (1972)

24 A. GUINIER, Théorie et Technique de la Radiocristallographie, Dunod (1964)

25 S. ARNOTT, Trans Americ of the Cristallo. Ass. 9, 31 (1973)

26 R.P. MILLANE et N.J. STROUD, Int. J. Biol. Macromol. 13, 202 (1991)

27 R.E. FRANKLIN et R.G. GOSLING, Acta Crystal. 6, 678 (1953)

28 R. LANGRIDGE, H.R. WILSON, C.W. HOOPER, M.H.F. WILKINS et L.D. HAMILTON, J. Mol. Biol. 2, 19 (1960)

29 A.G.W. LESLIE, S. ARNOTT, R. CHANDRASEKARAN et R.L. RATLIFF, J. Mol. Biol. 143, 49 (1980)

30 W. FULLER, M.H.F. WILKINS, H.R. WILSON et L.D. HAMILTON, J. Mol. Biol. 12, 60 (1965)

31 D.A. MARVIN, M. SPENCER, M.H.F. WILKINS et L.D. HAMILTON, J. Mol. Biol. 3, 547 (1961)

32 S. ARNOTT, Polymer 6, 478 (1965)

33 W. FULLER, Thèse, Université de Londres, 45 (1961)

34 H. EYRING, Phys. Rev. 39, 746 (1932)

35 J. HERMANS et D. FERRO, Biopolymers 10, 1121 (1971)

36 M. SUNDARALINGAM, Biopolymers 7, 821 (1969)

37 D. VOET et A. RICH, Prog. Nucl. Acid. Res. Mol. Biol. 10, 183 (1970)

38 N.C. SEEMAN, J.M. ROSENBERG, F.L. SUDDATH, J.J.P. KIM et A. RICH, J. Mol. Biol. 164, 109 (1976)

39 M.A. VISWAMITRA, Z. SHAKKED, P.G. JONES, G.M. SHELDRICK, S.A. SALISBURY et O. KENNARD, Biopolymers 21, 512 (1982)

40 S. ARNOTT et D.W.L. HUKINS, Biochem. J. 130, 453 (1972)

41 S. ARNOTT et D.W.L. HUKINS, J. Mol. Biol. 81, 93 (1973)

42 H. SUGETA et T. MIYAZAWA, Biopolymers 5, 673 (1967)

43 C. ALTONA et M. SUNDARALINGAM, J. Amer. Chem. Soc. 94, 9205 (1972)

44 R. TAYLOR et O. KENNARD, Acta Cryst. B 39, 133 (1983)

45 D. WRINCH, Acta Cryst. 3, 475 (1950)

46 R.D.B. FRASER, T.P. MACRAE et E. SUZUKI, J. Appl. Cryst. 11, 693 (1978)

47 O. KENNARD et W.N. HUNTER, Quant. Rev. Biophys. 22, 327 (1989)

48 W. FULLER, F. HUTCHINSON, M. SPENCER et M.H.F. WILKINS, J. Mol. Biol. 27, 507 (1967)

49 M.O. FENLEY, G.S. MANNING et W.K. OLSON, Biopolymers 30, 1191 (1990)

50 M.A. O'BRIEN, J. of Sciences Inst. 25, 73 (1948)

51 L.D. HAMILTON, R.K. BARCLAY, M.H.F. WILKINS, G.L. BROWN, H.R. WILSON, D.A.MARVIN, H. EPHRUSSI-TAYLOR et N.S. SIMONS, J. Biophys. Biochem. Cytol. 5, 397 (1958)

52 J. PILET et J. BRAHMS, Nature, New Biol. 236, 99 (1972)

53 S. BRAM, C.R. Acad. Sci. Paris 276, 657 (1973)

54 R.H.T. BATES, R.M. LEWITT, C.H. ROWE, J.P. DAY et G. RODLEY, J. Royal Soc. (New Zeeland), 7, 273 (1977).

55 R. WING, H. DREW, T. TAKANO, C. BROKA, S. TANAKA, K. ITAKURA et R. DICKERSON, Nature 287, 755 (1980)

56 P.B. KELLER et K.A. HARTMAN, Spectrochimica Acta 42 A, 299 (1986)

57 M. HARMOUCHI, Thèse Université Nancy I (1989)

58 H.R. DREW et R. DICKERSON, J. Mol. Biol. 151, 535 (1981)

59 M.J. DOKTYCZ, A.S. BENIGHT et R.D. SHEARDY, J. Mol. Biol. 212, 3 (1990)

60 J.J. MULLER, G. DAMASCHUN, H. DAMASCHUN, R. MISSELWITZ, D. ZIRVER et A. NOTHNAGEL, Biomed. Biochim. Acta 43, 929 (1984)

61 H. URATA, K. SHINOHARA E. OGURA, Y. UEDA et M. AKAGI, J. Am. Chem. Soc. 113, 8174 (1991)

62 W. POHLE, H. FRITZSCHE et V.B. ZHURKIN, Comm. Mol. Coll. Biophys. 3, 3, 179 (1986)

63 J. BRAHMS J. PILET, T.T. PHUONG LAN et L.R. HILL, Proc. Nat. Acad. Sci. USA 70, 3352 (1973).

64 R.M. IZATT, J.J. CHRISTENSEN et H. RYTTING, Chem. Rev. 71, 439 (1971)

65 G.L. EICHHORN, Adv. Inorg. Biochem. 3, 2 (1981)

66 M. LANGLAIS, H.A. TAJMIR-RIAHI et R. SAVOIE, Biopolymers 30, 743 (1990)

67 J.A. TABOURY, P. BOURTAYRE, J. LIQUIER et E. TAILLANDIER, Nucl. Acid. Res 14, 3501 (1986).

68 B. NORDEN, Y. MATSUOKA et T. KURUCSEV, Biopolymers 25, 1531 (1986).

69 V.P. CHUPRINA, A.A. LIPANOV O.Y. FEDOROFF, S. KIM, A. KINTANAR et B.R. REID, Proc. Natl. Acad. Sci. USA 88, 9087 (1991)

70 E. TAILLANDIER, J. LIQUIER et J.A. TABOURY, Adv. Infrared Raman Spectroscop. 12, 64 (1985)

71 H. FRITZSCHE et A. RUPPRECHT, J. Mol. Liquids 46, 39 (1990)

72 J. DOUCET, J.P. BENOIT, W.B.T. CRUSE, T. PRANGE et O. KENNARD, Nature 337, 190 (1989)

73 Y. WANG, G.A. THOMAS et W.L. PETICOLAS, J. Biomol. Struct. Dyn. 6, 1177 (1989)

74 J. LIQUIER, E. TAILLANDIER, W.L. PETICOLAS et G.A. THOMAS, J. Biomol. Struct. Dyn. 8, 295 (1990)

75 N. LAVALLE, S.A. LEE et A. RUPPRECHT, Biopolymers 30, 877 (1990)

UNIVERSITE DE NANCY I

NOM DE L'ETUDIANT : Monsieur ALBISER Guy

NATURE DE LA THESE : DOCTORAT D'ETAT ès SCIENCES PHYSIQUES

VU, APPROUVE ET PERMIS D'IMPRIMER

NANCY, le 18 FEV. 1992 n° 84

LE PRESIDENT DE L'UNIVERSITE DE NANCY I

UNIVERSITE NANCY I LE PRESIDENT

M. BOULANGÉ

RESUME

L'ADN et les polynucléotides étirés en fibres orientées sont étudiés par diffraction des rayons X en utilisant les possibilités de modifier leur environnement, à savoir :

- l'humidité relative,
- le pourcentage du cation alcalin associé,
- la fixation de cation métallique et la tension mécanique appliquée.

En utilisant les informations obtenues par diffraction R.X. et des contraintes structurales provenant d'autres techniques, il est proposé :

- une discrimination entre modèles conformationnels de la forme B,
- des modèles conformationnels pour les formes A, B, C de l'ADN et D du $[poly\ (dA\text{-}dT)]_2$.

Une méthode originale permet d'analyser les transitions A-B et B-C de l'ADN, D→A-B et D-B du $[poly\ (dA\text{-}dT)]_2$ et Z-B du $[poly\ (dC\text{-}dG)]_2$.

Pour chaque transition, on mesure les variations du nombre de molécules d'eau associé à chaque nucléotide.

MOTS CLES

- ADN
- POLYNUCLÉOTIDES
- DIFFRACTION R.X.
- FIBRES
- CONFORMATION
- MODÉLISATION
- TRANSITION
- HYDRATATION